

DISS. ETH NO. 30436

DECENTRALISED FLEXIBILITY IN  
RENEWABLE POWER SYSTEMS

A thesis submitted to attain the degree of

DOCTOR OF SCIENCES  
(Dr. sc. ETH Zurich)

presented by

ANYA HEIDER  
M.Sc. University of Stuttgart

born on 26.07.1993

accepted on the recommendation of

Prof. Dr. Gabriela Hug, examiner  
Dr. Philipp Blechinger, co-examiner  
Prof. Dr. Jalal Kazempour, co-examiner

2024

Anya Heider: *Decentralised Flexibility in Renewable Power Systems*, © 2024

DOI: 10.3929/ethz-b-000684451

To my family and friends, especially to my parents  
Xiaoli and Klaus to whom I owe so much.



## ABSTRACT

---

Power systems worldwide are transitioning towards a more sustainable electricity supply based on renewable energy sources. At the same time, other sectors, like heat and transport, are electrified to move away from fossil fuels to renewable electricity. This major transition comes with new challenges, opportunities, and players, some of which are addressed in this thesis. The focus is power system flexibility, a key enabler for renewable power systems, and the newly emerging sources of decentralised flexibility in households, whose role is changing in the transitioning power system. Traditionally, they acted as passive consumers, drawing electricity from the grid whenever needed. Nowadays, more and more households are equipped with photovoltaic systems, often in combination with battery storage, electric vehicle chargers and heat pumps. With their own electricity generation, storage and flexible demand of electric vehicles and heat pumps, the opportunity for a more active participation in the power system and flexibility provision by households arises.

This thesis provides tools and insights for integrating household flexibility into renewable power systems. In the first part, the flexibility from the decentralised flexibility options owned by households is estimated in terms of temporal availability, available power and flexible energy. Flexibility is important to various aspects of the power system, and different flexibility needs exist because electricity generation and demand need to be balanced temporally and geographically. In the second and third parts, the contribution of decentralised flexibility to the supply of geographic flexibility needs in German distribution grids and to the supply of temporal flexibility needs of a 100 % renewable German power system is estimated. The last part of the thesis deals with the activation of decentralised flexibility by economic incentives of electricity tariffs and how far well-designed tariffs can help supply geographic and temporal flexibility needs.

The results show a large flexibility potential from decentralised flexibility options. At the same time, the available flexibility depends on many aspects, like the time and location or consumer willingness to adapt their behaviour. Another factor is which flexibility needs should be supplied. The geographic flexibility needs in German distribution grids, measured

by reinforcement needs and resulting costs, can be significantly reduced by a flexible operation of decentralised flexibility options. However, they can not be fully avoided, and the distribution grids must be reinforced to a certain degree to incorporate high shares of decentralised photovoltaic, electric vehicles and heat pumps.

On the other hand, the temporal flexibility needs of a fully renewable German power system, supplied by photovoltaic and wind only, can be net decreased by deploying decentralised flexibility. Electric vehicles, especially, significantly reduce short- to medium-term flexibility needs if shifting between standing times and vehicle-to-grid is enabled. The total flexibility needs, their division into short-, medium- and long-term energy shifting, and the influence of decentralised flexibility also depend on the generation mix. A carefully chosen mix of photovoltaic and wind can thus reduce the temporal flexibility needs. Generally, decentralised flexibility options can supply short- to medium-term but not long-term flexibility needs. These would have to be supplied by other sources in future renewable power systems.

The right economic incentives can help to untap the potential of decentralised flexibility. Therefore, this thesis investigates the effect of different electricity tariff designs on geographic and temporal flexibility needs. The investigated tariffs are combinations of energy-based and capacity-based network tariffs with constant or time-varying suppliers' costs. The results show that if designed well, electricity tariffs can reduce geographic and temporal flexibility needs. On the other hand, time-varying purely energy-based tariffs pose the danger of synchronisation and increase in temporal and geographic flexibility needs, especially at high penetrations of decentralised flexibility. Capacity-based components on peak load and feed-in can counteract these effects and decrease the flexibility needs.

The supply of flexibility needs is not the only criterion electricity tariffs must fulfil. To this end, this thesis develops and applies a comprehensive evaluation framework with the criteria of an *efficient grid*, *fairness and customer acceptance* and *consistency with other political objectives*. The evaluation shows that purely energy-based tariffs overall perform worse than tariffs including capacity-based price components. It is therefore recommended to include capacity-based prices in future electricity tariffs.

This thesis highlights the importance of decentralised flexibility in renewable power systems. It shows that geographic flexibility needs in German distribution grids can be significantly reduced by an optimised operation of

residential electric vehicles, heat pumps and battery storage, and costly reinforcement measures delayed. Furthermore, decentralised flexibility options can supply temporal flexibility needs, especially short- and medium-term energy shifting on time scales up to a month. The right electricity tariff can help a system-friendly operation but must be designed carefully so as not to aggravate the effects of increased penetrations of decentralised flexibility options. The provided decision and simulation tools, which are all available open source, can help an informed choice.



## ZUSAMMENFASSUNG

---

Die Transformation des Energiesystems hin zu einer nachhaltigen Energieversorgung ist eine der großen gesellschaftlichen Herausforderungen der heutigen Zeit. Sie umfasst den Umbau des Stromsystems hin zu erneuerbaren Energien, aber auch die Elektrifizierung anderer Sektoren, wie Transport und Wärmeversorgung, um fossile Brennstoffe durch erneuerbaren Strom zu ersetzen. Dieser weitreichende Umbau birgt Herausforderungen, aber auch Chancen und neue Player, von denen einige in der vorliegenden Arbeit untersucht werden. Der Fokus ist dabei Flexibilität im Stromsystem, ein Schlüsselement für ein erneuerbares Stromsystem, und dezentrale Flexibilitätsoptionen in Haushalten, die die Rolle der Endverbraucher im sich wandelnden Stromsystem verändern. Traditionell agierten Haushalte als passive Verbraucher. Heutzutage sind immer mehr Haushalte mit dezentraler Photovoltaik, oftmals in Kombination mit Heimspeichern, Elektrofahrzeugen und Wärmepumpen ausgestattet. Mit eigener Erzeugung, Speichern und flexiblen Lasten eröffnet sich die Möglichkeit für eine aktive Partizipation der Haushalte im Stromsystem und das Potenzial, Flexibilität bereitzustellen.

Die vorliegende Arbeit beinhaltet Tools und Erkenntnisse zur Integration von Haushaltsflexibilitäten in ein erneuerbares Stromsystem. Der erste Teil behandelt Flexibilitätsoptionen und deren Flexibilitätspotential und bewertet das Flexibilitätspotenzial dezentraler Haushaltsflexibilitäten im Hinblick auf zeitliche Verfügbarkeit, abrufbare Leistung und flexible Energie. Flexibilität ist relevant für unterschiedliche Aspekte im Stromsystem und der benötigte Ausgleich von Stromerzeugung und -verbrauch führt zu verschiedenen Flexibilitätsbedarfen, da der Ausgleich sowohl geografisch als auch zeitlich gewährleistet sein muss. Im zweiten und dritten Teil der Arbeit wird der mögliche Beitrag der Haushaltsflexibilitäten zur Deckung des geografischen Flexibilitätsbedarfs in deutschen Verteilnetzen und des zeitlichen Flexibilitätsbedarfs in einem 100 % erneuerbaren deutschen Stromsystem untersucht. Der letzte Teil der Arbeit behandelt ökonomische Anreize durch angepasste Stromtarife und inwieweit solche Tarife zur Deckung von geografischem und zeitlichem Flexibilitätsbedarf beitragen können.

Die Ergebnisse zeigen ein hohes Flexibilitätspotential seitens dezentraler Flexibilitätsoptionen. Gleichzeitig ist das verfügbare Potential stark abhängig von verschiedenen Faktoren, wie Zeit und Ort oder der Bereitschaft der Kund\*innen, ihr Verbrauchsverhalten anzupassen. Ein anderer relevanter Faktor für die Effektivität des eingesetzten Flexibilitätspotentials ist, welcher Flexibilitätsbedarf gedeckt werden soll. Der geografische Flexibilitätsbedarf in deutschen Verteilnetzen, welcher in Netzausbaubedarf und den resultierenden Kosten gemessen wird, kann durch eine optimierte Fahrweise der dezentralen Flexibilitätsoptionen signifikant reduziert werden. Allerdings kann der Netzausbaubedarf für hohe Durchdringungen von Photovoltaik, Elektrofahrzeugen und Wärmepumpen in Haushalten nicht vollständig vermieden werden.

Im Gegensatz dazu kann der zeitliche Flexibilitätsbedarf in einem erneuerbaren deutschen Stromsystem, vollständig versorgt durch Photovoltaik und Windenergie, durch den Einsatz dezentraler Flexibilitätsoptionen effektiv verringert werden. Elektrofahrzeuge sind besonders geeignet, kurz- und mittelfristige Flexibilitätsbedarfe zu decken, wenn Verschieben des Ladebedarfs zwischen unterschiedlichen Ladevents und bidirektionales Laden möglich sind. Der gesamte zeitliche Flexibilitätsbedarf sowie dessen Unterteilung in kurz-, mittel- und langfristiges Schieben von Energie hängen auch von der Zusammensetzung des Einspeisemixes ab. Ein sorgsam ausgewählter Mix aus Photovoltaik und Windenergie kann daher dabei helfen, den zeitlichen Flexibilitätsbedarf zu begrenzen. Dezentrale Flexibilitätsoptionen können generell zur Deckung des kurz- und mittelfristigen Flexibilitätsbedarfs beitragen, nicht aber zum langfristigen Flexibilitätsbedarf. In einem zukünftigen erneuerbaren Stromsystem müssten andere Flexibilitätsoptionen dieses saisonale Verschieben von Energie decken.

Die richtigen ökonomischen Anreize können dazu beitragen, das Flexibilitätspotential von Haushaltsflexibilitäten zu heben und systemdienlich einzusetzen. Aus diesem Grund untersucht die vorliegende Arbeit den Einfluss von unterschiedlichen Stromtarifen auf den geografischen und zeitlichen Flexibilitätsbedarf. Die untersuchten Tarife sind Kombinationen aus energie- und leistungsbasierten Netzentgelten und konstanten oder zeitvariablen Strompreisen. Die Ergebnisse zeigen, dass gut designte Tarife den geografischen und zeitlichen Flexibilitätsbedarf reduzieren können. Auf der anderen Seite können zeitvariable energiebasierte Preise bei hoher Durchdringung von dezentraler Flexibilität zu erhöhten Gleichzeitigkeiten und dem Anstieg von zeitlichem und geografischem Flexibilitätsbedarf füh-

ren. Leistungsbasierte Preise auf die Spitzenlast und -einspeisung können diesen Effekt verhindern und die Flexibilitätsbedarfe reduzieren.

Zur Deckung der Flexibilitätsbedarfe beizutragen ist nicht das einzige Kriterium, was Stromtarife erfüllen müssen. Daher entwickelt diese Arbeit ein umfassendes Bewertungssystem für Stromtarife, in denen die Kriterien einer *effizienten Netznutzung*, der *Fairness und Kundenakzeptanz* and der *Konsistenz mit anderen energiepolitischen Zielen* quantifiziert und gewichtet werden. Die Anwendung auf Systeme mit hohen Durchdringungen dezentraler Flexibilität zeigt, dass über die untersuchten Tarife solche mit leistungs-basierten Kostenkomponenten im Allgemeinen besser abschneiden als rein energiebasierte Tarife. Es ist daher empfehlenswert, leistungs-basierte Preis-komponenten in zukünftige Stromtarife für Haushalte zu integrieren.

Zusammenfassend unterstreicht die vorliegende Arbeit die Relevanz dezentraler Flexibilitätsoptionen in erneuerbaren Stromsystemen. Sie zeigt, dass der geografische Flexibilitätsbedarf in deutschen Verteilnetzen signifikant reduziert, und kostenintensive Ausbaumaßnahmen verzögert werden können mit einer optimierten Fahrweise von Elektrofahrzeugen, Wärmepumpen und Heimspeichern. Außerdem können dezentrale Flexibilitätsoptionen zur Deckung des zeitlichen Flexibilitätsbedarfs beitragen, besonders zu kurz- bis mittelfristigem Flexibilitätsbedarf mit Verschiebebedarfen bis zu vier Wochen. Ein gut designer Stromtarif kann systemdienliches Verhalten der dezentralen Flexibilitätsoptionen anreizen, sollte aber leistungs-basierte Kosten beinhalten, um übermassige Synchronisationseffekte zu vermeiden. Die bereitgestellten offen verfügbaren Entscheidungs- und Simulationstools können zu einem informierten Entscheidungsprozess beitragen.



## ACKNOWLEDGEMENTS

---

The last four and a half years have been a great journey with many inspiring encounters and countless lessons learned. I want to thank the people who have made it such a unique and wonderful experience.

My deepest gratitude goes to my supervisor Prof. Gabriela Hug for her guidance and exceptional leadership style. Not only her professional expertise, but also her trust and constant support have been the foundation of this work. You are a real role model in how you balance professional and personal life. I consider myself extremely lucky to have had you as my supervisor. Merci vielmals for everything!

Many thanks to Dr. Philipp Blechinger for his supervision, his great motivation and visionary work. Thank you for founding the RLS graduate school which has been the most inspiring work environment and given so much opportunity to shape something new and to grow professionally and personally. I admire your ability to find the story line, how you provide and receive feedback, and I am extremely grateful for your support and efforts to make me finish things. I know I have not always been an easy case in that sense.

Thank you to Prof. Jalal Kazempour for agreeing to be part of my committee, for your time and dedication reading through the manuscript and the interesting discussion at my defense. It was a pleasure to have you in the committee!

In the course of the PhD I have further grown into the "Reiner Lemoine Family" to which I want to express my gratitude. Thank you to the Reiner Lemoine Foundation for the funding of my scholarship but also for your interest in our research, for sharing your knowledge and providing us the access to your expert networks. A special thanks to Fabian Zuber for his constant reminder of how important science communication is, for pushing us in that direction but also providing us with valuable feedback and his expertise. Thank you to the ESW network, especially my mentors Dr. Kathrin Goldammer, Eberhard Holstein, Stefan Jessenberger, Markus Meyer, Paul Neetzow and Carolin Schenuit for their support. It was great

to have your insights from different angles and institutions and I enjoyed our discussions a lot.

The warmest thank you to my mentor, colleague and friend Birgit Schachler who has been incredibly supportive in the past years. Thank you for the countless discussions and your input, for reading through so many of my texts, starting from the research plan to final chapters in this thesis, but also for the fun activities like beach volleyball and concerts. You are one of the smartest and most competent persons I know, and I honestly don't know what I would have done without your help. You are one of the persons with whom work is fun, and even more so after-work-activities. Thank you so much for everything, you are just great!

I had the pleasure of being part of two groups, both with amazingly talented and inspiring colleagues. Thank you to the RLS graduate school for giving meaning to the initial motto "The whole is bigger than the sum of its parts". It has been a great experience to form this new group, with all the freedom to contribute, group projects and joint workations. A special thanks to Ricardo Reibsch for his calm and structured way, for our collaborations in work but also outside, trying to push the energy system transition and a more sustainable way of life. Thank you to Marlin Arnz for his visionary way of work, combining professional excellence with his pronounced sense of free time and for letting us join him in beautiful Engelberg. Thank you to Alexandra Krumm for sharing her expertise on the social dimension of the energy system transition and for her remarkable way of giving constructive feedback. Both have extremely benefitted our group and work. Thank you to Martha Hoffmann and Philipp Diesing for joining and carrying on the spirit of the Kolleg.

Thank you to my colleagues of the power systems laboratory (PSL) in Zurich for always being so welcoming, for all their helpful feedback, the discussions on work and other topics and all the fun activities aside from work. A special thank you to Katharina Kaiser for our discussions on consumer modelling, for reading through the tariff chapter of my thesis but also for joining me in the night train, the hikes and exploring Budapest together. Thank you to Maria for all our conversations, be it on electric vehicle modelling, student supervision or simply life, and for your friendship! I would also like to thank Manolis for his input on heat pump modelling and the joint student project, Johanna for her great templates and the nice chats, Milos for his joyful energy, my office mates Kathi, Julie and Ognjen for the fun working environment in the final phase, Conor, Quentin and Maitraya for

the bouldering sessions and all other former and current PSL members for the great atmosphere in the lab.

In the past years, I had the pleasure to supervise a number of student projects. Thank you Sebastian Tews, Julian Endres, Maike Held, François Nzale, Hei Kern Leong, Benjamin Bossy, Seraina Wurster, Jill Huber, Mostafa Genena, Ladina Kundert, Florian Moors, Marta Puiggròs Vilalta and Shipra Mohan for your diligent work and your contributions to this thesis. I was impressed by your creativity, focus and styles of work. I learned a lot from all of you and I am extremely grateful to have had the possibility to work with you.

Outside my groups, I was able to work with other inspiring researchers and professionals who I would like to thank for the countless discussions and the joint research. Thank you to Adeleye Adetunji, Prof. Dr. Martin Weibelzahl, Dr. Alexandra März, Dr. Stephanie Halbrügge, Anne Michaelis, Simon Rusche, Yamshid Farhad, Dr. Yves Hertig and Leo Semmelmann for the fruitful exchange.

I would furthermore like to express my gratitude towards the numerous people who provided their support in organisational and technical aspects and who are overlooked so easily, especially when they do a good job. Thank you to the whole admin team at RLI for the great work that you do. A special thanks to Michaela Weiske who it was always a pleasure to talk to and who was extremely helpful with anything concerning personelle. Thank you Olaf Bernicke and the IT-team for all your support and the infrastructure you provide. At ETH, I would like to thank Judith Eberle for all her help but especially for her kindness and positive energy which made it so easy to come to her with anything. I also want to thank the IT support of ITET for their efficiency and their help during the last years.

Last but not least, I want to thank my friends and family for their unwavering support, their love and energy. Thanks for taking my mind off work, for the time spent together and the hearty laughs. My biggest thanks to my parents Xiaoli and Klaus for their support and trust, for giving us the freedom to find our own ways and for always being there to catch us. With time I have learned the value of the safe environment you have build around us, allowing us to grow and learn, and I cannot thank you enough for all you have done. Thank you to my brother Benyi for anchoring me by being so different in some ways yet so alike in others. Finally, I want to thank Hannes for his love and kindness, for his endless curiosity and his

continuous support. You have been the cherry on top of the cake and made life so much fuller and more enjoyable these past years. Thank you!

# CONTENTS

---

List of Acronyms	xx
1 Introduction	1
1.1 Background and Motivation . . . . .	1
1.2 Thesis Outline and Contributions . . . . .	4
1.3 List of Publications . . . . .	8
<b>I Flexibility Options and their Flexibility Potential</b>	
2 Representation in Open Energy Modelling Tools	15
2.1 Motivation . . . . .	15
2.2 Background to Flexibility Options and Energy System Models . . . . .	17
2.3 Research Design . . . . .	24
2.4 Results . . . . .	30
2.5 Discussion and Limitations . . . . .	44
2.6 Conclusion . . . . .	47
3 Modelling of Decentralised Flexibility Options	51
3.1 Distribution Grids . . . . .	51
3.2 Electric Vehicles . . . . .	70
3.3 Heat Pumps . . . . .	86
3.4 Battery Electric Storage . . . . .	95
4 Flexibility Potential of Decentralised Flexibility Options	101
4.1 Methodology - Estimation of Flexibility Potential . . . . .	101
4.2 Case Study - 100% DER Penetration . . . . .	106
4.3 Results and Discussion . . . . .	108
4.4 Conclusion . . . . .	118
<b>II Geographic Flexibility Needs in Distribution Grids</b>	
5 Motivation and Related Work	123
5.1 Introduction . . . . .	123
5.2 Background . . . . .	124
6 Methodology - Optimal Power Flow Formulation	131

7	Case Study I: Integration of Electric Vehicles	135
7.1	Comparison of Rule-Based and Optimised EV Charging	137
7.2	Comparison of Different Levels of EV Flexibility . . . . .	153
7.3	Sensitivities and Performance . . . . .	167
8	Case Study II: Simultaneous Integration of DERs	175
8.1	Distribution Grid Reinforcement Costs . . . . .	175
9	Discussion	187
9.1	Influence of Electric Vehicles . . . . .	187
9.2	Interplay of DERs . . . . .	189
9.3	Limitations . . . . .	192
10	Summary and Conclusions	195

### iii Temporal Flexibility Needs in the National System

11	Motivation and Related Work	199
11.1	Introduction . . . . .	199
11.2	Background . . . . .	200
12	Methodology - Storage Equivalent Model	207
12.1	Formulation of the Storage Equivalent Model . . . . .	207
12.2	Flexibility Indicators . . . . .	209
13	Case Studies	213
13.1	Study Setup . . . . .	213
13.2	Case Study I: Generation Mix . . . . .	218
13.3	Case Study II: Decentralised Flexibility Options . . . . .	221
13.4	Case Study III: Combined Analysis . . . . .	236
13.5	Sensitivities . . . . .	240
14	Discussion	247
14.1	Influence of the Generation Mix . . . . .	247
14.2	Influence of Decentralised Flexibility Options . . . . .	248
14.3	Limitations . . . . .	251
15	Summary and Conclusions	253

### iv Economic Incentives - Electricity Tariffs

16	Motivation and Related Work	257
17	Influence on Flexibility Needs	261
17.1	Methodology - Consumer Optimisation . . . . .	261
17.2	Data / Case Study . . . . .	264
17.3	Results and Discussion . . . . .	273
17.4	Conclusion . . . . .	296

18	Evaluation of Tariff Designs	299
18.1	Research Design . . . . .	300
18.2	Case Study - Application of the Proposed Framework .	316
18.3	Results and Discussion . . . . .	320
18.4	Conclusions and Policy Implications . . . . .	342
19	Conclusion	345
19.1	Main Findings . . . . .	345
19.2	Summary of Tools . . . . .	348
19.3	Further Research Needs . . . . .	350
<b>Appendix</b>		
A	Modelling of Flexibility Options	357
A.1	Overview of Models and Their Evaluation . . . . .	357
A.2	Additional Results for Individual Flexibility Categories	364
A.3	Modelling of Distribution Grids . . . . .	367
B	Additional Material on the Evaluation of Tariff Designs	369
	Bibliography	375

## LIST OF ACRONYMS

---

<b>AC</b>	Alternating current
<b>AHP</b>	Analytic hierarchy process
<b>AS</b>	Ancillary services
<b>BESS</b>	Battery energy storage systems
<b>BEV</b>	Battery electric vehicle
<b>CAES</b>	Compressed air energy storage
<b>CCGT</b>	Combined cycle gas turbine
<b>CHP</b>	Combined heat and power
<b>COP</b>	Coefficient of performance
<b>CR</b>	Consistency ratio
<b>DC</b>	Direct current
<b>DER</b>	Distributed energy resource
<b>DFO</b>	Decentralised flexibility option
<b>DG</b>	Distribution grid
<b>DHW</b>	Domestic hot water
<b>dRES</b>	Dispatchable renewable energy sources
<b>DSM</b>	Demand side management
<b>DSO</b>	Distribution system operator
<b>EMS</b>	Energy management system
<b>ESM</b>	Energy system model
<b>EV</b>	Electric vehicle
<b>GIS</b>	Geographic information system
<b>HP</b>	Heat pump
<b>HPC</b>	High power charging
<b>HV</b>	High voltage
<b>LP</b>	Linear programming
<b>LV</b>	Low voltage
<b>MCDA</b>	Multi-criteria decision analysis
<b>MDL</b>	Maximum deferrable load
<b>MILP</b>	Mixed-integer linear programming
<b>MV</b>	Medium voltage
<b>NDP</b>	Network development plan
<b>OCGT</b>	Open-cycle gas turbine
<b>OEP</b>	Open Energy Platform

<b>OPF</b>	Optimal power flow
<b>PEMFC</b>	Proton exchange membrane fuel cell
<b>PF</b>	Power flow
<b>PHEV</b>	Plug-in hybrid electric vehicle
<b>PHS</b>	Pumped hydro storage
<b>POI</b>	Point of interest
<b>PV</b>	Photovoltaics
<b>RE</b>	Renewable energy
<b>RES</b>	Renewable energy sources
<b>ResL</b>	Residual load
<b>RTestPSM</b>	Renewable test power system models
<b>SC</b>	Sector coupling
<b>SoC</b>	State of charge
<b>SOFC</b>	Solid oxide fuel cell
<b>TES</b>	Thermal energy storage
<b>V2G</b>	Vehicle-to-grid
<b>VPP</b>	Virtual power plant
<b>VRES</b>	Variable renewable energy sources



# INTRODUCTION

---

## 1.1 BACKGROUND AND MOTIVATION

The transition of the energy system towards a sustainable energy supply is one of the greatest challenges in Western society. This transition includes replacing conventional fossil-fueled and nuclear power plants with renewable energy sources and electrifying the transport and heat sectors. With many of these technologies installed at lower grid levels, the system becomes more decentralised.

While renewable generation from biomass and hydropower plants is dispatchable, a large share of the generation in a future renewable power system will be covered by variable renewable energy sources (VRES), particularly solar and wind generation [1], [2]. These sources depend on intermittent weather conditions and are hard to predict [2], [3]. Since power generation and demand must always be balanced for a stable system operation, the intermittency and uncertainty of generation from VRES increases the need for flexibility [4]. Therefore, power system flexibility is a key enabler for implementing high shares of renewable energy [1], [4]. Flexibility can be provided by many different sources and has always been a crucial part of power system planning and operations [2], [4]. Possible sources are the supply-side, demand-side, storage and sector coupling [2].

Traditionally, large-scale assets, like dispatchable power plants and pumped hydro storage, were the main provider of flexibility to balance supply and demand. However, conventional power plants, as one of the primary sources of flexibility, are being replaced by renewable generation [5]. Other technologies, like pumped hydro storage, have geological requirements and therefore a natural limit regarding possible expansion [6]. Therefore, the increasing need for flexibility faces a decrease in provision from conventional sources of flexibility, thus requiring more flexibility from other sources [2], [5].

Such possible sources include small-scale assets, like residential battery energy storage systems (BESS) and sector coupling technologies such as

electric vehicles (EVs) and heat pumps (HPs) equipped with thermal energy storage (TES). All these technologies are increasingly installed in the system [7]–[9].

While the primary goal of sector coupling technologies is the more efficient and sustainable use of energy in the non-electricity sector (i.e. heat and transport), these technologies also exhibit flexibility in their operation [2]. EVs are often parked much longer than the charging process takes place, and their electricity demand could therefore be shifted in time. If incentivised accordingly, they could even change the charging location, geographically shifting their demand. The thermal latency of buildings allows for shifting of the demand of HPs in time, and TES could further increase the shifting times. Thermal storage is usually cheaper than BESS and could pose a viable alternative [10].

Nevertheless, the costs for BESS have drastically decreased over the last years, and more and more BESS are installed in households alongside photovoltaics (PV) power plants [11]. Furthermore, the primary purpose of BESS is flexibility provision, and they can therefore contribute to many different system services [12], [13].

EVs, HPs and PV systems with BESS are increasingly being introduced to households, changing their role from passive consumers to prosumers actively interacting with the system. Figure 1.1 shows the recent development of decentralised flexibility options in Germany [14]–[16]. The numbers of EVs, HPs and BESS are increasing, and the growth shows an acceleration in the last years.

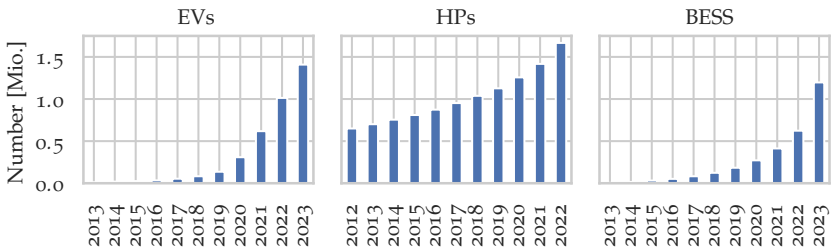


FIGURE 1.1: Numbers of installed distributed energy resources (DERs) in Germany in the last years, own representation with numbers from [14].

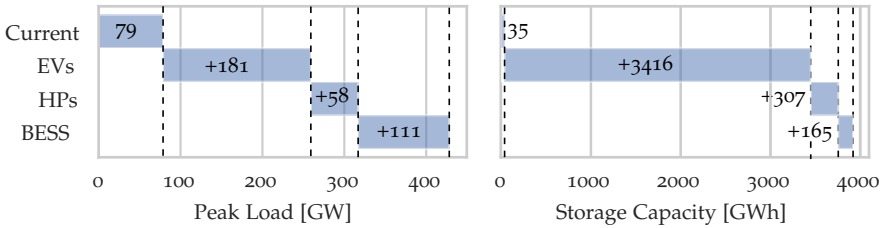


FIGURE 1.2: Peak load (left) and storage energy capacities (right) with a 100 % DERs penetration in Germany. The current values for peak load and storage capacity are obtained from [20] and [21].

With these technologies comes a massive increase in installed capacities at the lower grid levels but also in available storage. Figure 1.2 shows the increase in peak load (left) and storage energy capacity (right) for a 100 % penetration of EVs, HPs and BESS in Germany, i.e. all private vehicles (48.8 Mio.) are electrified<sup>1</sup> and all residential buildings (19.2 Mio.) own a HP and BESS<sup>2</sup>. The increase in peak load assumes a simultaneous operation of all units, which is unrealistic but still an interesting extreme case to consider. It shows that the newly installed capacities exceed the current peak load by more than fivefold. Similarly, the storage capacity of the decentralised flexibility options is not always available for load shifting and can therefore not be directly compared to existing large-scale storage capacities. The comparison still highlights that especially EVs introduce massive amounts of electrical storage into the system, which could be used to provide flexibility services. So, on one hand, EVs, HPs and BESS will increase the installed capacities, especially in lower grid levels, thus posing significant stress on the grids. On the other hand, they also introduce massive amounts of storage and flexible demand into the system, holding the potential to help integrate VRES if incentivised accordingly.

The EVs, HPs and BESS that are the focus of this PhD research are owned and operated by households. In contrast to larger flexible assets, like conventional power plants or large-scale storage units that directly interact with the market, these smaller assets are not yet incentivised to balance electricity supply and demand in the system. One possibility for using their flexibility are time-varying prices, but they also pose the danger of

<sup>1</sup> We assume a medium battery size of 70 kWh and slow charging at 3.7 kW chargers in this case.  
<sup>2</sup> The mean power capacities are assumed to be 3 kW [17] and 5.8 kW [18] and energy capacities of 16.0 kWh [19] and 8.6 kWh [18] for HPs with TES and BESS.

increasing simultaneities and peak loads in lower grid levels, requiring more grid reinforcement [22], [23]. Economic incentive systems, such as time-varying prices, should therefore try to find the right balance between the temporal flexibility needs of the whole system and the geographical flexibility needs of local distribution grids to achieve a system-friendly operation.

In summary, decentralised flexibility options, i.e. residential BESS, EVs and HPs, introduce large storage capacities into the system, thus holding the potential to provide flexibility. However, the available flexibility depends on the location and time, and consumer comfort should not be compromised. Under these considerations, it is not yet clear how much decentralised flexibility options can contribute to flexibility supply and how to accurately incentivise a system-friendly behaviour. This research contributes to overcoming these challenges by answering the following research questions:

- What is the flexibility need in a renewable German power system?
- What share of this flexibility need can be supplied by decentralised flexibility options?
- Which economic incentive systems are most suitable to stimulate a system-friendly operation of decentralised flexibility options?

It therefore develops models to quantify the temporal and geographical flexibility needs in future power systems with high shares of VRES. It furthermore investigates the influence of decentralised flexibility options on these flexibility needs. Lastly, different economic incentives are evaluated on their suitability to help integrate VRES and decentralised flexibility options.

## 1.2 THESIS OUTLINE AND CONTRIBUTIONS

This thesis investigates the contribution of decentralised flexibility in renewable power systems. It is divided into four parts, as visualised in Fig. 1.3. The first part focuses on *flexibility options*, i.e. technologies that can adapt their power output or consumption in response to an external signal. Furthermore, the *flexibility potential* of decentralised flexibility options is estimated, meaning the available range of power and energy values that the flexibility option can take. The second and third parts investigate the *geographical flexibility needs* in distribution grids and *temporal flexibility needs*

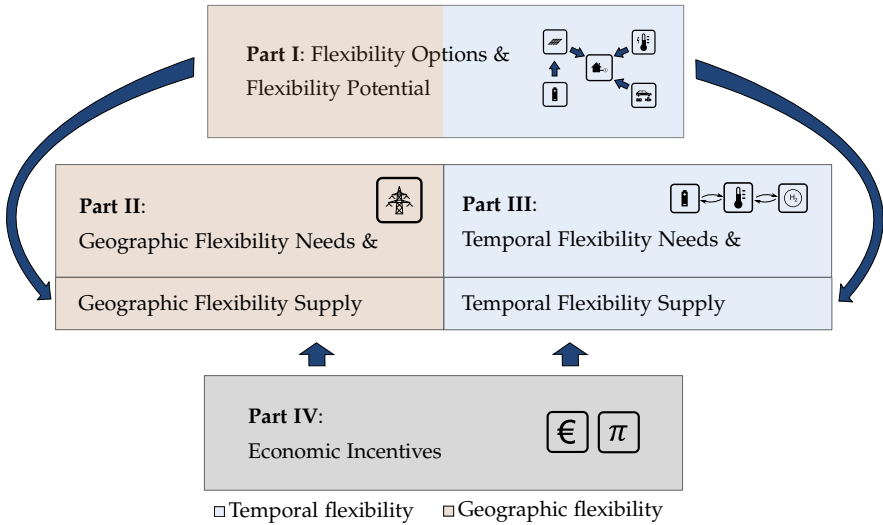


FIGURE 1.3: Structure of dissertation.

in the German national system. *Flexibility needs* arise from a mismatch of electricity generation and demand. These mismatches can occur in the *geographic* dimension, requiring transport capacities of electricity grids, and in the *temporal* dimension, requiring shifting of generation or demand in time. For both dimensions, it is investigated in how far an optimised operation of decentralised flexibility options can reduce the flexibility needs, in other words contribute to the *flexibility supply*. The last part investigates economic incentives to stir geographic and temporal flexibility supply and achieve a system-friendly operation of decentralised flexibility options. Furthermore, social and political implications are included in the final evaluation of the investigated incentives since these influence the practicability of the proposed measures.

All models and tools that were produced in the course of this PhD research are available open source for further use and refinement. They are introduced in the respective parts of the thesis, which are further detailed below.

### 1.2.1 *Part I: Flexibility Options and their Flexibility Potential*

Part one deals with the modelling of flexibility options and the estimation of their flexibility potential.

**Chapter 2** gives the theoretical background on the modelling of flexibility options and examines their representation in existing open energy modelling tools. Therefore, it introduces a new classification for flexibility and influencing factors and extracts and examines key factors of flexibility representation in the current modelling landscape. It furthermore provides an evaluation algorithm for decision support in choosing the right modelling tool for different research questions.

**Chapter 3** includes the chosen models and formulations for decentralised flexibility options used in this thesis, i.e. models for the sizing and operations of EVs, HPs and BESS. Furthermore, linearised models are provided for all investigated flexibility options. Such linear model formulations are important for studies with high geographic and temporal resolution, e.g. large-scale grid studies to investigate geographic flexibility needs.

In **Chapter 4**, the flexibility potential of decentralised flexibility options is estimated. The chosen concept accounts for the temporal availability and provides the mean available power and average flexible energy of the different flexibility options. It is used to approximate the flexibility potential for representative distribution grids and entire Germany for 100% penetration of decentralised flexibility options.

### 1.2.2 *Part II: Geographic Flexibility Needs in Distribution Grids*

Part two investigates geographic flexibility needs in distribution grids to incorporate increasing shares of renewable energy and sector coupling technologies, measured by curtailment and grid reinforcement needs. It furthermore assesses the potential of an optimised operation of decentralised flexibility options to decrease these geographical flexibility needs.

**Chapter 5** introduces the theoretical background and gives an overview of existing work. In **Chapter 6**, the optimal power flow formulation used in this thesis is introduced. The established model formulation is tractable for large-scale grid studies and allows the investigation of necessary curtailment and a grid-friendly operation that reduces the grid reinforcement needs. Such large-scale grid studies are required because of the distributed nature

of decentralised flexibility options, which are mainly introduced to the low voltage but also influence higher grid levels.

In **Chapters 7 and 8**, the model formulation is applied to investigate the reduction potential in geographical flexibility needs through an optimised operation of decentralised flexibility options in representative German distribution grids. **Chapter 7** focuses on EVs, which are complex to model since they can change locations and thus shift electricity demand in the temporal and geographic dimensions. The results of optimised charging are compared to rule-based charging strategies, and the influence of different levels of EV flexibility on geographic flexibility supply is investigated.

In **Chapter 8**, the investigations are expanded to a simultaneous integration of EVs, HPs and PV systems with and without BESS. The results provide mean reinforcement costs that can be used in large-scale energy system models to incorporate distribution grids. Furthermore, the potential to reduce reinforcement costs through an optimised operation is estimated. **Chapter 9** discusses the results and limitations, and **Chapter 10** presents conclusions drawn from this part of the thesis.

### 1.2.3 *Part III: Temporal Flexibility Needs in the National System*

Part three focuses on the temporal flexibility needs in a 100% renewable power system in Germany and investigates which influence and reduction potential decentralised flexibility options have on the flexibility needs.

**Chapter 11** summarises existing quantification methods for temporal flexibility. **Chapter 12** introduces a new linear optimisation model that quantifies energy shifting needs on different timescales. The main contribution is a basic model which allows the incorporation of existing model formulations of individual flexibility options to assess their influence on temporal flexibility needs on different time scales. This way, their contribution to the balance of supply and demand can be measured.

In **Chapter 13**, the model is applied to a 100% renewable power system in Germany to assess the influence of the generation mix and increasing shares of EVs, HPs and BESS on the temporal flexibility needs. Results and model formulation are discussed in **Chapter 14**, and conclusions are drawn in **Chapter 15**.

### 1.2.4 Part IV: Economic Incentives - Electricity Tariffs

Part four deals with the economic and social dimensions of flexibility supply from decentralised flexibility options, investigating the influence of electricity tariff structures on technical, economic and social aspects.

**Chapter 16** introduces the background and existing relevant work. **Chapter 17** investigates the economic incentives of different electricity tariffs and their influence on residential consumption profiles. The results allow a detailed comparison of different combinations of electricity prices and network tariffs and their effects on geographic and temporal flexibility.

**Chapter 18** introduces a two-stage process for evaluating tariff designs. The first stage comprises extracting the most important decision criteria and the second stage translating them into a coherent quantitative evaluation framework. The framework is then applied to the different combinations of electricity prices and network tariffs under increasing penetrations of DERs. It aims to provide a holistic and fact-based decision support by including social and political considerations in addition to technical and economic ones.

**Chapter 19** finally summarises and concludes the findings of this thesis and gives an outlook into future research directions.

## 1.3 LIST OF PUBLICATIONS

The following publications have reported the work presented in this dissertation:

1. **A. Heider**, R. Reibsch, P. Blechinger, A. Linke and G. Hug, *Flexibility options and their representation in open energy modelling tools*, Energy Strategy Reviews, Vol. 38, 2021, DOI: 10.1016/j.esr.2021.100737. ©2021 The Authors. Published by Elsevier Ltd.
2. **A. Heider**, K. Helfenbein, B. Schachler, T. Röpcke and G. Hug, *On the Integration of Electric Vehicles into German Distribution Grids through Smart Charging*, 2022 International Conference on Smart Energy Systems and Technologies (SEST), 2022, pp. 1-6, DOI: 10.1109/SEST53650.2022.9898464. Copyright ©2022, IEEE.
3. **A. Heider**, L. Kundert, B. Schachler and G. Hug, *Grid Reinforcement Costs with Increasing Penetrations of Distributed Energy Resources*,

- 2023 IEEE Belgrade PowerTech, Belgrade, Serbia, 2023, pp. 1-6, DOI: 10.1109/PowerTech55446.2023.10202913. Copyright ©2023, IEEE.
4. L. Kundert, **A. Heider** and G. Hug, *The Influence of Different Network Tariffs on Distribution Grid Reinforcement Costs*, 2023 IEEE Belgrade PowerTech, Belgrade, Serbia, 2023, pp. 1-6, DOI: 10.1109/PowerTech55446.2023.10202875. Copyright ©2023, IEEE.
  5. **A. Heider**, F. Moors and G. Hug, *The Influence of Smart Charging and V2G on the Flexibility Potential and Grid Expansion Needs of German Distribution Grids*, 2023 International Conference on Smart Energy Systems and Technologies (SEST), Mugla, Turkiye, 2023, pp. 1-6, DOI: 10.1109/SEST57387.2023.10257453. Copyright ©2023, IEEE.
  6. **A. Heider**, J. Huber, Y. Farhat, Y. Hertig and G. Hug, *How to choose a suitable network tariff? - Evaluating network tariffs under increasing integration of distributed energy resources*, Energy Policy, Vol. 188, 2024, DOI: 10.1016/j.enpol.2024.114050. ©2024 The Authors. Published by Elsevier Ltd.

Furthermore, parts of this dissertation are based on the following publications currently under review:

1. **A. Heider**, K. Helfenbein, B. Schachler, T. Röpcke and G. Hug, *On the Integration of Electric Vehicles into German Distribution Grids through Smart Charging*, submitted to Transactions on Industry Applications
2. **A. Heider**, F. Moors and G. Hug, *The Influence of Smart Charging and V2G on the Flexibility Potential and Grid Expansion Needs of German Distribution Grids*, submitted to Transactions on Industry Applications
3. **A. Heider**, M. Genena, B. Schachler, P. Blechinger and G. Hug, *Flexibility needs in a 100 % renewable German power system with growing shares of decentralised sector coupling technologies*, internal review for submission to Applied Energy

The following scientific publications have been published throughout the PhD but are not included in this dissertation:

1. B. Schachler, **A. Heider**, T. Röpcke, F. Reinke and C. Bakker, *Assessing the impacts of market-oriented electric vehicle charging on German distribution grids*, 5th E-Mobility Power System Integration Symposium (EMOB 2021), 2021, pp. 128-136, DOI: 10.1049/icp.2021.2515

2. L. Semmelmann, D. Schmid, S. Henni, **A. Heider**, B. Schachler and C. Weinhardt, *On the impact of heat pump installations and peak blocking strategies on grid expansion costs*, 2023 IEEE PES Innovative Smart Grid Technologies Europe (ISGT EUROPE), Grenoble, France, 2023, pp. 1-6, DOI: 10.1109/ISGTEUROPE56780.2023.10407931.

Additionally, the following non-scientific publications have been published during the PhD:

1. **A. Heider**, *Neue Technologie: Radikale Designänderungen für Systemstabilität*, Erneuerbare Energien, 2020, URL: <https://www.erneuerbareenergien.de/transformation/speicher/energiesystemwende-neue-technologie-radikale-designaenderungen-fuer-systemstabilitaet>
2. **A. Heider** and A. Krumm, *Die Bundestagswahl im Visier: Von der politischen Vision zum Fahrplan*, Erneuerbare Energien, 2020, URL: <https://www.erneuerbareenergien.de/energierecht/energiesystemwende-die-bundestagswahl-im-visier-von-der-politischen-vision-zum>
3. Reiner Lemoine Stiftung (2020): *Weichenstellungen ins Erneuerbare Energiesystem. Impulspapier zur EnergieSystemWende im Wahljahr 2021*, URL: [https://www.reiner-lemoine-stiftung.de/pdf/RLS\\_Impulspapier\\_Weichenstellungen\\_Ern\\_Energiesystem\\_Nov%202020\\_V2.pdf](https://www.reiner-lemoine-stiftung.de/pdf/RLS_Impulspapier_Weichenstellungen_Ern_Energiesystem_Nov%202020_V2.pdf)
4. Reiner Lemoine Stiftung (2022): *Leitplanken für die Gestaltung des Klimaneutralen Stromsystems. Erkenntnisse aus einer Expert\*innen-Umfrage.*, URL: [https://www.reiner-lemoine-stiftung.de/pdf/RLS\\_2022\\_Leitplanken\\_f\\_r\\_die\\_Gestaltung\\_des\\_Klimaneutralen\\_Stromsystems.pdf](https://www.reiner-lemoine-stiftung.de/pdf/RLS_2022_Leitplanken_f_r_die_Gestaltung_des_Klimaneutralen_Stromsystems.pdf)
5. **A. Heider**, R. Reibsch and B. Schachler, *Stromnetze in der Gaskrise - Der Einfluss von elektrischen Heizgeräten auf deutsche Verteilnetze*, Kurzstudie, 2022, URL: [https://www.reiner-lemoine-stiftung.de/pdf/Stromnetze\\_in\\_der\\_Gaskrise\\_Kurzstudie.pdf](https://www.reiner-lemoine-stiftung.de/pdf/Stromnetze_in_der_Gaskrise_Kurzstudie.pdf)

Lastly, the following student projects have been (co-)supervised during this PhD and partly contributed to its research:

1. François Nzale. *Cost-Optimized Mini-grid Design with Tree-Star Configuration*. Master Thesis, Power Systems Laboratory, ETH Zürich, 2020.
2. Hei Kern Leong. *Distribution Grid Flexibility Characterisation and Limits*. Semester Project, Power Systems Laboratory, ETH Zürich, 2021.

3. Benjamin Bossy. *Availability analysis of demand technologies for grid ancillary services*. Semester Project, Power Systems Laboratory, ETH Zürich, 2021.
4. Seraina Wurster. *Assessment of distribution grid extension costs with growing shares of electric vehicles*. Bachelor Thesis, Power Systems Laboratory, ETH Zürich, 2021.
5. Sebastian Tews. *Vergleich von synthetischen dingo-Netzen mit realen und synthetischen Netzen durch die Simulation von Speichern auf der Mittelspannungsebene*. Master Thesis, Fachgebiet Elektrische Energiespeichertechnik, Technische Universität Berlin, 2021.
6. Jill Huber. *Qualitative Analysis of Grid-Supportive Flexibility Procurement Methods*. Semester Project, Power Systems Laboratory, ETH Zürich, 2022
7. Mostafa Genena. *Flexibility quantification in distribution grids*. Semester Project, Power Systems Laboratory, ETH Zürich, 2022.  
(Contributed to Chapter 12)
8. Ladina Kundert. *The Influence of Residential Heat Pumps and Storage on Distribution Grid Extension Costs*. Semester Project, Power Systems Laboratory, ETH Zürich, 2022. (Contributed to Chapter 8)
9. Florian Moors. *The Influence of Smart Charging and V2G on the Flexibility Potential and Grid Expansion Needs of German Distribution Grids*. Master Thesis, Power Systems Laboratory, ETH Zürich, 2022.  
(Contributed to Chapter 7.2)
10. Jill Huber. *Evaluation Framework for Network Tariff Structures under Increased Integration of Distributed Energy Resources*. Master Thesis, Power Systems Laboratory, ETH Zürich, 2022. (Contributed to Chapter 18)
11. Marta Puiggròs Vilalta. *Flexibility potential of residential buildings for distribution grid services*. Master Thesis, Power Systems Laboratory, ETH Zürich, 2022.
12. Ladina Kundert. *Evaluating network tariffs as incentives for decentralised flexibility options*. Master Thesis, Power Systems Laboratory, ETH Zürich, 2022. (Contributed to Chapter 17)
13. Shipra Mohan. *Optimal Design of Decentralized Multi-energy Systems Considering Demand-Side Flexibilities*. Master Thesis, Power Systems Laboratory, ETH Zürich, 2022.

14. Maike Held. *Netzdienlich optimaler Einsatz von Flexibilitäten in radialen Verteilnetzen basierend auf einem AC-Lastflussmodell*. Master Thesis, Fachgebiet Energie- und Ressourcenmanagement, Technische Universität Berlin, 2023.
15. Julian Endres. *Evaluating load-balancing potential for the energy system provided through distribution grid flexibilities*. Master Thesis, Institut für Energietechnik, Technische Universität Berlin, 2023.

## Part I

# FLEXIBILITY OPTIONS AND THEIR FLEXIBILITY POTENTIAL



## REPRESENTATION IN OPEN ENERGY MODELLING TOOLS

---

*This chapter gives an introduction to flexibility options and their representation in existing open energy modelling tools. It is based on the published paper: A. Heider, R. Reibsch, P. Blechinger, A. Linke and G. Hug, "Flexibility options and their representation in open energy modelling tools", Energy Strategy Reviews, Vol. 38, 2021 [24]. ©2021 The Authors. Published by Elsevier Ltd.*

### 2.1 MOTIVATION

The decarbonisation of power supply systems is crucial for tackling climate change. For this reason, the international community has committed to ambitious goals for expanding renewable energy technologies within the Paris Agreement [25]. To achieve these goals, variable renewable energy sources (VRES) such as wind and photovoltaics (PV) must play a substantial role in the supply of electric energy in most countries [1].

The complexity of the energy supply system increases as the share of VRES grows. This increase in complexity is mainly due to three technological characteristics of VRES: variability, uncertainty and local distribution [3].

In conventional power systems, large-scale fossil-fuelled power plants provide dispatchable electricity to consumers, following a one-directional power flow from higher voltage levels to the distribution grid. By introducing VRES, uncertainty is added to the supply side, due to their varying output nature. In addition, we observe a much higher granularity of power plants following the introduction of small-scale decentralised VRES power plants. This leads not only to an increased challenge in controlling and operating the power plant fleet but also to bi-directional power flows in the grid. To keep the system stable and reliable, we must therefore add and use a broad range of flexibility options to balance supply and demand both geographically and temporally. In conclusion, flexibility is critical for designing and operating up to 100% renewable energy (RE) systems. It is

therefore essential for the planning and operation of future power systems to consider and study different flexibility options [1].

Since energy systems are highly complex, decision-makers rely heavily on the predictions of energy system models to find cost-optimal and sustainable future supply scenarios [26]. This affects different stakeholder groups from portfolio planners and power plant operators to grid operators and policymakers. The incorporation of flexibility into energy systems modelling is therefore a prerequisite for the proper modelling and simulation of high share RE systems. This can be achieved by accounting for operational constraints of supply-side technologies and adding new flexibility options such as strengthened grid networks, storage units and demand side management (DSM) to existing models.

However, there is no one-size-fits-all solution for including flexibility options in energy system models. Different research questions call for distinct modelling approaches. The evaluation of transient stability, for example, needs a tool with a high temporal resolution in the subsecond range and a realistic representation of the grid assets. Assessing investment decisions and long-term energy planning require a much lower temporal resolution because these models simulate years or even decades of the behaviour of future energy systems. In general, energy system modelling must strike a delicate balance between great technical detail and sufficient abstraction to make problems computable [26]. To achieve this, researchers and modellers have created a wide range of energy modelling tools covering various aspects and characteristics of energy systems.

A detailed overview of the existing modelling landscape is required when selecting the appropriate model to answer specific research questions. Various reviews and classifications have been introduced to provide such an overview [27]–[29]. However, there has not yet been an analysis of energy system models focusing specifically on flexibility representation. As the focus shifts towards high share VRES energy systems, it is crucial to understand the capabilities of existing energy system models (ESMs). Such understanding allows researchers to select appropriate energy system models for a specific representation of flexibility options and to identify aspects that are missing in existing models. In order to fill this research gap, we address the following open questions: What flexibility options exist, and how can they be categorised? How are the different dimensions and types of flexibility represented in open energy modelling tools? What recom-

mendations can be derived for future implementation of flexibility in open energy models?

In this study, we conduct a literature review to identify the key technologies and properties for modelling flexibility. Based on this review, we introduce a classification of flexibility in power systems and factors that influence the available flexibility. In the second step, we present a questionnaire that was sent out to identify the representation of these technologies and properties in current open energy system models. The results are examined for shortcomings and room for improvement in the representation of flexibility in the tools surveyed.

The chapter is structured as follows: **Section 2.2** summarises the existing literature on model overviews and classifications of flexibility. It also introduces a new classification of flexibility. **Section 2.3** describes the methodology we use to obtain the representation of flexibility and gives an overview on the models considered in the survey. **Section 2.4** presents the results, **Section 2.5** the discussion and **Section 2.6** the interpretation of the results.

## 2.2 BACKGROUND TO FLEXIBILITY OPTIONS AND ENERGY SYSTEM MODELS

Flexibility is the ability of a power system to adapt its operation to either foreseen or unforeseen changes in energy system behaviour, e.g. changes in network configuration, generation, or load according to local climate conditions, user needs, or network outage [30], [31]. The underlying principle is that supply and demand have to be balanced to allow for stable system operation. Many different options can enhance the flexibility of power systems so that high shares of VRES can be integrated. Lund et al. provide an extensive overview of such measures in [2]. To capture the representation of these options in modelling tools, it is necessary to identify all flexibility options and classify them into distinct categories.

A number of approaches exist to classify flexibility options. Table 2.1 summarises the classification schemes found in existing literature. All sources mention some variation of supply- and demand-side flexibility, storage and flexibility provided by the grid or its components. Most sources also mention sector coupling (SC) as another flexibility option. Aggregation concepts such as smart grids or exchange with neighbouring grid zones are mentioned as a possibility to increase the utilisation of available sources.

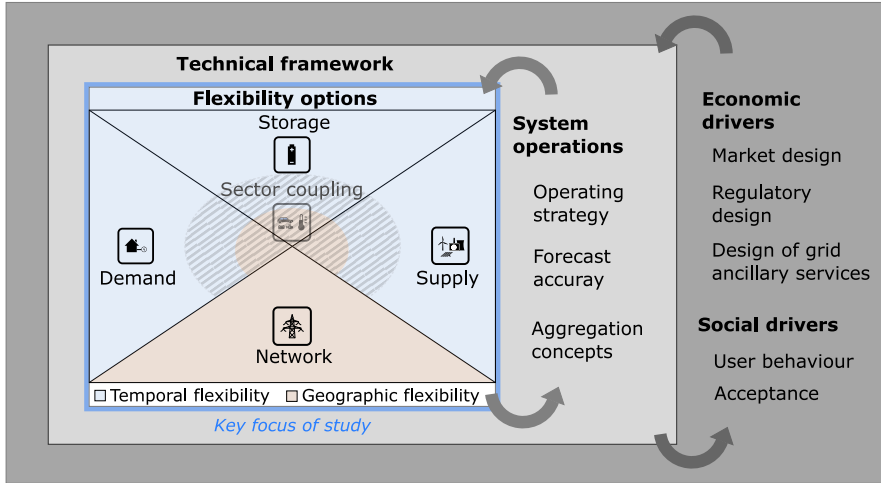


FIGURE 2.1: Classification of flexibility in energy systems

The influence of the operating strategy and forecast accuracy are mentioned less frequently. All of the papers examined also specify the market as a possibility to enhance power system flexibility. Other recurring factors are the design of ancillary services (AS) and regulatory design, such as grid codes.

The literature analysed provides a detailed overview of the different technical flexibility options. However, only one source introduces a hierarchy, putting the different types of options into relation with each other [36]. This interplay does not include all options, however. We therefore introduce a new classification scheme in an attempt to merge the above-mentioned approaches, relating technical flexibility and their operation with economic and social drivers and adding *temporal* and *geographical dimensions*. Figure 2.1 visualises the proposed classification. Temporal flexibility is the ability to alter the power input or output in time. This can be achieved by increasing or decreasing power generation or demand. Geographic flexibility is the ability to match supply and demand from different locations.

We call the technologies available in a power system, forming the basis of flexibility and therefore focus of the following investigations, *flexibility options*. These are further subdivided into five *flexibility categories*: supply side, demand side, storage, network and sector coupling. Flexibility options are restricted by technical constraints within their operation. We call these

TABLE 2.1: Overview of flexibility classifications

Source	Network	Supply	Demand	Storage	SC	Operations
[2]	x	x	x	x	x	o
[32]	x	x	x	x		x
[4]	o	x	x	x	(x)	o
[33]	x	x	x	x	o	
[34]	(x)	x	x	x		
[35]	x	x	x	x	o	
[36]	x	x	x	x	x	x
[37]	x	x	x	x	x	

Source	Aggregation	Forecasting	Regulations	Market	AS	Interplay
[2]	o	o	(o)	x	x	(o)
[32]	(x)	x	(x)	x	x	(o)
[4]	(x)			o	o	
[33]	x	o		x	x	x
[34]			x			x
[35]	o	x	o	o	x	o
[36]	o	(o)	o	x	(o)	x
[37]	x	(o)		x	(o)	

x - defined as own category; o - no own category, but mentioned in text;

(x/o) - only partly mentioned

constraints *operational characteristics*. Operational characteristics related to most of the flexibility options are efficiency, ramping, response and recovery time. Research questions addressing flexibility options and their optimal combination include: Will future power systems have sufficient flexibility to incorporate 100% renewable energy supply? What is the optimal mix of flexibility options in a highly decentralised future energy system? Which storage technologies are necessary to ensure system stability?

Traditionally, temporal flexibility has been provided by generation units. Supply-side flexibility options include fossil- or nuclear-based thermal generation or dispatchable renewable energy sources (RES). VRES can also provide temporal flexibility, e.g. by being controlled in curtailed operation and ramped up during peak demand or curtailed even further. Operational characteristics of the flexibility of generation units include minimum and maximum output, ramping constraints and minimum up and down time.

Another way to provide temporal flexibility is to include the demand side. This can be achieved using different mechanisms, such as the direct control of loads by the grid operator. Price incentives used to shift loads to periods of high power production are another possibility. Direct control has already been used in the case of industrial loads. Although price incentives and other control mechanisms for including households and the service sector have not been used widely, they have become an increasingly prominent topic of discussion in research [38]. The available flexibility of demand can be characterised by the maximum deferrable load, shifting time and recovery time after activation.

A third flexibility option - storage units - have the ability to shift load or supply over time. They can act as both supply and demand, being able to draw power from the grid, save it over time and feed it back later. The most commonly used power storage systems are pumped hydro storage (PHS). However, there are other storage technologies at different maturity levels, such as compressed air energy storage (CAES), flywheels, capacitors and a variety of battery technologies. The flexibility of storage units is influenced by their capacity, state-of-charge, self-discharge, efficiency and ageing.

Geographical flexibility is mainly provided by the network, i.e. transmission and distribution grids. Measures to increase geographical flexibility include grid extensions, interconnection to other power systems and dynamic

reconfiguration by switches. Limiting factors include the capacity of lines and transformers, as well as the current grid configuration.

Sector coupling introduces new technologies into the power system. These technologies represent a link to other energy sectors such as heat and transport. Connecting different sectors opens the possibility to use other energy storage and transport units. Viewing all flexibility options from a power system perspective, sector coupling elements may act like supply, demand and storage units. Power-to-X technologies and electric vehicles (EVs) can serve as both supply and demand technologies. Not only do sector coupling elements behave like more than one type of flexibility, but they also connect the temporal and geographic dimension. Fuels produced by power-to-X, for example, can be moved to other places before being converted back to power. The flexibility of sector coupling elements is dependent on the demand, infrastructure and flexibility of the connected sector; and it is restricted by operational characteristics of the transforming technology.

As stated in [39], technologies are not the only factors that influence energy systems. We therefore put the introduced technical flexibility options and their operation into relation with economic and social drivers. For the later analysis of the models, however, we focus on flexibility options as such as the basis of power system flexibility. Therefore, both system operations and economic and social drivers are considered only marginally in the further analysis. Nevertheless, they are briefly outlined below.

*System operations* do not include flexibility options as such, but describe the interplay and operations of the different players and technologies. It comprises how flexibility options are operated, which has a strong impact on the available flexibility. For example, the same battery storage can provide up and down regulation if operated at around 50% of its capacity, whereas it can only provide up regulation when kept at full charging level to increase supply security. These aspects include unit commitment or reserve procurement as well as improving the forecast quality of supply and demand as a measure to decrease the need for flexibility and increase flexibility supply [2]. Another concept attributed to system operations and able to make flexibility options available to the system are smart grids. This concept includes the intelligent monitoring, protection and optimisation of grid resources at all voltage levels [40]. It poses an alternative to conventional central grid planning with focus on grid reinforcement by expanding on distributed resources [41] and including storage and demand response.

New aggregation concepts such as virtual power plants (VPPs), microgrids and energy cells also fall into this category. VPPs and microgrids both enable the inclusion of distributed energy resources (DERs) [42]. Microgrids often allow an operation in islanded mode and include the grid and its components in a limited geographical area. They furthermore utilise hardware innovations such as smart inverters or switches [42]. VPPs on the contrary can include components in a large geographical area and combine these providing access to wholesale markets for smaller units. They depend more on smart metering and information and communication technology and already find application in the current system [42]. The idea of energy cells or so-called system-of-systems approach allows for a complexity reduction to reduce the operation of the system to a manageable problem size in times of increasing complexity [43].

Questions relevant to system operations include: How does bidding behaviour influence reserves? How much additional flexibility can aggregators provide? What is the optimal size of independently operating energy cells in a connected cellular system?

Overlaying drivers that influence system operations and therefore the availability of flexibility are *economic* and *social* ones. Economic drivers cover the system design, including the market, AS and regulations. Measures to create greater flexibility through economic drivers include shortening the trading and reserve procurement time horizons [34], location-specific pricing, integrating electricity markets [2], designing additional regulation reserves and flexible ramping products [33]. Research questions associated with these economic drivers include: What are the optimal procurement time horizons? Is it necessary to create an additional market for flexibility? Do we need different ancillary services in a system based on renewable energy?

Social drivers become increasingly important through the deployment of DERs as assets of private persons are added to the mix. User behaviour and acceptance therefore influence the amount of available flexibility. Social barriers for the deployment of flexibility are mainly behavioural aspects such as imperfect information, credibility and trust, bounded rationality, social inertia and personal values other than economic maximisation [43]. Research questions addressing social drivers are: How do user preferences influence the available flexibility of EVs? Which incentive structures are the most promising to increase user participation and acceptance in local flexibility markets?

Energy system modelling is a valuable tool for answering some of these questions. It was found that the optimal tool depends heavily on the specific research questions and the objectives required to answer them [44], [45]. It is therefore crucial to specifically assess the representation of flexibility options in models in order to evaluate their suitability to answer questions concerning power system flexibility.

Several papers and other sources provide an overview of the existing modelling landscape in energy system modelling [26], [29], [44]–[50]. Rinkjøb et al., for example, give a good overview of 75 models, general model characteristics, and technological and economic parameters, including the modelled markets [48]. Although they do not mention specific models, Deng and Lv evaluate the changes in model formulation owing to the incorporation of renewables [51]. They highlight the growing importance of short-term system operation, transmission constraints, storage units and demand-side response in the models. The authors of [52] focus on social aspects in energy system models and frameworks and find that these factors are mainly included through exogenous assumptions or in the discussion of results. They state that approaches exist such as agent-based modelling which allow for a better representation of social factors and behavioural aspects but there is still room for improvement within the examined models. Many of the energy system models and frameworks are under continuous development and evolve as new questions and energy policy challenges arise. Review papers can therefore only give a snapshot of the modelling landscape at the time of the study. To deliver continuous and up-to-date information on different modelling tools, the OPEN ENERGY PLATFORM provides factsheets on 132 models and frameworks used for energy system modelling [53]. The online list provided by the OPENMOD INITIATIVE, specifying 50 open source models and frameworks, has a similar purpose [54].

Considering the representation of flexibility in different models, single aspects were found to be missing [49] or posing a major challenge for energy system modelling [48], [51]. To the best of our knowledge, however, there has not yet been a systematic analysis of energy system models for the purpose of understanding their representation of flexibility options, which is why we address this in our study.

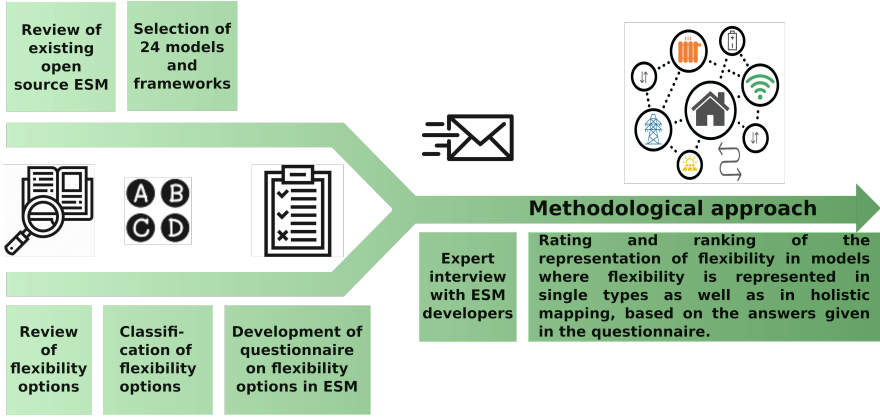


FIGURE 2.2: Methodological approach

## 2.3 RESEARCH DESIGN

The methodological approach of this study, shown in Figure 2.2, is divided into three main parts. The first part involved selecting the models under analysis. In the second part, we developed a questionnaire to evaluate the representation of flexibility options in energy system modelling, based on the classification introduced in Section 2.2. In the third part, we evaluated the models under examination to assess the representation of flexibility in the single categories and from a holistic perspective.

### 2.3.1 Model selection

Various open energy system modelling tools and frameworks exist, as described in the previous section. In the context of this study, we made a final selection of 24 models and frameworks<sup>1</sup>.

In the literature, balancing uncertainty and transparency is mentioned as one of the major challenges in energy systems modelling [26], and authors have suggested learning from the open source community. Later, the importance of opening up energy system models to increase the transparency and quality of research was stressed [55]. In recent model development,

<sup>1</sup> From now on, we denote models and frameworks together as models, since the differentiation between a model and a framework is of no importance for the examination of flexibility options.

there has been a recognisable trend towards open source and open access in energy system modelling [29], [56] and the maturity of open source energy models has been demonstrated [50]. For these reasons, our study focuses on open source modelling tools.

We preselected models based on the ESM review specified in Table 2.1, the OPEN ENERGY PLATFORM [53] and the OPENMOD INITIATIVE [54]. These sources were combined with a review of the classification of flexibility types, which was described in further detail in Section 2.2.

To reach out to a broad audience of open source model users and developers, we presented the research goal and questionnaire at a workshop hosted by the OPENMOD INITIATIVE, and sent an appropriate request to model developers in the OPENMOD forum and via its mailing list. The final selection of models was then made by the developers who responded to the request and were willing to complete the questionnaire. In addition, the developers of models that were interesting in terms of flexibility options were contacted directly and asked to complete the questionnaire (e.g. REGION4FLEX).

Finally, we collected data from 24 models (including six frameworks). The majority of these models classify themselves as ESMs, while the others are called electricity or power system models. Rinkj b mentions in [48] that, as a rule, energy models were not actively used before the 2010s. This is also reflected in our model selection, given that 19 of the 24 models were published after 2010. The oldest models - BALMOREL, ENERGYPLAN and OSEMOsYS - were developed in the early 2000s. This shows that holistic energy system modelling is relatively new and in constant evolution. We selected both widely used models and niche models. To identify how widely the models have been used, we determined the number of citations of their first scientific reference. Models such as TIMES, OSEMOsYS, EMMA, ENERGYPLAN, PANDAPOWER and PyPSA yield more than 100 citations, while GRIDCAL, XEONA or OMEGALPES are cited only a few times.

Appendix A.1 contains a list of all the models and frameworks surveyed, a brief description of the models and the modelling language on which they are based. The overview shows that more than half of the models considered are based on the general-purpose programming language PYTHON and about a quarter on the algebraic modelling language GAMS.

### 2.3.2 *Questionnaire with classification of flexibility*

As mentioned in Section 2.2, flexibility is becoming crucial when it comes to planning and designing of the future energy supply structures. In this context, it is important not only to focus on a few flexibility options, but also to consider different social and economic drivers and options with regard to supply, demand, storage, sector coupling, and the network (see all drivers and options in Figure 2.1). We call the integrated assessment of these different categories a holistic approach. To pursue this holistic approach, we derived the following evaluation categories: general characteristics, supply, network, storage, demand, and sector coupling. These categories provided the structure of our questionnaire<sup>2</sup>.

The first section of the questionnaire was dedicated to the general part which covers general model characteristics, such as temporal and geographic scope and aspects regarding social and economic drivers. The second part of the questionnaire focused on the technical operational characteristics of several flexibility options, such as efficiency, ramping rate, response and recovery time. In the third part of the questionnaire, we asked about other specifications concerning flexibility options that are connected to a specific category such as whether or not a minimum load is implemented in conventional power plants. The fourth and final part of the questionnaire focused on the representation of specific technologies in an effort to determine whether the model is general enough such that these technologies can be represented or whether the model already has its own specific representation. All the specific supply-side, demand-side, storage and network-related technologies were listed in this section.

Developers of open energy system models<sup>3</sup> were sent the questionnaire and asked to complete it. The flexibility options surveyed are discussed in more detail in the next subsection, where we evaluated the single categories and combined them to create a holistic flexibility approach.

### 2.3.3 *Model evaluation*

The methodology applied in this work aims to provide an initial evaluation to simplify the choice of an appropriate open energy model. It assesses

<sup>2</sup> The survey at full length is available in the appendix of the original publication [24].

<sup>3</sup> The questionnaire for IRENA FLEXTOL was completed by the authors because the developers did not respond to our request.

the level of modelling detail for each flexibility category, and outlines the suitability of the models for modelling energy or power systems using a holistic approach. This was realised by rating the models, as summarised in Table 2.3. For each answer in the questionnaire, a specific rating was given depending on its importance in the representation of flexibility.

The first part of the evaluation focused on general parameters such as the spatial and temporal scope, the temporal resolution, the decision-making process implemented and the representation of probabilistic behaviour and social factors.

The second part surveyed the technical parameters concerning several flexibility options. The operational characteristics that were relevant for all flexibility categories included efficiency, ramping, the response time and the recovery time after activation. The parameters relevant to the network were grid representation and the modelling of the import and export of energy. Another part of the evaluation addressed technology-specific parameters that influence flexibility. The parameters describing conventional power plants were minimum load and discrete power plant capacity expansion as well as those concerning variable renewable energies such as curtailed operation. Furthermore, the demand side was evaluated in terms of the implementation of maximum deferrable load, shifting time and price elasticity. Finally, this part also questioned whether and how storage, its ageing and self-discharge are implemented.

There are different types of ratings as shown in Table 2.3. Some parameters, such as temporal and geographic scope, are rated without any hierarchy, meaning that every ticked box counts as one point. Other factors, such as the representation of technology, are rated such that one option is preferable to another, resulting in a higher rating. As an example, predefined technologies score a whole point, whereas the possibility to implement that technology earns only half a point. Some parameters, such as decision-making, are evaluated by means of more complex functions. All detailed ratings can be found in Appendix A.2. To render the models comparable, the detailed ratings were added together by

$$rating_{model} = \frac{\sum_{i \in \mathbb{N}} rating_{model,i}}{n},$$

where  $n$  is the number of parameters.

TABLE 2.3: Model evaluation overview

Category		Content	Rating
General		Geographic scope, temporal scope, temporal resolution, probabilistic behaviour, social factors	All possibilities equally weighted or yes \ no
		Decision making	Descending from decision-/ agent-based to perfect foresight
Supply	Technologies	Conventional, dispatchable RES, VRES, fuel cells	Predefined 1 \ possible 0.5
	Detailed characteristics	Technology specifications, operational characteristics, discrete expansion	All possibilities equally weighted
Demand	Technologies	Household, industry, service	Predefined 1 \ possible 0.5
	Detailed characteristics	Technology specifications, operational characteristics, price elasticity	All possibilities equally weighted
Network	Technologies	Grid types, topology	Predefined 1 \ possible 0.5
	Detailed characteristics	Grid representation, import \ export, ancillary services	Mainly individual rating (see Table A.2 in Appendix)
Storage	Technologies	Long-term, medium-term, short-term	Predefined 1 \ possible 0.5
	Detailed characteristics	Technology specifications, operational characteristics, storage implementation	Mostly yes \ -no, sometimes individual rating (e.g. ageing)

*Continued on next page*

TABLE 2.3 – *Continued from previous page*

Category		Content	Rating
Sector Coupling	Technologies	Supply technology, demand technology, storage technology	Predefined 1 \ possible 0.5
	Detailed characteristics	Technology specifications, operational characteristics, sector representation	Individual rating for technology specifications and sector representation

## 2.4 RESULTS

The following section presents the results of the analysis. First, **Section 2.4.1** provides insights into the outcomes with regard to the general model characteristics. Second, **Section 2.4.2** gives an overview of the representation of the individual flexibility categories and the coverage of their technical characteristics. Finally, **Section 2.4.3** presents a holistic assessment of the models.

### 2.4.1 *General model characteristics*

Although general model characteristics are not considered to be flexibility options, they influence the representation of those options nonetheless. In this research, as mentioned above, the general model characteristics under evaluation are spatial and temporal scopes, temporal resolution, decision-making, social factors and probabilistic aspects.

Figure 2.3 shows how many models cover each spatial and temporal scope and resolution. The upper left plot shows that most models cover all spatial scopes. In approximately half of all models examined, a local, regional or international scope is usually used. It is striking that the national scope is usually used in almost 80 % of the models.

Other spatial scopes are possible or predefined by the model in nearly 50 % of cases. These scopes are based on the power grid levels, for example, or the area of a medium-voltage grid. Some of the models also allow for a continental or an arbitrary scope.

The upper right plot shows how many models cover each temporal scope. A period between days and years can be simulated in all the models under examination. This scenario period is usually used in more than 90 % of the models. Fewer models are able to simulate short-time scales for periods of less than a few days. Approximately 25 % of the models allow for the application in another temporal scope. In most of these models, the input data determine the temporal scope.

The bottom plot illustrates how many models cover each temporal resolution. Hourly resolution is the most common resolution in approximately 80 % of the models making it the most widely used resolution. Resolutions larger or smaller than one hour are usually used by around 30 % of the

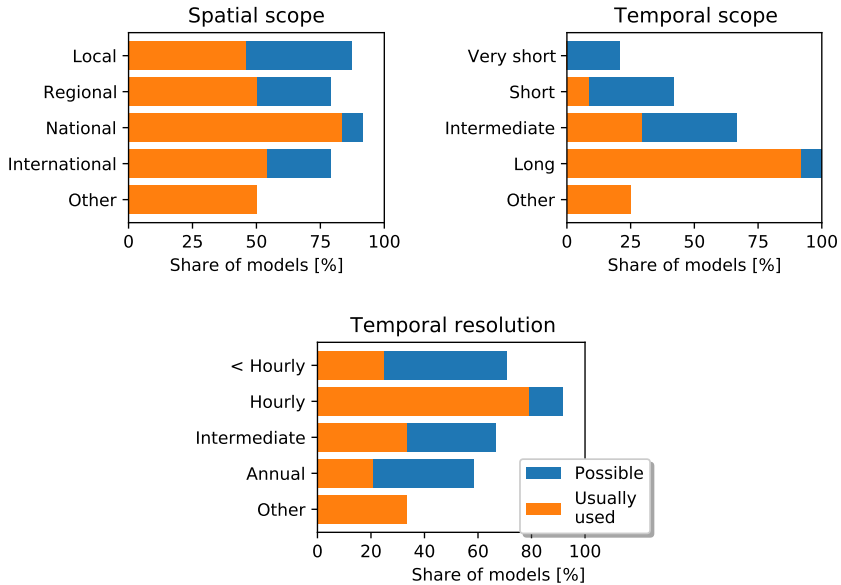


FIGURE 2.3: Representation of geographical scope (upper left), temporal scope (upper right) and temporal resolution (bottom)

models. In addition, a resolution of more than one hour or less than one hour is possible in a further 30 % of models.

Regarding decision-making processes, 80 % of the models can make decisions according to perfect foresight. Other decision-making processes such as the rolling horizon and the agent-based process are represented less frequently, in approximately 35 % and 15 % of the models. Detailed information is depicted in the Appendix in Figure A.1.

A probabilistic behaviour is implemented in less than 25 % of the models under investigation. Those models that are able to represent probabilistic behaviour often use Monte Carlo analysis, as well as other methods. Detailed information is depicted in the Appendix in Figure A.1.

Just over 20 % of the models include social factors. These factors refer mainly to economic parameters, such as taxes and costs, or user preferences. The questionnaire did not ask which social factors are mapped in which way

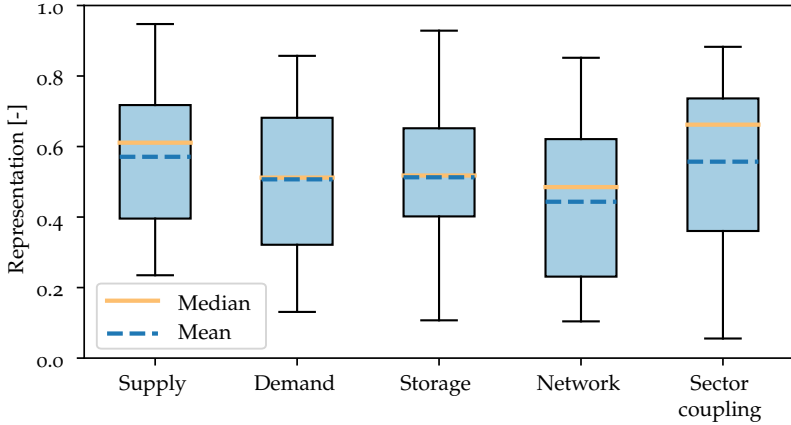


FIGURE 2.4: Representation of flexibility categories

and to what extent. Nevertheless, the results reveal that social factors are not implemented in most models and are therefore underrepresented.

#### 2.4.2 Flexibility categories

Figure 2.4 illustrates how well, based on our defined parameters and level of potential detail, each flexibility category is represented within the models under examination. The figure reveals that, on average, the flexibility of sector coupling is the category for which most models score in many of the questioned aspects. The majority of models reach a level of representation exceeding 65%. Considering that sector coupling is a relatively new field, this appears remarkable. In the supply category, approximately half of the models achieve a representation of more than 60%. On average, demand and storage are equally well represented. More than half of the models achieve a degree of representation of more than 50% in each category. However, both two categories have a wide range of representation. Furthermore, the results show that networks tend to be represented less well than the other categories, which may be because networks are often represented in a simplified way. The following subsections provide a detailed assessment of the flexibility categories. In these subsections, with the exception of the network representing non-temporal flexibility, operational characteristics comprise four elements: efficiency, ramping, response time and recovery time. The detailed operational characteristics are listed in Table A.2. The

reader should be aware that the level of fulfilment for all of these categories is also dependent on the type and level of questioned aspects. Hence, the comparison between categories for a specific model only has an informative value.

### *Supply*

Figure 2.5 gives insights into the representation of the supply side. Most models are able to represent the majority of supply-side technologies. However, there are differences in the level of representation in these technologies. Conventional technologies, such as fossil fuel-based generation and nuclear power, and dispatchable renewable supply technologies, such as bioenergy and hydro power (reservoir and run-of-river), can be implemented in 90 % to 100 % of the models under examination, and are predefined in roughly half of them. Variable PV, onshore and offshore wind technologies can also be implemented in almost all the models and are predefined in nearly 60 % of them. Geothermal, concentrated solar power, fuel cell technologies, and wave and tidal power are not as well represented in the models. While in the majority of models it is possible to implement these technologies, less than a fifth of them have predefined classes. Only ENERGYPLAN models dispatchable and variable renewable energy sources with the highest degree of representation with respect to the considered aspects.

Technology specifications comprise the minimum load of conventional power plants and curtailed operation as a specification of VRES. The minimum load is implemented in almost 80 % of the models. Curtailed operation is possible in nearly 50 % of them. Fewer than 40 % of the models enable a discrete power plant expansion.

The five models with the highest degree of representation (TRANSIENT, DISPA-SET, CALLIOPE, PYPSA, DIETER) are strong in conventional generation technologies and technology specifications compared to all the other models. In particular, with regard to technology specifications, all five models represent ramping, minimum load, and curtailed operation of RES. However, not only conventional energy sources have predefined classes in these models; commonly used RES such as bioenergy, hydro energy, photovoltaic and wind energy also show high levels of representation.

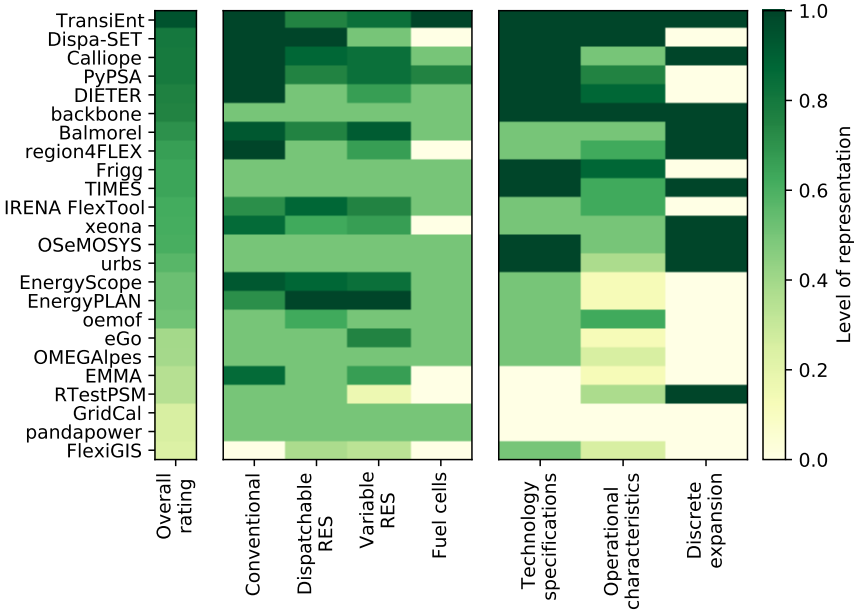


FIGURE 2.5: Representation of supply side technologies (left) and other specifications (right)

*Demand*

Figure 2.6 provides an overview of the representation of the demand side. Although 70 to 85 % of the models are able to represent individual load sectors such as households, services and industry, only around a quarter of them have predefined classes of the load sectors under examination. Households tend to be best represented, followed by the industrial sector and then the service sector.

Technology specifications include the possibility to determine a maximum deferrable load (MDL). This deferrable load can either be defined according to the time of day when the load can be shifted (time-dependent) or according to different load types with regard to technologies or load sectors, such as households, industry and the service sector (type-dependent). A deferrable load has the highest degree of representation if it can be mapped in both a time-dependent and type-dependent manner. More than 40 % of the models are able to define both time-dependent and type-dependent

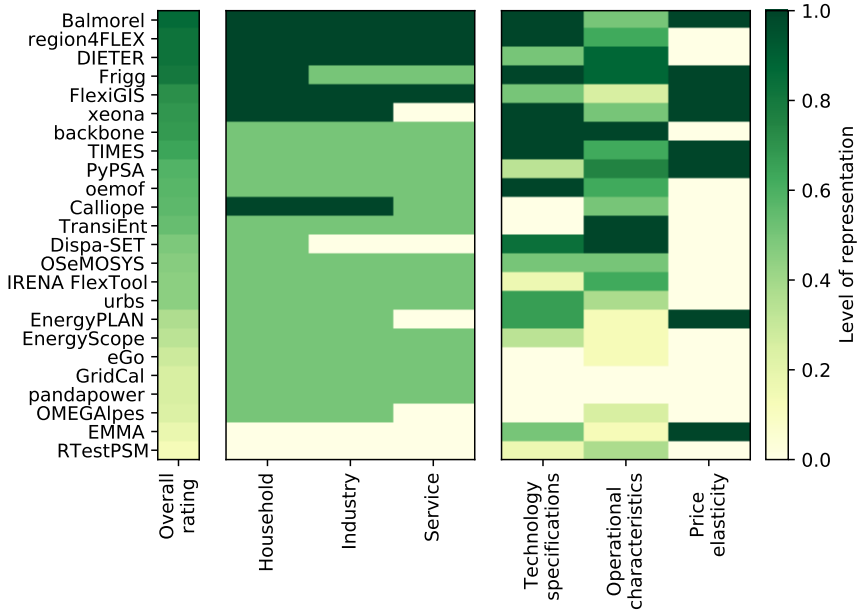


FIGURE 2.6: Representation of demand side technologies (left) and other specifications (right)

MDL. Around 15 % of the models can only map a time-dependent change of MDL; no MDL is implemented in further 15 % of the models.

All five models that score the highest in the area of demand based on our evaluation (BALMOREL, REGION4FLEX, DIETER, FRIGG, FLEXIGIS) are able to represent time-dependent and type-dependent deferrable loads. This is an essential requirement for representing flexible loads in a renewable energy system. In addition, these five models have predefined classes or methods for household loads. The service and industry sectors are also predefined in four of the five models. Also, all five models can map the efficiency of demand technologies. However, other operational characteristics, such as ramping, response time and recovery time, are implemented in only three of the five models. These operational properties are represented by only three models at the highest complexity level. These three models (BACKBONE, TRANSIENT, DISPA-SET) are not among the five highest-rated models in this category.

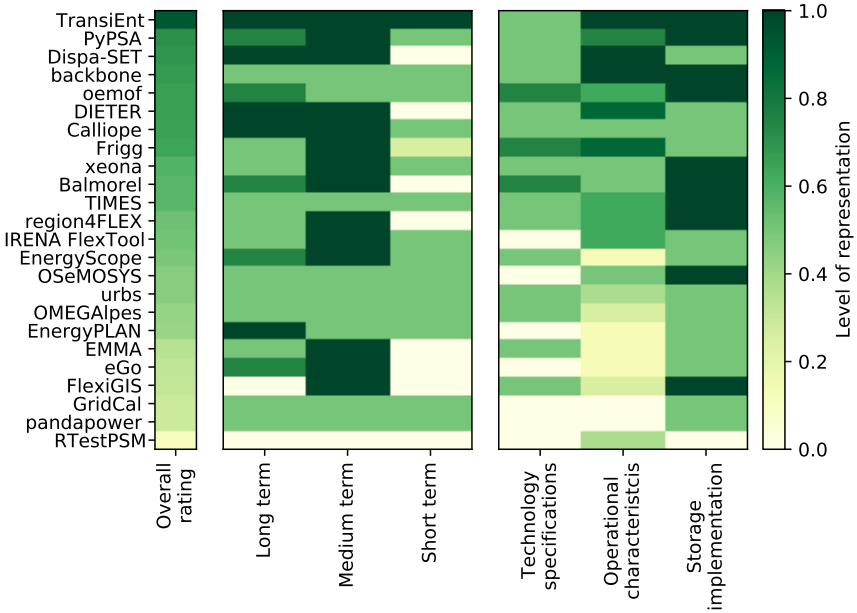


FIGURE 2.7: Representation of storage technologies (left) and other specifications (right)

### Storage

Figure 2.7 illustrates the representation of storage technologies and their characteristics in the various models. Among the storage technologies examined, capacitors and flywheels are considered to be short-term storage units. Batteries are categorised under medium-term storage technologies, whereas PHS and CAES are classified as long-term storage technologies.

Batteries tend to be best represented among all storage technologies related to the power sector, followed by PHS and CAES. Capacitors and flywheels are represented less frequently than the other technologies; only TRANSIENT has predefined classes for them.

Technology specifications in storage technologies comprise cycle and calendrical ageing, and self-discharge. Almost 80 % of the models do not cover storage ageing, while more than 15 % take calendrical ageing into account.

Only TIMES has implemented cycle ageing. Nearly 70 % of the models consider self-discharge over time.

Storage specifications describe how complex storage units are implemented. Storage units can either be modelled in a simplified static way or dynamically, e.g. considering a temperature-dependent efficiency or a seasonally varying storage capacity. Concerning these storage specifications, the results show that nearly 55 % of the models represent storage units with a fixed/simplified model, whereas more than 40 % are able to model storage units dynamically, e.g. with regard to efficiency dependent on temperature or seasonally varying storage capacity. One model has not implemented any storage technologies.

Among the five highest-rated models (TRANSIENT, PYPSA, DISPA-SET, BACKBONE, OEMOF) in the category of storage, only TRANSIENT has predefined classes or methods for all storage technologies under consideration. Long-term and medium-term storage technologies can be implemented in the other four models. Among the five models, short-term storage technologies are represented the worst. Furthermore, neither calendrical nor cycle ageing is implemented in four of the five models. Calendrical ageing is only specified in OEMOF.

### *Network*

Figure 2.8 illustrates how network-related technologies are mapped in the models under examination. Among the grid types, distribution grids are represented worse than transmission grids. Around 45 % of the models contain predefined transmission grids. Approximately 25 % of the models feature predefined classes or methods for distribution grids.

Grid topology includes properties such as automated network extension and the use of switches. The results reveal that grid extension is implemented in almost 35 % of the models. Switches are represented the least.

Grid representation refers to the method by which networks are represented electrically. Networks can be represented by a net transfer capacity or by power flow in alternating current (AC) networks (AC power flow) or as a direct current (DC) power flow approximation. DC power flow and transfer capacity can be used in less than 60 % and 45 % of the models, respectively. AC power flow is only represented in less than 40 % of the models.

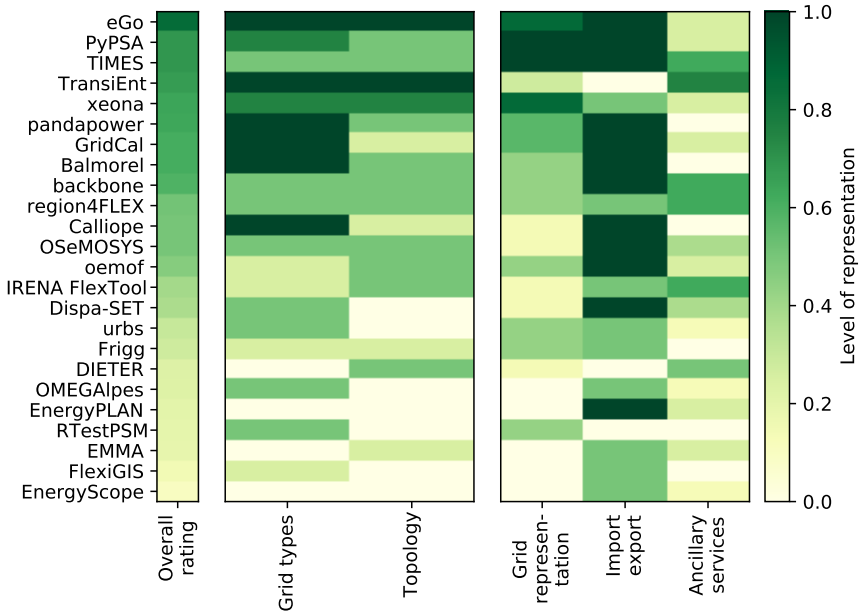


FIGURE 2.8: Representation of network side technologies (left) and other specifications (right)

Almost 55 % of the models enable the modelling of the import and export of power using a simplified method. Furthermore, the representation of import and export is flow-based in 45 % of the models. Approximately 10 % of these models facilitate the modelling of import and export using a simplified or a flow-based method. Less than 10 % of the models do not include import/export modelling. Just under 20 % of the models are based on other import/export methods; these refer, for instance, to representation by means of cost functions.

Ancillary services such as spinning reserve, balancing energy, sheddable loads, feed-in management, and curtailment of variable renewable energy technologies are represented in 20 % to 45 % of the models. In contrast, re-dispatch and power factor correction are represented in less than 20 % of them. All models still have room for improvement regarding ancillary services, e.g. none of them consider black start capability.

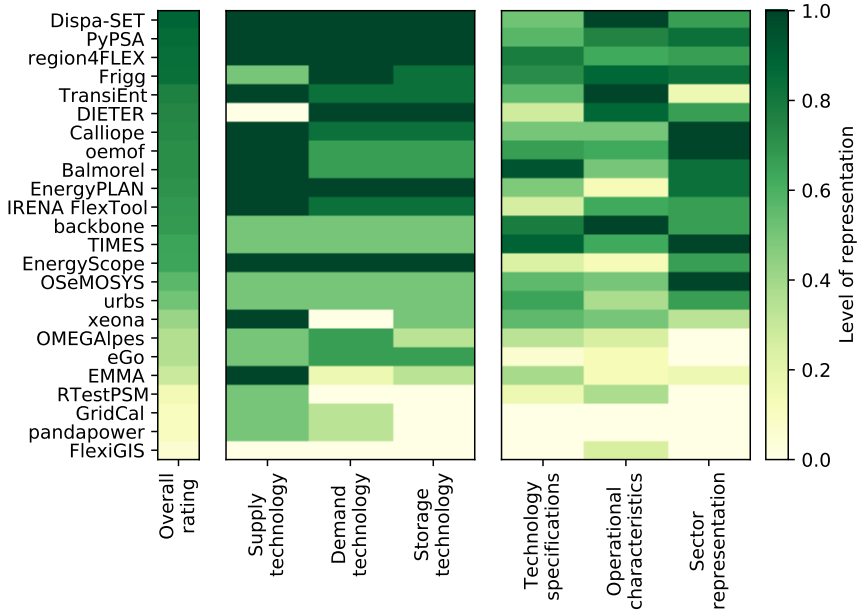


FIGURE 2.9: Representation of sector coupling technologies (left) and other specifications (right)

TRANSIENT has the largest variety of ancillary services (spinning reserve, balancing energy, sheddable loads, feed-in management, power factor correction, and curtailment). The five highest-rated models achieve a significant degree of representation because most of them cover both distribution and transmission grids, and are able to represent both AC and DC power flow.

### *Sector coupling*

Sector coupling is a cross-sectional issue in relation to the other categories. Figure 2.9 shows that sector coupling is generally well represented, particularly given that it is a relatively new area, especially when it comes to representing sector coupling supply, demand, and storage technologies.

Sector-coupled supply includes only combined heat and power (CHP) because it is capable of producing both heat and electricity. While fuel cells are

also capable of using waste heat, their primary goal is to generate electricity. As such, they have already been discussed in Section 2.4.2. Most models are capable of representing CHP. This corresponds to the previous conclusion that supply-side technologies are generally well represented.

Demand-side technologies include power-to-gas, heat pumps, and EV. Despite the fact that these are relatively new technologies, a considerable number of models are capable of representing them. In particular, the three best-rated models can represent sector-coupled demand at the highest level of complexity, as defined in the evaluation scheme employed.

Sector coupling storage technologies include fuels, heat storage, and vehicle-to-grid (V2G). A large number of models are able to represent one or more of these storage technologies.

Sector representation refers to how well heat and transport sectors are represented in terms of exogenous aggregated demand or endogenous disaggregated choices for demand or technologies. The results reveal that the heat sector is better covered than the mobility sector, which is neglected in almost 60 % of the models. In contrast, around 40 % of the models do not cover the heat sector.

Technology specifications include how technologies are implemented. These specifications, corresponding to those mentioned above under supply, demand and storage, include discrete expansion, curtailment for supply technologies, ageing for storage technologies and other specifications. These specifications do not reach the degree of representation that the technologies themselves achieve. Furthermore, no model meets the highest degree of representation in this area.

Among the five highest-scoring models in the sector coupling domain, DISPA-SET, PyPSA and REGION4FLEX feature the highest level of modelling details in representing sector coupling technologies. ENERGYPLAN and ENERGYScope also achieve the highest level of modelling details in sector coupling technologies.

### 2.4.3 *Holistic approach*

As mentioned in Section 2.2, flexibility is becoming crucial when it comes to planning and designing future energy supply structures. In this context, it is important not only to focus on a few flexibility options, but also to consider different options of supply, demand, storage, sector coupling,

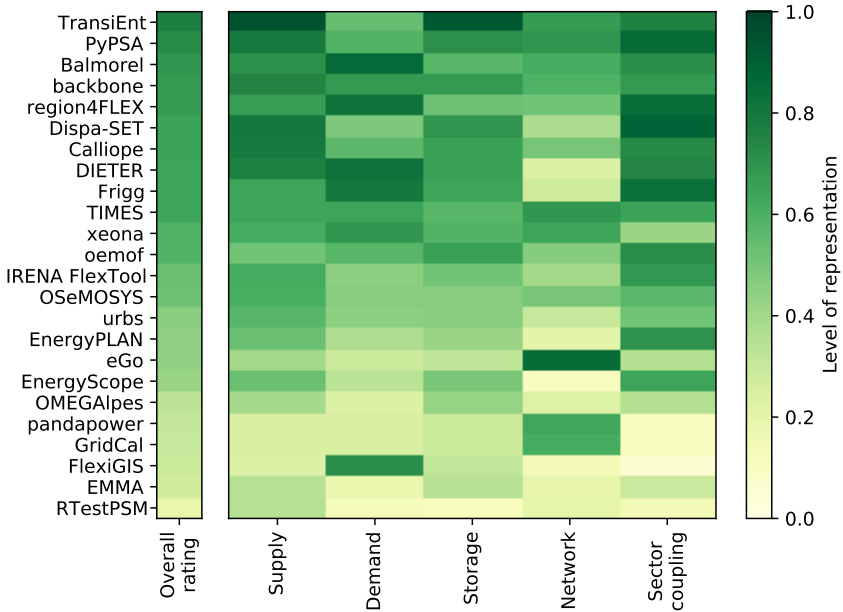


FIGURE 2.10: Holistic representation of all flexibility categories

and network. The following section shows the extent to which the models surveyed models represent a holistic approach to flexibility.

Figure 2.10 provides an overview of the ranking of the models under examination in the relevant categories, as defined in our evaluation scheme. Many models are powerful in individual categories but perform only moderately in others. TANSIENT, for instance, appears to be the most potent model. This model has a very high degree of representation with regard to supply and storage, while many other models perform better when it comes to demand. EMMA, for instance, achieves a high level of representation in the demand category compared to other categories. The same applies to eGo, PANDAPOWER and GRIDCAL, which exhibit an above-average performance in the network, but fare less well in the other categories. In the field of sector coupling, some models consider a wide range of sector coupling aspects. Other models, on the other hand, focus specifically on the electricity sector and only rarely consider elements related to the heating and transport sector. Many models map individual categories very well. Among the mod-

els that achieve a high degree of representation in a certain category, the representation is often over 80 %.

The results summarised in the previous section also show that many operational characteristics are not well represented. This may be because many models use perfect foresight, and therefore several operational parameters, such as ramp rate or response time, are neglected. Since the economic and social drivers were not specifically part of the questionnaire, it is difficult to draw conclusions on these aspects. It appears, however, that models such as EMMA and BALMOREL address economic drivers, given that they are market models. Economic aspects are implicitly included in other models via price structures or investment decisions.

However, the results also reveal that a wide range of models exists that are strong in specific areas and weaker in others, depending on the focus of the model. When selecting a model to answer a specific research question, the strengths and weaknesses of each model should be considered.

The question remains as to the extent to which the models feature a holistic approach to flexibility options. To this end, a threshold value was chosen that is slightly above the highest median of the individual categories. The sector coupling category exhibits the highest median (almost 70 %). For this reason, all models with a representation above 70 % in a particular category were examined and depicted in Table 2.4. Models that were unable to achieve more than 70 % representation in any category were excluded from the representation. This fact should not cause users to assume that these models are generally less convenient to use. These models probably focus on aspects that were not explicitly included in the questionnaire, meaning that they may address research questions that do not focus on flexibility. The following conclusions are therefore closely connected to the aspects of the questionnaire and the evaluation criteria.

Table 2.4 shows that sector coupling appears to be exceptionally well covered based on our evaluation criteria. Ten models achieve a representation level of 70 % or more. The comparatively large number of models may suggest that the open energy community is consciously promoting the relatively new topic of sector coupling. Note that this conclusion is drawn from a power sector perspective. Detailed aspects of the mobility and heat sector are not the subject of this examination. A specific evaluation of heat and mobility sector aspects may therefore lead to other conclusions. In contrast, there are only two models in the storage category and only one in the network category with a representation exceeding 70 %.

TABLE 2.4: Representation of holistic approach within models with more than 70% of representation in any category

Model	Supply	Demand	Storage	Network	Sector coupling
TRANSIENT	95 %		93 %		77 %
DISPA-SET	80 %				82 %
CALLIOPE	79 %				74 %
PyPSA	79 %		71 %		85 %
DIETER	76 %	82 %			
BACKBONE	75 %				
BALMOREL	71 %	86 %			70 %
REGION4FLEX		82 %			84 %
FRIGG		80 %			84 %
FLEXIGIS		71 %			
eGo				85 %	
OEMOF					70 %
ENERGYPLAN					70 %

To address specific research questions regarding one individual category, there is probably at least one appropriate model. However, a holistic approach, which shows flexibility across all categories considered with a high degree of representation, cannot be deduced from the results. Three models (TRANSIENT, PyPSA, BALMOREL) cover three of the five categories with a high degree of representation. Not one model achieves a high degree of representation in four or the five categories.

To answer specific research questions with a holistic approach of flexibility, different models can be combined to ensure broad coverage of the categories. Thus, it would be possible to use mainly one model with a comprehensive range covering almost all categories. In addition, one or two models could be used that are strong in the specific categories covered inadequately by the other model. One example of coupled models is eGo, which uses PyPSA to perform load flow calculations.

Moreover, many models will be expanded in the future by components that also affect flexibility. eGo, for example, will be upgraded with controlled charging for electric vehicles. The representation of power-to-X and the transport sector is likely to be improved in BALMOREL. OEMOF will address the heat sector more comprehensively by optimising and simulating district heating and absorption heat pumps.

Regarding grid aspects, it is likely that TRANSIENT will integrate a module that allows the investigation of voltage stability. Furthermore, a complete AC/DC simulation with additional components and harmonic analysis will be implemented in GRIDCAL. Power flow calculations in PANDAPOWER will be extended to allow the consideration of asymmetric grid situations.

Demand response will be enabled by model coupling in FRIGG, and automated model coupling will be implemented in DISPA-SET. Furthermore, FLEXIGIS will integrate socio-economic aspects and an urban policy perspective.

The results suggest that many categories are mapped very well by individual models. However, a holistic approach to flexibility across all categories appears to be inadequately represented as for now. It may be advantageous to couple several models in this context. Moreover, flexibility aspects will be added to many models in the future.

## 2.5 DISCUSSION AND LIMITATIONS

Our analysis revealed different levels of representation of technical flexibility options among the models surveyed. In this section, we critically reflect on our findings and discuss the limitations of this study.

First, the questionnaire itself contained certain biases due to the survey designers' understanding and interpretation of flexibility and modelling tools. We strove to minimise this bias by scanning the existing literature for model parameters and cross-checking the questionnaire with modeling experts before distributing it. To counteract deviations that may occur nevertheless due to different interpretations of the survey questions, we checked all of the completed questionnaires for consistency, and enquired and discussed matters with the developers if answers were unclear or suggested that the respondent may have had a different understanding of specific questions. With our methodology, we follow the line of argumentation of [56], where the authors recommend a dialogue with model developers

for model overviews and validation purposes. The approach is also in line with [44] who sent a survey to model developers and [48] who validated their outcomes with the developers of most of the investigated models. A case study to evaluate how well our results reflect the actual modelling capabilities would be a valuable extension of our work.

Second, the scope of the questionnaire is limited. As stated in the background section, flexibility is a broad field covering numerous aspects and dimensions. It is quite a challenge to cover all aspects and dimensions in detail, while ensuring that the questionnaire does not become too long, affecting the response rate. To this end, the primary focus of this study was narrowed down to the technical representation of flexibility options in the models under examination, focusing on the power sector. Some aspects of system operations are covered by the decision-making process and probabilistic aspects. The social drivers are touched by behavioural and social aspects. A more detailed examination of the system operations and the economic and social drivers would be interesting, but exceeds the scope of this work and is left to further research.

Finally, in spite of all attempts to reach out to a wide variety of open source models, it was not possible to capture all existing models. However, a sufficient quantity and variety of models enabling a good overview was ensured by disseminating the questionnaire via the website and mailing list of the OPENMOD INITIATIVES and reaching out to specific interesting models by sending additional emails. While the models surveyed do not therefore necessarily represent a perfect sample of the global open source ESM landscape, the results identify specific trends nonetheless.

We discuss these trends and the reasons for different levels of representation in ESMs along the five flexibility options. We are aware that the level of representation obtained is highly dependent on the parameters chosen and their weighting. In this study, they were chosen such that flexibility options could ideally be represented holistically. However, some parameters may not be of interest to several questions on the topic of flexibility, while others may weigh more heavily than represented in the current evaluation. We therefore provide an open source version of the algorithm<sup>4</sup>, which enables users to adjust the weighting as required and provides the level of representation of all models. The tool is intended to help scientists choose the right tool for their specific research question.

---

<sup>4</sup> Open ESM Flexibility Evaluation Tool: <https://github.com/r1-institut/OpFE1>

In this study, sector coupling exhibited the highest rate of representation in all ESMs surveyed. This is quite surprising because the flexibility of sector coupling is a relatively new approach [56], [57]. However, it must be noted that our study only examined sector coupling technologies from the perspective of the power system. The detailed evaluation of the representation of sector-specific aspects, such as their transport structure, was therefore excluded. As a result, all statements on the level of representation apply only to sector coupling technologies in power systems. Among these, many ESMs already include sector-coupling technologies such as PtG and heat pumps (HPs). These technologies enable electricity to be converted to different gas types and then used for heating, transport, industrial processes or reconversion to electricity. The existing literature shows an emerging trend in the investigation of cross-sectoral synergies [56], which explains the detailed mapping of sector coupling technologies. Since these technologies are an important long-term storage solution for high-share RE systems, they are included in many ESMs. This is also underlined by studies on high-level or 100 % RE that demonstrate the importance of PtG [57]–[59]. Nonetheless, a proper representation of the heat and transport sector in ESMs was often found to be missing. As such, there is room for improvement when it comes to comprehensively simulating sector-coupled flexibility [49], including behavioural aspects [60], [61] and demand-side management in other sectors than electricity [49].

Supply-side and demand-side flexibility options have the second and third highest representation. Providing flexibility via different supply technologies is the most established form of flexibility in power systems. As a result, almost all models include conventional and RE as flexibility options, but have limitations with regard to the operational constraints of these options, even though it is possible to implement most constraints in the most common temporal scope of hourly increments. Other studies also found that certain operational aspects were underrepresented [49], [50]. Demand-side flexibility, such as shifting the load of household appliances, the service sector and industrial loads, is enabled in most ESMs. The flexibility potential lies – as is the case with supply – within the range of hourly timesteps.

We observed a limited representation of storage flexibility options in the ESMs surveyed. While primarily medium-term and long-term storage options such as batteries and pumped hydro storage are included in almost all models, short-term storage such as capacitors and flywheels is missing in most cases. This result suggests that modelling the short-term storage

behaviour and ageing of battery systems is a complex field and beyond the scope of most ESMs that look at long-term scenarios. In [62], for instance, PyPSA is used to compare battery storage and long-term storage technologies for a year on a European scale. A transient short-term energy system simulation in TRANSIENT using batteries and a natural gas grid as storage units is described in [63]. A broader overview of energy storage in long-term system models is provided in [64].

In general, networks are not broadly covered as a flexibility option in any of the models aside from EGo. Modelling networks and the geographical flexibility associated with them requires a very detailed set of data and simulations. For this reason, most ESMs exclude this dimension and neglect geographical flexibility, with the exception of comparing different regions connected via transmission grids [57], [65]. Detailed analysis at the medium- and low-voltage grid level has traditionally been conducted for grid integration studies [66] or for improving grid operations [67], applying commercial software such as POWERFACTORY [68] or SINCAL [69]. The emerging field of including distribution grids in larger-scale energy system models has been shown to alter the results of long-term scenarios significantly [70]. In a recent study on the capabilities of energy system models, however, the representation of distribution grids was also found to be a possible field of improvement [49].

In summary, the results reveal the background of most models - they were designed to provide decision support for medium-term to long-term energy planning.

## 2.6 CONCLUSION

The importance of flexibility in the design of future energy systems is growing. Finding the appropriate flexibility option for planners and operators of power systems is crucial to provide reliable and cost-effective power, especially in high share VRES systems.

As the first result of our work, we introduced a new framework that captures the different characteristics of flexibility options. First, we distinguished between the geographical and temporal dimension. We then introduced aspects of system operation and presented economic and social drivers, which influence the utilisation of technical flexibility. Finally, we presented five different technological flexibility categories: network, supply, demand, storage and sector coupling and their operational characteristics. This framework

can be used to describe, develop and improve flexibility options. We have applied the framework to assess the representation of flexibility options in ESM in an effort to support future energy modelling tasks by finding the most appropriate tool for the question at hand as well as identifying future research and development needs for new tools.

The results show that the geographical dimension is adequately represented among the models analysed, generally covering all geographical scopes from local to international. With regard to the temporal dimension, most models focus on long-term assessments and planning using hourly increments as simulation time steps. As shorter timescales become increasingly relevant as the share of VRES, we suggest placing greater emphasis on shorter timescales in future model development.

We further analysed the technical flexibility categories - supply, demand, storage, network and sector- coupling, including their operational characteristics. All technical flexibility options are well represented in at least one of the models. Based on our analysis and assessment criteria, we recommend to apply TRANSIENT for modelling supply-side and storage flexibility, while BALMOREL scores the highest for demand-side flexibility. We found that EGO represents network flexibility most comprehensively. However, network-type flexibility in particular is still covered in limited detail in most models. DISPA-SET exhibits the highest representation of sector-coupling features for power system flexibility. Most models still cover storage and network-type flexibility in limited detail. Thus, this needs to be prioritized in the process of refining and improving models. Another possibility to overcome certain weaknesses of individual models is to facilitate a soft coupling of different models. This would allow for a holistic evaluation of flexibility and energy systems based on VRES.

Flexibility depends not only on technical parameters of flexibility options, but also on the system operations. Aspects addressing system operation parameters are generally represented less strongly than those covering technical parameters. Most models use perfect foresight as the basis for investment and dispatch decisions and did not include probabilistic and behavioural aspects. Perfect foresight is appropriate for managing foreseen changes in either supply or demand, but less so for unforeseen changes. We therefore recommend using probabilistic approaches and including behavioural aspects to ensure that system operation flexibility tackling unforeseeable changes can also be assessed.

In summary, the open energy modelling landscape provides a broad set of solutions for modelling flexibility options in power systems. The appropriate selection depends on the research task at hand. Having said that, most questions can be addressed using existing models. Our open source version of the evaluation algorithm may help scientists find the appropriate models for their specific research purposes. Future work in model development should focus on coupling models and increasing the temporal resolution.



## MODELLING OF DECENTRALISED FLEXIBILITY OPTIONS

---

This PhD research investigates the role of decentralised flexibility options (DFOs) in future power systems with high shares of variable renewable energy sources (VRES) and sector coupling technologies. The focus thereby lies on flexibility from electric vehicles (EVs), heat pumps (HPs) and battery energy storage systems (BESS). These are larger consumption units within households that display both high energy consumption and power values and therefore offer a higher flexibility potential than smaller devices.

The chapter is structured as follows. **Section 3.1** introduces the choice and methods of an existing model for distribution grids (DGs). **Sections 3.2, 3.3 and 3.4** introduce the relevant data and model formulations for EVs, HPs and BESS that were developed and used in this thesis<sup>1</sup>.

### 3.1 DISTRIBUTION GRIDS

The previous chapter found that the open-source modelling landscape covers diverse flexibility options. To use existing work, we apply an adapted version of the algorithm introduced in Section 2.3.3 to choose the most suitable model for further investigations. This model is then expanded with missing model formulations.

The first part of the PhD focuses on the interplay of decentralised flexibility options and the grid. We focus on the medium voltage (MV) and low voltage (LV) as many new technologies are installed within these voltage levels. Therefore, the chosen model should be able to adequately represent DGs on these voltage levels and decentralised flexibility options. **Section 3.1.1** describes the choice of an existing model to adequately represent DGs. **Sections 3.1.2, 3.1.3 and 3.1.4** describe relevant methods of the model, namely the identification of grid issues and the modelling of grid reinforcement and curtailment in the chosen tool.

---

<sup>1</sup> The code for sizing (and operations) of the DFOs is published open-source under <https://github.com/AnyHe/DFOs>.

### 3.1.1 *Model Choice*

We want to make use of existing models for the representation of DGs using the previously described decision algorithm. To be able to capture the varying importance of certain technologies and their representation, we use a Likert-scale [71] ranging from one to five (1: very low importance, 2: low importance, 3: moderate importance, 4: high importance, 5: very high importance) to weigh the representation of different parameters in the model. We thereby only evaluate aspects that are relevant for the interplay of decentralised flexibility options, namely EVs, HPs and BESS, and DGs.

#### *Evaluated Parameters*

Table 3.1 summarises the investigated parameters, the chosen weights and ratings. As DGs are our main focus, their representation and the possibility to perform alternating current (AC) power flow (PF) calculations are rated with very high importance. Network extension as the geographic flexibility option is rated as highly important, and all relevant temporal flexibility options (EVs, HPs and BESS) as slightly less important, i.e. of moderate importance, as they are easier to implement than grid related aspects.

The represented geographic and temporal scope and temporal resolution are also weighted as moderately important. The relevant geographical scope is the local scale as we focus on lower grid levels. The temporal resolution should enable calculations with 15 min or hourly time steps for temporal scopes of days to one year, i.e. intermediate and long durations. The representation of vehicle-to-grid (V2G) and thermal energy storage (TES) for the increased flexibility of EVs and HPs is rated as nice-to-have but of low importance. Similarly, the representation of VRES would be nice but should also be easy to integrate, so it is rated of low importance. The last category of very low importance comprises the more detailed representations of temporal flexibility options and the modelling language. These factors make an application easier or more accurate but are not necessarily required.

TABLE 3.1: Relevant parameters and their weights and ratings (in brackets) for model choice. Weights range from one to five (1: very low importance, 2: low importance, 3: moderate importance, 4: high importance, 5: very high importance) and ratings from zero to one (0: not represented at all, 1: full representation).

Category	Content	Rating
General	Geographic scope, temporal scope, temporal resolution (weight: 3)	All relevant possibilities equally weighted (rating: 1/n)
	Modelling language python (weight: 1)	yes (rating: 1) \ no (rating: 0)
Network	Technologies Distribution grid (weight: 5), network extension (weight: 4)	Predefined (rating: 1) \ possible (rating: 0.5)
	Specifications Grid representation ACPF (weight: 5)	yes (rating: 1) \ no (rating: 0)
Sector Coupling	Technologies EVs, HPs (weight: 3), V2G, TES (weight: 2)	Predefined (rating: 1) \ possible (rating: 0.5)
	Specifications Technology specifications, operational characteristics (weight: 1)	Individual rating for technology specifications
Storage	Technologies Batteries (weight: 3)	Predefined (rating: 1) \ possible (rating: 0.5)
	Specifications Storage implementation (weight: 1)	Dynamic (rating: 1) \ static (rating: 0.8)
Supply	Technologies PV, wind (weight: 2)	Predefined (rating: 1) \ possible (rating: 0.5)
	Specifications Curtailed operation (weight: 1)	yes (rating: 1) \ no (rating: 0)

### *Rating of Models*

We perform the introduced evaluation algorithm with the subset of relevant parameters to find the most suitable model. Figure 3.1 shows the resulting ranking of all investigated models. The highest ranked model is  $\epsilon$ Go followed by PyPSA and TRANSIENT. All three models show a very high representation of the relevant technologies, with PyPSA being slightly weaker in network representation and  $\epsilon$ Go and TRANSIENT weaker in the representation of sector coupling technologies. For the other specifications, all three models show the lowest values for detailed specifications of sector coupling technologies, where again PyPSA shows the strongest representation out of the three.

It is important to mention that the final ranking is extremely sensitive towards the chosen parameters and ratings. Even small changes in the weights can lead to a different order of the models since some show very similar overall ratings. However, the three models mentioned always rank the highest as they broadly cover the relevant parameters. Therefore, we base the final choice on these three models and consider additional relevant factors that were only partly covered in the survey. These are:

**INTEROPERABILITY:** As flexibility has different dimensions and is relevant on various geographical and temporal scales, performing a model coupling or switching between different models might be necessary.

**DATA AVAILABILITY:** While most models and frameworks work independently from input data and can be fed with several different data sources, it is advantageous if the model has already been applied to a specific use case. This way, relevant methods and intersections will already be available and do not need to be newly implemented.

In terms of *interoperability*,  $\epsilon$ Go and PyPSA outperform TRANSIENT as they are implemented using python, like 54,2 % of all investigated models. TRANSIENT, on the other hand, is the only model using Modelica as a language. Furthermore,  $\epsilon$ Go uses functionalities of PyPSA. Therefore, the data formats are very similar, and both models can easily be coupled.

On the other hand, the *data availability* for the given use case is best for  $\epsilon$ Go. While both PyPSA and TRANSIENT are mainly intended for an application on the transmission level (e.g. [72], [73]),  $\epsilon$ Go is designed for all voltage levels, ranging from the extra high voltage to the LV [74].  $\epsilon$ DisGo, a sub-module of  $\epsilon$ Go was specifically designed for DG modelling in the MV and

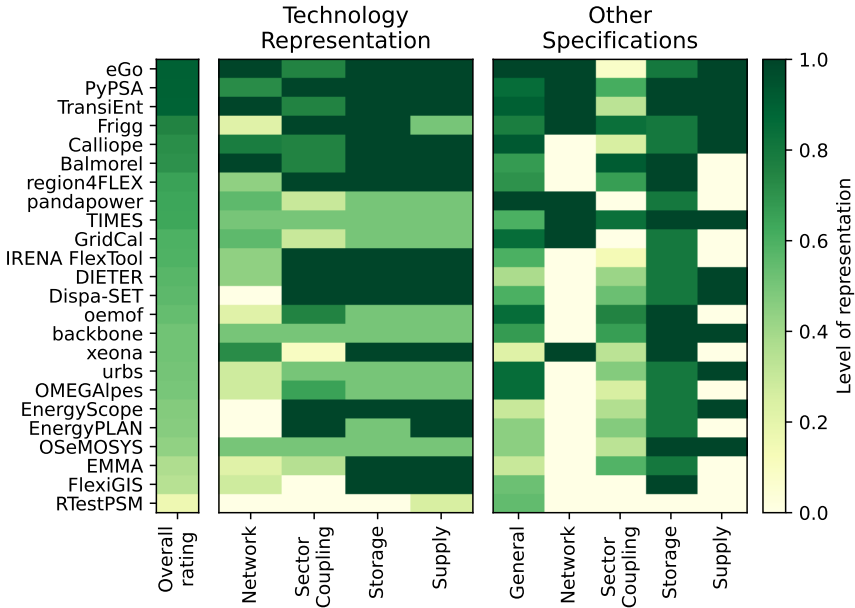


FIGURE 3.1: Representation of investigated parameters divided into technology representation (left) and other specifications (right)

LV [75]. It is directly coupled with DINGO, a tool which creates synthetic MV-LV-grids based on geographic information system (GIS) data for entire Germany [76].

With these additional criteria, we choose eDisGo, the sub-model for DGs of eGo, for our further investigations. During this PhD, the model was extended with an optimal power flow (OPF) formulation for the grid-optimised operation of EVs, HPs and BESS. The required model extensions were implemented in close collaboration with the modelling team and the eGo<sup>n</sup>-project [77]. Figure 3.2 displays the development of the representation of relevant parameters in eDisGo in the course of this thesis. While most relevant aspects were already covered to a large extent at the beginning of the thesis (eDisGo), improvements are visible in the representation of sector coupling technologies and storage in the current version (eDisGo<sub>new</sub>). While not all of these improvements were implemented during the thesis, some important aspects were integrated, like the modelling of EVs and HPs. The demand from these sector coupling technologies is still predetermined

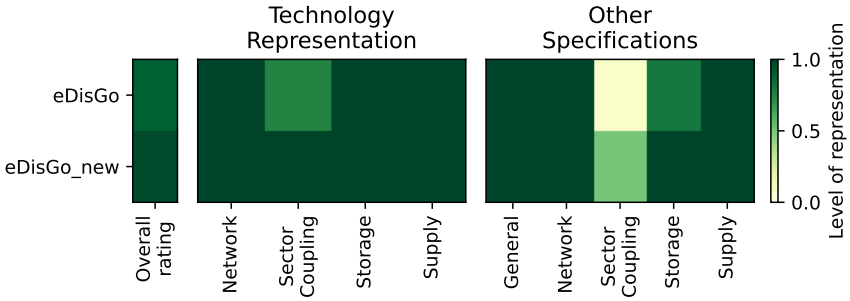


FIGURE 3.2: Development of representation of investigated parameters divided into technology representation (left) and other specifications (right)

and treated as an exogenous parameter in the model, which is why it still does not reach the highest score in the other specifications of this category. As mentioned, many of the relevant aspects were covered in the model at the start of the thesis, which is why the model was chosen in the first place. The following section explains the most important previously existing methods used in this thesis.

### 3.1.2 Grid Issues

The chosen open-source tool `EDisGo` allows us to analyse DGs by running an AC PF (using functionalities of `PyPSA` [78]) and comparing the resulting branch currents and bus voltages to grid-level- and case-specific voltage and loading bounds [75]. The cases that are differentiated are the load and feed-in cases, depending on whether the load exceeds the feed-in in the residual load of the grid or vice versa. If any of these bounds are violated, these violations are detected as grid issues. They can be resolved using grid reinforcement or curtailment measures (explained in Sections 3.1.3 and 3.1.4). The grid issues that are detected are voltage and overloading issues.

Our investigations use a time series based approach, meaning that load and feed-in time series are integrated into the grids and an AC PF is conducted for every time step. The utilised active power time series are described in Section 3.1.5, where the investigated grids are introduced. The reactive power is modelled with a constant technology-specific  $\cos(\phi)$ , summarised in Tab. 3.3.

TABLE 3.3: Standard values for  $\cos(\phi)$  used in eDisGo

	Load	Heat Pumps	Charging Points	Storage Units	Generation
MV	0.9	1.0	1.0	0.9	0.9
LV	0.95	1.0	1.0	0.95	0.95

### *Voltage Issues*

The voltage has to stay within grid-level- and case-specific voltage bounds [75] that are visualised in Fig. 3.3. The values are chosen following technical standards and guidelines [79]–[81]. In the case of voltage drops, the allowed voltage deviation is set to 0.015 p.u. in the MV, 0.02 p.u. for MV-LV-transformers and 0.065 p.u. in the LV. In the case of voltage increase, the allowed voltage deviation equals 0.05 p.u. in the MV, 0.015 p.u. for MV-LV-transformers and 0.035 p.u. in the LV. In both cases, the grid-level-specific bounds add up to a total deviation of 0.10 p.u., i.e. 10% of the nominal voltage, thus fulfilling DIN EN 50160 [79].

### *Component Overloading*

Regarding component loading, the thermal limit of lines and transformers should not be exceeded. The MV furthermore has to be operated (n-1)-secure, meaning that the system still needs to be operated safely within the operational boundaries in case of the contingency of any of the grid components [82].

For the component loading (summarised in Tab. 3.4), we therefore differentiate two simulation setups: the normal operation and contingency case. For normal operation, the maximum allowed loading is 100% of the thermal component limit in all investigated voltage levels and cases.

For the contingency case, we use voltage level and case-specific standard values provided by eDisGo [75]. It follows the approach introduced in [83], where loading constraints are defined for the different voltage levels and depend on the grid residual load. If the grid residual load is positive, i.e. the load exceeds the feed-in, this is defined as the *load case*. If the grid residual load is negative, on the other hand, the situation is defined as *feed-in case*. The LV does not have to be operated (n-1)-secure. The allowed maximum component loading of LV lines and for MV-LV-transformers is therefore 100% of the thermal limit for both load and feed-in case. In the

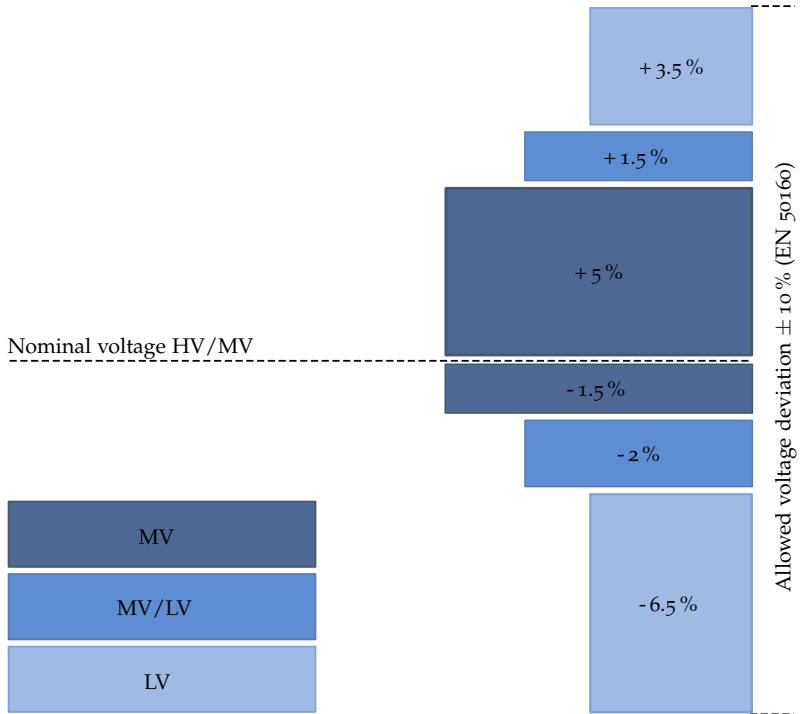


FIGURE 3.3: Default voltage bounds implemented in eDisGo (own representation based on [75])

TABLE 3.4: Loading constraints for different grid levels in percent of thermal limit of the components

<b>Normal Operation</b>				
<b>Case</b>	<b>HV/MV</b>	<b>MV</b>	<b>MV/LV</b>	<b>LV</b>
Feed-in/load	100%	100%	100%	100%
<b>Contingency Case</b>				
<b>Case</b>	<b>HV/MV</b>	<b>MV</b>	<b>MV/LV</b>	<b>LV</b>
Feed-in	100%	100%	100%	100%
Load	50%	50%	100%	100%

MV and for high voltage (HV)-MV-transformers, on the other hand, there is a differentiation between the load and feed-in case because of (n-1)-security. In the load case, the allowed component loading for HV-MV-transformers and MV-lines in open ring topologies is 50 % of the thermal limit to be able to compensate for contingencies. The distribution system operator (DSO) can disconnect the feed-in from the grid in case of a fault or overloading [80]. Therefore, the allowed component loading in the feed-in case is equal to 100 % of the thermal limit.

### 3.1.3 Grid Reinforcement

The chosen open-source tool `EDisGo` [75] allows us to determine the necessary grid reinforcement and resulting costs. The tool iteratively installs parallel components or splits single feeders until all occurring voltage and overloading issues are resolved.

The basic principle of this functionality is displayed in Fig. 3.4. In case of voltage or overloading issues at transformer stations, the transformer is either replaced or parallel standard transformers are installed. If a line is overloaded, the line is either replaced or parallel standard lines are added until the overloading is solved. In case of voltage issues within a feeder, a feeder separation is performed, where the feeder is split after two-thirds of the feeder length. For a more detailed description of the methodology of this tool, we refer to [74].

Standard components according to [83] are used for the reinforcement measures. These are summarised in Tab. 3.5. The resulting costs are calculated

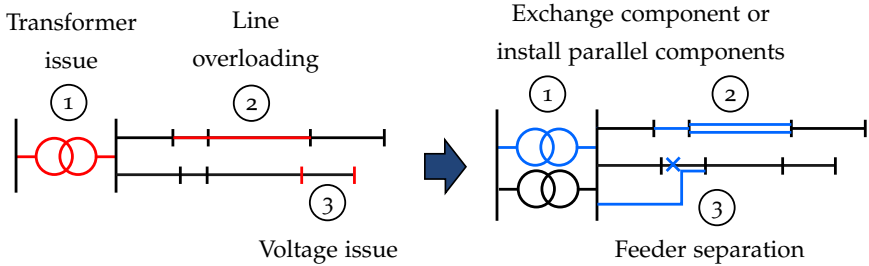


FIGURE 3.4: Heuristics for grid reinforcement measures implemented in eDisGo (own representation based on [75])

with the help of standard values for equipment changes, summarised in Tab. 3.6. The costs for cables without earthworks are adopted from [84], and all other values stem from [85]. The population density differentiates the region type (rural, urban). Areas with a population density  $\leq 500/\text{km}^2$  are classified as rural, and areas with a population density  $> 500/\text{km}^2$  as urban [75].

TABLE 3.5: Standard components for grid reinforcement measures used in eDisGo

MV Lines	HV/MV-Transformer	LV lines	MV/LV-Transformer
NA2XS2Y 3x1x185 RM/25 <sup>1</sup> NA2XS2Y 3x1x240 <sup>2</sup>	40 MVA	NAYY 4x1x150	630 kVA

<sup>1</sup> For 10kV MV grids; <sup>2</sup> For 20kV MV grids

TABLE 3.6: Standard costs for grid reinforcement measures used in eDisGo

Voltage level	Cable	Cable incl. earth-works - rural	Cable incl. earth-works - urban	Transformer
MV	20 t€/km	80 t€/km	140 t€/km	1 M€
LV	9 t€/km	60 t€/km	100 t€/km	10 t€

### 3.1.4 Curtailment

While grid reinforcement is the traditional way of dealing with grid issues and therefore a good measure of comparison, grid reinforcement needs

depend only on the highest occurring grid issue per component, i.e. very short periods. Some could be solved with relatively small interventions, like using storage to shift feed-in or demand. Therefore, we assess the curtailment needs for load and feed-in to solve arising grid issues as a second measure of comparison. It allows a more detailed investigation of when, to what extent, and how long the DSO would have to enact countermeasures to solve the arising grid issues. The curtailment thereby measures the need for temporal flexibility instead of the increase of geographic flexibility by grid reinforcement. Temporal flexibility measures like the utilisation of storage or load shifting will likely become more important in future active distribution grids.

To calculate the necessary curtailment of load and feed-in to solve arising grid issues, we use the methodology developed in [23]. The demand respectively feed-in is iteratively reduced in steps of 1 %, and after each iteration, it is rechecked for grid issues as described in Section 3.1.2. Since the curtailment of load and feed-in in lower grid levels can alleviate grid issues in higher grid levels, the grid issues are solved from the LV to the MV: first in the LV, second at MV-LV transformers and lastly in the MV. Similarly, the grid issues farthest away from the transformer station are solved first within one voltage level (i.e. in the LV or MV), successively moving closer to the station. The reason is that solving issues further away from the station can alleviate the other grid issues.

### 3.1.5 Investigated Grids

Distribution grids can vary greatly depending on local conditions. The influence of increasing penetrations of DFOs will likely also vary depending on the grid type. We therefore investigate different types of grids to capture the influence of DFOs, namely load-, PV- and wind-dominated grids. In the following, we introduce the representative grid topologies that serve as the base of our investigations. Thereby, two base scenarios are simulated: the status quo and a future scenario for 2035, which shows higher levels of DFOs.

#### *Grid Topologies*

We use synthetic medium- and low-voltage DGs provided by the open-source tool DINGO [76]. It provides a data basis of 3608 MV-DGs with underlying LV-grids for entire Germany. This work focuses on the simul-

taneous integration of DFOs and renewable energy sources (RES) with a specific focus on the influence of different technological compositions of DGs. As the future RES penetration and influence on the grids are expected to be higher in suburban and rural grids [86], we only consider these types of grids. In previous work, the grids were clustered using the k-means-algorithm to obtain 15 representative grids, further divided into four categories: load-, PV-, wind-dominated grids and other [23]. For this work, the two grids with the most dominant characteristics classified as load-, PV- and wind-dominated while representing sufficiently high numbers of grids are chosen for the investigations. These six typical grids and the represented grids are displayed in Fig. 3.5.

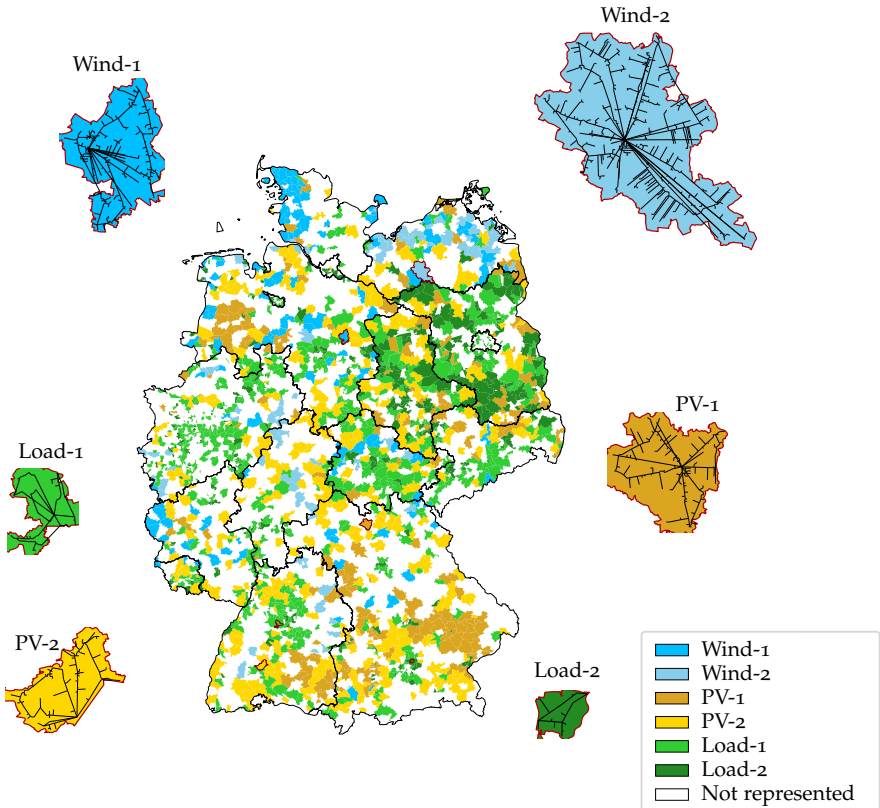


FIGURE 3.5: Representative grid topologies and represented grids on a map of Germany.

The provided grid topologies include lines and transformers as well as various loads and generators connected to specific buses. The MV-buses are georeferenced and obtained with the help of a routing algorithm. Typical LV-grids are connected to the MV/LV-transformers. The connected loads are subdivided into *agricultural, industrial, residential* and *retail* loads.

Following [87], time series data of the demandlib [88] is used for the load and time series data for the weather year 2011 extracted from the *Open Energy Platform (OEP)* [53] for solar and wind generation. Dispatchable renewable energy sources (dRES) are assumed to produce at constant capacity factors, namely 0.57 for biomass and 0.41 for hydropower plants. These values are obtained by dividing the total energy produced in 2019 by the total installed capacity in that year. All time series data are obtained in a resolution of 15 minutes. In some of the following investigations, the temporal resolution is decreased to one hour to limit the computational complexity.

### *Status Quo Grids*

We use the DINGO-grids and update them to 2018 installed capacities for the status quo. Fig. 3.6 shows the installed capacities of generation units and peak loads of residential and other loads. The status quo grids are the basis for most grid investigations. However, increasing penetrations of distributed energy resources (DERs) are integrated and connected to residential loads to study their effect on different distribution grids.

### *2035 Grids*

One specific setup we investigate is the status of the grids for the target year 2035. For this scenario, we use data from the *eGo 100*-scenario of the *open\_eGo*-project [87] and predictions provided by the German network development plan (NDP) [17]. Fig. 3.7 visualises the resulting peak load of the conventional load including HPs and installed capacities of EV charging stations as well as generation, differentiated into wind, PV and other generation (i.e. dispatchable renewable energy plants), in the considered grids. Table 3.7 additionally contains structural parameters and private and public charging demands within the grids.

The *eGo 100*-scenario gives information on generator capacities and conventional load as well as the spatial distribution and assignment to the different voltage levels. The *eGo 100*-scenario only considers an expansion

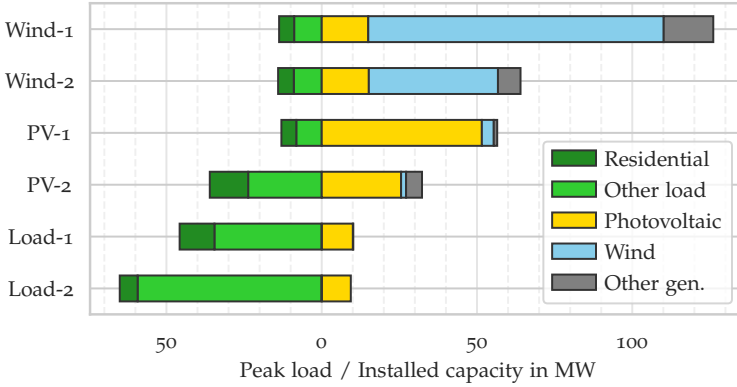


FIGURE 3.6: Considered grids in status quo with peak load of residential and other conventional load and installed capacities of generation technologies.

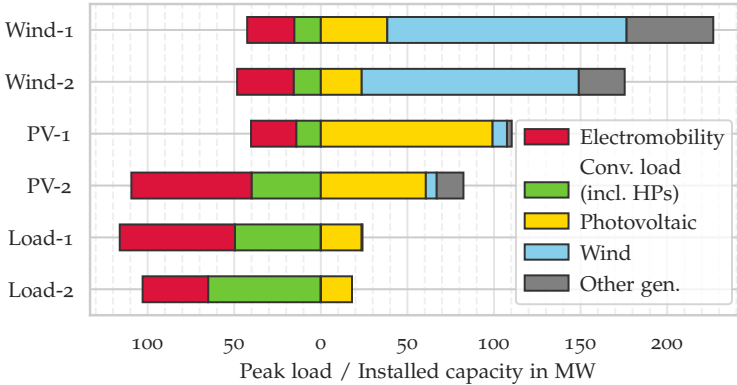


FIGURE 3.7: Considered grids for 2035 with peak load of conventional load (including HPs) and installed capacities of EV charging points and generation technologies.

of renewables, however, and does not take sector coupling into account. We therefore expand it by EVs and HPs as these are the most important sector coupling elements for the MV and LV. For the number and total annual consumption of HPs as well as the number of EVs, the *NEP C 2035*-scenario of the German NDP [17] serves as input. The demand profile for HPs is adopted from [89] if not optimised<sup>2</sup>. As HPs are assumed to be predominantly installed in households, the demand is allocated to households proportionally to the annual electricity demand of the respective household and added to its load profile. The total number of EVs for Germany are regionalised and assigned to the DGs based on current statistics on registered vehicles [90]. To incorporate their demand into the grids, charging stations are added as new loads. The sizing of these charging stations and the modelling of EV driving and charging patterns is further detailed in Section 3.2.

### 3.1.6 Critical Reflection

Here, input data and modelling assumptions, as well as their potential influence on the results, are discussed. Furthermore, areas for future research are pointed out.

#### *Input Data*

Due to the lack of openly available distribution grid data for entire Germany, we use synthetic data for the distribution grids, provided by DINGO [76]. While these are based on GIS data and follow current grid planning principles, they will still differ from real-world distribution grids since these also depend on historical decisions and grid planning principles can differ based on the DSO [91]. In the original publication, the authors compared the created data basis with statistical parameters from German distribution grids and found deviations of +10.3 % for the number of HV/MV-transformers, -8.2 % for MV/LV-transformers and -2.3 % for the total length of MV lines [91]. In a master thesis supervised during this PhD, the grids were compared to real-world distribution grids and SIMBENCH grids based on visual, structural and mathematical criteria [92]. SIMBENCH is another source of synthetic grid data which is based on real-world data, i.e. 74 distribution grids for the MV benchmark grids [93], [94].

---

<sup>2</sup> The modelling of HPs in case of optimised operation is explained in the following Section 3.3.

TABLE 3.7: Grid topologies and included technologies for the 2035 grids.

<b>Structural grid parameters</b>					
<b>Grid ID</b>	<b>#feeder</b>	<b>#MV-buses</b>	<b>#LV-buses</b>	<b>#MV-LV-stations</b>	
Load-1	29	159	13,812	110	
Load-2	30	96	6,514	56	
PV-1	11	240	7,992	130	
PV-2	18	196	20,275	196	
Wind-1	15	419	9,071	179	
Wind-2	24	798	11,722	381	

<b>Installed generator capacities in [MW]</b>					
<b>Grid ID</b>	<b>Wind</b>	<b>Large PV</b>	<b>Small PV</b>	<b>Hydro</b>	<b>Bio</b>
Load-1	0.0	6.8	16.8	0.0	0.5
Load-2	0.0	13.5	4.5	0.0	0.0
PV-1	8.3	72.2	27.0	0.3	2.4
PV-2	6.3	13.7	47.0	0.8	14.6
Wind-1	138.2	24.6	13.8	0	50.1
Wind-2	125.4	14.9	8.7	0.1	26.4

<b>EV integrated capacities <math>P</math> in [MW] and charging demand <math>E</math> in [MWh]</b>					
<b>Grid ID</b>	<b>#EVs</b>	<b><math>P_{\text{public}}</math></b>	<b><math>P_{\text{private}}</math></b>	<b><math>E_{\text{public}}</math></b>	<b><math>E_{\text{private}}</math></b>
Load-1	6771	6.0	60.5	344.6	286.7
Load-2	3769	3.4	34.4	188.7	163.1
PV-1	2696	2.5	23.6	128.7	111.5
PV-2	7739	5.8	63.6	368.3	286.8
Wind-1	2665	3.3	23.9	107.7	93.2
Wind-2	3240	3.9	28.7	140.4	119.7

The general structure of the DINGO grids was found to be in good accordance with the real grids, all being operated in open ring structures [92]. However, the number of satellite buses, i.e. buses connected to the ring by an extra line, was much higher than in the real grids. Furthermore, the minimum and maximum line lengths were more extreme in the DINGO grids than in the compared real-world grids. One reason are aggregated load areas in the original DINGO grids. For the data basis of this PhD, these are removed and replaced by spatially resolved grid data. Furthermore, very short lines are removed to gain more realistic grids. The master thesis found that despite the structural differences, the diversity of real grids was captured well by the DINGO grids [92]. For the investigations of this thesis, where the focus lies on the influence of DERs on differently composed grids, the DINGO grids are therefore evaluated as suitable. We trust that the general trends and tendencies can be trusted even though individual grids might show different behaviour in the real world. Therefore, all tools are published open-source for DSOs and future research. This way, the presented investigations can be repeated for individual grids.

This thesis focuses on the interplay of DFOs with renewable energy generation. We therefore focus on rural and suburban grids, as renewable generation in urban areas is assumed to be neglectable for the grid. However, urban grids would be an interesting subject for future research since the density of EVs and HPs is expected to be high in these areas. On the other side, the grid structure tends to be more robust in these grids with lower line lengths and higher shares of meshed grids. In the literature, some studies found a higher influence of DERs on urban grids (e.g. [22], [23]) and others found the opposite (e.g. [86], [95], [96]). We thus recommend including urban grids in future investigations.

Lastly, six distribution grids might not be enough for a representative study for entire Germany. While they represent a large share of the 3608 MV grids (see Fig. 3.5), there are also large areas that are not represented and urban grids are not considered. Therefore, we recommend expanding the investigations in this thesis to a more representative set of distribution grids. The provided methods and tools can be used for such a representative study.

### *Modelling Assumptions*

While EDisGo is a useful tool to analyse grid issues and estimate the necessary grid reinforcement or curtailment, it also has some limitations

we want to discuss in the following. Furthermore, some modelling choices within this PhD omit certain factors that might influence the results.

First, we compare flexibility provision from DERs with curtailment or grid reinforcement, omitting alternatives to tackle grid issues, like reactive power compensation or on-load-tap-changing transformers. These could represent viable alternative solutions to grid reinforcement and result in lower total costs [97]. However, reactive power compensation from decentralised flexibility and adjustable transformers with tap changers are not yet widespread. Therefore, this thesis focuses on the active power provision from DFOs and its effects on grid reinforcement. Reactive power provision is accounted for with a fixed  $\cos(\phi)$ . In future work, it would be interesting to expand the work with more sophisticated reactive power provision (e.g.  $Q(U)$ ) from these sources and its potential to limit voltage violations and reduce the required grid reinforcement.

Another strong assumption is that as soon as a grid issue occurs in one of the simulated time steps, this violation results in grid reinforcement. If violations are short, other measures such as feed-in curtailment or load shedding might be the cheaper alternative. However, DSOs are not likely to accept structural congestion in their grids, and we use mean values with a temporal resolution of 15 minutes or one hour. Shorter peak values are therefore already smoothed out. Furthermore, we allow for a loading of 100% without applying any security factor. In this light, the assumption that reinforcement will be undertaken when any grid issue is detected will still lead to comparably low values and is a valid assumption. Furthermore, our investigations estimate the reduction potential of reinforcement needs through temporal flexibility provision by DERs and therefore already account for alternative measures to grid reinforcement. Nevertheless, it could be interesting to investigate the interplay of curtailment and grid reinforcement in future work to find the optimal combination.

The simulated reinforcement is based on time series and, therefore, an optimistic way of determining grid reinforcement costs. The current practice is to run a worst-case analysis with simultaneity factors of load and feed-in and size the grids accordingly [22]. This approach will lead to higher grid reinforcement needs than the time series based approach. Figure 3.8 shows the reinforcement costs for the 2035 grids with both approaches<sup>3</sup>.

---

<sup>3</sup> For the worst case analysis, we use the predefined simultaneity factors of eDisGo, which are summarised in Tab. A.3 in the appendix.

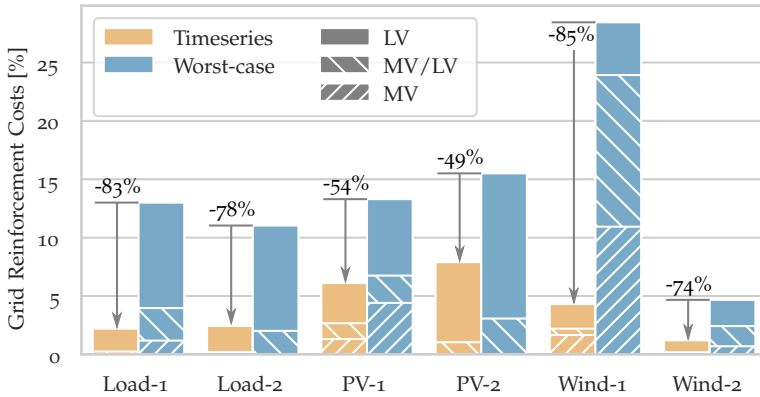


FIGURE 3.8: Grid reinforcement costs in percent of total grid value obtained with timeseries based vs. worst-case approach.

The results are displayed in percent of the current value of the grid<sup>4</sup>. In all the investigated grids, the reinforcement costs are significantly lower using the time series based approach, with relative reductions of 49–85%. These values mean that if grid planning moves from worst-case analysis to time series based reinforcement, the reinforcement costs can be reduced by 49–85% in the investigated grids. However, this would also require perfect knowledge of the consumption behaviour and renewable feed-in. Furthermore, no security margin is applied so the grids would be operated closer to their limits. Time series based modelling is necessary to estimate the reduction potential of a grid optimised operation of DFOs. When interpreting the results, it should be considered that the obtained values constitute a lower bound and that there is already a significant potential to decrease reinforcement costs using the time series based approach instead of the worst-case analysis.

Last but not least, the simulated reinforcement follows a heuristic. Therefore, the solutions that are obtained are not necessarily cost-optimal. However, optimising grid reinforcement requires integer values and is therefore not feasible for large-scale grids. Furthermore, real-world grid planning does not follow a centralised optimal solution but consists of case-by-case decisions. The implemented heuristics might therefore reflect reality better

<sup>4</sup> To estimate the current value of the grid, we calculate the costs of all existing lines and transformers using the standard cost values introduced in Tab. 3.6.

than a central optimisation. Lastly, our studies cover larger areas, and on average, the implemented methods have proven to yield results in the same range as other large-scale grid studies [87]. Therefore, we conclude that the methods implemented in eDisGO are also suitable for the grid studies in this thesis, which focus on larger areas of different MV distribution grids. It has to be noted that the literature shows quite a wide range of different values for the reinforcement costs in future systems with high penetrations of DERs [98] and results should therefore rather be interpreted for trends and tendencies than for absolute values.

### 3.2 ELECTRIC VEHICLES

EVs will become an important part of the future power system. Their high charging powers and electricity consumption can pose significant stress on the grids and require additional generation capacity [99]–[101]. At the same time, they will introduce great amounts of storage capacity, which can provide flexibility to the system [100]–[102]. However, EVs are primarily means of transport and therefore move around, which means the storage is not always available and changes location [100], [103]. Modelling EV flexibility is therefore a complex task combining the temporal and geographical dimension [103]. The following subsections describe the chosen modelling approaches for EVs, later used for the evaluation of the influence of EV integration on DGs and the national balancing of generation and demand in renewable power systems.

**Section 3.2.1** includes the generation of travel profiles to obtain charging demand and standing times of individual EVs. **Section 3.2.2** explains the sizing of charging stations. **Section 3.2.3** introduces the reference operation of EVs, if charging remains uncoordinated. In **Section 3.2.4**, different levels of EV flexibility are explained. **Sections 3.2.5 and 3.2.6** introduce two model formulations for smart charging of EVs, one modelling each EV and its battery individually and one aggregating the charging demand of groups of EVs or charging stations into flexibility envelopes.

#### 3.2.1 *Charging Demand and Parking Times*

We want to model a large fleet of different EVs to cover different vehicle types and driving patterns. Therefore, we use the open-source tool SIM-

BEV [104] to generate travel profiles and charging processes of individual EVs in a 15-minute resolution.

The underlying data basis is historical mobility data from a large-scale German mobility survey, giving information on the trip destination, start and end times of trips, distance travelled, travel speed and standing time [105]. SIMBEV uses probability distributions extracted from this data to simulate travel profiles of individual EVs. The travel profiles depend on region type<sup>5</sup>, season and weekday. In the first step, the trip destination is randomly chosen. Trip destinations are differentiated between work, business, school, shopping, private/ridesharing, leisure and home. Per trip destination, probability distributions for distance travelled, travel speed and standing times are the basis for a random choice of these attributes for each trip in the second step.

The last step translates the travel profiles into scheduled charging demand during specific standing times. For this, SIMBEV uses assumptions on the availability and charging capacity of charging points at different destinations. Therefore, the trip destinations are mapped to three different types of charging locations - *home*, *work*, and *public* charging. Business and work trips are mapped to work or public charging, trips back home to home or public charging and all remaining trip destinations to public charging<sup>6</sup>. Whether a charging event will occur upon arrival at the trip destination is randomly chosen based on predefined probabilities. For example, it is assumed that the availability of charging opportunities for home charging points at single-family homes is the highest at 85 % while it is the lowest for roadside public charging points at 25 %. On the other hand, home charging consists mainly of 11 kW chargers while charging in public settings is dominated by 22 kW chargers<sup>7</sup>. Further, high power charging (HPC) at 50-150 kW is considered as a fallback option in case the state of charge (SoC) of any EV drops below a minimum threshold of 20 %. In all charging sessions, it is assumed that the EV charges at full capacity until the battery is fully charged or the standing time ends. Based on a recent study [89], the efficiency during the resulting charging sessions is assumed to be  $\eta_{EV} = 90\%$  within

---

5 Region types from RegioStaR 7 are used: Urban region – Metropolis, Large cities/Second-tier cities, Medium-sized cities, Small towns and villages, Markets towns in rural areas, Towns in rural areas, Small towns in rural area [106].

6 The exact shares and a more detailed breakdown of charging locations can be found in Table II.19 of [107].

7 The probability distribution of charging at different locations and charging powers can be found in Table II.20 of [107].

all charging processes. For more detailed information on the underlying assumptions and modelling in SIMBEV, we refer to [107].

The obtained driving profiles contain information on driving and parking times, the consumed energy during driving, and the scheduled charging demand at specific destinations. We expand this information with the minimum required SoC to cover the upcoming trip  $SOC^{min}$ . The initial SoC  $SOC^{initial}$ , minimum required SoC  $SOC^{min}$ , the driving and parking times, energy consumption and charging demands are used as input for the reference operation as well as the model formulation of smart charging and V2G described in Sections 3.2.5 and 3.2.6. The minimum required SoC  $SOC_{c,t}^{min}$  is thereby set for every last time step of a parking event such that the next driving session can be met without falling below a SoC of 20%, if possible. In our simulations, EVs are available for smart charging or V2G whenever they are plugged into a charging station. Of all parking events, they are plugged in for 45% of the parking time. Specifically, they are plugged in for 51.3% of the time when parked at home, 41.5% when parked at work, 36.5% when parked in public and 100% when parked at a high power charging station. In the remaining time, the EVs are not plugged in.

### 3.2.2 Sizing and Grid Connection of EV Charging Stations

In this thesis, an extended version of the travel profiles and charging demand created during a master thesis [108] is used. In total, 26 880 EVs, divided into 16 597 battery electric vehicles (BEVs) and 10 283 plug-in hybrid electric vehicles (PHEVs) of different types in the six investigated grids were modelled for a full year. Table 3.8 summarises the technical parameters of the modelled vehicle types (see also [108]) and Table 3.9 the shares of the different vehicle types in the simulated grids. The different regions of the grids were chosen to cover different driving profiles and charging infrastructure setups. In the national investigations, we assume that the simulated number of EVs is large enough to account for statistical deviations, such that the aggregated time series can be scaled up with the number of EVs.

In order to allocate the charging processes to specific sites, we use the tool TRACBEV [109], where potential charging points within each DG are identified and weighted on geospatial attributes. For home charging, the potential charging sites are weighted with the total number of apartments

TABLE 3.8: Technical characteristics of simulated vehicle types

	BEV Types			PHEV Types		
	luxury	medium	mini	luxury	medium	mini
Max. Charging Power [kW]	350	350	120	120	120	120
Battery Energy Capacity [kWh]	120	100	70	40	30	25
Mean Consumption [kWh/100km]	17.8	14.8	11.9	18.2	15.2	12.1

TABLE 3.9: Percentages of simulated vehicle types in the investigated grids

	BEV Types [%]			PHEV Types [%]		
	luxury	medium	mini	luxury	medium	mini
Wind-1	10.7	35.2	15.8	6.6	21.8	9.8
Wind-2	9.2	36.8	15.7	5.7	22.8	9.8
PV-1	9.7	38.4	13.6	6.0	23.8	8.4
PV-2	10.8	35.9	15.0	6.7	22.3	9.3
Load-1	13.8	34.1	13.8	8.6	21.1	8.6
Load-2	14.7	35.3	11.7	9.1	21.9	7.2
Total	11.8	35.7	14.3	7.3	22.1	8.8

in the area based on [110]. The weighting of work charging sites depends on the area and type of industrial, commercial or retail areas provided by [111]. Potential public and high power charging are assigned to point of interests (POIs) and existing gas stations [111], respectively. Public charging sites are weighted according to the density of POIs while HPC stations are equally weighted. The charging processes are then randomly mapped to the potential charging points, considering the weight of each charging point that was determined beforehand. One or more such charging points connected to the grid at the same grid connection point are defined as a *charging park* in the following.

Figure 3.9 shows the distribution of installed capacities of all integrated charging parks in the six investigated distribution grids for 2035. The number of home and work charging parks is much higher than that of public and high power charging parks. The installed charging capacities, on the other hand, are much higher for the public and high power charging parks.

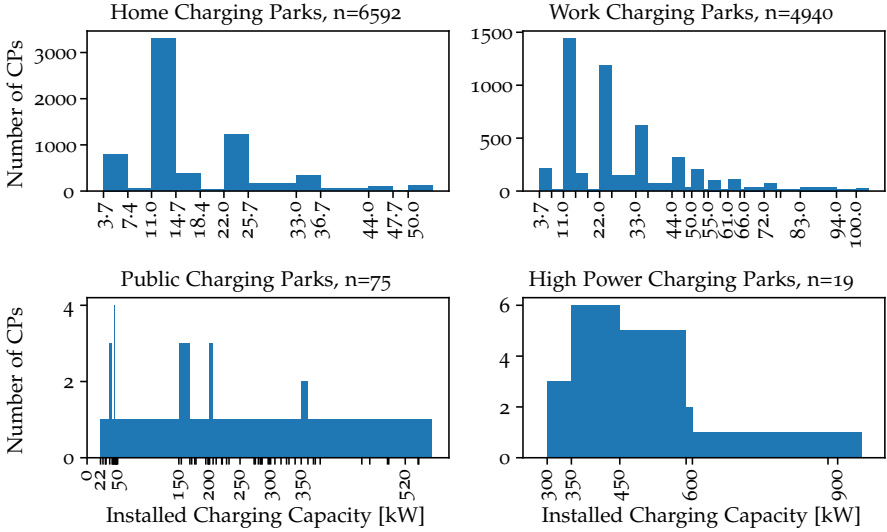


FIGURE 3.9: Distribution of installed capacities of charging parks in all investigated grids. The ticks on the x-axis mean that charging parks with the respective installed capacity exist. The bar on the right of this tick indicates the number of charging parks with this installed capacity. For clarity, not all of the tick labels are displayed.

The grid integration per charging park is based on the total capacity of all connected charging points. Charging parks with capacities of up to 300 kVA are integrated into the LV and above that in the MV level. In the MV grids, new charging parks are connected to the closest grid connection point or line. In the case of integration into LV grids, the charging park is integrated into the LV grid whose MV-LV substation is closest. Above a nominal capacity of 100 kVA, the grid connection is made via a cable connection directly to the MV-LV substation. Below, the integration process depends on the use case of the charging park. For home charging, the charging park is connected to a random household load. In the case of work charging, the connection is made to a random commercial, industrial, or agricultural load. In contrast, public charging infrastructure is connected to a random LV grid connection point. We refer the interested reader to [108] for more details.

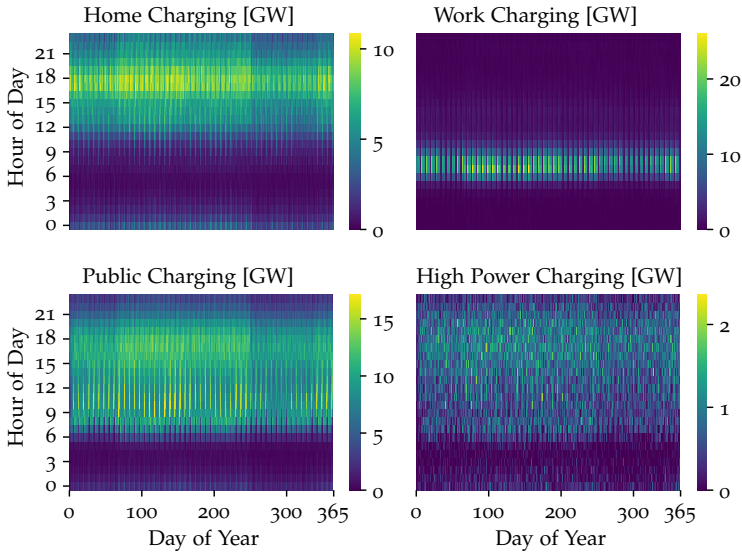


FIGURE 3.10: Reference charging with 100% EV penetration for the different charging use cases.

### 3.2.3 Reference Operation

The reference charging is obtained with a heuristic approach. It resembles a behaviour where the EVs charge directly after arrival with the nominal charging power until the charging demand of that charging session is fully met. Figure 3.10 displays the resulting charging powers for full electrification (i.e. only BEVs) of all private vehicles in Germany (i.e. 48.8 Mio. [112]) over the hour of the day and day of the year. Displayed are home, work, public and high power charging. Home charging displays the highest charging powers at around 18:00, work charging around 7:00. The simultaneity of work charging is higher than for home charging, with high charging demands from 6:00-9:00. For home charging, on the other hand, the time of charging is spread over a longer period from 12:00-23:00, with the highest values from 16:00-19:00. Public and high power charging show less pronounced peaks than the other two use cases and are distributed between 6:00-22:00.

### 3.2.4 *EV Flexibility*

We model different levels of flexibility for EVs, summarised in Tab. 3.10. In the reference scenario without flexibility (*EVs Ref.*), an uncoordinated operation with reference charging is assumed. Furthermore, we model four different flexible scenarios for EVs with increasing levels of flexibility. For each level of flexibility, the underlying assumptions are detailed below.

*EVs Flex*: Only home and work charging are assumed to be flexible. For public and high power charging, a fixed time series as per reference charging is assumed. To model flexible charging, we assume that the charging demand of a charging session can be freely scheduled within the entire standing time of the originally scheduled charging session.

*EVs Flex+*: In this scenario, in addition to home and work charging, public charging is also flexible. As in the *Flex* scenario, shifting is only allowed within the same charging session.

*EVs Flex++*: In the *Flex++*-scenario, the flexibility of EV charging is further increased. Like in *Flex+*, charging at home, work and in public is assumed to be flexible, and high power charging to be inflexible. However, in this case, shifting over different parking events is allowed. For example, the charging demand originally scheduled at work can be shifted to a later charging event at home.

*EVs V2G*: In this scenario, vehicle-to-grid, i.e. feeding power back into the grid, is allowed additionally to shifting between different standing periods. Again, home, work and public charging are assumed to be flexible.

### 3.2.5 *Model Formulation Based on Battery State of Charge*

A first model formulation describes every EV separately. Such detailed modelling is necessary if the charging location matters and charging demand can be shifted between different charging locations, i.e. when investigating the influence of EV charging on the grid and allowing shifting over different standing times. A simpler approach can be applied if the charging location is irrelevant or predefined (introduced in Section 3.2.6). The detailed model formulation is based on a master thesis that was supervised in the course of this PhD, where a mixed-integer linear programming (MILP) and linearised problem set for smart charging with V2G were developed [113].

TABLE 3.10: Levels of flexibility modelled for EVs

Name	Level of Flexibility
EVs Ref.	None - Charging with reference operation
EVs Flex	Flexibility to shift within standing times for charging use cases <i>home</i> and <i>work</i>
EVs Flex+	Flexibility to shift within standing times for charging use cases <i>home</i> , <i>work</i> and <i>public</i>
EVs Flex++	Flexibility to shift over standing times for charging use cases <i>home</i> , <i>work</i> and <i>public</i>
EVs V2G	Flexibility to shift over standing times for charging use cases <i>home</i> , <i>work</i> and <i>public</i> , utilisation of V2G

Since this work focuses on large-scale DGs, which requires a linear problem formulation, only this version of the problem set is introduced in the following.

The development of the SoC  $soc_{c,t}$  of every EV  $c$  is modelled by:

$$soc_{c,t} = soc_{c,t-1} + \frac{(p_{c,t}^{in} - p_{c,t}^{out}) \cdot \Delta t}{CAP_c} \quad \forall c \in C, t \in T, \quad (3.1)$$

$$SOC_{c,t}^{min} \leq soc_{c,t} \leq 1.0 \quad \forall c \in C, t \in T, \quad (3.2)$$

$$p_{c,t}^{out} = p_{c,t}^{V2G} + \frac{E_{c,t}^{driving}}{\Delta t} \quad \forall c \in C, t \in T, \quad (3.3)$$

where  $CAP_c$  is the EV's battery capacity,  $p_{c,t}^{in}$  the charging power and  $p_{c,t}^{out}$  the power flowing out of the EV, either by discharging using V2G ( $p_{c,t}^{V2G}$ ) or during driving ( $E_{c,t}^{driving} / \Delta t$ ). Parameter  $E_{c,t}^{driving}$  thereby represents the consumed energy at time step  $t$  while driving. For the first time step,  $soc_{c,t-1}$  needs to be replaced by  $SOC_c^{initial}$  in (3.1). The SoC has to stay within certain limits as defined in (3.2). The minimum is time dependent as it needs to be ensured that the vehicle is sufficiently charged at the time of the next departure to make its next scheduled trip. Furthermore, the SoC can not exceed 1.0.

Both charging and discharging are constrained by the maximum charging power  $P_c^{max}$  limited by vehicle characteristics defined for each vehicle  $c$

and the maximum charging power  $P_s^{max}$  of the station  $s$  to which the car is connected:

$$p_{c,t}^{in} \leq P_c^{max} \quad \forall c \in C, t \in T, \quad (3.4)$$

$$p_{c,t}^{V2G} \leq P_c^{max} \quad \forall c \in C, t \in T, \quad (3.5)$$

$$\frac{p_{c(s),t}^{in}}{\eta_{EV}} + \eta_{V2G} \cdot p_{c(s),t}^{V2G} \leq P_s^{max} \quad \forall c \in C, t \in T. \quad (3.6)$$

For times when the car is not connected to any station, charging  $p_{c(s),t}^{in}$  and discharging  $p_{c(s),t}^{V2G}$  are inhibited by  $P_s^{max} = 0$ .

The charging power at every charging station  $s$  is the sum of charging and discharging events of EVs connected to that station  $C(s)$  at time  $t$ :

$$p_{s,t}^{EV} = \sum_{c \in C(s)} \left( \frac{p_{c,t}^{in}}{\eta_{EV}} - \eta_{V2G} \cdot p_{c,t}^{V2G} \right) \quad \forall s \in S, t \in T. \quad (3.7)$$

With the given problem formulation, simultaneous charging and discharging can occur, e.g. to reduce necessary feed-in curtailment. The standard measures to counteract this behaviour are to include binaries or the product of charging and discharging as a penalty term in the objective function. However, both of these implementations lead to a significant increase in complexity and result in the larger numbers of EVs being no longer solvable. We therefore choose a linear penalty term  $pen_{EV}$  instead, that is added to the objective function:

$$pen_{EV} = \delta_{charge} \left( \sum_{s \in S} \sum_{t \in T} p_{s,t}^{EV} \cdot \Delta t - E^{tot} \right), \quad (3.8)$$

$$E^{tot} = \sum_{s \in S} \sum_{t \in T} (p_{s,t}^{EV,ref} \cdot \Delta t). \quad (3.9)$$

Thereby, the additional energy consumption through charging losses is penalised by subtracting the total energy consumption  $E^{tot}$  with reference operation  $p_{s,t}^{EV,ref}$  from the charged energy with unconstrained optimised charging. The weighting of this penalty term influences the overall utilisation of V2G. For very high  $\delta_{charge}$ , V2G utilisation is completely avoided as it leads to more losses. For very low values, V2G is used to waste energy by simultaneously charging and discharging to avoid feed-in curtailment. Therefore, it is necessary to choose a reasonable value for the weight and

correct results if simultaneous charging and discharging occur nevertheless.

### 3.2.6 Model Formulation Based on Energy and Power Envelopes

The second formulation is based on energy and power envelopes [114] and was developed in [115] and [116]. The idea is that energy and power must stay within predefined time-dependent lower and upper bounds but can be scheduled freely within these boundaries. This concept can be applied to charging stations if their charging demand is predefined or for groups of vehicles or charging stations if the charging location is irrelevant, e.g. all vehicles in one LV grid if we assume the grid will not constrain the charging. The application to the different levels of EV flexibility is explained later in this section.

Fig. 3.11 shows an exemplary course of lower and upper bounds of energy and charging power of a work charging park containing eight charging points. The envelopes are displayed for the *Flex* scenario, only allowing shifting within the originally scheduled charging session. The lower bound of the charging power is assumed to be zero, and the upper bound equals the sum of charging powers of connected EVs. The lower bound of energy corresponds to a charging behaviour where the cars are left uncharged as long as possible to be charged at full capacity for the last time steps within the standing time. On the other hand, the upper energy bound corresponds to direct charging at full capacity until the charging demand is met. When a charging park contains several charging points, the aggregated bands are obtained by adding up the individual upper and lower bands.

The general formulation of the model is:

$$e_{c,t} = e_{c,t-1} + \eta_{EV} \cdot y_{c,t}^{EV} \cdot p_{c,t}^{EV} \cdot \Delta t - \eta_{V2G} \cdot y_{c,t}^{V2G} \cdot p_{c,t}^{V2G} \cdot \Delta t \quad \forall c \in C, t \in T \setminus \{0\}, \quad (3.10)$$

$$0 \leq p_{c,t}^{EV} \leq \bar{P}_{c,t}^{EV} \quad \forall c \in C, t \in T, \quad (3.11)$$

$$0 \leq p_{c,t}^{V2G} \leq \underline{P}_{c,t}^{EV} \quad \forall c \in C, t \in T, \quad (3.12)$$

$$\underline{E}_{c,t} \leq e_{c,t} \leq \bar{E}_{c,t} \quad \forall c \in C, t \in T, \quad (3.13)$$

$$e_{c,t} = \frac{1}{2} \cdot (\underline{E}_{c,t} + \bar{E}_{c,t}) \quad \forall c \in C, t \in \{0, t_{end}\}, \quad (3.14)$$

$$y_{c,t}^{EV} + y_{c,t}^{V2G} \leq 1 \quad \forall c \in C, t \in T, \quad (3.15)$$

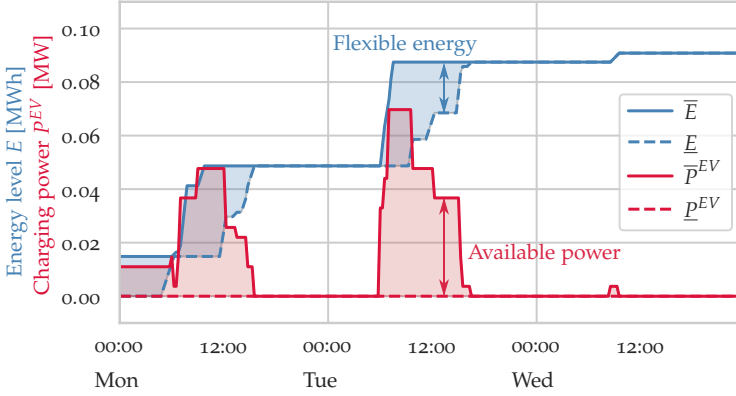


FIGURE 3.11: Lower and upper bounds of charging power and energy level at exemplary charging park.

$$y_{c,t}^{EV}, y_{c,t}^{V2G} \in \{0, 1\} \quad \forall c \in C, t \in T, \quad (3.16)$$

where  $e_{c,t}$  is the energy level for station or aggregate of EVs or stations  $c$ , i.e. cumulative electricity consumption of  $c$ ,  $\eta_{EV}$  and  $\eta_{V2G}$  are the charging and discharging efficiencies and  $\underline{p}_{c,t}^{EV}$  and  $\bar{p}_{c,t}^{EV}$ ,  $\underline{E}_{c,t}$  and  $\bar{E}_{c,t}$  are the time-dependent lower and upper bound on charging power and energy level. These are obtained with the help of the EV driving schedules and depend on the assumed level of EV flexibility. The binaries  $y_{c,t}^{EV}$  and  $y_{c,t}^{V2G}$  are introduced to prevent simultaneous charging and discharging of the EVs. In (3.14), the cumulative actual energy withdrawal at each station is fixed to the mean of the lower and upper energy band at the beginning and end of the simulation period to avoid that EVs simply minimise their consumption by converging towards the lower energy bound towards the end of the simulation.

If V2G is not possible, (3.10) can be simplified to:

$$e_{c,t} = e_{c,t-1} + \eta_{EV} \cdot p_{c,t}^{EV} \cdot \Delta t \quad \forall c \in C, t \in T \setminus \{0\}, \quad (3.17)$$

and (3.12), (3.15) and (3.16) omitted. We then arrive at a simplified linear version of the problem set comprising (3.17), (3.11), (3.13) and (3.14).

### *Application to Flexibility Scenarios*

The flexibility scenarios defined in Section 3.2.4 result in different energy and power envelopes. The considered use cases thereby change which stations or charging use cases are included in set  $C$ . The influence on the envelopes themselves is described below for each flexibility scenario.

*EVs Flex and Flex+*: The upper power  $\bar{P}_{c,t}^{EV}$  is restricted by the charging power of connected EVs and charging stations. The lower power is set to  $\underline{P}_{c,t}^{EV} = 0$  since no discharging is allowed in this case. The energy boundaries are determined for each charging station by applying two different charging strategies. The upper band  $\bar{E}_{c,t}$  represents a charging strategy where the EV directly charges upon arrival with the maximum charging power until the charging demand is met. The lower bound  $\underline{E}_{c,t}$  represents a behaviour where the EV charges as late as possible with full charging power.

*EVs Flex++*: This scenario's power and energy bands are obtained for individual EVs instead of aggregated to charging stations. They follow the assumption that the SoC of an EV has to stay within certain limits: a minimum SoC ( $SOC_{min}$ ) and a maximum SoC ( $SOC_{max}$ ) that should both not be exceeded at any point in time. The minimum SoC is assumed to be  $SOC_{min} = 20\%$  and the maximum SoC is set to  $SOC_{max} = 100\%$ . The lower energy band is calculated so that the EV charges as late as possible. This means that the EV charges at the latest possible occasion, with just enough energy for the next driving event such that the SoC does not drop below  $SOC_{min}$  during the driving session. The upper energy boundary represents a charging as early as possible, meaning that after every driving session, the EV charges as soon as possible until  $SOC_{max}$  is reached. The minimum power is set to zero. The maximum charging power is the nominal power of the charging point if the car is plugged in for a parking session; otherwise, it is zero.

*EVs V2G*: In this scenario, V2G is allowed in addition to shifting over standing times. To account for this, the lower power bound  $\underline{P}_{c,t}^{EV}$  is set to the same values as  $\bar{P}_{c,t}^{EV}$ , meaning that the EVs can discharge at the same rates as they can charge. If the EV is disconnected, the lower power band stays at zero. The discharging efficiency is assumed to be the same as the charging efficiency  $\eta_{V2G} = \eta_{EV} = 0.9$ .

### 3.2.7 *Critical Reflection*

In this section, we want to critically reflect on input data and modelling assumptions and their influence on the results.

#### *Input Data*

Modelling results are always dependent on the input data. As large-scale measured data sets with all the required information to model flexible charging are still missing, we use synthetically created travel and charging profiles to model EVs and their flexibility. To assess the plausibility of the modelled profiles, we compare the annual electricity consumption per EV and the resulting charging profiles with other studies and measured data from the literature in the following.

The integration of EVs leads to an increase in electricity consumption. Therefore, the influence of EV integration will also depend on how much additional consumption is expected. To put the results into perspective, we therefore compare the resulting mean electricity consumption per EV with values from other studies ( [117]–[120] ) in Fig. 3.12. It is visible that our assumed electricity consumption for EVs is on the lower end. However, it still lies within assumed literature values and therefore shows a reasonable order of magnitude. The relatively low value might be because our investigations are limited to private vehicles, which show different driving behaviours from commercially used vehicles. To showcase the influence of this factor, we include the values of total electricity consumption per vehicle in the German development plan when accounting for all vehicles (NEP2035) and when only accounting for privately used vehicles (NEP2035 - only private) [17]. When only accounting for privately used vehicles, the annual electricity consumption per vehicle decreases by 26.5 %, and the value is much closer to our assumed electricity consumption.

The comparison with other studies indicates that the influence of EVs could be higher than the results of this thesis imply, as the assumed consumption is on the lower end. On the other hand, technology development could increase efficiency and reduce the electricity consumption of EVs. Overall, projections of technology uptakes are always subject to uncertainty. Therefore, all results for temporal and geographic flexibility needs should not be interpreted with absolute numbers but more for trends and tendencies.

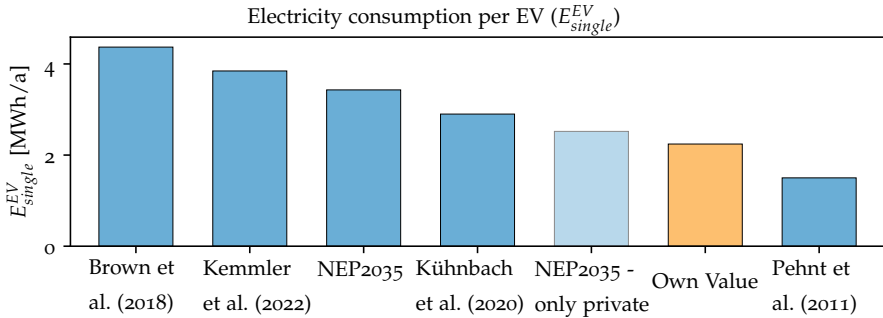


FIGURE 3.12: Annual electricity consumption of a single EV in comparison with other studies.

Not only the overall electricity consumption of EVs is an important factor but also when this additional demand occurs and what is the peak demand. We therefore qualitatively compare the charging pattern with empirical data from [121]. The empirical data comprised charging events collected in three field trials: *CROME*, *iZEUS* and *Get eReady*. The over 100 EVs in *CROME* and 327 EVs in *Get eReady* were mainly used by companies, while the over 50 EVs in *iZEUS* were mainly used privately. Figure 3.13 shows the mean daily (top) and weekly (bottom) charging patterns from the literature (left) and the simulated values used in this thesis (right). The daily consumption is standardised to 4.44 kWh and the weekly profile to 41.051 MWh following [121] to enable a direct comparison.

Overall, the daily charging pattern resembles the load profile in [121] well, showing a similar shape and peak value. In both profiles, there are peaks in the morning and evening. However, the morning peak in [121] seems to be slightly later, around 9:00. In contrast, the peak in our data occurs around 8:00. Furthermore, the morning peak in their measured profiles is wider, showing the lowest value around 13:30 while in our data, the lowest value occurs around 11:00. Another difference is that there are two separate afternoon/evening peaks in the measured profiles, around 16:00 and 18:00 in the measured profiles. In the simulated profiles, only one broader peak around 18:00 is visible.

The weekly profiles show larger differences but are also more difficult to compare because of the different temporal resolutions. Both profiles show different charging behaviours during the week and over the weekends. However, the difference is more pronounced in the measured profiles

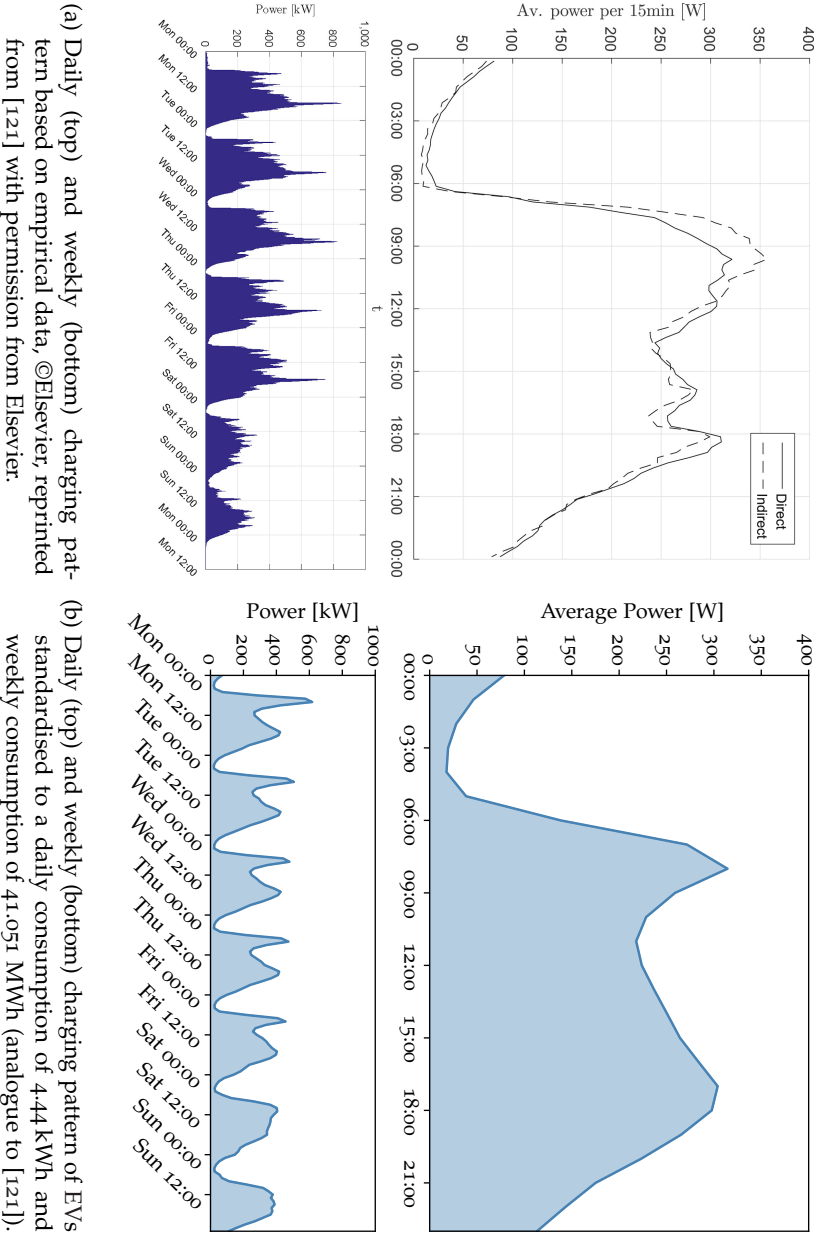


FIGURE 3.13: Comparison of daily and weekly charging patterns with empirical data from the literature.

in [121], showing significantly lower weekend consumption. One reason for the difference in measured and simulated profiles could be that in the measured trial runs, two of the three studies consisted of vehicle fleets used within organisations or companies [121]. Naturally, their utilisation on the weekends will be lower than for privately owned cars. This effect was also visible in the comparison with the third case study, where most cars were privately used. There, the difference between charging processes on weekdays and weekend days was less pronounced [121].

In general, the simulated profiles resemble the measured profiles in [121] well and therefore constitute a good basis for our investigations.

### *Modelling Assumptions*

We applied several simplifications for the modelling of EVs. First, we allow the full range of charging powers from zero to the nominal charging capacity at all times and apply a constant efficiency value. We thereby omit that with higher SoC values, the active charging power decreases [121]. Furthermore, users might oppose very low active charging power values since the charging efficiency decreases [122]. While this assumption introduces inaccuracies, it is a necessary simplification to reduce the complexity to a manageable size. In aggregate, this simplification should be acceptable. Control algorithms for individual EVs or charging stations should consider these changes in efficiency, however.

Second, we use the strong assumption that the users always plug in the EV when charging infrastructure is available to estimate the maximum potential of smart charging and V2G to relieve the stress on the grids or participate in the balancing of generation and load. In reality, it would need incentives to achieve such a behaviour and use its full potential. However, we want to showcase the maximum potential of EVs in this thesis. Providing adequate incentives to users to achieve system-friendly behaviour is a second step and a different research question, which is partly touched on in Part IV but not the main focus of this thesis.

Lastly, we assume the same driving behaviour as in the historic surveys underlying `simBEV` to model the travel behaviour of EV users. This assumption omits that the charging behaviour will also be influenced by the availability of charging infrastructure and policy measures [123]. Therefore, the driving and charging behaviour might change in the future, which strongly influences the effects on the grid [124]. With this respect, efforts

exist to move from a system mainly based on individual transport to a sufficient transport system with a higher share of public transport [125]. Such a mobility transition would lead to a decreased number of private vehicles and a different utilisation of them [125], [126]. While the decreased number can be easily accounted for in scenario variations, it would be interesting to investigate the influence of adapted driving behaviour on the flexibility potential of private EVs in future work. Furthermore, the influence of autonomous driving could be integrated into future investigations.

### 3.3 HEAT PUMPS

Heat pumps offer the potential to decarbonise the heating sector by using renewable electricity for heating. Compared to other residential appliances, their nominal power values are relatively high. Furthermore, high simultaneousities are expected as the heating demand depends on the outside temperature, which is the same for neighbouring buildings. They might therefore pose high stress on the grids. Additionally, their consumption shows a seasonal pattern as heating demand is much higher in winter with additional space heating demand than in summer with only demand from domestic hot water. This seasonality poses an additional challenge for balancing supply and demand as it is exactly opposite to renewable generation from PV. On the other side, the electrification of heating also offers flexibility potential, as the latency in heating allows for a shifting of electricity demand without compromising user comfort. Furthermore, TES is much cheaper than electricity storage and could offer additional flexibility to shift the electricity demand of HPs.

The following sections explain the modelling of HPs including TES. **Section 3.3.1** includes heat demand and coefficient of performance (COP), **Section 3.3.2** the sizing of HPs and **Section 3.3.3** explains their assumed reference operation. In **Section 3.3.4**, different levels of HP flexibility are introduced. **Sections 3.3.5 and 3.3.6** describe the modelling of HPs with lossy and ideal TES for flexibility provision. We want to critically reflect on the chosen input data and modelling assumptions in **Section 3.3.7**.

#### 3.3.1 Heat Demand and COP

We want to investigate the influence of increasing penetrations of residential HPs on geographical and temporal flexibility needs. The HPs cover residen-

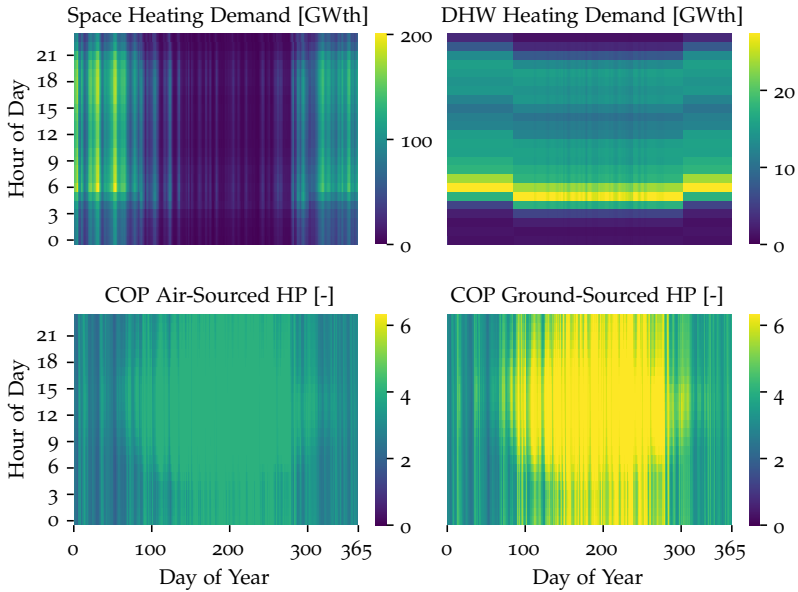


FIGURE 3.14: Heat demand for space heating (upper left) and DHW (upper right) and COP for air- (lower left) and ground-sourced (lower right) floor heating.

tial heat demand and operate with a time-varying COP. For heat demand and COP, we use input data from *WHEN2HEAT* [127], [128]. This data set comprises national building heat demand time series in an hourly resolution and COP time series that depend on the heat source and sink.

Figure 3.14 displays the thermal heating demand for space heating (upper left) and domestic hot water (DHW) (upper right) for single family houses and the COP time series for air- (lower left) and ground-sourced (lower right) heat pumps for floor heating. The time series are displayed for a representative year<sup>8</sup> and the heating time series are scaled with the space heating and DHW demand of private households in Germany in 2020 (space heating: 504 TWh, DHW: 105 TWh) [129].

Both space heating demand and COP show a seasonal effect. While the space heating demand is higher in winter, the COP values show the opposite tendency. In general, the COP time series of air- and ground-sourced HPs show a similar pattern, but ground-sourced HPs display higher absolute

<sup>8</sup> In line with later investigations, we use 2011 as a representative weather year [87].

TABLE 3.12: Parameters of  $\gamma$ -distribution for HPs.

Shape	Location	Scale	Min	Max
5.43	-0.77	2.54	0 kW	35 kW

values for the COP. On the other hand, the heating demand for DHW does not show a strong seasonality. However, it shows a daily pattern with a peak in the morning hours. All displayed time series show higher values during the day than at night. This effect is most pronounced for DHW heating demand.

### 3.3.2 Sizing of HPs and TES

We use a probabilistic approach to simulate increasing penetrations of residential HPs inside the distribution grids. Therefore, residential loads inside the simulated grids are randomly selected until the desired penetration is reached. The size of the HPs is again randomly chosen from a probability distribution, and heat demand and TES are scaled accordingly. For the six investigated grids, a total of 31 518 heat pumps has thus been modelled at a 100 % penetration of HPs. For the national investigations, we assume that this number is large enough to account for statistical deviations and use the resulting mean values for HP and TES sizes.

We size HPs according to current sales statistics and fit a gamma distribution to input data on the number of installed HPs by nominal thermal capacity in 2021 [130]. Since no capacity-specific values were available for Germany, we use data from Switzerland. The extracted values are displayed in Tab. 3.12 and result in a distribution with a mean thermal capacity of  $P_{mean}^{HP,th} = 13.0 \text{ kW}$ , which is displayed in Fig. 3.15. The size of residential HPs is assumed to lie between 0 kW and 35 kW. Random draws from the gamma distribution outside this window are mapped to 0 kW and 35 kW, respectively. In accordance with [131], a share of 80 % air-source and 20 % ground-source HPs is assumed.

The electrical power  $P_{hp}^{HP,el}$  of the HP is obtained by:

$$P_{hp}^{HP,el} = \frac{P_{hp}^{HP,th}}{\min(COP_{hp,t})} \quad \forall hp \in HP, \quad (3.18)$$

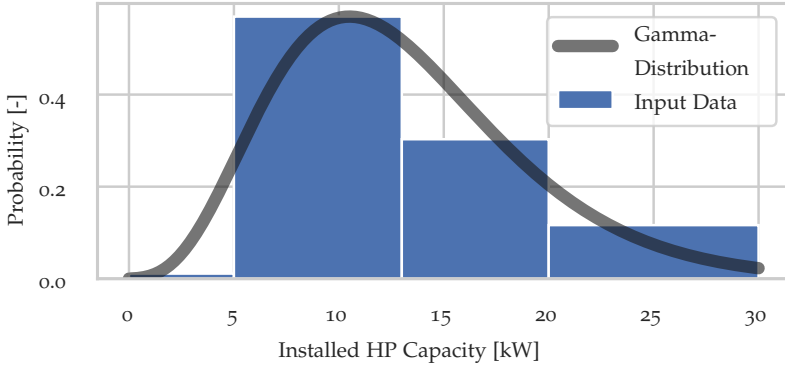


FIGURE 3.15: Input data and fitted gamma-distribution for sizing of residential HP systems.

where  $P_{hp}^{HP,th}$  is the nominal thermal capacity drawn from the gamma distribution and  $\min(COP_{hp,t})$  the minimum of the annual COP time series provided by [127]. We assume that the installed thermal capacities of the HPs are chosen in a way that the maximum heat demand of the household can be met while also accounting for blocking hours imposed by the grid operator. In [17], these blocking hours are set to a total of six hours per day, i.e.  $T_{day}^B = 6$  h, with a maximum of two consecutive hours, i.e.  $T_{cons}^B = 2$  h. The installed thermal power  $P_{hp}^{HP,th}$  of the HP is assumed to be oversized in a way that it can compensate for the daily blocking hours. It follows:

$$P_{hp}^{HP,th} = \frac{24h}{24h - T_{day}^B} \cdot \max(P_{hp,t}^{D,th}) \quad \forall hp \in HP, \quad (3.19)$$

where  $P_{hp,t}^{D,th}$  is the heat demand of the building for time step  $t$ . With  $P_{hp}^{HP,th}$  drawn from the distribution, we obtain this building-specific heat demand time series by using the rated heat demand time series from [127] and scaling it so that (3.19) is fulfilled. The mean annual heat demand of the resulting time series equals 21.5 MWh. The heat storage installed with a HP is assumed to be configured such that it can cover the heat demand of the two consecutive blocking hours  $T_{cons}^B$ . We therefore scale the size of the TES to meet the maximum heat demand of two consecutive hours in  $P_{hp}^{D,th}$  and obtain a medium storage size of 18.3 kWh. The size of the TES is later varied to model different levels of flexibility (see Section 3.3.4).

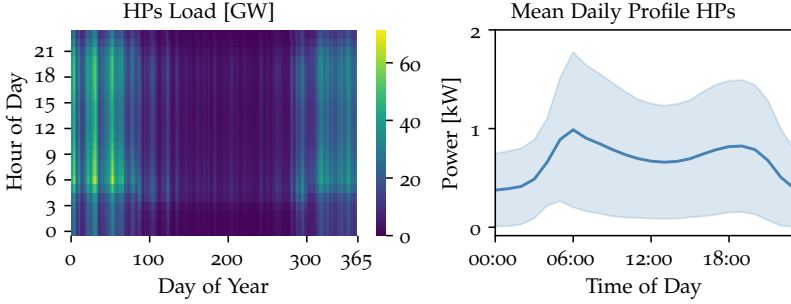


FIGURE 3.16: Electrical power of 100% HP penetration (left) and mean daily pattern per HP with standard deviation (right).

### 3.3.3 Reference Operation

In the case of reference operation, HPs are assumed to provide the heat demand directly, so their active power consumption  $p_{hp,t}^{HP,el}$  is calculated by:

$$p_{hp,t}^{HP,el} = \frac{P_{hp,t}^{D,th}}{COP_{hp,t}} \quad \forall hp \in HP, t \in T, \quad (3.20)$$

where  $P_{hp,t}^{D,th}$  is the thermal demand of the household and  $COP_{hp,t}$  the coefficient of performance of the heat pump.

Figure 3.16 shows the resulting electricity demand for 100% HP penetration on the left, meaning that all residential buildings in Germany (i.e. 19.4 Mio.) are equipped with a HP. On the right, the mean daily electricity consumption profile per HP with the standard deviation as the shaded area is displayed. The electricity consumption shows a strong seasonal pattern, with higher consumption in the winter, which is caused by higher space heating demand and lower COP values. On the daily scale, a peak is present in the early morning hours and the late afternoon.

### 3.3.4 HP Flexibility

We want to investigate the influence of HP integration with different levels of flexibility. Table 3.13 includes the different modelled levels of flexibility. In the reference scenario (*HPs Ref.*), HPs are operated with reference operation and do not offer any flexibility. In the flexible scenarios (*HPs Flex*, *Flex+*

TABLE 3.13: Levels of flexibility modelled for HPs

Name	Level of Flexibility
HPs Ref.	None - HP reference operation
HPs Flex	Flexibility to shift heat demand by at least two hours; 2 h-TES, $C_{mean}^{TES} = 18.3$ kWh
HPs Flex+	Flexibility to shift heat demand by at least four hours; 4 h-TES, $C_{mean}^{TES} = 36.6$ kWh
HPs Flex++	Flexibility to shift heat demand by at least eight hours; 8 h-TES, $C_{mean}^{TES} = 73.2$ kWh

and *Flex++*), HPs are equipped with TES to offer the flexibility to shift the thermal demand without compromising user comfort. The originally scheduled heat demand  $P_{hp,t}^{D,th}$  stays the same and has to be always covered. The electricity demand of the HP, on the other hand, can be altered using the TES.

*HPs Flex*: In this scenario, the HPs are equipped with TES that can shift the highest thermal demand of two consecutive hours. This is the period that DSOs were allowed to block thermal devices (cf. § 7 BTOElt<sup>9</sup>). In combination with the heat demand time series and sales statistics of HPs (further detailed in Section 3.3.2), we arrive at a mean thermal capacity of  $C_{mean}^{TES} = 18.3$  kWh.

*HPs Flex+* and *HPs Flex++*: For these scenarios, the energy capacity of the TES is doubled, respectively quadrupled, compared to the *HPs Flex* scenario. This way, a minimum of four, respectively eight, hours of heat demand can be shifted by the TES.

### 3.3.5 Model Formulation with Lossy TES

HPs are modelled including a TES, which can be used to shift the demand:

$$p_{hp,t}^{HP,el} = \frac{p_{hp,t}^{HP,th}}{COP_{hp,t}} \quad \forall hp \in HP, t \in T, \quad (3.21)$$

<sup>9</sup> In new regulations starting from 2024, the power of controllable loads can be capped to 4.2 kW instead of blocking them entirely [132].

$$p_{hp,t}^{HP,th} = P_{hp,t}^{D,th} + y_{hp,t}^{TES,ch} \cdot p_{hp,t}^{TES,ch} - y_{hp,t}^{TES,dis} \cdot p_{hp,t}^{TES,dis} \quad \forall hp \in HP, t \in T, \quad (3.22)$$

$$\begin{aligned} soe_{hp,t}^{TES} &= \eta_{stat}^{TES} \cdot soe_{hp,t-1}^{TES} + (\eta_{dyn}^{TES} \cdot y_{hp,t}^{TES,ch} \cdot p_{hp,t}^{TES,ch} \\ &\quad - y_{hp,t}^{TES,dis} \cdot p_{hp,t}^{TES,dis}) \cdot \Delta t \quad \forall hp \in HP, t \in T \setminus \{0\}, \end{aligned} \quad (3.23)$$

$$soe_{hp,t}^{TES} = \frac{1}{2} \cdot C_{hp}^{TES} \quad \forall hp \in HP, t \in \{0, t_{end}\} \quad (3.24)$$

$$0 \leq p_{hp,t}^{HP,th} \leq P_{hp}^{nom,th} \quad \forall hp \in HP, t \in T, \quad (3.25)$$

$$0 \leq soe_{hp,t}^{TES} \leq C_{hp}^{TES} \quad \forall hp \in HP, t \in T, \quad (3.26)$$

$$y_{hp,t}^{TES,ch} + y_{hp,t}^{TES,dis} \leq 1 \quad \forall hp \in HP, t \in T, \quad (3.27)$$

$$y_{hp,t}^{TES,ch}, y_{hp,t}^{TES,dis} \in \{0, 1\} \quad \forall hp \in HP, t \in T, \quad (3.28)$$

where  $p_{hp,t}^{HP,el}$  is the electricity demand of the HPs and  $p_{hp,t}^{HP,th}$  the thermal demand of the HPs constrained by the nominal thermal capacity of the HPs  $P_{hp}^{nom,th}$ ,  $COP_{hp,t}$  the coefficient of performance,  $P_{hp,t}^{D,th}$  the heat demand,  $p_{hp,t}^{TES,ch}$  and  $p_{hp,t}^{TES,dis}$  the thermal charging and discharging of the TES,  $soe_{hp,t}^{TES}$  the state of energy of the TES constrained by its total energy capacity  $C_{hp}^{TES}$ . Heat losses of the TES are represented by the static efficiency  $\eta_{stat}^{TES}$  and losses during the charging process by the dynamic efficiency  $\eta_{dyn}^{TES}$ . For simplicity, the dynamic losses are implemented as round-trip losses and are only applied to the charging process. The binaries  $y_{hp,t}^{TES,ch}$  and  $y_{hp,t}^{TES,dis}$  are introduced to prevent simultaneous charging and discharging of the TES.

### 3.3.6 Model Formulation with Ideal TES

While the introduced formulation allows to model losses of the TES, the necessary binary variables significantly increase the complexity compared to a linear ideal formulation. Thus, for large-scale grid studies, the model formulation with lossy TES is not tractable. We therefore introduce a second, simplified formulation with ideal TES where all losses are neglected and the storage efficiency is assumed to be 100%.

The model formulation can thus be simplified to:

$$p_{hp,t}^{HP,el} = \frac{P_{hp,t}^{D,th} + p_{hp,t}^{TES}}{COP_{hp,t}} \quad \forall hp \in HP, t \in T, \quad (3.29)$$

$$soe_{hp,t}^{TES} = soe_{hp,t-1}^{TES} + p_{hp,t}^{TES} \cdot \Delta t \quad \forall hp \in HP, t \in T \setminus \{0\}, \quad (3.30)$$

$$soe_{hp,t}^{TES} = \frac{1}{2} \cdot C_{hp}^{TES} \quad \forall hp \in HP, t \in \{0, t_{end}\} \quad (3.31)$$

$$0 \leq p_{hp,t}^{HP,el} \leq P_{hp}^{nom,el} \quad \forall hp \in HP, t \in T, \quad (3.32)$$

$$0 \leq soe_{hp,t}^{TES} \leq C_{hp}^{TES} \quad \forall hp \in HP, t \in T, \quad (3.33)$$

where thermal charging and discharging of the TES are combined to a single variable  $p_{hp,t}^{TES}$ , which makes the binary variables obsolete. The thermal (dis-)charging  $p_{hp,t}^{TES}$  is indirectly constrained by the capacity of the TES, the thermal power provided by the heat pump and the heat demand at time  $t$ , assuming these are the binding limitations. The state of energy at the beginning and end of each simulated day is set to  $\frac{1}{2}C_{hp}^{TES}$ .

### 3.3.7 Critical Reflection

Again, we want to reflect on input data and modelling assumptions and how they affect the modelling results.

#### *Input Data*

First, we compare the assumed electricity consumption per HP to other studies ([117], [118], [133], [134]) in Fig. 3.17. We can see that the electricity consumption for HPs is comparably high but lies within the range of other literature values. The relatively high values could be because we use current sales statistics for the sizing, which do not include possible increases in efficiency and building retrofits. Literature values considering these developments might obtain lower values. Furthermore, it is likely that currently, mostly wealthy consumers with single family houses purchase HPs. Their heat demand tends to be higher because of the larger size of the house compared to flats, and therefore, current sales statistics might overestimate the mean size of HPs in a fully electrified system.

We use input data from WHEN2HEAT, which provides national time series data, as input for the heat demand. While these are suitable for an applica-

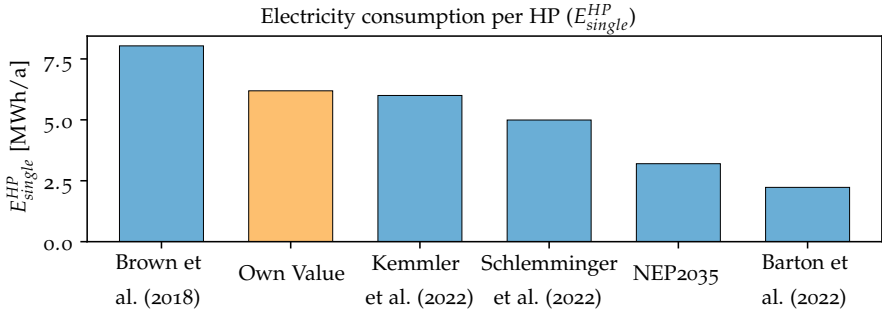


FIGURE 3.17: Annual electricity consumption of a single HP in comparison with other studies.

tion to the national system, they introduce inaccuracies when applied to individual HPs in the DGs. Aggregated time series data already smoothed out the peak demands of individual consumers. Therefore, the grid reinforcement needs in the lower voltage levels will likely be underestimated when using aggregated demand time series. Similarly, the reduction potential through a smart operation will most likely be underestimated, as peaks are already smoothed out and all consumers have the same heating demand profile. However, a comparative study showed that while aggregated time series data underestimated the influence of HPs on grid issues, the main insights stayed the same [135]. We therefore trust that the main results are still robust even with the aggregated profiles. For further investigations, we want to point out that the newer version of the grids comes with disaggregated building-specific heating profiles and could serve as a basis for future case studies with more realistic heating profiles [98].

### *Modelling Assumptions*

On the modelling side, we use a simplified energy-based modelling of HPs and TES. These models are of low accuracy but can be used for determining seasonal energy use or economic investigations [136]. In reality, the COP not only depends on the time but also the operation point of the heating system and the temperatures of the inlet and outlet [137]. With higher compressor speeds, the COP decreases, which correlates with high power values [137]. Therefore, peak demand might be higher than estimated in our investigations and, consequently, also the influence on the grid.

Part of the simplified energy-based model is the assumption that the original heating demand is not altered. In reality, the thermal inertia of the building allows a limited shifting of the heating demand without compromising user comfort [138]. While directly including a detailed building model is not feasible, a soft coupling of models could allow for a more realistic representation of building flexibility in future work. In a master thesis co-supervised in the course of this thesis [139], this was done by including flexibility envelopes determined with detailed building models from [138] into the optimisation. This way, other influencing factors, such as gains from solar radiation and building occupancy, could be included in the simulations. However, a comparison of both approaches has not been carried out but would be interesting for future work.

In our work, heat pumps operate continuously between zero and the nominal thermal capacity. Traditionally, thermal devices operated differently, using a control scheme where the heat pumps are either fully turned on at nominal capacity or turned off. The heat pump would turn off when a maximum temperature is exceeded and turn on again when the temperature drops below a minimum bound. However, with future technological advancements, an adapted operation is possible. We furthermore model a temporal resolution of 15 minutes to one hour, within which on-off cycling could also result in continuous values. When on-off cycles have to be deployed, the potential to decrease peaks might be lower, and the original peaks higher than in our investigations. This would likely mean a higher stress on the grids and additional shifting requirements to balance demand and supply (although the influence on the latter should be low).

### 3.4 BATTERY ELECTRIC STORAGE

Already nowadays, many residential PV systems are equipped with BESS to increase the self-consumption of PV [18]. Naturally, BESS offer a high flexibility potential as their primary use is flexibility provision. They could both benefit the grid by reducing peaks from PV feed-in and electricity demand and the balancing of generation and load by shifting PV feed-in into times of higher demand. Current regulations incentivise self-consumption. While residential BESS therefore help balance local PV generation and demand, there are no real incentives to reduce the grid impacts. In this thesis, we investigate the potential of BESS to target both flexibility needs, the temporal shifting of generation and demand and the geographical needs of the grid.

TABLE 3.15: Parameters of  $\gamma$ -distribution for PV.

Shape	Location	Scale	Min	Max
190.89	-46.09	0.29	0 kW	20 kW

The remainder of the Section is structured as follows. In **Sections 3.4.1 and 3.4.2**, the sizing and reference operation of BESS is explained. **Sections 3.4.3 and 3.4.4** describe the modelling of lossy and ideal BESS and **Section 3.4.5** critically reflects on input data and modelling assumptions.

### 3.4.1 Sizing of Batteries

We assume that BESS are only installed in households that also own a PV system and that batteries are sized relative to the size of the PV plant. The energy capacity of the BESS is scaled with a fixed ratio of 1 kWh/kWp [140] relative to the installed capacity of the PV plant. The rating of charging power to energy capacity is set to 0.6 kW/kWh [140].

The size of the PV plant, in turn, is drawn from a gamma distribution fitted to input data from [140], which contains sales statistics of PV systems in Germany for the years 2019 to 2021. For our investigations, we use the 2021 values. The obtained values for the fitted gamma distribution are summarised in Tab. 3.15 and both input data and fitted distribution are displayed in Fig. 3.18. The resulting distribution has a mean of 8.4 kW whereas, in line with the input data, the minimum size of a PV plant is assumed to be 0 kW and the maximum size 20 kW. If a random draw from the gamma distribution returns a value outside this range, it is adjusted to the respective extreme value.

### 3.4.2 Reference Operation

In the case of reference operation, BESS charge as soon as the PV feed-in exceeds the demand and discharge as soon as the demand exceeds the PV feed-in. Figure 3.19 shows the battery operation over the year for a scenario where every residential building in Germany is equipped with a PV-battery-system on the left. The right shows the mean daily charging profile per BESS and its standard deviation. It shows that the batteries

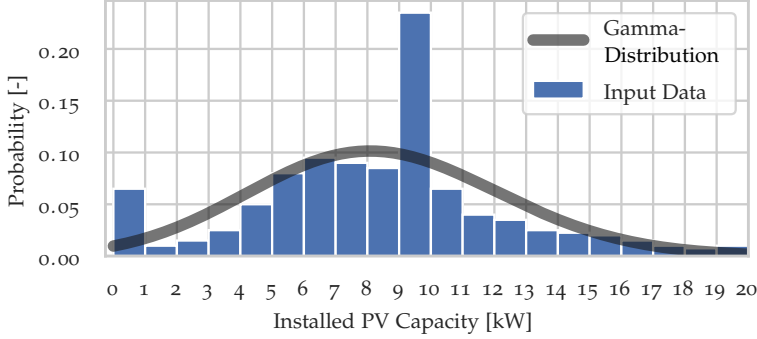


FIGURE 3.18: Input data and fitted gamma-distribution for sizing of residential PV systems.

mainly charge before noon and discharge in the evening. Next to the daily, there is also a seasonal pattern, where in summer, the charging starts earlier and the discharging later than in winter. This effect is caused by the PV feed-in, which shows the same seasonality. However, while PV feed-in is highest around noon and in the early afternoon, the battery charging shows close to no charging in these times. The low values imply that usually, the batteries are fully charged at that time and will not reduce feed-in peaks of PV.

### 3.4.3 Model Formulation with Lossy Battery

BESS are modelled with the following formulation:

$$soe_{bs,t}^{BS} = soe_{bs,t-1}^{BS} + \left( \eta_{bs}^{BS,ch} \cdot y_{bs,t}^{BS,ch} \cdot p_{bs,t}^{BS,ch} - \frac{y_{bs,t}^{BS,dis} \cdot p_{bs,t}^{BS,dis}}{\eta_{bs}^{BS,dis}} \right) \Delta t \quad \forall bs \in BS, t \in T \setminus \{0\}, \quad (3.34)$$

$$soe_{bs,t}^{BS} = \frac{1}{2} \cdot C_{bs}^{BS} \quad \forall bs \in BS, t \in \{0, t_{end}\} \quad (3.35)$$

$$0 \leq soe_{bs,t}^{BS} \leq C_{bs}^{BS} \quad \forall bs \in BS, t \in T, \quad (3.36)$$

$$0 \leq p_{bs,t}^{BS,ch} \leq p_{bs}^{nom} \quad \forall bs \in BS, t \in T, \quad (3.37)$$

$$0 \leq p_{bs,t}^{BS,dis} \leq p_{bs}^{nom} \quad \forall bs \in BS, t \in T, \quad (3.38)$$

$$y_{bs,t}^{BS,ch} + y_{bs,t}^{BS,dis} \leq 1 \quad \forall bs \in BS, t \in T, \quad (3.39)$$

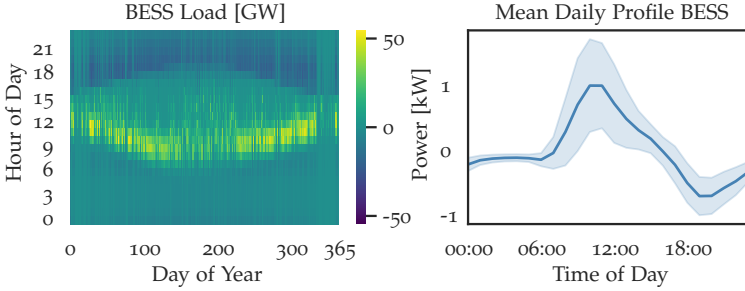


FIGURE 3.19: Electrical power of 100 % PV and BESS penetration, i.e. every residential building owns a PV system with BESS, (left) and mean daily pattern per BESS with standard deviation a shaded areas (right).

$$y_{bs,t}^{BS,ch}, y_{bs,t}^{BS,dis} \in \{0,1\} \quad \forall bs \in BS, t \in T, \quad (3.40)$$

where  $C_{bs}^{BS}$  is the battery capacity,  $P_{bs}^{nom}$  the nominal charging power and  $\eta_{bs}^{BS,ch}$  and  $\eta_{bs}^{BS,dis}$  are the charging and discharging efficiencies of the battery. The state of energy  $soe_{bs,t}^{BS}$  evolves according to charging  $p_{bs,t}^{BS,ch}$  and discharging  $p_{bs,t}^{BS,dis}$  of the battery. In order to ensure that charging and discharging never occur at the same time, the binaries  $y_{bs,t}^{BS,ch}$  and  $y_{bs,t}^{BS,dis}$  are introduced.

#### 3.4.4 Model Formulation with Ideal Battery

To investigate the maximum positive effect, we model the BESS with an efficiency of 100 %, resulting in the following set of constraints:

$$soe_{bs,t}^{BS} = soe_{bs,t-1}^{BS} + p_{bs,t}^{BS} \cdot \Delta t \quad \forall bs \in BS, t \in T \setminus \{0\}, \quad (3.41)$$

$$soe_{bs,t}^{BS} = \frac{1}{2} \cdot C_{bs}^{BS} \quad \forall bs \in BS, t \in \{0, t_{end}\} \quad (3.42)$$

$$-P_{bs}^{nom} \leq p_{bs,t}^{BS} \leq P_{bs}^{nom} \quad \forall bs \in BS, t \in T, \quad (3.43)$$

$$0 \leq soe_{bs,t}^{BS} \leq C_{bs}^{BS} \quad \forall bs \in BS, t \in T, \quad (3.44)$$

where  $soe_{bs,t}^{BS}$  is the state of energy of the battery system  $bs$ ,  $C_{bs}^{BS}$  the battery capacity,  $p_{bs,t}^{BS}$  the (dis-)charging power and  $P_{bs}^{nom}$  the nominal power. The

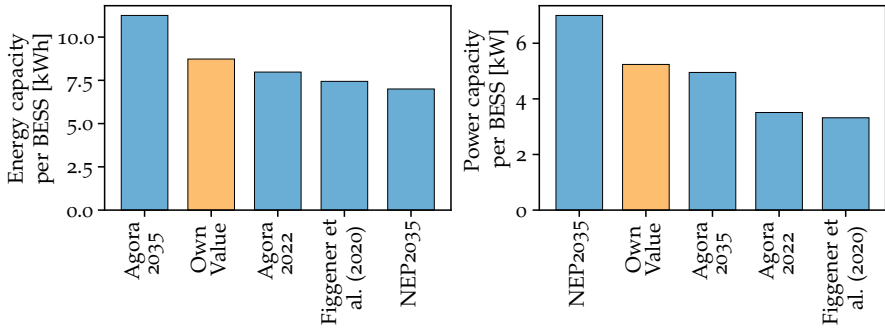


FIGURE 3.20: Mean battery energy and power capacities in comparison with selected studies.

state of energy at the beginning and end of each simulated day is set to  $\frac{1}{2}C_{bs}$ .

### 3.4.5 Critical Reflection

As for the other flexibility options, we want to discuss the input data and modelling assumptions, their limitations and their influence on the results.

#### *Input Data*

In Fig. 3.20, we compare the obtained mean values for energy and power capacity per BESS with the values used in the German network development plan [17], a recent study on household flexibility (evaluated for the years 2022 and 2035) [141] and a study comprising empirical data (evaluated for the year 2018) [142]. The values are in good accordance with the investigated literature values, especially when considering the trend for increasing capacities in the future [141].

In our studies, battery storage is always sized relative to PV systems. While this is a reasonable assumption, the values might differ and vary in reality. When accounting for differences in relative size, some of the BESS might be full earlier than others and the total flexibility potential consequently lower.

Furthermore, we do not account for the influence of possible policy measures. Their influence is clearly visible in the input data for the size of PV

systems in Fig. 3.18. There are peaks for sizes below 1 kW and 10 kW. These are caused by regulations that apply for PV systems with sizes larger than 1 kW and 10 kW. To avoid the more complex rules, customers choose PV systems sizes accordingly. It can thus be assumed that if other regulations come into place, the sizes of both PV systems and connected BESS might change accordingly. While these effects are out of scope for this thesis, it would be interesting to investigate the interplay with political incentives in future research.

### *Modelling Assumptions*

We choose a relatively simple static model for battery storage to limit the complexity. First, the efficiency is modelled by a fixed value. In reality, the efficiency also depends on the charging power. While this introduces inaccuracies, these are acceptable for our large-scale investigations. Furthermore, no aging is implemented. The available flexibility is therefore overestimated since the available battery capacity decreases with time and the number of cycles.

Another strong assumption is that the full battery capacity is available for the flexibility service at hand. This allows us to investigate the maximum potential of BESS to reduce the stress in the distribution grid and balance supply and demand on a system level. However, in reality, only a limited share of the battery storage might be available for these services if there are also other objectives of the customer, e.g. increasing PV self-consumption or limiting battery ageing.

## FLEXIBILITY POTENTIAL OF DECENTRALISED FLEXIBILITY OPTIONS

---

In the introduction of this thesis, a rough estimation of the power and energy capacities being introduced into the German system by decentralised flexibility options was provided (see Fig. 1.2). It shows that with increasing shares of decentralised flexibility options (DFOs), massive amounts of storage are introduced to the system. However, these are not always available for EVs and HPs. EVs are not always connected to the grid since their main purpose is to provide mobility and not all parking opportunities offer charging infrastructure. HPs, on the other hand, show a high seasonality in heat demand, which also influences the energy available for shifting [143].

In this chapter, we want to approximate the flexibility from DFOs that can be used for different flexibility services. Therefore, we determine the flexible energy and available power within the six different distribution grids for a 100 % penetration of DERs and provide an estimate for entire Germany. We thereby account for the temporal availability of EVs and HPs and the different levels of flexibility described in the previous chapter.

The remainder of the chapter is structured as follows. **Section 4.1** introduces the method for estimating the flexibility potential. **Section 4.2** introduces the case study, including investigated numbers of DFOs and the different levels of flexibility. In **Section 4.3**, the results are presented and discussed. Lastly, **Section 4.4** draws conclusions.

### 4.1 METHODOLOGY - ESTIMATION OF FLEXIBILITY POTENTIAL

To estimate the flexibility potential within the grids, we use the concept of flexibility envelopes, introduced in Section 3.2.6. It is applied to estimate the available power (difference between maximum and minimum power bounds), further detailed in **Section 4.1.1**, and the available flexible energy (difference between maximum and minimum energy bounds), further detailed in **Section 4.1.2**. Figure 4.1 displays the principal concepts for the estimation of the flexibility potential of the different DFOs and flexibility

levels, described in more detail in the following sections. For simplification, we assume ideal storage units, i.e. 100% efficiency for BESS and TES.

#### 4.1.1 Available Power

We define the available power  $AP_{dfo,t}$  as the difference between maximum and minimum power values ( $\bar{P}_{dfo,t}$  and  $\underline{P}_{dfo,t}$ ), that a DFO can take at a certain time step if the component is connected to the power system:

$$AP_{dfo,t} = \bar{P}_{dfo,t} - \underline{P}_{dfo,t} \quad \forall dfo \in \{BESS, EV, HP\}, t \in T. \quad (4.1)$$

If the component is not connected to the power system (e.g. an EV while driving), the available power is zero  $AP_{dfo,t} = 0$ .

For EVs, the power bounds depend on the modelling assumptions (see Section 3.2.6). If V2G is not available, the lower power bound is always zero. In case of V2G, on the other hand, the lower power bound is equal to the negative upper power bound (see Fig. 4.1 - upper left, lower subplot). The upper power bound depends on whether the EV is parked and on the charging location. For parking events where the EV was originally scheduled to charge, the upper power bound is limited by the maximum powers of the EV and the charging infrastructure. In driving sessions, the upper power is always zero since the EV is not connected to the grid in these times. Similarly, if the EV is parked but no charging infrastructure is available, the upper power is always zero. A difference between the investigated levels of EV flexibility (see Tab. 3.10) occurs for parking sessions where charging infrastructure is available but the EV was not originally scheduled to charge. If only shifting within the charging sessions is allowed (i.e. for *EVs Flex+* and *EVs Flex* - upper subplot in Fig. 4.1 upper left), the upper power bound is zero in these parking sessions. Conversely, if shifting between different charging sessions is allowed (i.e. for *EVs Flex++* and *EVs V2G* - lower subplot in Fig. 4.1 upper left), the upper power bound is limited by the maximum power of the EV and the charging infrastructure.

The upper power of HPs is calculated assuming that the TES is empty and filled as far as possible within the given time step in addition to the thermal heat demand of that time step  $P_{hp,t}^{D,th}$ . Furthermore, it is assumed that the TES is only filled to a level  $E_{hp,t}^{TES}$  that can be emptied within 24 hours. This additional constraint is added to avoid unrealistically high flexibility in summer when heat consumption is low. The maximum electrical power of

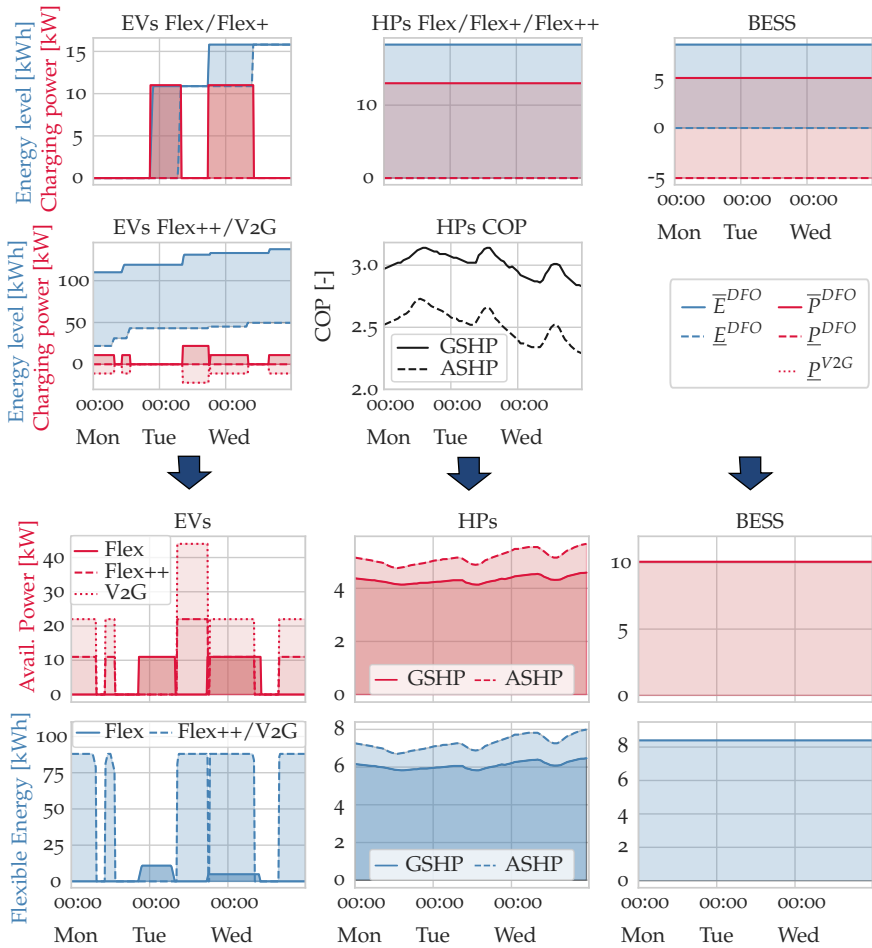


FIGURE 4.1: Concept for the estimation of the flexibility potential of EVs, HPs and BESS. Note that the energy levels and charging powers for EVs are displayed for a charging station for *EVs Flex* and *EVs Flex+* and for an individual EV for *EVs Flex++* and *EVs V2G*. The charging sessions are thus not aligned in these cases.

the HP  $\bar{P}_{hp,t}^{HP,el}$  is additionally constrained by the installed thermal power of the heat pump  $P_{hp}^{nom,th}$ :

$$\bar{P}_{hp,t}^{HP,el} = \min \left( \frac{P_{hp}^{nom,th}}{COP_{hp,t}}, \frac{E_{hp,t}^{TES} / \Delta t + P_{hp,t}^{D,th}}{COP_{hp,t}} \right) \quad \forall hp \in HP, t \in T, \quad (4.2)$$

$$E_{hp,t}^{TES} = \min \left( C_{hp}^{TES}, \sum_{t_1=t+1}^{t+25} P_{hp,t_1}^{D,th} \right) \quad \forall hp \in HP, t \in T, \quad (4.3)$$

where  $COP_{hp,t}$  is the coefficient of performance of the HP. In winter with high heat consumption, the installed capacity of the HP is the constraining factor (as displayed in Fig. 4.1 - upper center).

The minimum bound  $\underline{P}_{hp,t}^{HP,el}$  describes a situation where the TES is filled and supplies the thermal demand  $P_{hp,t}^{D,th}$  as far as possible. Again, we assume that the storage is only filled to a level  $E_{hp,t}^{TES}$  that can be used in the following 24 hours:

$$\underline{P}_{hp,t}^{HP,el} = \max \left( 0, \frac{P_{hp,t}^{D,th} - E_{hp,t}^{TES} / \Delta t}{COP_{hp,t}} \right) \quad \forall hp \in HP, t \in T, \quad (4.4)$$

where  $COP_{hp,t}$  is the coefficient of performance of the HP, and  $\Delta t$  is the time increment of the calculation (one hour in our investigations). The underlying assumption is that the TES can supply its full capacity within that time horizon. An additional constraint would have to be included for shorter temporal resolutions that limits the thermal power of the TES.

Battery storage has no temporal restrictions on the available power. Both upper and lower limits are thereby constrained by the nominal power capacity of the battery since discharging is allowed to the same extent as charging (see Fig. 4.1 - upper right).

#### 4.1.2 Flexible Energy

Similar to the available power, we define the flexible energy  $FE_{dfo,t}$  as the difference between maximum and minimum energy values ( $\bar{E}_{dfo,t}$  and

$\underline{E}_{dfo,t}$ ), that a DFO  $dfo$  can take at a certain time step if the component is connected to the power system:

$$FE_{dfo,t} = \bar{E}_{dfo,t} - \underline{E}_{dfo,t} \quad \forall dfo \in \{BESS, EV, HP\}, t \in T. \quad (4.5)$$

Again, the flexible energy is zero  $FE_{dfo,t} = 0$  if the component is not connected to the power system since the flexibility is unavailable at these times. This is the case for EVs that are driving or parking in locations where no charging infrastructure is available. In Fig. 4.1 (left), this effect can be observed for *EVs Flex++* and *EVs V2G* Monday around noon to Tuesday morning.

The upper bound of the cumulative energy consumption of EVs is obtained by simulating a charging behaviour to charge as early as possible. For *EVs Flex* and *EVs Flex+*, this means charging at nominal power at the beginning of the charging session until the originally scheduled charging demand of that session is met. For *EVs Flex++* and *EVs V2G*, it means that after each driving event, the first opportunity is used to recharge the EV battery fully. Conversely, the lower bound reflects a behaviour where EVs charge as late as possible, always charging just enough to make the next trip without violating a minimum state of charge in case of *EVs Flex++* and *EVs V2G*. For *EVs Flex* and *EVs Flex+*, the lower bound is obtained by charging the originally scheduled amount at the end of the charging session at nominal charging capacity. For further details, see Section 3.2.6.

For HPs, the TES provides flexibility to shift the heat demand. To estimate the flexible energy available to the power system, we calculate the thermal flexible energy (i.e. maximum minus minimum cumulative thermal energy consumption) for every time step and divide it by the COP. The maximum cumulative energy consumption translates into a consumption as early as possible and the minimum cumulative energy consumption as late as possible. For the minimum cumulative thermal energy consumption, the TES would thus be emptied initially supplying the heat demand of the initial time steps, and the thermal demand would be directly supplied by the HP in the subsequent time steps. Similarly, for the maximum cumulative thermal energy consumption, the TES would be filled in the beginning to achieve a higher consumption at the start. In the subsequent time steps after the TES is fully charged, the thermal heat demand would also be directly supplied by the HP. Again, we assume that the TES is only filled to a level

that can be consumed within 24 hours. If losses of the TES were accounted for, these would be added to the upper energy band.

As described, consuming as early as possible and consuming as late as possible lead to the same behaviour of directly supplying the heat demand with the HP after the initial phase of filling, respectively emptying, the TES. After these first time steps, the thermal available flexible energy (i.e. the difference between upper and lower energy bound) is therefore equal to the energy level of the TES in the previous time step  $E_{hp,t-1}^{TES}$  as defined in (4.3)<sup>1</sup>. Since we are interested in the electrical available flexible energy  $FE_{hp,t}^{HP,el}$ , the thermal value is adjusted by the coefficient of performance  $COP_{hp,t}$ :

$$FE_{hp,t}^{HP,el} = \bar{E}_{hp,t}^{HP,el} - \underline{E}_{hp,t}^{HP,el} = \frac{E_{hp,t-1}^{TES}}{COP_{hp,t}} \quad \forall hp \in HP, t \in T, \quad (4.6)$$

where  $\bar{E}_{hp,t}^{HP,el}$  and  $\underline{E}_{hp,t}^{HP,el}$  are the upper and lower energy bands of the heat pump. In winter with high heat demand, the thermal capacity of the TES is the constraining factor, and the thermal available energy is constant (as displayed in Fig. 4.1 - upper center). On the other hand, the energy consumption of the previous 24 hours (determining the energy level of the TES) is limiting in summer, leading to a variation in thermal flexible energy in these times.

Like the available power, the flexible energy of BESS is always available and has no temporal restrictions. The flexible energy of a BESS is therefore equal to its energy capacity  $C_{bs}^{BS}$  (see Fig. 4.1 - upper right).

#### 4.2 CASE STUDY - 100 % DER PENETRATION

We want to estimate the absolute flexibility potential for the six investigated distribution grids in case of 100 % DER penetration, i.e. every residential load owns a home charging station, a HP with TES and PV system with battery storage. Since we assume that in future renewable power systems PHEVs will not play a significant role [144], only BEVs are considered in this investigation. The resulting values for the numbers, aggregated power and energy capacities, and electricity consumption of the integrated DFOs are summarised in Table 4.1. All values are obtained following the

<sup>1</sup> For the following investigations, we assume a settled operation, i.e. do not account for the initial time steps of filling, respectively emptying, the TES.

TABLE 4.1: Number, installed power and energy capacities of DFOs in the six investigated grids at 100 % DER penetration.

	Number [-]	Power Capacity [MW]	Energy Capacity [MWh]	Electricity Consumption [MWh]
EVs	128 520	1495.2	7901.6	292 340.5
HPs	31 518	173.9	560.8*	179 491.1
BESS	31 518	165.1	275.2	-

\*The energy capacity for HPs is the *thermal* capacity of the TES in the *HPs Flex* scenario.

TABLE 4.2: Extrapolated number, installed power and energy capacities of DFOs in Germany at 100 % DER penetration.

	Number [Mio.]	Power Capacity [GW]	Energy Capacity [GWh]	Electricity Consumption [TWh]
EVs	48.8	567.8	3000.2	111.0
HPs	19.4	107.0	345.2*	110.5
BESS	19.4	101.6	169.4	-

\*The energy capacity for HPs is the *thermal* capacity of the TES in the *HPs Flex* scenario.

modelling assumptions introduced in the previous chapter (see Section 3.2 for EVs, Section 3.3 for HPs and Section 3.4 for BESS).

For the extrapolation for entire Germany, we scale the numbers such that 48.8 Mio.<sup>2</sup> EVs and 19.4 Mio.<sup>3</sup> HPs and PV systems with BESS are present in the system. The resulting power and energy capacities, and electricity consumption are displayed in Table 4.2.

The flexibility potential is calculated for the different levels of EV and HP flexibility, introduced in Sections 3.2.4 and 3.3.4, and a battery scenario with standard sizing of BESS as explained in 3.4.1, denoted as *Battery* in the following. For clarity, the most important assumptions for the different scenarios are briefly summarised in the following.

<sup>2</sup> Number of private cars in Germany at the beginning of 2023 [112].

<sup>3</sup> Number of residential buildings in Germany in 2021 [145].

**EVS FLEX & EVS FLEX+:** For these lower levels of EV flexibility, only shifting within the originally scheduled charging session is allowed. For *Evs Flex*, only charging at home and work charging stations is assumed to be flexible. For *Evs Flex+*, public charging is additionally assumed flexible.

**EVS FLEX++ & EVS V2G:** For these higher levels of EV flexibility, shifting between different charging sessions is allowed (as long as charging infrastructure is present), even if not charging demand was originally scheduled in some of these sessions. For this, charging at home, work and public charging stations is assumed flexible. This charging use case including all charging sessions with available charging infrastructure will be denoted as *extended* in the following. For *Evs Flex++*, only unidirectional charging is allowed while for *Evs V2G*, discharging of the EVs is possible.

**HPS FLEX, HPS FLEX+ & HPS FLEX++:** In all HP scenarios, each HP is equipped with a TES. The size of TES varies between the investigated levels of flexibility. In *Hps Flex*, the TES is sized to supply the two hours of highest consecutive heat demand, resulting in a mean thermal energy capacity of 18.3 kWh. For *Hps Flex+* and *Hps Flex++*, the size of the TES is doubled and quadrupled.

**BATTERY:** Batteries are sized according to the PV system with which they are installed. These are scaled according to recent sales statistics. The resulting mean power and energy capacities for batteries amount to 5.2 kW and 8.7 kWh.

### 4.3 RESULTS AND DISCUSSION

We present the flexibility potential of DFOs along their temporal availability (over the year), their aggregated potential in the investigated distribution grids, appliance-specific and extrapolated values for entire Germany in the following.

#### 4.3.1 Flexibility Potential over the Year

We first present the available power and flexible energy over the year for EVs and HPs. These results are only presented for EVs and HPs since BESS are always available for flexibility services in our investigations. While the real available power and flexible energy of BESS are dependent on the

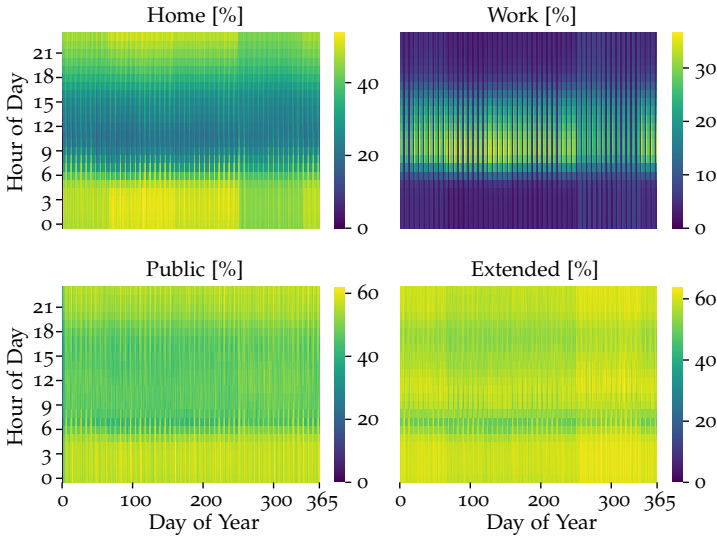


FIGURE 4.2: Available power of flexible EVs over time of day and day of year relative to the installed charging capacity.

temperature and consequently also on the time, we do not model battery storage in sufficient detail to account for these effects. However, they are assumed to be small in comparison with the changing availability of EVs and HPs and therefore not considered.

The available power and flexible energy of EVs depend on the time of the day and considered charging use cases. Figure 4.2 displays the available power in percent of installed charging capacity for home, work, public charging and the extended case. For home, work and public charging, only parking sessions are included when the EV is originally scheduled to charge (i.e., not allowing shifting between standing times in *EVs Flex* and *EVs Flex+*). In the extended case, all charging use cases (i.e. home, work and public) and parking events when the EV is plugged in are considered (to account for shifting between standing times in *EVs Flex++* and *EVs V2G*).

The relative available power for home charging is highest at night and shows low values during the day. For work charging, the opposite is the case. Public and extended charging combine both, showing a more evenly distributed availability, where public charging still shows lower values during the day. The mean available powers relative to installed charging

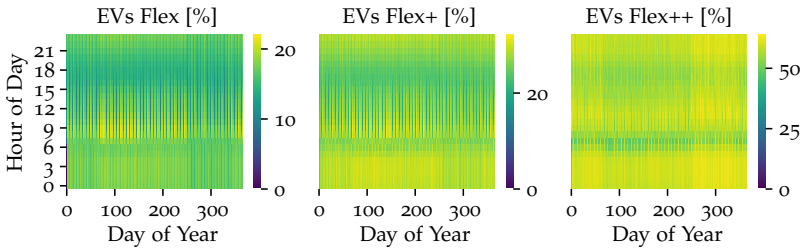


FIGURE 4.3: Available power of EVs over time of day and day of year for different levels of flexibility relative to installed charging capacity of all home, work and public charging stations.

capacity are 35.8 %, 10.6 %, 50.5 % and 57.2 % for home, work, public and extended charging. The installed charging capacities differ, with 489.2 MW, 633.6 MW and 306.1 MW of home, work and public charging stations and extended charging being the combination of the other three charging use cases.

Combining the different charging use cases for the investigated levels of flexibility leads to the distribution in Fig. 4.3, displaying the available power relative to the installed charging capacity of all home, work and public charging stations over the day of year and hour of the day. For *EVs Flex*, the highest available power occurs in the mornings, which can be explained by the higher installed charging capacities for work charging. On the other hand, the available power is similarly high in the mornings and at night when including public charging stations in scenario *EVs Flex+* since the available power is higher at night for public charging (see Fig. 4.2). For *EVs Flex++*, the available power significantly increases since parking sessions where charging did not originally occur are included. Furthermore, the available power is always relatively high, showing the minimum values in the mornings when many cars travel to work and in the late afternoon when driving home. The mean available powers relative to the installed capacity of all home, work and public charging stations are 16.1 %, 26.4 % and 57.2 % for *EVs Flex*, *EVs Flex+* and *EVs Flex++*. For *EVs V2G*, the available power would be double that of *EVs Flex++* since negative charging powers of the same magnitude are allowed in this case.

The flexible energy relative to total battery capacity of EVs is displayed for the scenarios *EVs Flex*, *EVs Flex+* and *EVs Flex++* in Fig. 4.4. For *EVs V2G*, the values are the same as for *EVs Flex++*. For the scenarios *EVs*

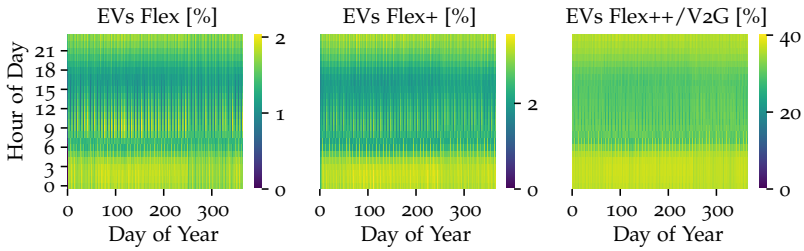


FIGURE 4.4: Flexible energy of EVs over time of day and day of year for different levels of flexibility relative to total battery capacity of the EVs.

*Flex* and *EVs Flex+*, the highest relative values occur at night and the lowest in the early morning (around 7:00) and in the late afternoon (around 17:00). These are the times when most vehicles are driving and therefore unavailable for shifting. The higher flexible energy at night is in contrast to the highest available power in the mornings (see Fig. 4.3). This indicates that the charging powers are higher at work but more of the charging demand is charged at home. Scenario *EVs Flex++* shows a more even distribution for the flexible energy during the day but also lower values than at night. The mean flexible energy relative to total EV battery capacity drastically increases when allowing shifting over standing times, from 1.5% and 2.6% for *EVs Flex* and *EVs Flex+* to 32.5% for *EVs Flex++* (and *EVs V2G*).

Figure 4.5 shows the available power relative to installed HP capacity (top) and the flexible energy in percent of thermal storage capacity of the TES divided by the minimum COP (bottom). Both show very similar patterns over the year, and the relative values for available power are independent of the level of flexibility. The available power is therefore only displayed once, while the flexible energy is differentiated for the different levels of flexibility. Both available power and flexible energy show the highest values in winter and tend to be higher during the night. The relative flexible energy during summer decreases with an increasing size of the TES. In these times, the thermal demand is low and therefore constrains the flexible energy ( $E_{hp,t}^{TES} < C_{hp}^{TES}$ ). The average available power equals to 56.5%. The mean flexible energy amounts to 54.1%, 46.8% and 39.8% for *HPs Flex*, *HPs Flex+* and *HPs Flex++*. While the relative values for flexible energy decrease with increasing flexibility level, the absolute values increase since the reference value is doubled and quadrupled in *HPs Flex+* and *HPs Flex++* relative to *HPs Flex*. The decrease in relative flexible energy can be explained by the

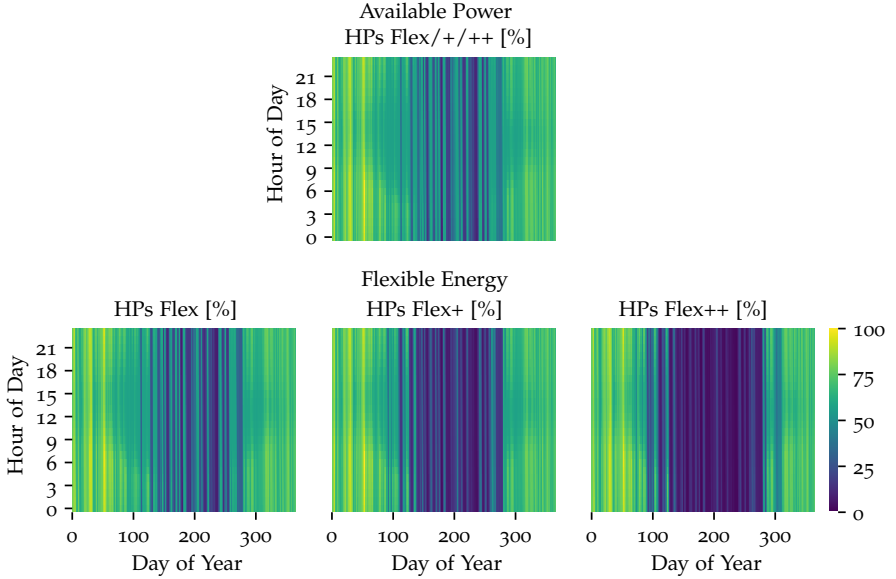


FIGURE 4.5: Available power relative to installed capacity (top) and flexible energy relative to storage capacity (bottom) of HPs over time of day and day of year.

fact that with increasing TES size, the flexible energy is constrained more often by the heat consumption, i.e. when  $E_{hp,t}^{TES} < C_{hp}^{TES}$ .

The general pattern of flexibility potential is in accordance with a previous study investigating the flexibility potential of a residential HP pool [143]. The study also showed longer periods in summer with close to no flexibility and higher flexibility in winter. In another study, the possible power deviation of a building with both EV and HP proved to be higher at night [146], which our results also indicate.

#### 4.3.2 Flexibility Potential of Investigated Distribution Grids

Next, we determine the absolute flexibility potential in the investigated distribution grids for the different flexibility scenarios in case of a 100% DER penetration, i.e. every residential load owns a HP, BESS and home charging station. The work and public charging infrastructure is scaled proportionally to the number of home charging stations. Figure 4.6 displays

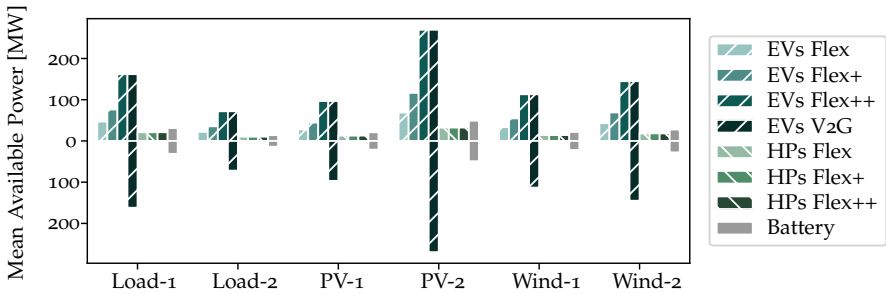


FIGURE 4.6: Mean available power in the investigated distribution grids with a 100 % DER penetration.

the mean available power over the year for the investigated distribution grids and scenarios. The results show that the available power is highest for the EV scenarios, followed by BESS and HPs in all of the grids. There is a large variance between the grids, with the largest values (PV-2) being 3.1 to 3.7 times as high as the smallest values (Load-2). This is because the grid Load-2 is mainly industrial, and the investigated flexibility is that of households and private EVs. Batteries and EVs using V2G allow discharging into the grid. Therefore, *Battery* and *EVs V2G* display negative power values as the only scenarios.

The differences in mean flexible energy, displayed in Fig. 4.7, show even higher differences. Since the flexible energy for *EVs Flex++* and *EVs V2G* is much higher than for the other scenarios, the values are displayed separately on the right. While these two EV scenarios show by far the highest values, *HPs Flex++* shows the highest values for the remaining scenarios. Again, the values vary between the different grids, with factors between the highest and lowest value per scenario ranging between 3.0 and 3.7.

The differences between the distribution grids mainly depend on the number of components. Figures 4.8 and 4.9 therefore display the mean available power and average flexible energy for individual components, i.e. per EV in the scenarios including EVs and per residential load for HPs and BESS. The black lines indicate the standard deviation between the investigated grids. For HPs and BESS, the observed differences mainly stem from the random choice of their size (see Sections 3.3.2 and 3.4.1). For EVs, additionally the driving behaviour and available charging infrastructure differs (see Sections 3.2.1 and 3.2.2). Overall, the differences prove to be small and the values in the same range for all investigated grids.

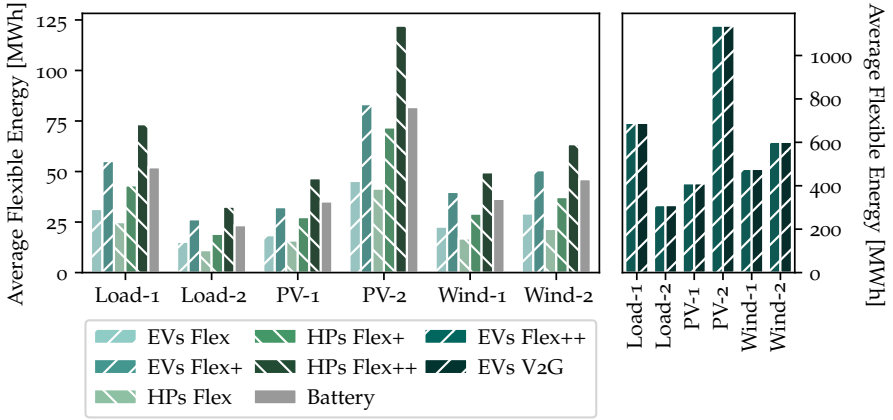


FIGURE 4.7: Mean flexible energy of the hourly profiles in the investigated distribution grids with a 100% DER penetration.

The values for mean available power and average flexible energy are highest for EVs at higher levels of flexibility (i.e. *EVs Flex++* and *EVs V2G*) with 6.6 kW per vehicle. However, the temporal availability varies over the day (see Fig. 4.2). Battery storage offers a mean available power of 5.2 kW (both charging and discharging) without temporal restrictions. Heat pumps offer a mean of 3.5 kW available power but with a high seasonal variability (see Fig. 4.5). EVs at lower flexibility levels (i.e. *EVs Flex* and *EVs Flex+*) display the lowest values with 1.9 kW and 3.1 kW. However, these require much lower coordination between the EVs and less interference with user behaviour than the higher levels of EV flexibility. They might therefore be easier to harness than the flexibility requiring shifting between standing times.

The mean flexible energy is highest for EVs when allowing shifting between standing times (i.e. for *EVs Flex++* and *EVs V2G*) with 28.1 kWh. As a comparison, the mean size of the battery for the simulated EVs is 86.5 kWh. HPs show values between 4.1-12.1 kWh for the differently sized TES in the scenarios. BESS are roughly in the same range with 8.7 kWh. When not allowing shifting between standing times, the flexible energy from EVs shows relatively low values of 1.3 kWh and 2.3 kWh for *EVs Flex* and *EVs Flex+*.

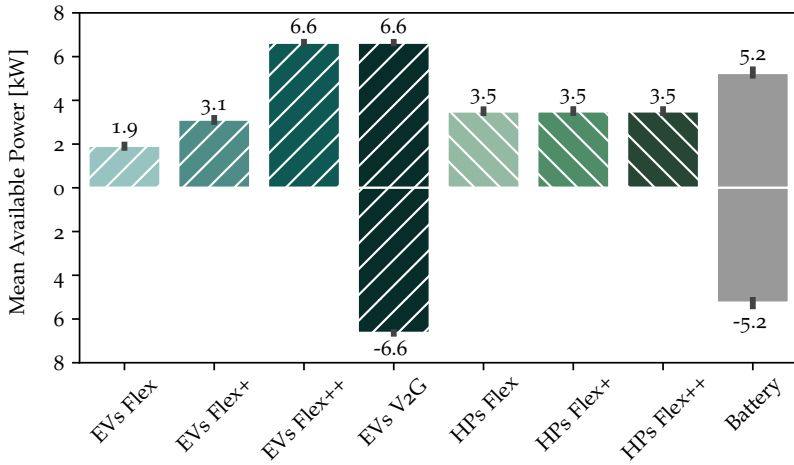


FIGURE 4.8: Mean available power per component, i.e. for an individual EV, HP or BESS.

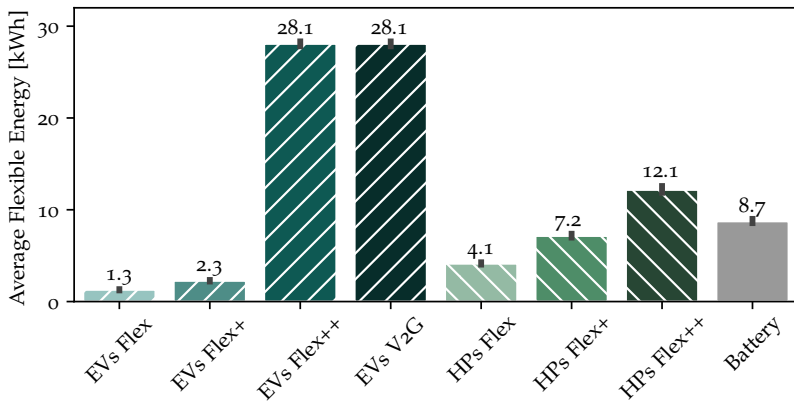


FIGURE 4.9: Average flexible energy per component, i.e. for an individual EV, HP or BESS.

### *Extrapolation for Entire Germany*

In the last step, we extrapolate the flexibility potential for entire Germany for a 100% DER penetration, i.e. 48.8 Mio. EVs and 19.4 Mio. HPs and BESS. We therefore use the mean values from Fig. 4.8 and Fig. 4.9 and scale them with the number of EVs, HPs and BESS to estimate the flexibility potential for entire Germany in the different flexibility scenarios. The obtained values only give a rough idea of the flexibility potential for 100% DER penetration since all components of the six grids are scaled linearly. For a more representative study, more grids should be included and a more realistic scaling undertaken (e.g. using the number of represented grids during the clustering and updated grids from [98]). Furthermore, it is the maximum potential without accounting for possible grid constraints that will likely occur at high DER penetrations.

The mean available power of EVs equals 92 GW, 150 GW and 325 GW for *EVs Flex*, *EVs Flex+* and *EVs Flex++*. For *EVs V2G*, the same values are available for charging (+325 GW) and discharging (-325 GW). The available power of HPs is mainly constrained by the installed HP capacity and daily heat demand. We do not vary these values in the scenarios, and therefore the available power is relatively constant at 67 GW. The available power for residential BESS is 102 GW, again available for charging (+102 GW) and discharging (-102 GW). These values are in a similar order of magnitude as in a recent study that estimated the installed capacity of decentralised flexibility options at ~500 GW in 2045, with the largest share from EVs [147]. Another study estimated the installed capacities by 2035 with ~330 GW for EV charging infrastructure, and respectively ~50 GW for HPs and BESS [141]. While they accounted for lower numbers of EVs, HPs and BESSs (roughly ~32 Mio. EVs, ~9 Mio. HPs and ~13 Mio. BESS), they did not consider the availability, thus showing similar power values for EVs and HPs but lower ones for BESS.

The estimated mean flexible energy is by far highest for EVs when allowing shifting between standing times (i.e. for *EVs Flex++* and *EVs V2G*) with 1371 GWh. HPs show values of 81 GWh, 140 GWh and 239 GWh for the differently sized TES in the scenarios *HPs Flex*, *HPs Flex+* and *HPs Flex++*. BESS are in a similar range with 169 GWh. When limiting the shifting to the originally scheduled charging session, the flexible energy from EVs shows lower values of 61 GWh and 109 GWh for *EVs Flex* and *EVs Flex+*. The flexibility potential thus strongly depends on the level of flexibility for EVs and HPs. The temporal availability reduces the available flexibility

compared to only accounting for installed power and energy capacity (e.g. [141], [147]) and should therefore be considered.

Comparing the estimated values with currently installed storage capacities from [21], both power and energy capacity would be drastically increased. The current power capacity amounts to 13 GW, 7 GW being battery storage and 6 GW pumped hydro storage (PHS) [21]. The estimated HP power is roughly five times as high as the current power capacity. However, it has to be mentioned that HPs only draw power from the grid, while the reference storage technologies allow charging and discharging. BESS show even higher values of eight-fold the reference storage capacities, allowing both charging and discharging like the other storage technologies. The highest increase in power capacity is observed by EVs at high levels of flexibility. The four investigated levels of flexibility amount to seven, twelve and twenty-five times the reference storage capacities. The higher flexibility scenarios *EVs Flex++* and *EVs V2G* lead to the same values (twenty-five-fold) but *EVs V2G* allows a discharging back into the grid. In contrast, all other scenarios only account for smart charging.

The energy capacity currently installed in Germany is 35 GWh, 11 GWh stemming from battery storage and 24 GWh from PHS [21]. The estimated flexible energy of HPs is double, four and seven times as high for the three investigated levels of flexibility. The BESS energy capacity is five times as high as the current storage capacities, and the flexible energy of EVs amounts to double, triple and thirty-nine times the current values. While both power and energy are multiples of the currently installed storage capacities, it should be considered that leveraging decentralised flexibility is much more complex than that of the central storage units. These are directly integrated into the market, and their primary purpose is to provide flexibility. The investigated DFOs, on the other side, are distributed in the system and much larger in their number but smaller in the capacities of individual units. The usable flexibility is therefore likely lower than for the central units, and the large number of assets is more difficult to coordinate than a few large ones. Furthermore, the primary goal of households is not to provide system services but to meet other needs, such as mobility or heating.

The provided numbers therefore only give a rough estimation of flexibility and constitute an upper bound. A potential use case is the provision of flexibility to overlying grid levels either for load levelling in the market or grid services like redispatch. The larger the range of energy and power

values that the DFOs has available, the higher the potential to provide these flexibility services. However, the displayed values do not consider the location or grid constraints, only the temporal availability of EVs and HPs.

While the available flexible energy reasonably estimates the potential maximum shiftable energy, it usually cannot be fully exploited. In reality, the value is significantly lower because perfect foresight in the future would be necessary to reach these extreme values. Additionally, EV owners would most probably not be willing to fully discharge their EVs to provide grid flexibility. Furthermore, if flexibility is analysed in the *EVs Flex++* and *EVs V2G* scenarios, the load shifting required to achieve such flexibility spans over longer periods. For the charging in *EVs Flex* and *EVs Flex+*, flexibility provision is limited to one charging event without influencing the later operation. Thus, the different scenarios cannot be compared directly, and the displayed values are rather used to give an idea of the order of magnitude of the available flexibility. Shifting heat demand with a TES and electricity demand with BESS, on the other side, should not compromise user comfort since the original consumption is not altered. However, for all investigated flexibility options, the right incentives would have to be given to consumers, and intelligent management would be necessary to use the available flexibility.

#### 4.4 CONCLUSION

We approximated the flexibility potential of residential EVs, HPs and BESS in terms of available power and flexible energy. To this end, we investigated the mean values per component and the temporal availability. Lastly, we determined the flexibility potential in the investigated distribution grids for 100% DER penetration and provided an estimate for entire Germany.

The flexibility potential that decentralised flexibility options could provide is immense. However, it also depends on the assumed level of flexibility of the component and is time-dependent for EVs and HPs. For both, the flexibility potential is higher at night, and HPs show a strong seasonal pattern with higher values in winter.

Broken down to individual appliances, the mean available power ranges between 1.9-6.6 kW and average flexible energy between 1.3-28.1 kWh. Both are highest for EVs if shifting between standing times is allowed. On the other hand, if the charging demand is only shifted within the

originally scheduled session, both flexibility indicators show the lowest values for EVs between the investigated technologies. For available power, BESS show higher values than HPs, independent of the modelled levels of HP flexibility. For the flexible energy, on the other hand, HPs equipped with a TES allowing eight hours of shifting (highest modelled level of flexibility) show higher values than battery storage.

The flexibility potential within the investigated grids varies by a factor of up to 3.7. It thereby mainly depends on the number of residential loads and integrated EVs. The extrapolation to entire Germany shows that the available power and flexible energy of the investigated decentralised flexibility options are drastically higher than the currently installed power and energy capacities of storage technologies in the system. The power values range between five- to twenty-five-fold. The energy values even reach between two- to thirty-nine-fold. Both show the highest values for EVs at high levels of flexibility. While these numbers prove the huge potential of decentralised flexibility options, they constitute the upper bound for flexibility, not accounting for many constraining factors like uncertainties, user preferences and grid constraints.

Furthermore, the value of flexibility largely depends on the use case. In the remaining parts of the thesis, we therefore investigate two concrete use cases: limiting the stress on distribution grids and thus reducing reinforcement needs in Part II and helping balance supply and demand in renewable power systems in Part III.



## Part II

# GEOGRAPHIC FLEXIBILITY NEEDS IN DISTRIBUTION GRIDS



## MOTIVATION AND RELATED WORK

---

### 5.1 INTRODUCTION

The energy system is undergoing a massive transition to achieve the climate targets that the international community has agreed upon [25]. Next to the shift in the power supply towards renewable energy sources (RES), there are also attempts to decarbonise the transport and heat sectors by electrification. This trend leads to growing numbers of electric vehicles (EVs) and heat pumps (HPs). Many of these technologies are directly connected to the distribution grids (DGs), leading to increased transport requirements within these lower grid levels. Additionally, residential photovoltaics (PV)-systems, which are also connected to the DGs, can lead to reverse power flows, grid congestion, and voltage issues [148]. Because of these new challenges, distribution system operators (DSOs) expect a need for grid reinforcements to accommodate the increasing shares of distributed energy resource (DER) [149].

On the other side, new consumers and battery energy storage systems (BESS) that are installed alongside PV can be operated flexibly and therefore release stress on the grids. If installed within the same grids, flexible EVs and HPs might even be able to help with the integration of RES. In this part of the thesis, we want to investigate the potential of a flexible operation of EVs, HPs and BESS to relieve distribution grids and lower reinforcement costs.

In Germany, the electricity demand for EV charging is expected to reach up to 8% of the total electricity demand in the year 2030 [150]. If all EVs would charge at the same time, e.g. when arriving at work in the morning, which is unrealistic but still interesting to consider, the peak demand would reach 74 GW [151]. This would result in a major increase in the German peak demand, which reached 79.5 GW in 2020 [151]. On the other hand, the deployment of EVs will come with massive amounts of storage introduced into the system since battery sizes of EVs are comparably large. With the ability of vehicle-to-grid (V2G) operation, meaning discharging back into

the grid, EVs could thus provide significant flexibility to the system. In a first case study, we therefore focus on the integration of EVs and the influence of different charging strategies on grid issues, reinforcement needs and flexibility potential in **Chapter 7**.

In a second case study in **Chapter 8**, we investigate the influence of increasing penetrations of EVs, HPs and PV systems with and without BESS. Again, we estimate the potential of a flexible operation to reduce the necessary reinforcement costs. We thereby investigate the uptake of each technology individually and compare it with a simultaneous integration of all investigated DERs. This comparison allows us to determine the cost driving factors and to better understand the interplay of different DERs.

## 5.2 BACKGROUND

There have been numerous studies on the grid integration of DERs. This section gives an overview over existing work and puts the contributions of this thesis into perspective. **Section 5.2.1** thereby focuses on the integration of EVs with different charging strategies and **Section 5.2.2** on the simultaneous integration of DERs.

### 5.2.1 *Integration of Electric Vehicles*

As an overview of existing studies, Table 5.1 summarises selected studies on the grid integration of EVs, which voltage levels (high voltage (HV), medium voltage (MV), low voltage (LV)) are covered in the study, whether curtailment and grid reinforcement are evaluated and which EV charging strategies are considered (rule-based, smart charging without and with V2G).

In a case study on individual MV- and LV-grids from Germany, Sweden, Spain, Portugal and Italy, the authors investigated the grid impacts of different EV charging strategies on the grids [95]. They found that most investigated MV grids had a lower EV hosting capacity than the LV grids, where sub-urban and rural grids showed higher restrictions to accommodate EV charging stations than urban ones. They found a reduction in grid reinforcement by a rule-based reduced charging strategy of 60% and by real-time smart charging by even 95% compared to uncontrolled charging. Another study compared two smart charging strategies of a work charging park within an industrial 37-bus MV distribution grid [152]. In one strategy,

TABLE 5.1: Overview on existing studies on the grid integration of EVs

Voltage Level	Grid Reinf.	Curt.	EVs Rule	EVs Smart	EVs V2G	Ref.
MV & LV	✓	✗	✓	✓	✗	[95]
MV	✗	✗	✗	✓	✓	[152]
MV	✗	✗	✗	✓	✓	[153]
MV	✓	✗	✗	✓	✓	[154]
LV	✓	✗	✗	✓	✓	[155]
LV	✗	✗	✓	✓	✗	[96]
MV & LV	✗	✓	✗	✓	✗	[23]
LV	✗	✓	✓	✓	✗	[156]
MV & LV	✓	✓	✓	✓	✓	This work

the charging costs were minimized, while the other minimised the peak-to-average ratio of the charging. While the first strategy naturally resulted in lower charging cost, only 10% EV penetration could be achieved with the existing grid infrastructure in case of slow and 0% in case of fast charging. The second strategy increased the integrated share to 60% in both cases. Similarly, the hosting capacities of the industrial IEEE 38-bus test system for coordinated work charging was assessed in [153]. The authors investigated the integration of workplace charging and applied a particle swarm optimisation to coordinate smart charging and V2G. With the optimised charging, all 800 modelled EVs could be incorporated without congestion, reducing total operational costs and improving the state of charge (SoC) at departure as well as losses.

In another study on the MV IEEE 33-bus test system, an optimised V2G operation achieved an 82% reduction of the grid reinforcement costs compared to the case without V2G [154]. In [155], the authors investigated the potential of smart charging with and without V2G to reduce CO<sub>2</sub>-emissions and charging costs and whether grid reinforcement makes sense from an economic and emissions point of view. They found that the charging costs could be reduced by a maximum of 23% by unidirectional smart charging (no V2G) and by 32% with V2G compared to uncoordinated charging. However, if only optimising for costs, the emissions partly increased. Transformer

reinforcement had positive effects on costs and emissions when leveraging V<sub>2</sub>G. For unidirectional smart charging, the additional gained flexibility did not compensate for the supplementary costs and emissions.

In a study on representative rural and urban LV-grids in Germany, the influence of EV integration with different charging strategies on grid issues was investigated [96]. The results showed that rural grids are more affected and that market-based charging leads to high peak loads and stress on the grids. A reduced charging strategy, on the other hand, can reduce the stress on the grids significantly. In another study on representative German MV grids with underlying LV grids, the authors investigated the influence of market-based EV charging on curtailment needs within the distribution grids [23]. They found that market-based charging increased load-driven curtailment and slightly decreased feed-in-driven curtailment, mainly caused by PV. Overall, the influence on feed-in-dominated, rural and suburban grids was moderate, but there was a significant increase in grid issues in urban grids.

In [157], the authors investigated the value of smart charging and time-of-use charging to lower grid costs and curtailment in California by integrating EV charging with different strategies into a power sector dispatch model. They found that overnight charging induced by a time-of-use scheme lowers grid costs but increases curtailment of RES. A study on DGs in the Netherlands assessed the influence of grid-supportive charging to minimise peak load and market-based charging to minimise charging costs [158]. The authors therefore formulated optimisation problems following different objectives for 25 typical driving profiles. In the price-based scenario, the authors found a strong influence of wind feed-in on the price, which could lead to a high simultaneity of EV charging, causing an increase in peak load.

While many aspects of the grid integration of EVs were covered, like grid reinforcement [95], [154], [155] and curtailment needs [23], none of the presented studies covers both at the same time. However, these two values allow insights into different dimensions of the grid integration of DERs. Grid reinforcement is the conventional way of dealing with grid issues and therefore a good measure to estimate the costs for integrating EVs with different charging strategies. At the same time, grid reinforcement needs depend only on the highest occurring grid issue per component, i.e. very short periods. Some of them could therefore be solved with relatively small measures, like it is currently done in Germany for smaller PV units. Since

they cannot be directly controlled by the DSO in case of emergency, they have to limit the feed-in peaks to 70% of their nominal capacity. To this end, the curtailment needs allow a more detailed investigation of when, how severe and how long the DSO would have to enact countermeasures to solve the arising grid issues. Of course, it is also an option to only assess the grid issues without a specific solution strategy, like in [96]. It allows an investigation of the severity and the duration of grid issues. However, ultimately, the goal is to avoid grid issues and estimate the required intervention. Therefore, we choose to compare grid reinforcement and curtailment needs to allow for a more holistic investigation of EV integration.

Furthermore, while all studies investigate some smart charging, none includes rule-based charging and the possibility for V2G at the same time. Our work simulates both to estimate the highest potential of EV flexibility with V2G and to compare it to simple rule-based approaches. These are less complex and have a lower need for communication between the EVs and the DSO and are therefore an attractive alternative to centrally optimised charging strategies for a real-world application. Lastly, V2G has only been studied in separate MV or LV grids of relatively small system sizes. We combine both in large-scale realistic MV grids with underlying LV grids.

### 5.2.2 *Integration of Distributed Energy Resources*

While EVs are especially interesting because of their high charging powers and storage capacities, future households will likely own more than one DER at a time. There might be synergies between different DERs, especially between local PV and new consumers like EVs and HPs. Studying the combination of EVs, HPs and PV with or without BESS is therefore a second topic addressed in this part of the thesis. Different studies in the literature have already worked in a similar direction, of which selected ones are summarised in Tab. 5.2 and further described below.

In a UK case study, the authors investigated the influence of EVs and HPs on the grid reinforcement needs in distribution grids [159]. They therefore simulated three scenarios and found that in all scenarios, there was a significant growth of electricity load by these appliances which could cause a high increase of peak load and grid expansion costs when not coordinated.

TABLE 5.2: Overview on selected studies on the grid integration of DERs

Voltage Level	EVs	HPs	PV	BESS	Smart Operation	Grid Reinforcement	Ref.
HV & LV	✓	✓	✗	✗	✓	✓	[159]
MV & LV	✓	✓	✓	✓	(✓)	✓	[22]
LV	✓	✓	✓	✓	(✓)	✓	[86]
MV	✓	✗	✓	✓	✓	✗	[160]
LV	✓	✓	✓	✓	✓	✗	[156]
MV & LV	✓	✓	✓	✓	✓	✓	This work

The smart control however could significantly reduce both peak load and grid expansion costs in all scenarios.

In a German case study, the authors investigated the effect of new electricity appliances, i.e. EVs, HPs, combined heat and power (CHP) units and PV systems with BESS, on the grid reinforcement costs of 113 real MV and LV grids. They found that there was a significant increase in grid reinforcement costs, by 145 % in the LV and 33 % in the MV. A market-oriented smart operation further increased these costs, by 16 % in the LV and 51 % in the MV. However, they used simultaneity factors for their investigations, which neglects the fact that the new peaks might not coincide with old ones and therefore do not necessarily require grid reinforcement. Furthermore, they investigated the effects of flexible charging but market-driven instead of grid-friendly.

The authors of a Swiss case study investigated the influence of increasing penetrations of EVs, HPs and PV on distribution grid reinforcement costs in LV grids [86]. They used simultaneity factors for the DERs in power flow calculations to determine grid violations and estimated the resulting costs for required grid reinforcements in an iterative approach. In their case studies, they investigated rural, suburban and urban grids. They found that PV caused more voltage violations, EVs and HPs slightly more overloading. The costs for required grid reinforcement depended on the urban setting, with higher costs in rural grids. Overall, the highest costs occurred for the integration of HPs, followed by EVs and PV. Again, the costs largely varied between different grids. While the authors gave a good indication of required grid reinforcements for DERs, they only investigated

a reference operation of these. Flexibility provision was only accounted for by additional BESS, which were found to be a cost-effective alternative for 15 % of the transformer reinforcements.

In a case study on eleven distribution grids with characteristics from the U.S., a central grid-optimised and local cost-optimised operation of DERs were compared in terms of their grid integration [160]. The authors thereby considered rooftop PV, stationary BESS, EVs and flexible demand of electric furnaces, air conditioners and water heaters. They found that the centralised approach could reduce the violations at transformers from 81 % with the local scheme to 28 %, and voltage violations from 28 % to 18 % in 2050 with high DER penetrations. They also found a reduction in peak load. However, they did not model grid reinforcement explicitly and did not include HPs in their investigations.

In a study on German LV grids, the influence of high penetrations of PV systems, EVs, HPs and BESS on grid violations and curtailment needs were investigated [156]. Without coordination, both load and feed-in needed to be curtailed to stay within the limits of the grids. Load curtailment could be avoided entirely by a smart operation of the DERs and PV self consumption doubled. While all DERs were studied in reference and smart operation, grid reinforcement was not explicitly modelled and the study was limited to the LV.

In summary, it was shown in the literature that increasing penetrations of combined DERs will lead to stress in the distribution grids if uncoordinated. In many studies, it was found that using the flexibility of EVs, HPs and battery energy storage systems (BESS), which are installed together with PV-systems, can reduce issues in the distribution grids and consequently grid reinforcement costs. However, most of them only considered single technologies and their flexibility, e.g. [10], [115], [158]. In the studies combining several DERs either not all DERs were included in the analysis [159], [160], no grid-optimised operation of the DERs was investigated [22], [86] or no grid reinforcement needs were determined [156]. In contrast, our study investigates the integration of PV with BESS, HPs and EVs, both as single components and in a combined scenario to determine the main drivers of the necessary grid reinforcement costs. Additionally, we study their effect on different medium voltage (MV)-grids with underlying low voltage (LV)-grids, where most studies only account for one or the other, e.g. [86], [156], [160], [161]. In this way, we can analyse the effect of increased penetrations of DERs and the utilisation of their flexibility on the different

grid levels as it was shown that reinforcement needs occur in both voltage levels [22].

## METHODOLOGY - OPTIMAL POWER FLOW FORMULATION

---

*This chapter introduces the optimal power flow formulation used in the following chapters. It was first introduced in the published paper: A. Heider, K. Helfenbein, B. Schachler, T. Röpcke and G. Hug, "On the Integration of Electric Vehicles into German Distribution Grids through Smart Charging", 2022 SEST [115] as part of this PhD and slightly adapted for this thesis.*

We introduce a linear power flow formulation which is applicable to large-scale distribution grid topologies. Instead of directly integrating grid reinforcement, which is intractable for large scale grids, we use a proxy to mimic a grid-optimised operation of decentralised flexibility options (DFOs). Therefore, we define a quadratic optimisation of the operation of decentralised flexibility options under consideration of grid constraints with linearised power flow equations.

### *Model Formulation*

In the following problem set, all variables are denoted by lowercase Arabic letters, while parameters are denoted by uppercase Arabic or Greek letters. Sets  $T$ ,  $N$  and  $B$  contain all investigated time steps, nodes and branches, respectively.

The objective contains two elements representing different optimisation goals. One is to minimise the required curtailment at each node  $p_n^{curt}$  to keep the power flow on lines and transformers and the voltage within allowed boundaries. The second is to minimise the component loading  $l_b$  for every line and transformer. It is an indirect way of limiting the necessary grid expansion. This leads to the following objective function:

$$\min \delta_{curt} \sum_{n \in N} \sum_{t \in T} p_{n,t}^{curt} + \delta_{load} \sum_{b \in B} \sum_{t \in T} l_{b,t}^2, \quad (6.1)$$

where  $\delta_{curt}$  and  $\delta_{load}$  are weighting factors for the two terms. For the following investigations, these are set to  $\delta_{curt} = 1$  and  $\delta_{load} = 10^{-5}$ .

The curtailment at every node  $p_{n,t}^{curt}$  is the weighted sum of curtailment of inflexible load  $p_{t,n}^{curt,l}$ , feed-in  $p_{t,n}^{curt,f}$  and DFOs  $p_{t,n}^{curt,dfo}$ :

$$p_{n,t}^{curt} = \delta_{curt,l} p_{n,t}^{curt,l} + \delta_{curt,f} p_{n,t}^{curt,f} + \delta_{curt,dfo} p_{n,t}^{curt,dfo} \quad \forall n \in N, t \in T, \quad (6.2)$$

where the weighting factors are fixed to  $\delta_{curt,l} = 1$ ,  $\delta_{curt,f} = 0.5$  and  $\delta_{curt,dfo} = 0.5$  to model a behaviour where the curtailment of feed-in and flexible units is preferable over the curtailment of conventional load.

The reactive power curtailment  $q_{n,t}^{curt,l}$  and  $q_{n,t}^{curt,f}$  are assumed to follow proportionally, i.e. the power factors of loads and generators stay constant. As reactive power provision is not the focus of this work, the power factor is assumed to be  $\cos(\phi) = 1$  for DFOs. The curtailment of active power of load, DFOs and feed-in at a node are positive and restricted by the nodal active power of load, DFOs and feed-in at that node.

The component loading  $l_b$  represents the active power flow  $p_{b,t}^*$  on a branch without curtailment of load or feed-in divided by the maximum active power  $P_{b,t}$ :

$$l_{b,t} = \frac{p_{b,t}^*}{P_{b,t}} \quad \forall b \in B, t \in T, \quad (6.3)$$

$$p_{b,t}^* = \sum_{n \in \text{down}(b)} \left( P_{n,t}^{fix} + p_{n,t}^{dfo} \right) \quad \forall b \in B, t \in T. \quad (6.4)$$

The maximum active power  $P_{b,t}$  of branch  $b$  is determined with the help of the nominal apparent power (i.e. thermal limit)  $S_b^{nom}$  of branch  $b$  and the reactive power flow  $Q_{b,t}^{fix}$  caused by all inflexible units downstream of branch  $b$ :

$$P_{b,t} = \sqrt{(S_b^{nom})^2 - (Q_{b,t}^{fix})^2} \quad \forall b \in B, t \in T. \quad (6.5)$$

To model the power flow equations, we use the linearised *Dist-Flow* equations described in [162]. It assumes that line losses can be neglected and is only applicable to radial networks. As the LV grids under inspection are all radial grids and the MV grids are assumed to be operated as open rings,

the method is suitable for this study. We therefore integrate the following set of equations for power flow on branches:

$$p_{b,t} = \sum_{n \in \text{down}(b)} \left( P_{n,t}^{\text{fix}} + p_{n,t}^{\text{dfo}} - p_{n,t}^{\text{curt,dfo}/l} + p_{n,t}^{\text{curt,f}} \right) \quad (6.6)$$

$$\forall b \in B, t \in T,$$

$$q_{b,t} = \sum_{n \in \text{down}(b)} \left( Q_{n,t}^{\text{fix}} - q_{n,t}^{\text{curt,l}} + q_{n,t}^{\text{curt,f}} \right) \quad (6.7)$$

$$\forall b \in B, t \in T,$$

$$-P_{b,t} \leq p_{b,t} \leq P_{b,t} \quad \forall b \in B, t \in T, \quad (6.8)$$

where  $p_{b,t}$  and  $q_{b,t}$  correspond to the active and reactive power flows on branch  $b$ , respectively, which are determined by active and reactive power drawn from all nodes  $n \in \text{down}(b)$  downstream of the branch in a radial network. The parameters  $P_{n,t}^{\text{fix}}$  and  $Q_{n,t}^{\text{fix}}$  describe the sum of active and reactive power of all inflexible units at node  $n$ , respectively, and  $p_{n,t}^{\text{dfo}}$  the flexible power consumption of all DFOs connected to node  $n$ .

The node voltages and the voltage drop between two neighbouring nodes  $m$  and  $n$  are described by:

$$v_{\text{slack},t} = V_{\text{nom}}^2 \quad \forall t \in T, \quad (6.9)$$

$$v_{m,t} = v_{n,t} + 2 \cdot (p_{b,t} \cdot R_b + q_{b,t} \cdot X_b) \quad \forall b \in B, t \in T, \quad (6.10)$$

$$V_{\text{min}}^2 \leq v_{n,t} \leq V_{\text{max}}^2 \quad \forall n \in N, t \in T, \quad (6.11)$$

where  $v_{n,t}$  is the squared magnitude of voltage at node  $n$ . The slack  $v_{\text{slack},t}$  at the MV-side of the station connecting the grid to the HV is set to the squared nominal voltage of the grid. Equation (6.10) describes the voltage drop over a branch, where  $R_b$  and  $X_b$  are the resistance and the reactance of branch  $b$ , respectively, and  $n$  and  $m$  are neighbouring nodes of branch  $b$ . The line capacitance is neglected in all following investigations.  $V_{\text{min}}$  and  $V_{\text{max}}$  give the allowed lower and upper bounds of the voltage and are here set to  $V_{\text{min}} = 0.9 V_{\text{nom}}$  and  $V_{\text{max}} = 1.1 V_{\text{nom}}$ .



## CASE STUDY I: INTEGRATION OF ELECTRIC VEHICLES

---

*The following chapter is extended from two published conference publications. The first case study is based on: A. Heider, K. Helfenbein, B. Schachler, T. Röpcke, and G. Hug, "On the Integration of Electric Vehicles into German Distribution Grids through Smart Charging," in 2022 International Conference on Smart Energy Systems and Technologies (SEST), 2022 [115], Copyright ©2022, IEEE. The second case study is based on: A. Heider, F. Moors, and G. Hug, "The Influence of Smart Charging and V2G on the Flexibility Potential and Grid Expansion Needs of German Distribution Grids," in 2023 International Conference on Smart Energy Systems and Technologies (SEST), 2023 [163], Copyright ©2023, IEEE. We provide more in-depth results for the first case study and investigate additional levels of flexibility in the second case study compared to the original publications.*

The emission reduction goals for the transport sector adopted by the German government call for a reduction of 40-42 % of CO<sub>2</sub>-emissions by 2030 [164]. With these emission targets, a growing share of electric vehicles (EVs) seems without alternative. A high share of the electric vehicle (EV) charging will thereby take place in medium voltage (MV) and low voltage (LV) grids. Recent research has found that a high penetration of EVs can lead to severe voltage and component overloading issues within the grids [100]. However, the negative impact can be reduced by making use of the available flexibility of the charging process and adapting the charging strategies of EVs [165], [166]. Both the severity of grid issues and the effectiveness of different charging strategies likely depend on the types of grids. In grids with high shares of variable renewable energy sources (VRES) such as wind and PV, a coordinated charging could even support the integration of VRES [167].

Literature furthermore shows different effects for the simultaneous integration of EVs with photovoltaics (PV) and wind feed-in (e.g. [23]). It indicates that the optimal charging strategy is dependent on the composition of technologies present in the distribution grids (DGs). However, a systematic analysis of the influence of different charging strategies on such differently

composed grids is still missing. We close this research gap by examining typical German DGs divided into PV-, wind- and load-dominated grids to address the following research questions:

- How do different charging strategies influence the simultaneous integration of EVs and renewable energy sources (RES) into the different grid types?
- What are the main factors determining the effectiveness of the charging strategies?
- How do different levels of flexibility influence the effects on the grid?

In the following, we compare smart charging that allows shifting within the originally scheduled charging session with other rule-based charging strategies and investigate different levels of EV flexibility.

In the first case study in **Section 7.1**, we investigate the potential of centrally optimised charging to reduce grid issues and curtailment or grid reinforcement needs to solve these issues. Since centrally optimised charging might be hard to implement, we compare the results to rule-based charging strategies to extract suggestions for the effective grid integration of EVs.

In the second case study in **Section 7.2**, we compare optimised EV charging at different levels of EV flexibility with respect to their potential to reduce the necessary curtailment and grid reinforcement. The levels of flexibility differ in three aspects. First, which charging use cases are assumed to be flexible; Second, if charging is only allowed within the originally scheduled charging session or between different parking events; And last, whether or not the vehicle-to-grid (V2G) service is available. This way, the effectiveness of different flexibility measures to increase EV flexibility is evaluated regarding their ability to reduce geographic flexibility needs.

## 7.1 COMPARISON OF RULE-BASED AND OPTIMISED EV CHARGING

In the first step, we want to compare optimised and rule-based charging strategies. While the optimisation of EV charging is a good way to measure the maximum potential to limit the stress on DGs, it might not be feasible to implement a centrally optimised charging of EVs in reality. We therefore compare it to rule-based charging strategies. They might be easier to implement and could therefore replace the central optimisation, which is computationally expensive and requires high coordination between grid operators and EV owners.

The remainder of the section is structured as follows. **Section 7.1.1** describes the setup of the study, including investigated grids, charging strategies and the measures of comparison. In **Section 7.1.2**, the results are presented and discussed, further divided into the obtained EV charging patterns, the flexibility potential, arising grid issues as well as curtailment and grid expansion needs to solve these issues, and in **Section 7.1.3** conclusions are drawn.

### 7.1.1 Study Setup

Fig. 7.1 shows the research design used in this study. The individual steps are further detailed in the indicated sections or below. We use the six representative grids for the target year 2035 introduced in Section 3.1.5. The charging demand is determined as described in Section 3.2.1 and integrated to the grids as described in Section 3.2.2. With the help of charging demand and standing times, we determine the flexibility potential in terms of shiftable energy and available power and the resulting charging time series with the different charging strategies. In a last step, curtailment and grid reinforcement costs are determined.

To allow for a manageable problem size with the temporally and spatially highly resolved data, we choose two representative weeks for each grid for all following investigations. To account for extreme load and feed-in conditions, the weeks of maximum and minimum residual load are used.

#### *Flexibility Potential*

Flexibility is modelled as described in Section 3.2.4. For our study, we use the *Flex* scenario for EVs (see Tab. 3.10). It assumes that charging is only

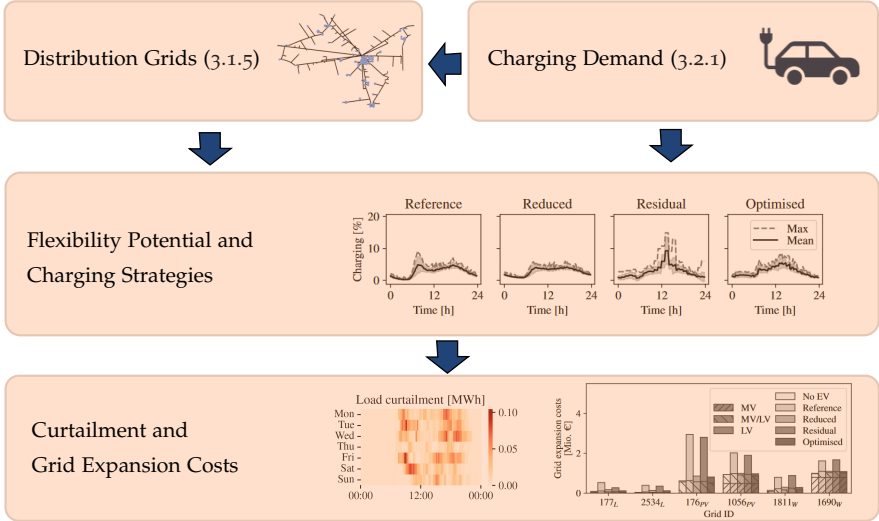


FIGURE 7.1: Research design of study.

shifted within the original standing time and not between different parking events so that consumer convenience is not compromised. Further, only charging at home and work is considered flexible, as in the case of public charging and high power charging (HPC) the priority lies in the fulfilment of the service.

### *Optimised Charging*

Since in the *Flex* scenario, charging demand and charging location are predetermined, we use the concept of flexibility envelopes introduced in Section 3.2.6. The charging of EVs is modelled with constraints (3.17), (3.11), (3.13) and (3.14) and is used as a flexible resource in the optimal power flow (OPF) formulation (6.1)-(6.11) in Section 6.

To allow for reasonable computation times, we apply spatial and temporal complexity reduction for the optimisation. Spatially, all feeders connected to the high voltage (HV)-MV-station are treated separately in the optimisation. As the MV-side of the transformer is set as slack in the power flow calculations, the feeders do not influence each other in terms of power flows on branches and node voltages. On the temporal scale, the optimisation is solved iteratively for the individual days of the two selected weeks. Each day is solved with an overlap of six hours into the next day to determine

the initial charging power and energy level for the following day. To ensure the feasibility of the optimisation problem, (6.8) and (6.11) as well as the initial charging state for consecutive days are relaxed through respective slack variables, which are strongly penalised in the objective function. For clarity, we do not include the slack variables in the equations.

### *Rule-Based Charging*

The optimised charging is compared to uncoordinated charging, referred to as reference charging, as well as two heuristic charging strategies, namely reduced and residual load charging, developed in [108].

**REFERENCE CHARGING** assumes an uncontrolled charging of charging processes. This corresponds to a start of the charging process immediately after arriving at a charging point and charging at full capacity until the full charging demand is met.

**REDUCED CHARGING** aims to reduce the stress on the grid by lowering charging powers to a minimum. It does so by expanding the charging process over the full standing time and charging at a reduced rate. This reduced rate is thereby bound by an assumed technical lower limit of 10 % of the nominal power of the respective charging point.

**RESIDUAL LOAD CHARGING** is based on [168]. It aims at smoothing the residual load within the MV grids by shifting charging demand into times with low residual load. For this, charging of an EV takes place at nominal capacity within the time steps that show the lowest residual load.

### *Curtailement and Grid Expansion Costs*

With the obtained charging profiles as well as feed-in of generators and demand profiles of the other loads described in Section 3.1.5, the results of an AC power flow calculation performed with the open-source tool *PyPSA* [78] serve as the basis for calculating the required curtailment and grid expansion necessary to stay within the voltage and current flow constraints. We use the values for normal operating conditions, described in Section 3.1.2. The maximum allowed voltage deviation is thus set to 10 % and the maximum allowed component loading to 100 %. To calculate the necessary curtailment to stay within these bounds, we use the methodology described in Section 3.1.4. The feed-in respectively load is therein iteratively reduced in steps of 1 % until all grid issues are resolved. The calculation of

grid expansion measures utilises the reinforcement method implemented in eDisGo [75], more thoroughly described in Section 3.1.3. It comprises heuristics of grid expansion measures to solve voltage and overloading issues.

### 7.1.2 Results and Discussion

The following sections present and discuss the results of our investigations. First, the charging profiles and charging peak load for the different charging strategies are displayed. Next, we showcase the flexibility potential of smart charging. Lastly, we evaluate the influence of the charging strategies on arising grid issues, necessary curtailment and grid expansion costs, respectively.

#### *EV Charging*

Fig. 7.2 shows the charging profiles of the different charging strategies for a representative PV-dominated grid (*PV-1*). Table 7.1 additionally contains absolute charging peaks and simultaneities relative to the installed capacity of charging infrastructure for all investigated grids and charging scenarios. In the case of reference charging, we see a charging peak at 7:45 and a slightly lower one around 18:00. These times correspond to times when a high share of cars arrive at work and home, respectively. Reduced charging decreases these peaks but displays a similar charging profile. While the charging peak load for reference charging ranges between 7.5-9.2% of the installed charging capacity in the different grids, it is lowered to 5.6-6.9% through reduced charging. Residual load charging displays a peak around 14:15, which results from a relatively high PV feed-in and decreasing load towards the afternoon and therefore a trend of shifting the charging to this time. Another smaller peak is visible in the early morning hours. The charging profile of residual load charging differs for the different types of grids but always displays the described peaks. In wind-dominated grids, higher variability of the daily charging pattern is observed. The charging peak load for residual load charging ranges between 9.7-14.9% of the installed charging capacity. This constitutes a significant increase in the EV peak load compared to the reference charging. However, this increase is seen in times of low residual load, therefore the peak of the overall residual load in the DG is not increased. As expected, the residual load charging strategy leads to the biggest smoothing effect of the overall residual load (see Fig. 7.3). The optimised charging displays a similar course as the residual

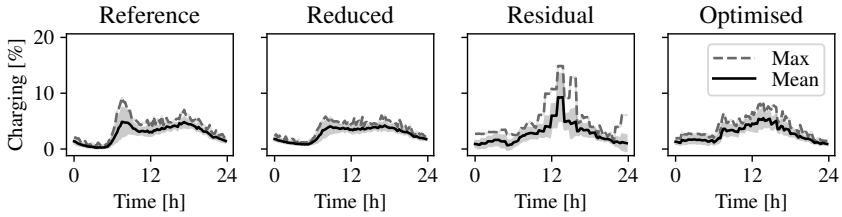


FIGURE 7.2: Daily mean and maximum of charging profiles of the different charging strategies in percent of total installed charging capacity for representative PV-dominated grid *PV-1*. Grey area displays the standard deviation computed from the 14 simulated days of the two representative weeks.

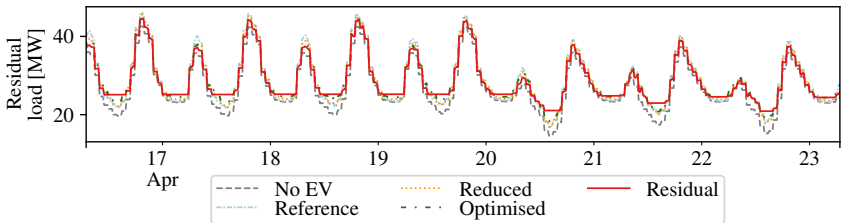


FIGURE 7.3: Residual load of the representative load-dominated grid *Load-1* in the week of minimum residual load for the different charging strategies.

load charging but lowers the charging peaks. This effect leads to a decreased charging peak load for the optimised charging of 5.8-8.3% of the installed charging capacity.

### *Flexibility Potential*

With the proposed method, it is possible to quantify and visualise the expected flexibility potential of EV charging in terms of available power and shiftable energy. The available power and shiftable energy are calculated by subtracting the lower bounds from the upper bounds, respectively. Fig. 7.4 shows the shiftable power in percent of the installed capacity of charging stations and the shiftable energy in percent of mean daily energy consumption using reference charging in a representative load-dominated grid.

TABLE 7.1: Maximum (absolute and relative) charging peaks in the different grids and EV charging scenarios.

	Maximum EV charging peak [MW] / (Simultaneity [%])			
	Reference	Reduced	Residual	Optimised
Load-1	5.8 (8.7)	4.1 (6.2)	6.4 (9.7)	4.3 (6.4)
Load-2	3.1 (8.3)	2.4 (6.3)	3.9 (10.3)	2.7 (7.1)
PV-1	2.4 (9.2)	1.6 (6.1)	3.9 (14.9)	2.1 (8.1)
PV-2	5.4 (7.8)	3.9 (5.6)	7.2 (10.3)	5.7 (8.3)
Wind-1	2.0 (7.5)	1.9 (6.9)	3.0 (11.1)	1.7 (6.4)
Wind-2	3.0 (9.1)	2.0 (6.2)	3.7 (11.4)	1.9 (5.8)

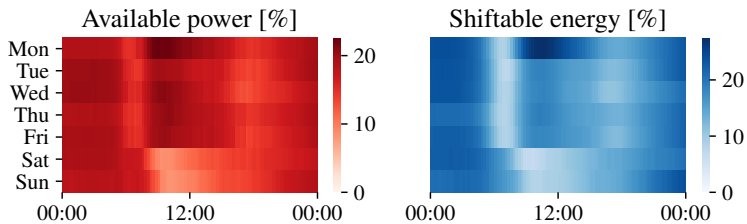


FIGURE 7.4: Mean available power (left) and shiftable energy (right) for the load-dominated grid *Load-1* for both weeks.

The highest available power is displayed around noon at weekdays with a maximum of 22.6% of the total installed charging station capacity, which is approximately 1.7 times the peak charging load in the reference case. The higher available power in day time results from higher installed charging capacities for work charging than for home charging. On the contrary, the consumed energy is higher for home charging. Therefore, a generally higher shiftable energy can be observed in night hours. There is limited shifting potential for weekend days, especially in terms of shiftable energy. The reduced charging demand for these days in turn leads to a high charged amount on Mondays and therefore the highest shifting potential of 27.5% of the mean daily consumption by reference charging. This indicates longer trips on weekends, leading to higher charging demands on Mondays.

### *Grid Issues*

Fig. 7.5 and Fig. 7.6 show the distribution of violations of voltage bounds and overloading in a representative load- (*Load-1*, left) and PV-dominated (*PV-1*, right) grid, i.e. they show the deviations from the bounds and only for cases when the bounds are violated. All violations are displayed on the top, while the bottom shows the most severe incidents per component, namely the highest undervoltage per bus and overloading per branch. In both cases, the probability distribution (obtained with a kernel density estimation) is displayed. The width of each violin within one subplot is thereby scaled with the number of occurrences of voltage violations and overloading events. The violation of voltage or loading bounds for one component and time step thereby counts as one occurrence. Only the violins within one subplot can be directly compared to each other. A smaller width means fewer occurrences, while the position on the y-axis indicates the severity of the grid issues. The area of the violins within one subplot can be interpreted as an indicator for the total number of occurrences of the respective grid violations in the upper subplots and the total number of components facing grid violations in the lower subplots.

The only voltage violations in the load-dominated grid are undervoltage events, as Fig. 7.5 (left) shows. The undervoltage incidents in the *No EV*-case stem from the integration of heat pumps (HPs). It can be seen that the integration of EV charging increases the number and severity of undervoltage incidents. Coordinated charging can decrease the number and severity of these events compared to reference charging. The most severe undervoltage events (bottom) are more substantially reduced than the total number of

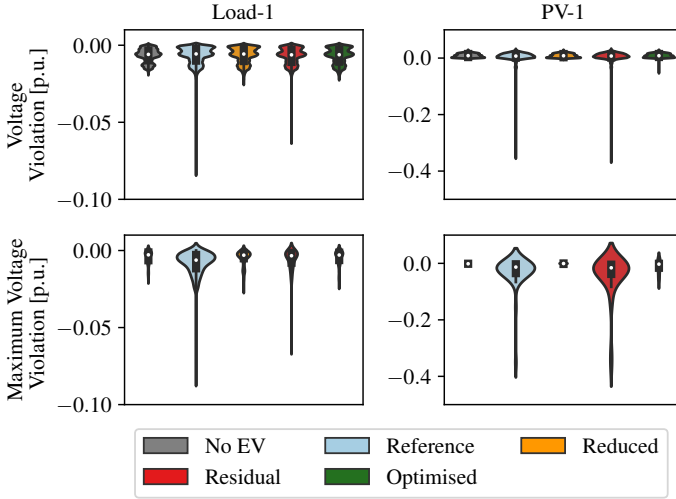


FIGURE 7.5: Distribution of voltage issues in load-dominated grid *Load-1* (left) and PV-dominated grid *PV-1* (right) with EV charging using the different charging strategies and without EVs. On the top, all occurring voltage issues are displayed. On the bottom, only the most severe undervoltage event per bus is displayed.

occurrences (top). In this case, optimised and reduced charging outperform residual load charging. For the reduction of the number of occurrences, on the other hand, residual load charging performs equally well as optimised charging and outperforms reduced charging.

In the PV-dominated grid (right), the main voltage violations are overvoltage events caused by the integration of RES. With the integration of EVs, undervoltage events also occur. The most severe undervoltage event depends again on the charging strategy, but in this case, residual load charging leads to an even lower undervoltage extreme value than the reference charging. As shown in Fig. 7.2, the residual load charging can lead to a high simultaneity in charging. When charging and the feed-in, which causes the simultaneous charging, are not located in the same areas of the grid, there is no local balancing of feed-in and demand. Combined with a high density of charging stations in certain parts of the grid, this can lead to the displayed effect of an increase in the severity of grid issues.

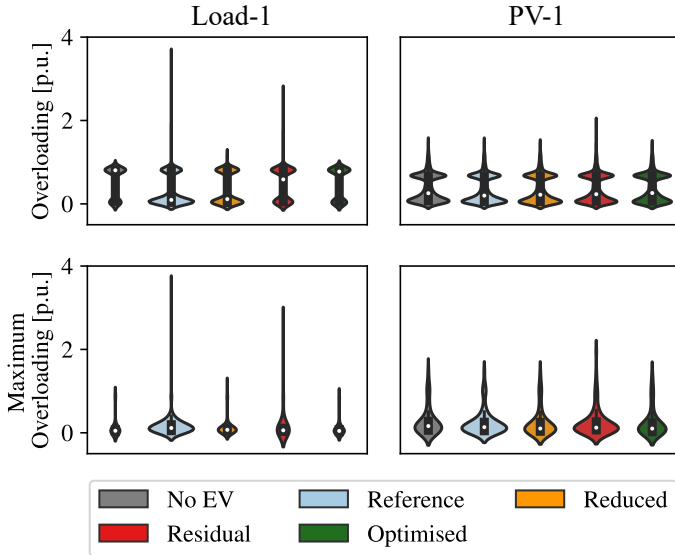


FIGURE 7.6: Distribution of overloading issues in load-dominated grid *Load-1* (left) and PV-dominated grid *PV-1* (right) with EV charging using the different charging strategies and without EVs. The top shows all occurring overloading events while the bottom displays only the most severe overloading event per branch.

The effects of the charging strategies on the overloading issues are similar as observed for voltage violations in both grids, as shown in Fig. 7.6. In the load-dominated grid (upper left), the number of small overloading incidents can be significantly reduced with coordinated charging strategies compared to reference charging. The more significant overloading events remain similar with the integration of EV charging and the different charging strategies. It has to be mentioned that the number of occurrences for overloading incidents is significantly smaller than for voltage issues in this grid. The maximum overloading per branch (lower left) can also be significantly decreased by all coordinated charging strategies, most effectively by optimised charging, followed by reduced and residual load charging.

In the PV-dominated grid, the total number of overloading events (indicated by the area of the violins in the upper right) is not significantly impacted by any of the different charging strategies. This implies that a large share of the overloading events is caused by RES integration. Smaller overloading

issues slightly increase with uncoordinated charging and can be reduced by coordinated charging, most effectively by the optimised charging. For the most severe overloading per branch (lower right), the integration of EVs shows a stronger effect. For the reference charging, the number of overloaded components increases compared to the *No EV*-case, which can be estimated from the total area of the violins. Optimised and reduced charging reduce the number of overloaded components. The residual load charging, however, shows no such reduction and even increases the most severe overloading event. The displayed results effectively showcase the possible negative effects of residual load charging. Its grid-wide incentive can lead to high simultaneities and increased local stress on the grids.

### *Necessary Curtailment*

To assess the influence of the different charging strategies on the necessary curtailment, we study the change in curtailment needs caused by EV integration. To this end, necessary curtailment is determined for a scenario without EVs and used as the reference to determine changes in curtailment needs due to EV integration. Fig. 7.7 shows the results normalised to the integrated charging demand for the different grids and charging strategies. Positive values indicate an increase in load curtailment, and negative values display a reduction of feed-in curtailment compared to the reference case without any EVs. Generally, all coordinated charging strategies, i.e. reduced, residual and optimised charging, lead to a decrease in total necessary curtailment compared to the reference charging.

In the feed-in dominated grids, we see a reduction of feed-in curtailment additionally to the reduction of load curtailment. In the PV-dominated grids, this effect even leads to a net reduction of curtailment needs with the integration of EVs compared to the reference scenario without EVs. Optimised charging shows the highest reduction potential in all of the grids, followed by residual load and reduced charging.

However, the overall potential of the assessed charging strategies to decrease necessary curtailment proves to be limited. Including the additional load of uncoordinated EV charging leads to an increase in load curtailment of 27.8% within all the grids. Optimised charging as the most effective strategy can reduce this additional load curtailment to 23.6%. Feed-in curtailment is reduced by 0.5% by the reference charging. This reduction can be increased to 0.7% by the optimised charging. It has to be stressed that the largest share of the absolute necessary curtailment is feed-in curtailment with

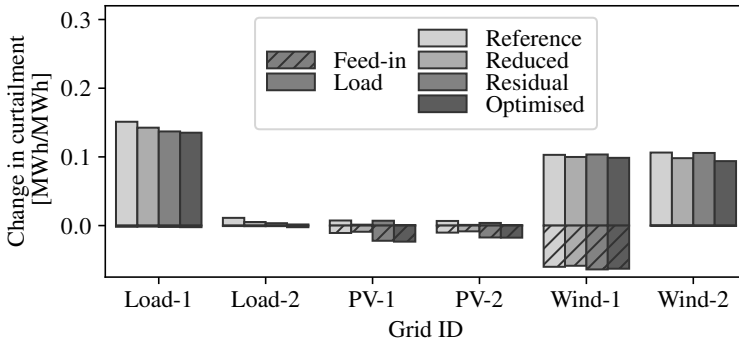


FIGURE 7.7: Change in curtailment necessary to solve grid issues caused by EV integration with different charging strategies compared to the case without EVs. The values are normalised to the integrated charging demand.

87.1% of the total curtailment of all grids in case of reference charging. The potential to reduce this feed-in curtailment by smart charging proves to be small because of the geographical distribution of load and feed-in. The grid with the highest feed-in curtailment, *Wind-1*, includes the smallest amount of flexible charging. Additionally, flexible charging and curtailment needs are not necessarily located in the same area of a grid. Topology plots show that in some grids, feed-in curtailment and flexible charging are located relatively far from each other (see Fig. 7.8). Additionally, they can be installed at different voltage levels. So even if the temporal flexibility to balance excessive feed-in from PV or wind exists, the grid cannot transport the power with the status quo grid capacities considered in this study.

The limited reduction of load curtailment, on the other hand, has two main reasons. First, in *Load-1*, *Wind-1* and *Wind-2*, the grids that show higher additional curtailment due to the integration of EVs and cause 93.4% of the total additional load curtailment, the share of the curtailment of flexible charging, i.e. home and work charging, compared to inflexible charging, i.e. public and HPC, is very low with 2.0-4.2%. Since only flexible charging can be shifted, the larger share of curtailment of inflexible charging cannot be influenced by the charging strategies. The other reason is the limited shifting potential between day and night hours when shifting is only allowed within the standing time of the originally scheduled charging. Fig. 7.9 shows the load and feed-in curtailment in the wind-dominated grid

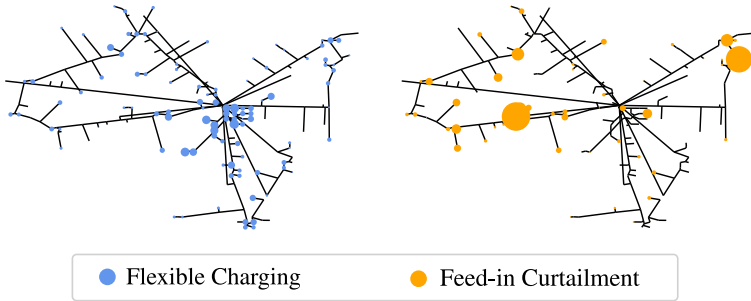


FIGURE 7.8: Topology plot for flexible charging (left) and feed-in curtailment (right) in the grid *PV-1*. The size of the circles indicates the cumulative energy of the respective quantity in the two investigated weeks.

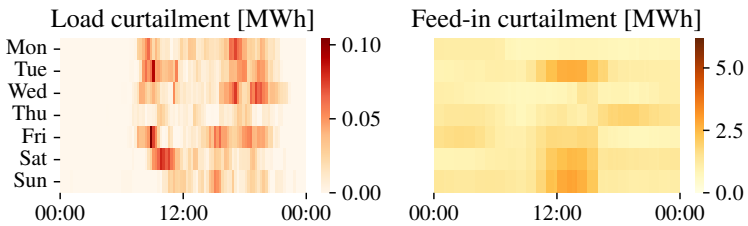


FIGURE 7.9: Load curtailment (left) and feed-in curtailment (right) in the case of reference charging in the representative wind-dominated grid *Wind-1* for the week of maximum residual load.

*Wind-1* for EV integration with reference charging in the week of maximum residual load. Flexible charging can reduce the necessary curtailment in two ways: by shifting away from times with high load to reduce load curtailment and by shifting the demand into times of high feed-in to reduce feed-in curtailment. Fig. 7.9 shows no load curtailment during night hours. However, work charging, which leads to additional load curtailment in the daytime, cannot be shifted into these night hours. On the other side, PV curtailment, which occurs during the day around noon, cannot be reduced by the flexibility of home charging which shows high flexibility potential at night (see Fig. 7.4).

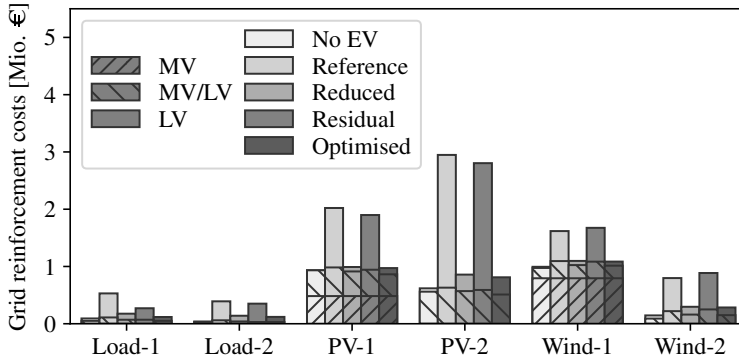


FIGURE 7.10: Reinforcement costs caused by RES, HP and EV integration in the different grids.

### Grid Expansion Costs

As an alternative to providing temporal flexibility, grid expansion measures can be deployed to solve the occurring grid issues. We therefore also examine the influence of EV integration on the costs of necessary grid expansion for the different grids and charging strategies. The results are shown in Fig. 7.10. In contrast to the curtailment, there is a strong influence of the charging strategy on the overall grid expansion costs. The reference charging increases grid expansion costs of all six considered grids by 194 % compared to the costs without EV integration. Optimised charging, as the most efficient strategy, can reduce the increase to 20 %. The difference in the impact of the charging strategies on curtailment and grid expansion costs stems from the fact that for grid expansion, only the most severe grid issues influence the necessary measures. In the case of curtailment, on the contrary, the frequency and duration of all grid issues play a role. Hence, it can be concluded that the influence of the charging strategies on the most severe grid issue is stronger than on the frequency and duration, which was also shown in Fig. 7.5 and Fig. 7.6.

Studying the different charging strategies, we again see the highest reduction potential in the optimised charging. This reduction might still not be the global optimum as neglecting the losses in the optimisation can lead to sub-optimal solutions. The optimisation might underestimate the flow on lines and require curtailment or grid expansion measures where

a slight change in charging might have been sufficient to solve the issues. However, by minimising the component loading in the objective function, these situations should be reduced to a minimum, and our results therefore still give a good estimation of the reduction potential. Within the rule-based approaches, the reduced charging proves to be more efficient than the residual load charging. In the wind-dominated grids, the residual load charging even leads to a small increase in grid expansion costs compared to the case with reference charging. This behaviour can be explained by false incentives received by a charging based on the residual load of the whole grid instead of a more locally resolved incentive. In grids with very differently composed feeders, such as the wind-dominated grids, it can lead to high load peaks in feeders with a high number of EVs, resulting in additional grid expansion measures. An increase in peak load and grid issues due to the influence of wind feed-in on EV charging was also shown in [158] and [23], respectively.

Overall, all investigated charging strategies reduce the total grid reinforcement costs observed in the investigated grids compared to the reference charging. The rule-based reduced charging shows a similarly high reduction potential with 57% as the optimised charging with 59% compared to the costs with reference charging. The residual load charging shows significantly lower potential, with 5% reduction compared to the grid reinforcement costs with reference charging.

To investigate the sensitivity towards the chosen grid limits, Fig. 7.11 displays the change in total reinforcement costs with increasing tolerance for overloading (left) and voltage deviations (right). Therefore, the allowed component loading and voltage deviations are increased by 10% and 50%. For the increase of allowed component loading, the reduction is mainly in the MV and at MV/low voltage (LV)-transformers. A large share of the costs caused by (RES and HP) can be reduced, up to 64% of the cost in the *No EV* scenario in case of a 50% increase of the allowed loading. The difference between the charging scenarios is comparably small. When increasing the allowed voltage deviation, on the other hand, there is a large difference between the charging strategies, implying that mainly reinforcement caused by EV integration is reduced. The cost reduction mainly occurs in the LV, reaching 35% of the additional costs caused by EV integration for reference charging and 50% increase of the allowed voltage deviation. The reduction is higher for the charging strategies that cause a high cost increase, i.e. reference and residual load charging.

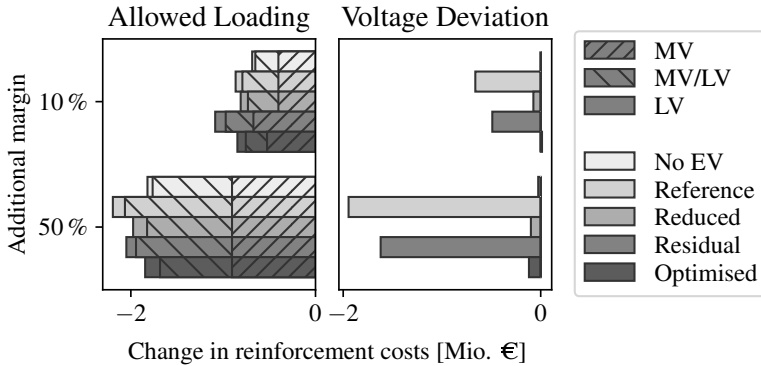


FIGURE 7.11: Change in total reinforcement costs with increasing tolerance towards overloading (left) and voltage deviation (right).

### 7.1.3 Conclusion

We investigated the influence of different EV charging strategies on the simultaneous integration of EVs and VRES into typical German suburban and rural MV-grids, including underlying LV-grids. Representative load-, PV- and wind-dominated grids were therefore expanded with renewable capacities from the *eGo 100*-scenario as well as HPs and EVs according to the *NEP C 2035*-scenario. We then compared optimised charging and rule-based approaches, namely reduced and residual load charging, with reference charging. While studies have individually focused on grid issues, curtailment and reinforcement needs, we investigated all three aspects to cover different aspects of EV grid integration. Furthermore, we focused on the influence of the technological composition of different types of grids to showcase the interplay of VRES adoption and smart EV charging.

The results show that, on average, all investigated charging strategies reduce curtailment needs and necessary grid expansion costs compared to reference charging. However, the potential of EV charging to reduce curtailment and grid expansion needs caused by the integration of VRES proves to be limited. Only the curtailment needs in PV-dominated grids can be slightly decreased compared to the curtailment needs without EVs. The grid expansion costs for all grids and the curtailment in the load- and wind-dominated grids increase with the integration of EVs. The additional grid expansion costs, mainly occurring in the LV, are thereby highly dependent on the charging

strategy and can be significantly reduced given the right strategy. The optimised charging as the most efficient strategy achieves a cost reduction of 59 % compared to the reference charging over all investigated grids. The influence of the charging strategies on curtailment needs, on the other hand, is small in the considered cases.

While the optimised charging strategy holds the highest reduction potential for both measures, the rule-based charging strategies show different tendencies. Reduced charging decreases the grid expansion costs to a similar extent as optimised charging, achieving a reduction of 57 % compared to the reference charging over all investigated grids. It could therefore serve as a relatively simple alternative to the centrally optimised charging when it comes to the reduction of grid expansion costs. However, it does not perform equally well with the reduction of curtailment needs. It decreases load curtailment but increases feed-in curtailment compared to the reference charging. Residual load charging, on the other hand, holds little potential to decrease the grid expansion needs, only reducing the grid total reinforcement costs by 5 % compared to the reference operation over all investigated grids. In the wind-dominated grids, it even leads to an increase in grid expansion costs compared to the reference charging. This is due to high charging peaks that result from charging based on the residual load of the grid. When charging and feed-in are located in different areas of the grid, the high charging powers can lead to additional congestion in areas with high charging demand. The same phenomenon leads to relatively high load curtailment needs in feed-in dominated grids. On the other hand, the shifting of charging demand into times of high feed-in reduces the feed-in curtailment.

Our investigations show that in addition to the type of grid, the geographical distribution of load and feed-in influences the efficacy of the different charging strategies. For future research, we therefore recommend to use several differently composed grids when investigating smart charging in distribution grids and take both the temporal and geographical dimension of flexibility provision into consideration.

## 7.2 COMPARISON OF DIFFERENT LEVELS OF EV FLEXIBILITY

In the previous section, we compared optimised EV charging with rule-based alternatives and proved that the influence of the different strategies on the grid reinforcement costs in the distribution grids is high. However, the optimised charging in the previous section represents a limited level of EV flexibility, only allowing the shifting of home and work charging within the originally scheduled charging session.

There are different ways to further increase the flexibility of EV charging, such as making other charging use cases (e.g. public charging) flexible as well or to allow shifting of the charging demand between standing times. To increase flexibility further, EVs can provide electricity to the system when needed, referred to as vehicle-to-grid (V2G). With this bidirectional power flow, EVs can operate as moving storage. For the estimated flexibility potential in Part I of this thesis, these measures proved to increase the available flexibility significantly (see Section 4.3). In this section, we want to investigate the influence of the different levels of EV flexibility considering specific flexibility needs, i.e. their influence on curtailment needs and grid reinforcement costs in distribution grids. To this end, we investigate strategies which allow to shift charging demand between standing times to different charging locations and the utilisation of V2G additionally to shifting within standing times, which was assessed in the previous section. We compare the results of four optimised strategies with different levels of flexibility with an uncoordinated reference operation (i.e. plug and charge). The necessary curtailment and grid reinforcement to avoid curtailment are evaluated for each strategy and put into perspective with the previously estimated flexibility potential.

### 7.2.1 *Study Setup*

Figure 7.12 shows the general setup of the case study. The charging demand (further detailed in Section 3.2.1) is integrated into a subset of the DGs introduced in Section 3.1.5. We model different levels of flexibility for EVs and determine the grid-optimised charging. In a last step, the different levels of flexibility are compared in terms of flexibility potential, curtailment and grid reinforcement needs. The single steps are described in more detail in the following.

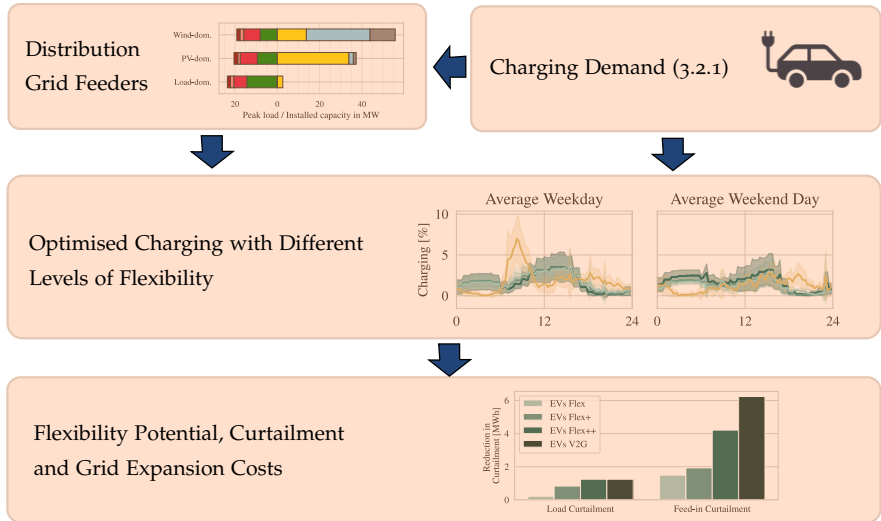


FIGURE 7.12: Research design of study.

### *Distribution Grid Feeders*

Due to a lack of real-world distribution grid topology data, synthetic MV-grid topologies with underlying LV-grids were generated with the software DINGO [76] and expanded with renewable generation, HPs and EV charging stations as explained in Section 3.1.5. We use the described setup of the *NEP2035* scenario.

We use a subset of these grids, which were subdivided into load-, PV- and wind-dominated grids to investigate grids with different characteristics. To reduce the problem to a manageable size, we use representative feeders of the grids with a similar technological composition as the original grids, which allows us to compare the effect of optimised charging on different types of grids. In total, we investigate 20 MV-feeders with underlying LV-grids. This includes seven load- and wind-dominated feeders and six PV-dominated feeders. Fig. 7.13 reflects the composition of the investigated feeders summed up over the considered grid types. For generation technologies, the installed capacities are displayed, while for EV charging and the conventional load, the peak load values are shown.

Generally, the feeders show high installed EV charging capacities since only feeders with a high number of EVs are selected for further investigation. In

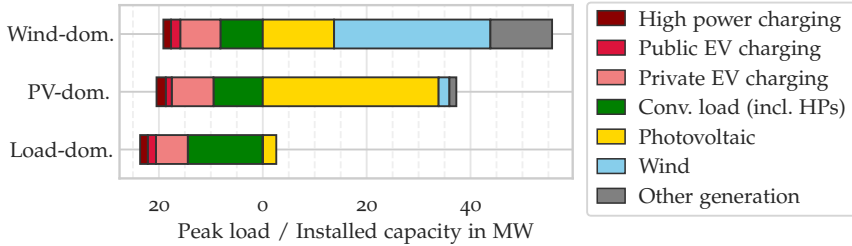


FIGURE 7.13: Peak load of reference EV charging and conventional load as well as installed capacities of generation technologies of the investigated feeders. The values are displayed summed up over the different grid types.

total, 762 EVs in the load-dominated feeders, 853 EVs in the PV-dominated feeders and 906 EVs in the wind-dominated feeders are integrated into the grids. If possible, charging stations are added to existing grid connection points. Otherwise, new connection lines to the closest grid connection points (e.g. for parking lots not close to existing electrical installations) or transformer stations, depending on the nominal capacity of the charging station, are installed.

### *Charging Demand*

For the integration of EVs, we use synthetic driving profiles created with the simulation tool SIMBEV [169] and map the obtained charging demands to the feeders. In reality, EV owners might commute long distances between different charging use cases and thus charge in different feeders of the grids. Since the geographical shift between different grids or feeders is not the focus of this study, we use the simplifying assumption that the charging demands of each EV occurs within a single feeder and map the entire charging demand to charging stations within that feeder.

The reference charging is obtained with a heuristic approach and resembles a behaviour where the EVs charge directly after arrival with the nominal charging power until the charging demand of that charging session is fully met.

### Optimised Charging with Different Levels of Flexibility

We want to compare the effect of different levels of flexibilisation of EVs on their flexibility potential and their influence on the grid. For the later, we use the OPF formulation introduced in Chapter 6, where the necessary curtailment to stay within the grid limits and the component loading are minimised. We furthermore model the levels of flexibility introduced in Section 3.2.4 to investigate the influence of EV flexibility. For readability, we briefly repeat the levels, their underlying assumptions and modelling in the following.

*EVs Flex* and *EVs Flex+*: EVs have the flexibility to shift charging demand within the originally scheduled charging session. As the charging location is thus predefined, we use the concept of flexibility envelopes introduced in Section 3.2.6. In *EVs Flex*, only home and work charging stations can shift their demand, whereas in *EVs Flex+*, public charging is additionally made flexible.

*EVs Flex++* and *EVs V2G*: To increase the flexibility, shifting between standing times and to other charging locations is allowed in these cases. Since it is an outcome of the optimisation at which location the charging demand occurs, the battery-based modelling of EVs introduced in Section 3.2.5 is used. In the case of *EVs V2G*, discharging is additionally allowed, while for *EVs Flex++*, only smart charging is allowed, i.e.  $p_{c,t}^{V2G} = 0$ .

### Model Parameters

Allowing the utilisation of V2G introduces a new penalty term  $pen_{EV}$  to the original objective function (6.1) to prevent excessive simultaneous charging and discharging (further detailed in Section 3.2.5). The weighting  $\delta$  of the different terms in the objective function

$$\min \delta_{curt} \sum_{n \in N} \sum_{t \in T} p_{n,t}^{curt} + \delta_{load} \sum_{b \in B} \sum_{t \in T} l_{b,t}^2 + pen_{EV} + \delta_{slack} pen_{slack}, \quad (7.1)$$

s.t.

$$p_{n,t}^{curt} = \delta_{curt,l} p_{n,t}^{curt,l} + \delta_{curt,f} p_{n,t}^{curt,f} + \delta_{curt,ev} p_{n,t}^{curt,ev} \quad \forall n \in N, t \in T, \quad (7.2)$$

$$pen_{EV} = \delta_{charge} \left( \sum_{s \in S} \sum_{t \in T} p_{s,t}^{EV} \cdot \Delta t - E^{tot} \right), \quad (7.3)$$

TABLE 7.2: Parameter values for weights in objective function.

$\delta_{curt}$	$\delta_{load}$	$\delta_{curt,l}$	$\delta_{curt,f}$	$\delta_{curt,ev}$	$\delta_{charge}$	$\delta_{slack}$
1	$10^{-3}$	1.0	0.5	0.5	2	$10^2$

greatly influences the results of the optimisation and their weight relative to each other is important. For the adapted objective, the original weights are therefore adjusted. Table 7.2 summarises the weights chosen for the given case study, which are the result of a sensitivity analysis (see Section 7.3). The total weighted curtailment  $p_{n,t}^{curt}$  is weighted as more important than the component loading  $l_{b,t}$ , which is used to achieve a unique solution. It is further assumed that the curtailment of flexible charging  $p_{n,t}^{curt,ev}$  and feed-in  $p_{n,t}^{curt,f}$  is preferable to the curtailment of inflexible load  $p_{n,t}^{curt,l}$ , therefore  $\delta_{curt,ev} = \delta_{curt,f} = 0.5$  and  $\delta_{curt,l} = 1.0$ .

To allow for reasonable levels of V2G but prevent excessive utilisation thereof, we choose a weighting factor of  $\delta_{charge} = 2$  for the penalty term of simultaneous charging and discharging of EVs. This value leads to an equally high penalty for the additional charging demand as for feed-in curtailment (for further justification, see [113]). The additionally increased component loading (leading to higher values of the second term in the objective function) leads to feed-in curtailment being slightly preferable to simultaneous charging and discharging. If simultaneous charging and discharging occur nevertheless, the results are corrected by using the net consumption and subtracting the additional consumption caused by losses. The obtained feed-in curtailment is equally corrected by the amount of additionally caused losses. With the linear penalty term, the computation times are reduced to similar values as for the constrained optimised charging (for more details and values, see [113] and Section 7.3).

Last, the sum of all slacks that are used to relax the constraints for the voltage and component loading limits ((6.8) and (6.11)) as well as battery state of charge (SoC) and maximum charging of the EVs ((3.2) and (3.6)) are heavily penalised with  $\delta_{slack} = 10^2$ .

### *Measures of Comparison*

To investigate the efficacy of the optimised charging strategies compared to the reference charging, we compare the necessary curtailment to stay

within the grid restrictions directly obtained by the optimisation. The maximum component loading is restricted to 100% and the maximum voltage deviation to  $\pm 10\%$ . If any of these limits are exceeded, conventional load, EV charging, or feed-in are curtailed by the optimisation. For comparison, the curtailment of conventional load and EV charging are classified as *load curtailment* and the curtailment of PV, wind and other generation as *feed-in curtailment*.

As an alternative to curtailment, the grids could be reinforced to incorporate the additional load and feed-in at all times. For this, the optimised charging strategies and the reference charging are integrated into the investigated feeders by assigning the obtained charging patterns to the respective charging stations and the respective grid flows are computed. If grid issues are detected (see Section 3.1.2), the affected components are reinforced. We use the approach introduced in Section 3.1.3 to estimate the necessary reinforcement and the *reinforcement cost* as a measure of comparison. The optimised charging strategies are thereby compared to the reference charging and a case without the integration of EVs. In that latter case, the resulting costs are entirely caused by integrating additional renewable generation and heat pumps.

To limit the complexity while still accounting for the weekly charging patterns as well as high loading of the grids, we choose two extreme weeks for all investigations: the week of highest and lowest residual load of the respective feeder. The optimised charging is obtained for one week at a time.

### 7.2.2 Results and Discussion

In the following, the results are shown and discussed. For additional results and more in depth discussion of the results and modelling assumptions, we refer to [113].

#### *Charging Patterns*

Fig. 7.14 shows the charging patterns of all levels of flexibility for a load- (top), PV- (center) and wind-dominated (bottom) feeder. The values are displayed relative to the installed capacities of all charging stations in the respective feeder. The reference charging shows a peak in the morning hours when EVs arrive at work and in the afternoon when EVs arrive at home. Charging on the weekends shows less pronounced charging

peaks. In the PV-dominated feeder, all optimised charging strategies shift the demand into the early morning and noon hours to use the high PV feed-in around noon. The mean charging peak for optimised charging increases with the level of flexibility and can obtain higher values than for the reference charging which however is aligned with the PV infeed. In the load-dominated grid, where a small share of PV is present, the same effects can be observed but to a smaller extent and the overall peak is reduced compared to the reference charging. In the wind-dominated grid, all optimised charging strategies lead to a lower overall peak in charging compared to the reference case and a relatively flat charging profile.

With higher flexibility, more charging demand is shifted to the weekends (see Fig. 7.15) as the conventional load is lower in these times. For reference charging, 22.0 % of the overall charging occurs on weekends. The optimised charging in case of *EVs Flex* and *EVs Flex+* shifts an additional 1.8 % and 2.1 % of the charging demand into the weekends. In these scenarios, only charging events spanning from weekday to weekend can shift charging demand to the weekend. In the case of *EVs Flex++* and *EVs V2G*, with the flexibility to shift between standing times, larger shares of 9.9 % and 9.7 % of the charging demand are shifted to the weekends.

### *Curtailment Needs*

Fig. 7.16 shows the reduction in necessary curtailment for the optimised charging strategies compared to the reference charging strategy within all simulated feeders (the absolute load curtailment in the reference case is 1.4 MWh and the feed-in curtailment 368.5 MWh). In general, additional flexibility in optimised charging increases the reduction in both load and feed-in curtailment. The absolute reduction of feed-in curtailment by optimised charging is higher than that of load curtailment for all optimised charging strategies. However, in relative terms, the potential to reduce load curtailment is much higher than the reduction of feed-in curtailment. The optimised operation in the *EVs Flex* scenario can reduce load curtailment by 15.4 %. Allowing shifting of public charging additionally to home and work charging (*EVs Flex+*) increases the reduction to 59.4 %. Allowing shifting between standing times in *EVs Flex++* even reduces the necessary curtailment of load by 88.6 %. Including the utilisation of V2G in *EVs V2G*, on the other hand, does not lead to a further reduction but shows the same value as *EVs Flex++* of 88.6 %. On the other hand, the relative reduction of feed-in curtailment only amounts to 0.4 %, 0.5 %, 1.1 % and 1.7 % for the

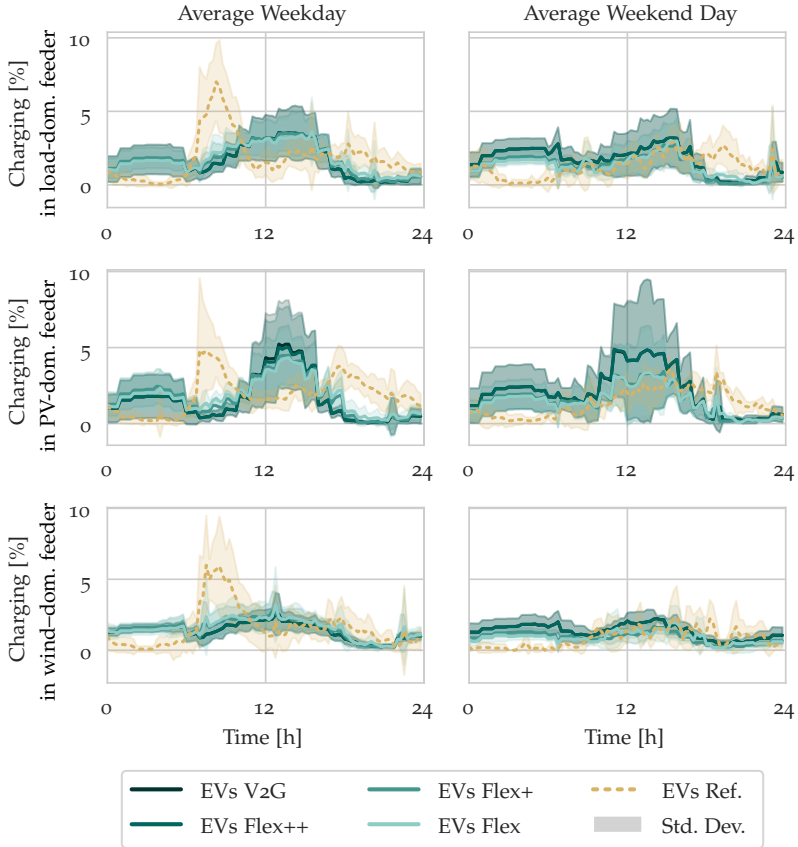


FIGURE 7.14: Charging pattern during the week (left) and the weekend (right) for a load- (top), PV- (center) and wind-dominated (bottom) feeder, displayed relative to installed charging station capacities. The shaded areas indicate the standard deviation over the simulated days.

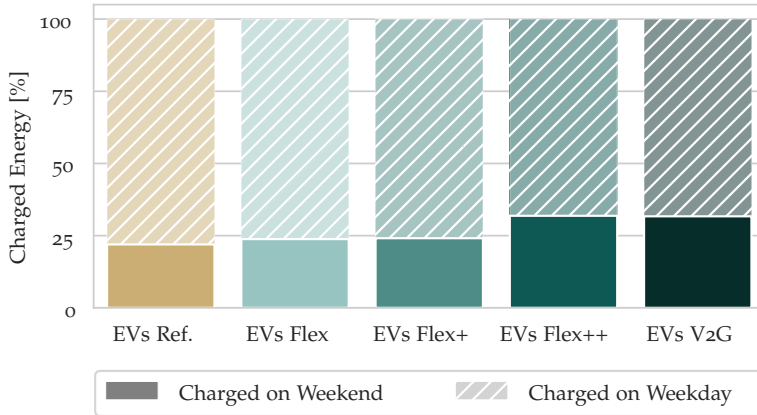


FIGURE 7.15: Charging demand occurring during the week and on weekends in percent of total charging demand for the different levels of EV flexibility.

four levels of EV flexibility. In this case, allowing V2G shows a positive effect and significantly increases the reduction of feed-in curtailment. The additional reduction in feed-in curtailment is the same as when allowing shifting between standing times and is much higher than when only including public charging in addition to home and work charging is considered. Hence, the different levels of flexibility exhibit different potentials to reduce load and feed-in curtailment.

The main reason for the different magnitudes of relative reduction in load and feed-in curtailment is that the curtailment of the load is much lower than the curtailment of feed-in in the reference charging case. Only 1.4 MWh of the 221.5 MWh additional load through EV charging have to be curtailed whereas 368.5 MWh of the 4181.5 MWh total feed-in have to be curtailed. One reason for the limited reduction potential for feed-in curtailment is the geographical distribution of feed-in and EV charging, already found in the previous case study. While larger generation units are directly connected to the MV, EV charging mainly occurs in the LV. If components between feed-in and EV charging are overloaded, the EV flexibility cannot be used to reduce feed-in curtailment. On the other hand, the load curtailment is mainly caused by the integration of EV charging. Flexibility from smart charging will thus always be at the right location to reduce load curtailment if all charging use cases are made flexible.

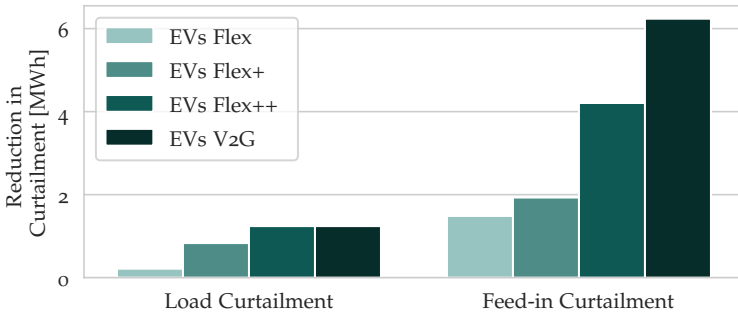


FIGURE 7.16: Reduction of the necessary curtailment for the optimised charging strategies compared to the *reference* strategy.

Since the curtailment values are directly obtained from the optimisation, no losses are accounted for in the displayed values. Therefore, the absolute curtailment needs would be slightly higher in the case of load curtailment and slightly lower in the case of feed-in curtailment as losses correspond to additional load. The reduction of load curtailment by optimised charging would likely increase when accounting for losses as these scale with the squared magnitude of the current, and both optimised charging strategies lead to lower charging peaks. Hence, there would be less additional load in times of high stress on the grid, which is when curtailment is necessary.

### *Reinforcement Cost*

Fig. 7.17 shows the grid reinforcement costs over all considered grids by grid type for all investigated charging strategies. The required reinforcement without EV integration is also displayed for comparison. In this case, the required grid reinforcement is mainly caused by an increase of RES and, to a minor extent, by HP integration. In the load-dominated feeders, almost no reinforcement is necessary (a single transformer is reinforced; the level of reinforcement differs due to different peak loadings). In the feed-in-dominated feeders, the cost in the PV-dominated feeders is higher than in the wind-dominated feeders, even though the overall required curtailment is lower. The reason is that only the most severe overloading or voltage issue determines the grid reinforcement cost. For the curtailment, on the other hand, the duration and frequency of grid issues are also important factors.

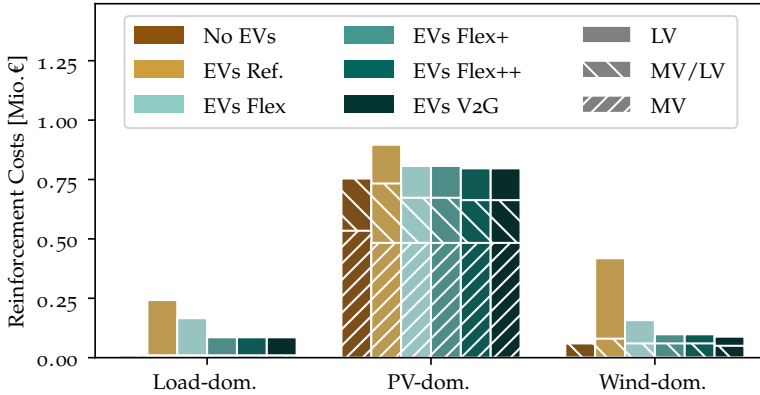


FIGURE 7.17: Comparison of the reinforcement costs per component for the charging strategies and *No EVs*.

It also must be mentioned that specific individual feeders cause a large share of the reinforcement costs, while others do not require reinforcement. For example, the entire reinforcement costs in the MV occur in a single feeder. The results are especially sensitive to these costs since reinforcement in the MV is more expensive than in the LV. In selected feed-in dominated feeders, the integration of EV charging with a high level of flexibility can lead to lower reinforcement costs than in the *No EVs* scenario but in the aggregate, the integration of EVs leads to additional reinforcement costs that can, however, be reduced significantly using EV flexibility.

The costs for the additional integration of EV charging depend on the charging strategy. The reference charging leads to a significant cost increase of 88.4% of the total costs in the *No EVs* scenario summed over all considered feeders. Optimised charging can reduce the additional reinforcement costs by 58.3% in the *EVs Flex* scenario and 77.4% in *EVs Flex+* compared to the reference scenario. Making public charging flexible additionally to home and work charging decreases the reinforcement costs in the load- and wind-dominated feeders but shows little effect in the PV-dominated feeders. The lower peak load of public charging relative to private charging in the PV-dominated feeders could be an explanation for this. With *EVs Flex++* and *EVs V2G*, the reduction with respect to reference charging can be further increased to 78.8% and 80.2%, respectively. Hence, overall, the

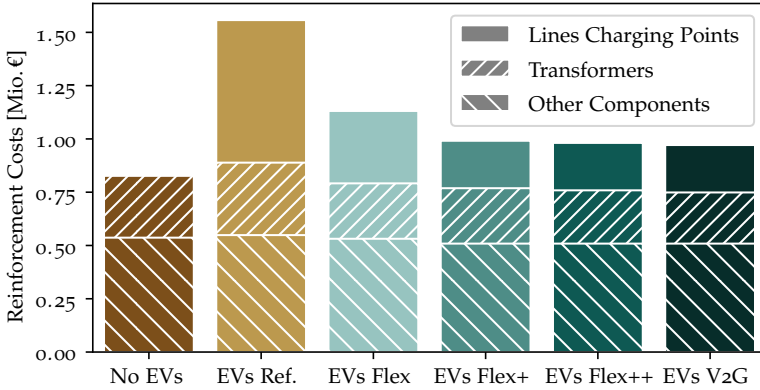


FIGURE 7.18: Grid reinforcement costs caused by different types of components in the investigated scenarios.

additional flexibility of shifting between standing times and using V2G only leads to a small additional reduction of the grid reinforcement costs.

Most of the additional costs for the integration of EVs occur in the LV, with small shares also at transformers at the MV/LV connection. The only feeder showing reinforcement needs in the MV is PV-dominated. However, these are caused by the integration of PV and are even slightly reduced by the integration of EVs. When studying the type of reinforced components in Fig. 7.18, the results show that a large share of the additional costs is caused by lines connecting the charging points to the next grid connection point or transformer station. The optimised charging strategies can effectively reduce these costs by lowering the peak load and thus the required number of parallel lines. They also reduce the costs of transformer reinforcement to a smaller extent. Lastly, the costs caused by the reinforcement of other components are not reduced significantly.

Since the objective of the optimised charging strategies is only a proxy for the minimisation of grid reinforcement cost, the real potential of the optimised charging strategies to reduce the cost further might be higher. If integer values for the reinforcement of lines and transformers were included and their real costs added to the objective function, the flexibility could be pooled more effectively to reduce the maximum loading at a particular location to avoid grid reinforcement of the overloaded component. How-

ever, the resulting optimisation problem is computationally expensive and therefore not applicable to the investigated large-scale grids [113].

### 7.2.3 Conclusions

We investigated the influence of different levels of flexibility in EV charging on the flexibility potential and grid reinforcement requirements of characteristic German distribution grids. We modelled 20 MV-feeder with underlying LV-grids and integrated a total of 2431 EVs and additional RES capacities. We then compared four optimised charging strategies at different levels of EV flexibility with reference charging, where the EVs directly charge after plug-in at full charging capacity until the charging demand is met. The first level of EV flexibility allows shifting within the initially scheduled charging event for home and work charging. In the second level, public charging is additionally made flexible. The third level of EV flexibility allows shifting charging demand to other charging events, thus also making it possible to change the charging location. The last level additionally enables the usage of V2G.

The additional flexibility available by including public charging, shifting between standing times, and V2G proves to be differently effective in reducing necessary curtailment and reducing grid reinforcement cost.

Load curtailment can be reduced by roughly 15 % for flexible home and work charging at the lowest level of EV flexibility compared to the reference charging. This reduction can be significantly increased by including public charging (to 59 %) and by allowing shifting between standing times (to 89 %). No further increase is achieved for the highest level of flexibility including V2G. The feed-in curtailment can also be reduced, and V2G increases the reduction significantly in this case. However, the reduction is relatively small for feed-in curtailment, with 0.4 %, 0.5 %, 1.1 % and 1.7 % for the four levels of flexibility.

Grid reinforcement costs can be significantly decreased by optimised charging compared to reference charging. The total grid reinforcement cost caused by the integration of RES and EV charging can be reduced by 27.4 %, 36.4 %, 37.0 % and 37.7 % with the four levels of flexibility, respectively, compared to the reference charging. Shifting between standing times and allowing V2G shows limited potential to reduce grid reinforcement costs further. The flexibility to shift within the standing times seems sufficient to reduce the reinforcement costs significantly. This result is in contrast with

the flexibility potential estimated in the first part of the thesis (see Section 4.3). There, the flexibility potential could be drastically increased by allowing shifting between standing times and the utilisation of V2G. The reason for this discrepancy is partly that the estimated flexibility potential is a purely temporal measure. While the temporal flexibility might be available, it must be located close to the grid issues to reduce reinforcement. Additionally, flexibility is necessary at specific times to reduce reinforcement needs which is also not captured in the estimated flexibility potential.

The value of increasing the flexibility by incentivising smart charging at public charging stations, shifts between standing times and the utilisation of V2G therefore strongly depends on the use case. For the reduction of grid reinforcement and load curtailment, shifting within the standing times already shows high reduction potential in the investigated grids. On the other hand, when reducing feed-in curtailment, shifting between standing times and V2G prove to be more effective.

### 7.3 SENSITIVITIES AND PERFORMANCE

In the optimisation, we use several weighting terms. We investigate the influence of different choices of these on the results in **Section 7.3.1**. Furthermore, we want to compare the performance of the different optimised charging strategies in terms of runtime and memory usage in **Section 7.3.2**.

We evaluate only a subset of the feeders to limit the computational burden. The considered five differently sized feeders have varying numbers of integrated EVs which is summarised in Tab. 7.3. The sensitivity runs are performed on a server with the following specifications: Intel(R) Xeon(R) Gold 6154 CPU @ 3.00GHz, 2993 Mhz, 11 Core(s), 11 Logical Processor(s), 381 GB RAM. The memory usage is determined with the TRACEMALLOC package [170], which is a debug tool to trace the memory allocation. We use it to measure the memory allocation during the solving process. It has to be mentioned that it significantly increases the solving time. However, since the solving times are only used to compare the runs relative to each other, the absolute values are not that relevant. To measure the solving time, we use the *perf\_counter* method of the TIME package [171]. Furthermore, we use GUROBI [172] as a solver and the model is created using PYOMO [173].

#### 7.3.1 Sensitivity towards Weightings

Table 7.4 summarises the sensitivity runs for the different weighting terms. The *Base* scenario uses the same weighting terms as used in Section 7.1 and as explained in Section 6. In scenario  $\delta_{curt}$ , the effect of equally weighting all three types of curtailment is investigated. Scenarios  $\delta_{charge-1}$  and  $\delta_{charge-2}$  vary the weighting of the penalty term to limit simultaneous charging and discharging. *Obj-c* investigates the effect if only the curtailment and penalties are accounted for in the objective function. Scenarios *Obj-1*, *Obj-2* and *Obj-3* investigate different weightings of curtailment and component loading against each other and *Obj-l* the case, where only the component

TABLE 7.3: Investigated feeders for sensitivity and performance evaluation.

	Load-I	PV-I	PV-II	PV-III	Wind-I
<b>Number buses</b>	51	188	488	1374	1449
<b>Number EVs</b>	19	41	79	200	189

TABLE 7.4: Scenario values for sensitivity analyses of different weights.

Scenario	$\delta_{curt}$	$\delta_{load}$	$\delta_{curt,l}$	$\delta_{curt,f}$	$\delta_{curt,ev}$	$\delta_{charge}$	$\delta_{slack}$
<b>Base</b>	1	$10^{-5}$	1.0	0.5	0.5	2	$10^4$
$\delta_{curt}$	1	$10^{-5}$	1.0	<b>1.0</b>	<b>1.0</b>	2	$10^4$
$\delta_{charge}^{-1}$	1	$10^{-5}$	1.0	0.5	0.5	<b>1</b>	$10^4$
$\delta_{charge}^{-2}$	1	$10^{-5}$	1.0	0.5	0.5	<b>4</b>	$10^4$
Obj-c	1	<b>0</b>	1.0	0.5	0.5	2	$10^4$
Obj-1	1	<b><math>10^{-3}</math></b>	1.0	0.5	0.5	2	$10^4$
Obj-2	1	<b>1</b>	1.0	0.5	0.5	2	$10^4$
Obj-3	1	<b>100</b>	1.0	0.5	0.5	2	$10^4$
Obj-l	<b>0</b>	<b>1</b>	1.0	0.5	0.5	2	$10^4$
$\delta_{slack}^{-1}$	1	$10^{-5}$	1.0	0.5	0.5	2	<b><math>10^0</math></b>
$\delta_{slack}^{-2}$	1	$10^{-5}$	1.0	0.5	0.5	2	<b><math>10^2</math></b>
$\delta_{slack}^{-3}$	1	$10^{-5}$	1.0	0.5	0.5	2	<b><math>10^6</math></b>

loading and penalties make up the objective function. In scenarios  $\delta_{slack}^{-1}$ ,  $\delta_{slack}^{-2}$  and  $\delta_{slack}^{-3}$ , different weightings of the slack variables are investigated.

We evaluate for these different weightings whether the solver finds a solution for all the investigated feeders and compare the total reinforcement costs, total slack usage, curtailment needs and usage of V2G. Figure 7.19 displays the solving times for the evaluated five feeders. Shaded red areas indicate that the solver exited because of numerical issues, and no solution was returned. This was the case in scenario  $\delta_{slack}^{-3}$  for three of the five feeders, in scenario  $\delta_{curt}$  for two and in the *Base* and  $\delta_{charge}^{-1}$  scenarios for one of the five feeders. This result indicates that the difference in  $\delta_{curt}$  and  $\delta_{slack}$  tends to be too high in these scenarios. In general, the solving times are relatively similar within one grid for all the simulated scenarios.

In Figure 7.20, the total reinforcement costs (upper left), slack usage (upper right), curtailment needs (lower left) and V2G usage, as well as simultaneous charging and discharging (lower right), are displayed. The displayed values include only the grids that were solved for all scenarios, i.e. PV-II and PV-III. In terms of reinforcement costs, we want to achieve a charging behaviour that minimises the costs. The results show the same value in all scenarios

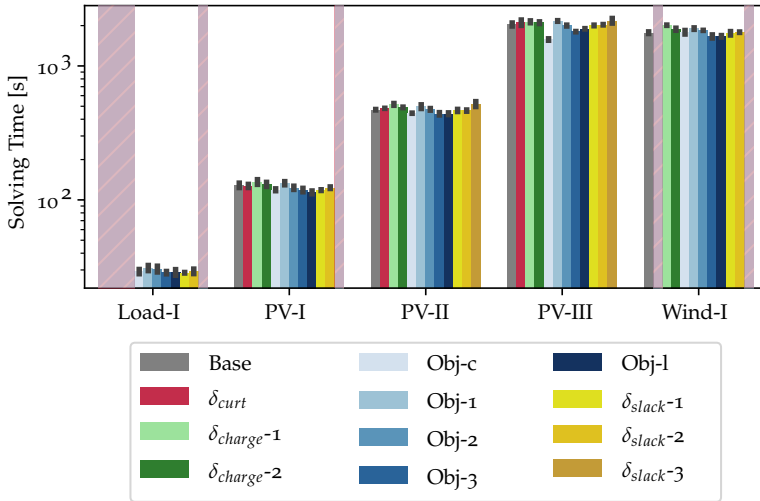


FIGURE 7.19: Solving times for sensitivity runs. Shaded areas in red indicate that the respective run did not solve due to numerical troubles.

except for *Obj-c*. Only using the curtailment needs in the objective function in *Obj-c* without the second term of squared component loading leads to higher reinforcement costs, which is not desired.

Slacks are only introduced to ensure the feasibility of the optimisation problem. The slack usage should therefore be as low as possible. The results show that for scenarios *Obj-3* and  $\delta_{slack-1}$ , an excessive slack usage occurs. Interestingly, increasing the weight of the loading term in the objective for *Obj-3* thereby shows higher slack values than a comparably low weighting of the slack penalty in  $\delta_{slack-1}$ .

Similar to reinforcement costs, optimised charging should also minimise curtailment needs. The results for the different weighting combinations show that the values are similar for most scenarios. Only in the case of scenario *Obj-1*, where the necessary curtailment is not part of the objective function, there are extremely high values for the curtailment of feed-in, inflexible load and EVs. Relatively small in comparison is an increase in feed-in curtailment in scenarios *Obj-2* and *Obj-3*. The reason is an excessive use of V2G, leading to high simultaneous charging and discharging of EVs. For the optimisation, this is a way to decrease feed-in curtailment. However, after correcting the simultaneous charging and discharging, the

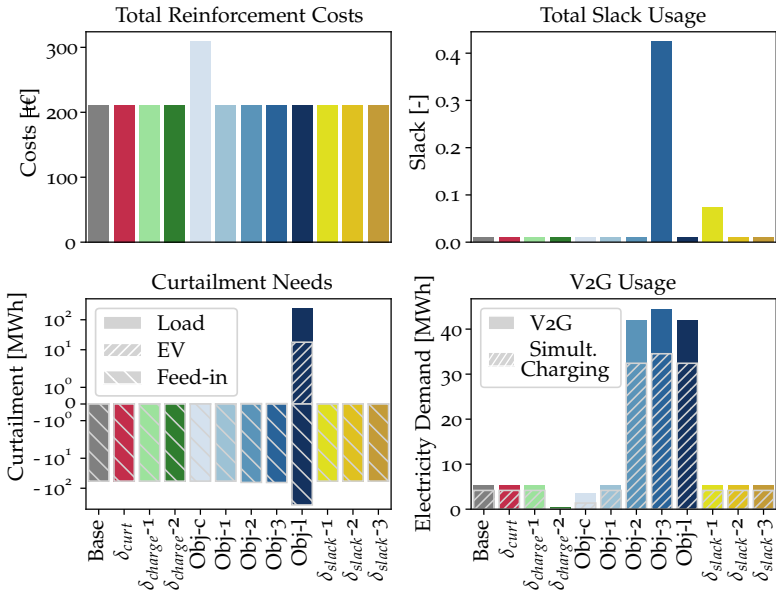


FIGURE 7.20: Comparison of sensitivity runs for grids that were solved for all investigated scenarios, i.e. PV-II and PV-III.

TABLE 7.5: Decision criteria for sensitivity scenarios.

Scenario	Decision Criterion	Acceptable
<b>Base</b>	Numerical troubles encountered	✗
$\delta_{curt}$	Numerical troubles encountered	✗
$\delta_{charge-1}$	Numerical troubles encountered	✗
$\delta_{charge-2}$	V2G usage prevented	✗
Obj-c	Increase in reinforcement costs	✗
Obj-1		✓
Obj-2	Excessive simultaneous charging and discharging	✗
Obj-3	Excessive usage of slacks	✗
Obj-l	Excessive curtailment needs	✗
$\delta_{slack-1}$	Excessive usage of slacks	✗
$\delta_{slack-2}$		✓
$\delta_{slack-3}$	Numerical troubles encountered	✗

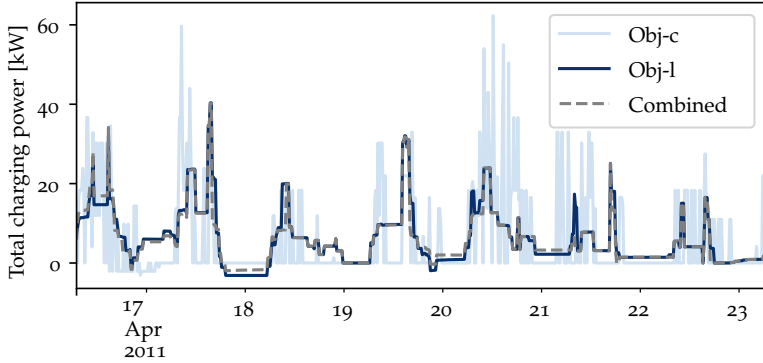
feed-in curtailment increases compared to the other cases. This indicates that the loading term in the objective should be weighted with a lower value than the curtailment term if excessive simultaneous charging and discharging should be prevented. While excessive simultaneous charging and discharging is not desirable, V2G should still be used if it can reduce the stress on the grid. With a high weight on additional losses through V2G like in  $\delta_{charge-2}$ , V2G usage is completely prevented.

Table 7.5 summarises the sensitivity analysis scenarios and whether they are acceptable for further use. If not, the reason is given as a decision criterion. Overall, only the scenarios *Obj-1* and  $\delta_{slack-2}$  yield favourable results in all investigated categories. To increase robustness, we combine the variations of both scenarios into a new one, which is also used for the investigations of the previous section. The final weights are summarised in Tab. 7.6. All results for this combination of weights (not shown) also comply with all criteria deemed necessary for an acceptable performance.

Figure 7.21 shows the total charging in feeder *Load-1* for the sensitivity runs *Obj-c*, *Obj-l* and the combined scenario. In all investigated feeders, scenarios *Obj-2* and *Obj-3* show a very similar pattern to *Obj-l* and the other sensitivity runs similar charging behaviour as the combined scenario. For easier interpretability, these other runs are therefore not displayed. Scenario

TABLE 7.6: Resulting combination of weights after conducting the sensitivity analysis.

Scenario	$\delta_{\text{curt}}$	$\delta_{\text{load}}$	$\delta_{\text{curt},l}$	$\delta_{\text{curt},f}$	$\delta_{\text{curt},ev}$	$\delta_{\text{charge}}$	$\delta_{\text{slack}}$
<b>Combined</b>	1	$10^{-3}$	1.0	0.5	0.5	2	$10^2$

FIGURE 7.21: Charging patterns of sensitivity runs *Obj-c*, *Obj-l* and the combined scenario.

*Obj-c* shows the highest charging peaks and strong fluctuations in the time series. Since, in this scenario, only the necessary curtailment is penalised, there is no incentive to reduce the charging peaks in times where either no curtailment is necessary or if curtailment cannot be prevented by reducing the charging power. The other two scenarios show a similar pattern with lower charging peaks. Only in selected instances, *Obj-l* shows additional peaks, like in the late mornings of the 20th and 21st of April. These are achieved by higher utilisation of V2G in the previous periods; however, they also result in higher simultaneous charging and discharging.

Overall, the sensitivity analysis shows that optimisation results are relatively robust if the weights are chosen in a reasonable order of magnitude.

### 7.3.2 Performance Evaluation

We want to compare the performance of the implemented charging strategies in terms of solving time and memory usage. Figure 7.22 shows the

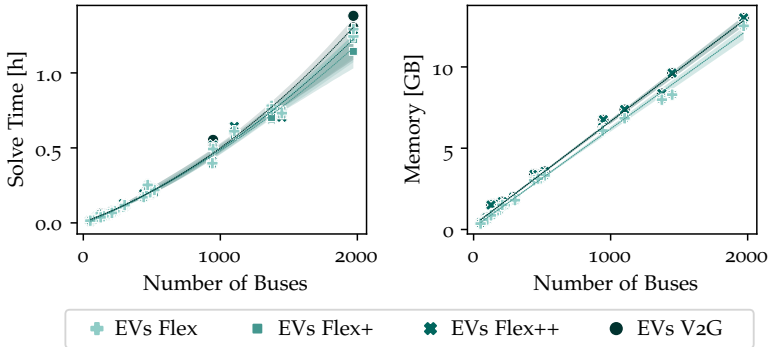


FIGURE 7.22: Comparison of memory allocation and solving time for the different optimised charging scenarios in all investigated grids.

solve time (left) and memory usage (right) for the investigated levels of flexibility over the number of buses in the feeders.

Both the solve time and the memory usage increase with the number of buses, the memory usage shows a linear trend. For the solution time, it is not clearly distinguishable whether it increases linearly or quadratically with the number of buses. In a master thesis co-supervised in the course of this dissertation, a similar analysis showed linear trends for both solving time and memory usage for a comparable problem formulation [174].

Between the different formulations of EV flexibility, there is no significant difference visible. For the solving times, *EVs V2G* tends to show slightly higher values but the order also changes between different grids. The memory allocation is slightly higher for scenarios *EVs Flex++* and *EVs V2G* than for the other two scenarios. Still, the order of magnitude is comparable. All formulations only contain linear constraints and continuous variables and therefore perform similarly well. In another master thesis, the more exact formulation with binary values for EV charging and discharging was compared to the linear version of the optimisation [113]. In that case, the solution times were significantly higher and larger grids could not be solved due to increasingly high memory usage.

Figure 7.23 shows the solving time (left) and memory usage (right) divided by the number of buses in the feeders for optimisations of different numbers

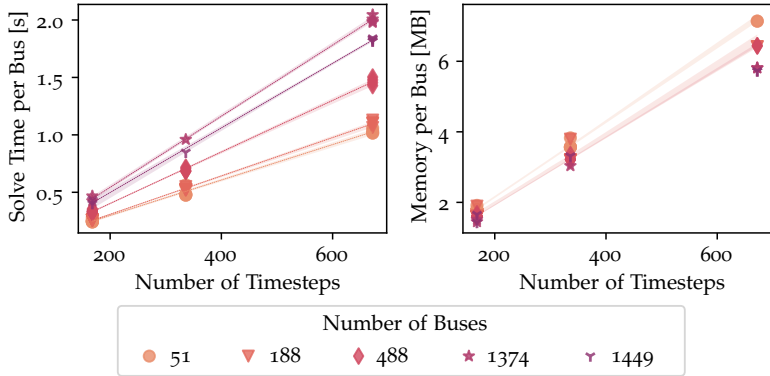


FIGURE 7.23: Comparison of memory allocation and solving time relative to number of buses in the grid for different number of time steps.

of time steps<sup>1</sup>. Again, we see linear trends for solving time and memory usage with increasing number of time steps. Comparing the values for feeders of different sizes, the solving time per bus seems to increase with larger grids while the memory usage slightly decreases.

Overall, a linear dependency of solving time and memory usage on both number of buses and number of simulated timesteps seems favorable for the investigation of large-scale grids. We furthermore do not see large differences between the different model formulations of EV flexibility.

<sup>1</sup> The scenarios *EVs Flex* and *EVs V2G* were simulated. Since the results showed close to no difference, they are not further distinguished in the displayed results.

## CASE STUDY II: SIMULTANEOUS INTEGRATION OF DERS

---

*This chapter includes the investigation of the influence of increasing penetrations of distributed energy resources (DERs) on distribution grid reinforcement costs and the flexibility potential within the distribution grids. It is based on the published paper: A. Heider, L. Kundert, B. Schachler and G. Hug, "Grid Reinforcement Costs with Increasing Penetrations of Distributed Energy Resources", 2023 IEEE Belgrade PowerTech [175], Copyright ©2023, IEEE. The results for the optimised charging are updated according to the adapted model formulation.*

### 8.1 DISTRIBUTION GRID REINFORCEMENT COSTS

In this case study, we investigate the grid reinforcement costs that are required to incorporate increasing penetration of DERS. To this extent, our study investigates the integration of photovoltaics (PV) with battery energy storage systems (BESS), heat pumps (HPs) and electric vehicles (EVs), both as single components and in a combined scenario to determine the main drivers of the costs. Additionally, we compare the uncoordinated operation with a grid-optimised operation using the flexibility of EVs, HPs and BESS.

The following sections are structured as follows. **Section 8.1.1** gives an overview on the research design of the study, including the integration of the DERS into the grids, their operational strategies and the calculation of grid reinforcement costs. In **Section 8.1.2**, the results are presented and discussed.

#### 8.1.1 *Research Design*

We use a probabilistic approach to approximate the costs of the required grid reinforcement to incorporate different penetrations of DERS. In a first step, PV, BESS, EVs and HPs including thermal energy storage (TES) are randomly connected to residential loads inside the grids. Two different op-

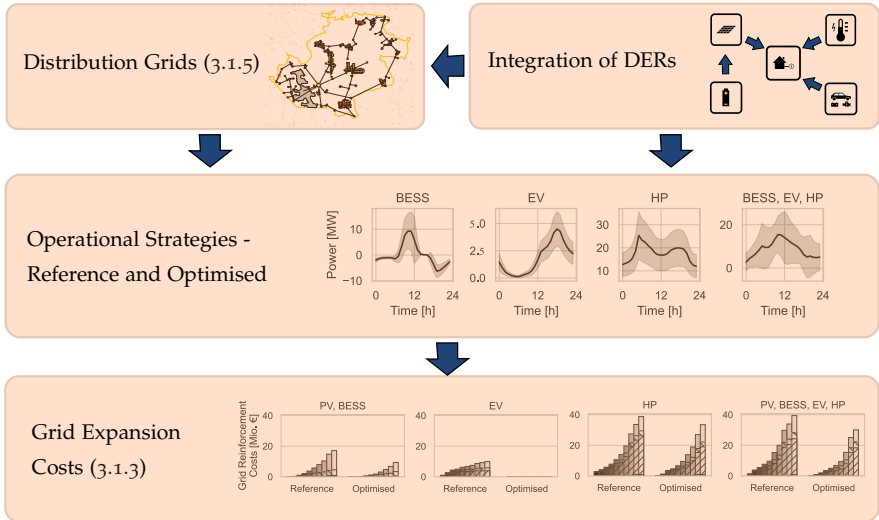


FIGURE 8.1: Research design of study.

erational strategies are simulated: the reference and an optimised operation. With the resulting time series, the grid expansion costs are calculated and the reduction potential of the optimised operation is estimated.

### *Integration of DERs*

In our study, different DERs are randomly distributed to the residential customers of the investigated grids.

**RESIDENTIAL PV-SYSTEMS** are randomly connected to residential loads that do not already own a PV power plant. If BESS are included, a battery is connected to every residential PV plant, also the ones already existing in the grids without further PV expansion. PV and BESS are sized as described in Section 3.4.1, resulting in mean installed PV capacities of 8.7 kW and mean BESS power and energy capacities of 5.2 kW and 8.7 kWh.

**HEAT PUMPS** including TES are randomly connected to a pre-specified share of all residential consumers following the sizing described in Section 3.3.2. The resulting mean thermal capacity of the HPs is 13.0 kW, and the connected TES has a mean thermal storage size of 18.3 kWh.

ELECTRIC VEHICLES are integrated through home charging points from the previous chapter. These are randomly added to residential loads. The added charging points can have nominal charging powers of  $P_{nom}^{EV} = \{3.7, 11.0, 22.0\}$  kW. Note that in this way, only the charging demand at home charging stations is added to the grids. Charging demand that would occur at work, in public or at high power charging stations, is not included in this study as it focuses on residential loads.

The DERs are integrated to the status quo grids, further described in 3.1.5. To gain a better understanding of the influence of the different technologies, we simulate five different scenarios: 1) PV on its own, 2) PV in combination with BESS, 3) only HPs, 4) only EVs and 5) the combination of all of them, added to the initial grid. We furthermore increase the penetration of these technologies in steps of 10% from 0% to 100%. A penetration of 100% thereby means that every residential load in the grid owns the respective DERs.

### *Operational Strategies*

We investigate two operational strategies for all flexible technologies: reference and optimised operation. PV plants are not assumed to operate flexibly on their own. BESS, HPs and EVs, on the other hand, are modelled in a way that they can adapt their operation. Descriptions for the reference operation of BESS, HPs and EVs can be found in Sections 3.4.2, 3.3.3 and 3.2.3, respectively. Sections 3.4.4, 3.3.6 and 3.2.6 contain the model formulations used for the optimised operation of BESS, HPs and EVs. For both battery and thermal storage units, the efficiencies are assumed to be 100% to determine the maximum potential to reduce the grid reinforcement costs. Thus, the ideal formulations are used.

For the *optimised operation*, the operation of the DERs is optimised for one day at a time using the optimal power flow formulation introduced in Chapter 6. As reactive power provision is not the focus of this study, it is assumed that all flexible units operate at a power factor of 1.0.

### *Grid Reinforcement Costs*

The grid reinforcement costs are calculated using the contingency case explained in Sections 3.1.2 and 3.1.3. This means that in the load case, medium voltage (MV)-lines and the high voltage (HV)/MV transformer are only allowed to be loaded to 50% of their thermal limit (to account for

( $n-1$ )-security). For all other components as well as the feed-in case, this limit amounts to 100 %. The voltage has to stay between 0.9 and 1.1 p.u. in the grids. Additionally, there are grid-level- and case-specific voltage bounds which are further detailed in Section 3.1.2. If any of the boundaries are violated, the heuristic approach of grid reinforcement implemented in  $\epsilon$ DisGo [75] is used to solve them and to estimate the required costs (for further details see Section 3.1.3).

In order to keep the simulation time reasonable, we make use of the fact that for the necessary grid reinforcement, only the highest overloading or voltage violation of a component is relevant. Consequently, only time steps where at least one component shows its highest overloading or voltage deviation are of interest. To determine these, we simulate the entire year for the reference operation and three different runs for each grid and scenario at the maximum penetration of 100 %. Different runs for the same scenario, grid and penetration of DERs only differ in the seed that is used for the random draws. Therefore, the installed capacities at specific sites differ, and for penetrations below 100 %, the locations of DERs can differ as well. Since the optimisation is conducted for entire days, the run with the largest number of days with at least one highest overloading or voltage violation of a component is chosen from the three runs. Only the days with grid violations of this run are later evaluated for the respective grid and scenario.

For the reference operation, the simulations are repeated ten times. From these ten runs, the run with the lowest root mean square deviation from the mean of all runs is chosen as a representative run. For this representative run, we additionally analyse the optimised operation.

### 8.1.2 Results and Discussion

In the following, we present the results along the DER operations, grid reinforcement costs and cost reduction by optimised operation.

#### *DER Operations*

Fig. 8.2 shows the mean power consumption of BESS (when combined with PV), EVs and HPs over a day in the reference (top) and optimised (bottom) operation with 100 % penetration of DERs across all the grids. The grey area around the mean thereby displays the standard deviation for the different simulated days. For the combination of PV and BESS, we see a shift in BESS

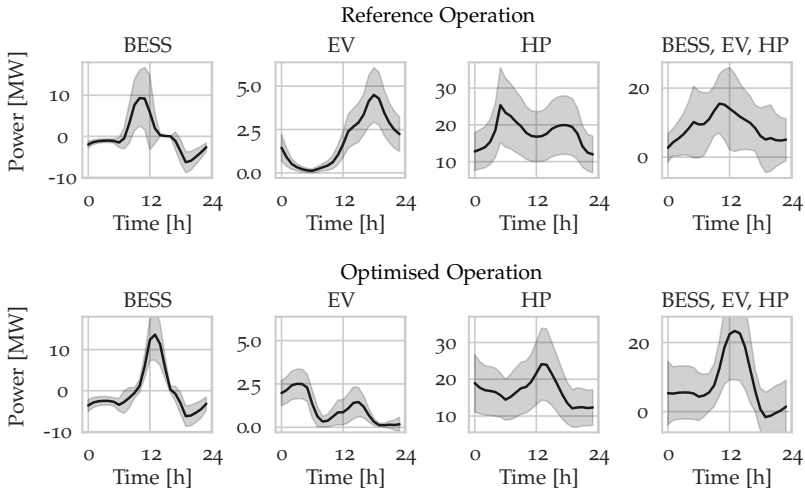


FIGURE 8.2: Mean power consumption of flexibility options over a day for reference (top) and optimised (bottom) operation. The grey areas denote the standard deviation.

charging from morning hours to noon. In this way, the local PV-production peak can be reduced. Similar to the reference operation, the discharging process shows a peak in the evening hours, when the residential load is highest. The reference charging of EVs shows a peak in the evening hours when most cars arrive at home. This peak coincides with the already existing load peak of residential loads. Therefore, the optimised operation shifts the charging demand towards early morning hours and, where possible, to noon hours. Since few cars are parked at home during the day, the peak in the morning hours is more pronounced. The reference operation of HPs shows peaks in the morning and evening. To avoid coinciding with existing peaks in residential load and to make use of local PV-production and high coefficient of performance (COP)-values around noon, the demand is shifted into these hours by the optimised operation. When all DERs are integrated, the reference operation shows the highest consumption during daytime around noon. The optimised operation even further increases the noon peak to leverage the PV in-feed and reduces consumption in the evening hours.

### *Grid Reinforcement Costs*

Fig. 8.3 shows the grid reinforcement costs for all six grids when all components operate with the reference strategy. The scenario with only PV is not displayed as the results are essentially the same as for the case of both PV and BESS. This leads to the conclusion that the operation of BESS, where the self-consumption is maximised, does not reduce the stress on the distribution grids. In some cases, including BESS even leads to additional reinforcement needs for individual MV-low voltage (LV)-transformers. However, the overall change in reinforcement costs is minimal. The results show that the integration of HPs causes the highest grid reinforcement costs. When all components are simultaneously integrated, the costs of integrating individual types of components do not accumulate but the total costs mostly reflect the costs of the HP integration. In some cases, e.g. for high penetrations in grid *PV-2*, synergies between PV with BESS and HPs reduce the costs compared to the integration of only HPs.

Fig. 8.4 shows the marginal grid reinforcement costs for additional capacity of the different DERS. To obtain these values, we divide the additional costs for each step of the calculation (e.g. from 10% to 20% penetration) by the added capacity of the respective component. All simulated values for PV and BESS in case of the reference operation are displayed on the left and for HPs on the right. For the scenario with PV and BESS, the marginal costs increase until an installed capacity of  $\sim 30$  MW. At higher capacities, it stabilises around  $\sim 100$  €/kW. There is no significant increase at small installed capacities visible for EVs (not shown) and HPs, but the values scatter around mean values already for small penetrations. A possible explanation is that most grids are designed for the existing load in the grid. Some parts of the grids therefore have free capacity for feed-in technologies. With increased penetrations, more and more components reach their limits, which results in increasing costs per newly installed kW. If all components have reached their hosting capacities for feed-in, in this case around  $\sim 30$  MW, the marginal costs plateau. For additional load, on the other hand, the capacities are already close to their limits. Therefore, no such increase in marginal costs at low additionally installed capacities is visible.

Another effect observable in the scatter plots is that the results show comparably high marginal costs around an installed capacity of  $\sim 40$  MW for the grid *Load-1* and a further increase in PV and BESS capacities. A similar effect is also visible for the grid *PV-2* around an added capacity of HPs of

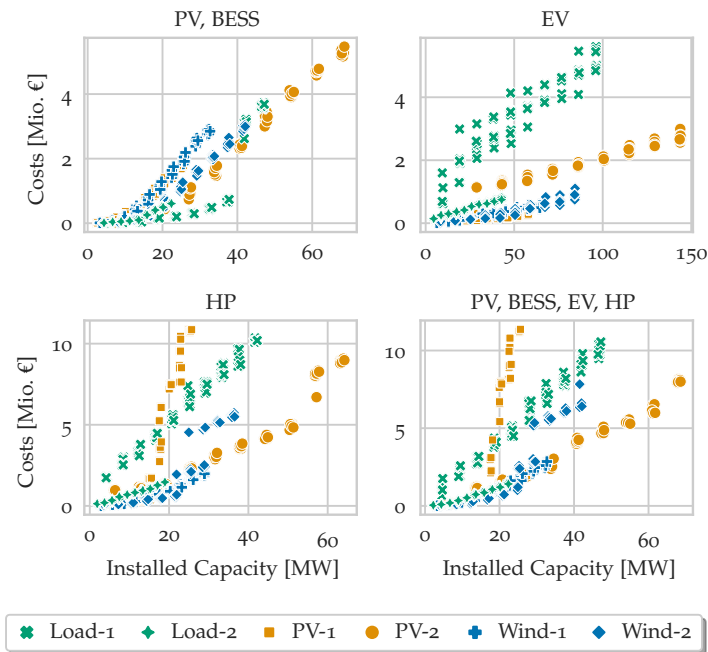


FIGURE 8.3: Grid expansion costs for the simulated scenarios with reference operation. For PV with BESS, the costs are plotted against the installed PV capacity and for the integration of all DERs the costs are plotted against the sum of installed capacities of PV, HPs and EVs.

$\sim 20$  MW. Several other grids show the same effect with increased penetrations of EVs and HPs. These spikes can occur when very long MV-lines start to be overloaded and need to be replaced. For the displayed case of grid *Load-1* with increased penetrations of PV and BESS, additionally long LV-lines start to be overloaded as well, causing the high marginal cost values. In the case of grid *PV-2* and uptake of HPs, overloading of the HV-MV-transformer in addition to long MV-lines is another reason for the observed cost spikes.

### *Cost Reduction by Optimised Operation*

The boxplots in Fig. 8.5 show the marginal grid reinforcement costs for reference and optimised operation of PV with BESS, EVs and HPs. The light-blue triangles display the mean values. For readability, the plot is cropped at the y-axis and does not show all outliers. The results for the

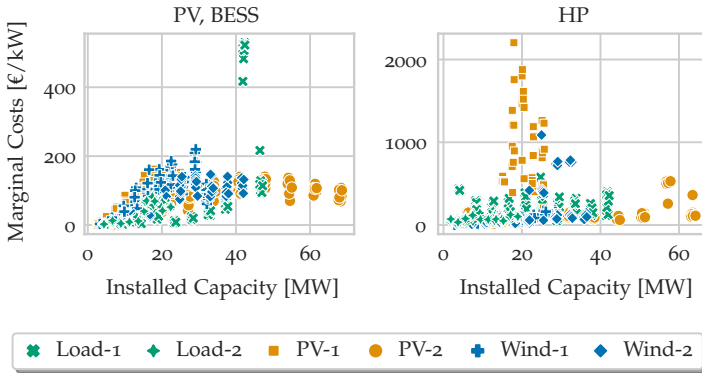


FIGURE 8.4: Marginal grid reinforcement costs per added capacity of DERs against the installed capacity for the reference operation.

reference operation show the highest marginal cost for HPs with a mean of 185.1 €/kW and values up to 2203.2 €/kW. Additional PV capacities cause marginal costs with a mean of 74.04 €/kW and maximum values of up to 541.6 €/kW. The lowest values are observed for EVs with a mean of 19.1 €/kW and maximum values up to 170.1 €/kW. However, it has to be mentioned that we only account for home charging and omit the charging demand that would occur at other charging stations. Therefore, the marginal costs accounting for all charging use cases are likely significantly higher. First, a larger overall charging demand occurs when also accounting for the other use cases. And second, the charging powers are higher, especially for public and high power charging. In [86], median values of 46-1385 CHF/kW were obtained for HPs, 51-213 CHF/kW for PV and 34-143 CHF/kW for EVs. Comparing these with the median of every step of increase and grid, we see comparable values in our simulations: 0.0-1493.3 €/kW for HPs, 0.8-522.2 €/kW for PV and 1.5-133.3 €/kW for EVs. The higher values for HPs can be explained by the fact that we additionally account for the MV. In fact, we see a large share of the costs in the MV in that case. The lower values for the case with EVs might be due to the limitation on home charging.

The optimised operation shows different effects for the PV with BESS, EVs and HPs. Note that the number of simulated runs is smaller for the optimised operation since this case is only simulated for one representative run instead of ten as is done for the reference operation. While we choose the run closest to the mean, the smaller sample size with one occurrence per grid and step of increase of the penetration still influences the results.

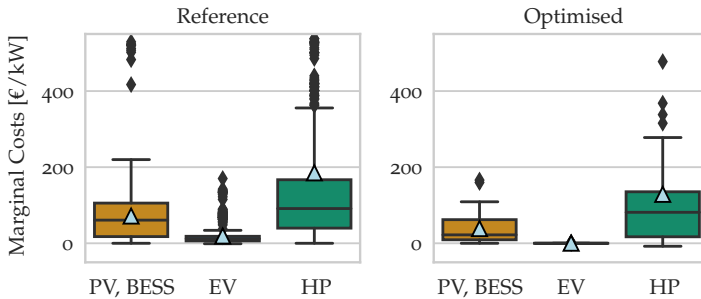


FIGURE 8.5: Boxplots showing the marginal grid reinforcement costs per added capacity of DERs for the reference (left) and optimised (right) operation. The light-blue triangles mark the mean values.

The optimised operation of HPs reduces the mean marginal cost by 30.5 % to 128.6 €/kW, and the median by 10.8 %. However, the relative decrease in costs depends on the penetration of HPs. As a trend, the reduction potential decreases with increasing penetrations. For lower penetrations, on the other hand, the optimised operation leads to significantly decreased costs. For the grid *PV-1*, the decrease in cost is very high, because of the synergies with the previously existing PV. PV with BESS achieve a reduction of 46.1 % of mean marginal cost to 38.6 €/kW and even a reduction of 63.7 % of the median with the optimised operation compared to the reference operation. For EVs, the optimised operation reduces the marginal costs to nearly 0.0 €/kW.

Fig. 8.6 shows the sum of grid reinforcement costs of all grids for reference and optimised operation of the representative run divided into costs for the different grid levels. The integration of all DERs at the same time leads to grid reinforcement costs of 39.4 Mio. € summed up over all grids, the integration of only HPs to 38.8 Mio. € for a penetration of 100 %. For PV with BESS, the costs at a 100 % penetration amount to 17.1 Mio. € and for EVs to 9.9 Mio. € summed up over all grids. For EVs and HPs, a large share of these cost occur in the MV. For PV with BESS, on the other hand, almost no costs occur at this voltage level. The reason is the different operational constraints for load and for feed-in. For load, the (n-1)-security constraint leads to a maximum allowed loading of 50 % in the open rings of the MV whereas for feed-in, a loading of 100 % is allowed since feed-in can be curtailed in case of overloading or a fault. Therefore, there is more free

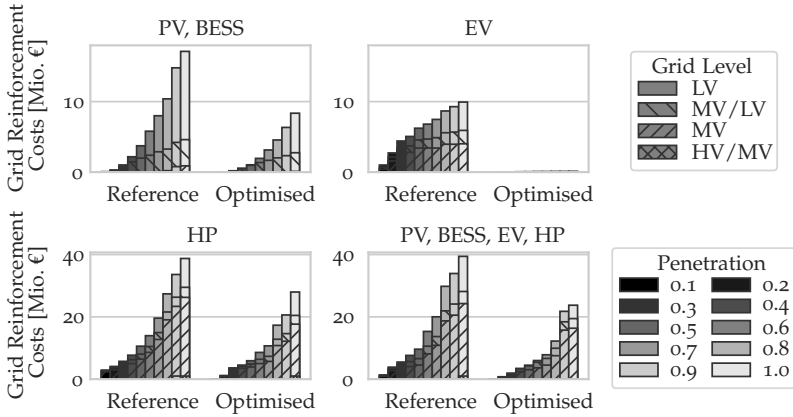


FIGURE 8.6: Sum of grid reinforcement costs for all grids divided into the different grid levels for reference and optimised operation.

capacity for PV in the MV than for the technologies that lead to additional load.

In all cases, the optimised operation reduces the grid reinforcement costs. The most significant cost decrease compared to reference operation occurs for EVs. Nearly all required grid reinforcement can be deferred, reducing the costs by almost 99%. For PV with BESS, the reduction summed over all grids and penetrations amounts to 58.8% of the costs with reference operation. However, with higher penetrations, the reduction decreases. There are relative reductions of up to 88.9% of the costs with the reference operation for small penetrations. The reduction decreases to 51.2% for a penetration of 100%. The same trend holds for HPs and the combination of all investigated DERS as well. For HPs, the mean decrease in costs over all penetrations and grids is equal to 38.9% of the costs with reference operation. In the case of 10% penetration, the reduction reaches 99.3% whereas this value is reduced to 27.8% for a penetration of 100%. In case of a combined increase of PV with BESS, EVs and HPs, the mean reduction of costs over the sum of all penetrations and grids equals 50.7%. The reduction can reach up to 97.0% for low penetrations. Again this value is significantly lower for a penetration of 100%, amounting to 39.8% reduction compared to the costs with reference operation.

This decrease in relative reduction with increasing penetrations of DERS indicates a saturation effect in the grids. With low penetrations, the flexibility to shift demand and feed-in effectively avoids grid issues. However, with

increasing penetrations, even with the ability to shift demand and feed-in, the grids reach the limit of their hosting capacities, leading to a limited potential to reduce costs. Still, even at very high penetrations, significant cost reductions are possible with an optimised operation of decentralised flexibility options.

The optimised charging does not necessarily reflect the minimum-cost solution. One reason is that losses are neglected in the chosen formulation. Since the losses grow quadratically with the current, they are especially high in cases of high penetrations of HPs and EVs as additional load. Even though the values are small compared to the consumption of these technologies, they accumulate for underlying elements. In situations with high load, it can therefore happen, that when accounting for the losses, some elements show an overloading whereas neglecting the losses leads to a situation without overloading issues. In these situations, the optimisation, which neglects losses, might schedule the flexibility options in a way that leads to overloading and consequently grid reinforcement needs. Another factor is that the chosen objective is only a proxy to reduce the grid reinforcement costs. It reduces continuous variables (the necessary curtailment and component loading) whereas the grid reinforcement is a discrete process. Therefore, there might be situations where the optimization reduces loading of components that are not close to a critical transition and accepts higher loading for another component that then requires reinforcement. However, in aggregate, the optimised charging still shows a significant reduction in costs and therefore provides a viable solution.



## DISCUSSION

---

In this chapter, we want to discuss the results of the presented case studies in **Sections 9.1 and 9.2** and put them into perspective with previous work. In **Section 9.3**, we critically reflect on the chosen model formulation .

### 9.1 INFLUENCE OF ELECTRIC VEHICLES

In the first case study, we investigated the influence of different EV charging strategies on the grid integration of EVs.

The potential of flexible EV charging to help the integration of renewable energy sources (RES) into the distribution grids proves to be limited in our investigations. While the necessary feed-in curtailment can be slightly reduced, the reduction only amounts to 1.7% of the overall feed-in curtailment with the highest level of EV flexibility. The grid reinforcement needs caused by the integration of RES can also only be partly avoided (mainly in PV-dominated grids) and the costs with the integration of EVs always exceeds the costs without. From our investigations we therefore conclude that the synergies of flexible EV charging and RES are limited on the lower grid levels. Only local PV generation can be effectively utilised by EVs. Using the generation of larger RES that are directly connected to the transformer stations or to the MV, on the other hand, does not relieve the local distribution grids. Our results therefore imply that the potential of smart EV charging to help the integration of RES on a local scale is limited.

However, this does not mean that EV flexibility does not have the potential to help with RES integration on a larger scale. The previous investigations of Chapter 4 found that the flexibility potential can be significantly increased when allowing shifting over standing times and the utilisation of vehicle-to-grid (V2G). The positive effects of such flexibility provided to the overlying grids and entire system have been proven in various studies. It was able to significantly reduce the RES curtailment (by up to 40%) [151], [157], [176]. Furthermore, production costs for additional electricity for EV charg-

ing [176] and total system costs [102], [157] could be reduced significantly. So on the system level, EV flexibility can contribute largely.

However, the system wide flexibility procurement might come at the cost of increased stress on the distribution grids [22], [23], [96]. To this respect, our results show that the charging strategy highly influences the additional stress that the integration of EVs poses on distribution grids (DGs) and the required countermeasures. With an uncoordinated plug-and-charge, both the necessary load curtailment and the grid reinforcement costs show high values. Load curtailment can be largely avoided through EV flexibility with a reduction of up to 88.6%. The additional reinforcement needs through EV charging can also be reduced by up to 80.2%. In [95], the reinforcement costs could even be avoided almost entirely by real-time control of the EVs. So overall, coordinated EV charging shows great potential to limit the additionally required reinforcement caused by the integration of EVs. Shifting the charging demand within the originally scheduled charging session thereby already shows the largest reduction potential. Further increasing EV flexibility by shifting between standing times and the utilisation of V2G only showed marginal improvement. Therefore, shifting within the standing times seems to provide sufficient flexibility to limit grid reinforcement needs.

From a practical point of view, the simple rule-based strategy of reduced charging thereby performs similarly well as the grid-optimised charging strategy. Significant decrease of grid issues with a simple balanced charging strategy was also found in [96]. In [95], the authors similarly found a significant decrease of grid reinforcement costs with a reduced charging. However, their real time optimised operation could even further decrease the reinforcement costs to very low values even for 100% EV penetration. However, grid reinforcement also occurred without EV integration in their case, implying that their grids might not have been designed for the integrated charging demand time series. For already highly stressed grids, a reduced operation might therefore not be as beneficial as a smart control. Still, due to its simplicity, the reduced charging seems to be a viable alternative to an optimised operation concerning the reduction of grid reinforcement costs.

The majority of additional grid reinforcement in our investigations occurred in the LV, a smaller part at MV/LV-transformers. A higher increase in costs in the LV than in the MV was also found in a previous study on real German distribution grids [22]. However, they also found a significant cost increase

in the MV, which was not the case in our study. One reason could be their more conservative approach to grid expansion, using simultaneity factors. These assumed that the additional demand of new loads (such as EVs and HPs) is added to the existing peak load. However, they also mentioned that the analyses of time series data showed a delay of new and existing peaks [22]. Therefore, the necessary reinforcement was likely overestimated. Furthermore, they investigated the simultaneous integration of EVs and HPs while our study focused on the integration of EVs alone. In [95], they also found a higher sensitivity of MV grids towards the integration of EVs. However, most of the grids that showed low integration capabilities were urban, which are not accounted for in our investigations. It has to be noted, that the results in the literature also largely differ. As an example, the effects of EV integration are stronger in rural areas in some studies (e.g. [86], [95], [96]) while others attest a higher influence in urban areas (e.g. [22], [23]). The results therefore seem to depend strongly on the investigated grids and simulation setups.

Lastly, the results show that even with the highest level of EV flexibility, grid issues cannot be fully avoided at the simulated penetration of EVs. This means that either load and feed-in have to be curtailed or the grids need reinforcement to avoid violations of the grid constraints. In contrast, the grid reinforcement costs for the integration of EVs could almost be fully avoided in [95]. However, they only accounted for home and work charging [177], while in our investigations, part of the reinforcement costs are caused by inflexible high power charging (HPC). This part of the costs cannot be reduced since in case of HPC, it is assumed that the priority lies in the fulfillment of the service and charging demand can therefore not be shifted within these charging sessions. In the second case study, where we only investigate the effect of home charging, we achieve similarly high reduction potentials as in [95]. Our results therefore indicate that when accounting for public and high power charging, the distribution grids need reinforcement to a certain extent. Using flexibility can reduce the reinforcement needs but not fully avoid them.

## 9.2 INTERPLAY OF DERS

In a second case study, we analysed the necessary grid reinforcement for increasing penetrations of residential PV, BESS, EVs and HPs in six different MV-grids with underlying LV-grids. To gain a better understanding of the main cost drivers, we simulated scenarios for an uptake of PV, PV with

BESS, HPs and EVs on their own as well as a combined scenario with all investigated DERs. The different technologies were randomly added to the residential loads of the grids and the resulting costs were calculated. For one representative run per grid, we additionally calculated the costs for an optimised operation of the DERs to quantify the potential decrease in grid reinforcement costs through utilisation of the DER's flexibility. Our results help to explore different effects for the integration of DERs into typical DGs. Furthermore, the calculated values can be used to incorporate DG reinforcement caused by residential DERs into large-scale energy system models.

The results show the highest absolute and marginal costs for integrating HPs and the lowest for integrating EVs. In [86], the authors also found HPs to cause the highest specific costs at a mean. However, PV and EVs showed similar distributions. The difference might be caused by the fact, that we only account for home charging, so a limited share of the total charging demand in our study. If other use cases are included as well, the specific costs might increase and costs might also add up differently in the combined scenario, since charging would occur at different locations and cause violations in other parts of the grids. In the current setup, the costs of the combined scenario largely reflect the costs induced by the integration of HPs and are only slightly higher than in the case of HPs only. This means, that peaks of the different DERs do not add up but HP peaks determine the necessary grid reinforcement. In [86], the costs for a combination of EVs and HPs also showed only slightly higher values than for the single investigations. However, including PV increased the costs significantly in their case. The reason might be that they use a worst-case approach with simultaneity factors to determine the grid reinforcement costs. With this, there is limited room to account for synergies which can be assessed with the time series based approach we use. Furthermore, they include relatively more PV capacities. In future investigations, it would therefore be interesting to investigate whether PV has a higher influence on costs in the combined scenario if higher capacities are installed per household. In our investigations, a large share of the costs occurs in the MV for EVs and HPs, whereas the integration of PV mainly leads to costs in the LV. These results are different to the ones in the previous case study, where the costs of integrating EVs occurred mainly in the LV. This is because the first case study is undertaken under normal operating conditions while the second accounts for (n-1)-security. MV components can therefore only be loaded to 50% in the load case, leading to higher reinforcement needs in

the MV. When operating the grids (n-1)-secure, MV grids might also need higher reinforcements for the integration of new loads.

Investigating the marginal cost of integrating the different DERs into the grids, we also see a difference between the integration of PV and of the load technologies. For PV, an increase in marginal costs for small penetrations occurs. The reason is that the grids were initially designed to accommodate the load. Therefore, there is free capacity for feed-in technologies at low penetrations. More and more of this free capacity is used with increasing penetrations, leading to increasing marginal cost, which then plateaus at a particular value. For EVs and HPs, on the other hand, the marginal costs scatter around a particular value already at small penetrations as there is only limited free capacity for additional load and therefore no reduced marginal costs for low penetrations. An effect visible for all DERs are peaks in the marginal costs when long MV-lines or the HV-MV-transformer reach their limits and need to be reinforced.

The optimised operation shifts the demand to noon hours to use local PV-generation, thereby reducing the need for distribution capacities within the grids. For EVs, the demand is additionally moved to early morning hours since many vehicles are not parked at home during the daytime. The potential cost reduction by an optimised operation differs by the type of the DER and depends on their penetration within the grids. Except for EVs, where the optimised operation leads to cost reductions of almost 99 % even at a penetration of 100 %, the relative reduction in costs compared to the reference operation decreases with increasing penetrations of DERs. This effect indicates that there is a certain saturation effect within the grids. For low penetrations, the shift of demand and feed-in can mitigate reinforcement needs to a large extent. For high penetrations, the grids reach their limits even with an optimised operation of the DERs, leading to a limited reduction potential. However, it is still possible to significantly reduce the necessary reinforcement with an optimised operation, even at high penetrations. For the considered grids and for HPs, the costs can be reduced by 13.6 %, for PV with BESS by 45.2 % and for the combination of all DERs by 23.6 % at a penetration of 100 %. In [159], the authors also found a significant decrease of grid reinforcement costs with a smart operation of EVs and HPs. They furthermore showed that additional voltage regulation can further decrease the costs and the combination of all measures reduced the reinforcement costs by 66 %. It would therefore be interesting to include voltage regulation in future investigations and compare the effect in the investigated distribution grids.

This research focused residential DERs and their effect on the grid reinforcement costs. In future work, the study could furthermore be expanded to other loads and operational approaches, namely other EV charging use cases, industrial demand response and large scale BESS and HPs. Furthermore, it would be interesting to study the trade-off between flexibility procurement to reduce the grid reinforcement in the DGs and flexibility provision to overlying grid levels.

### 9.3 LIMITATIONS

In order to handle the high geographical and temporal resolution, certain simplifying assumptions and modelling decisions were made. In this section, we want to critically reflect on the limitations in the model formulation and the effects on the results.

First, the losses are neglected in the chosen model formulation. While this is a valid assumption for grids under normal conditions, the losses can become significantly more important in a situation with highly loaded grids. In our simulation setup, high shares of DERs are integrated into status quo grids, thus creating situations with such high loading. Losses might therefore be relatively high. For the estimated curtailment needs, the load curtailment will be underestimated while feed-in curtailment might be overestimated since losses constitute additional load. For the optimised operation, there might be situations where neglecting the losses leads to a situation without violations of the grid while the losses create overloading or voltage issues. However, the second term in the objective function that minimises the virtual loading of the component without accounting for curtailment should prevent that these situations occur frequently. A master thesis that was co-supervised during this PhD enhanced the introduced problem formulations and uses a second order cone relaxation that accounts for losses in the power flow [174]. For future investigations, we propose to use the updated approach and compare the results of the linearised optimal power flow with the second order cone version to estimate the trade-off between computational burden and performance.

Furthermore, we assume a balanced operation of the system, which is not necessarily the case, especially in LV grids. However, larger consumers like 11 kW chargers are connected to all three phases. Furthermore, assuming a balanced operation is a necessary and common simplification for large-scale studies.

Lastly, the chosen objective is only a proxy to minimise grid reinforcement needs. A direct minimisation would require integer values since the number of new lines and transformers is a discrete value. Including these in the optimisation would increase the complexity to an extent that the large-scale grids that are the basis of our investigations, are no longer solvable (see also [113]). While the chosen model formulation successfully decreased the reinforcement costs, the obtained values are likely not the global optimum. It would be interesting to investigate the difference in performance for smaller systems to estimate the gap between the introduced model formulation and a direct minimisation of the reinforcement costs.



## SUMMARY AND CONCLUSIONS

---

We investigated the geographic flexibility needs in German distribution grids with increasing shares of DERs. We therefore investigated six differently composed MV grids with underlying LV grids and calculated the necessary grid reinforcement to incorporate different shares and combinations of EVs, HPs, PV and BESS. We furthermore estimated the potential of a smart operation using the flexibility of EVs, HPs and BESS to decrease the necessary grid reinforcement. Specific attention was thereby given to EV flexibility because of their large charging powers and storage capacities.

Our results showed that even with a smart operation of DERs, grid reinforcements are necessary. However, these can be delayed when using DER flexibility and reduced by almost one fourth for a 100% penetration of EVs, HPs, PV and BESS in households. A delay of necessary reinforcements might become especially interesting when a large share of the German distribution grids faces reinforcement needs and resources such as technical material and skilled labour are limited.

For the combined integration of household DERs, heat pumps proved to be the main cost driver causing the highest specific and absolute costs. The total costs were much lower than the sum of the individual DERs and largely resembled the costs of HPs on their own. This result stresses the importance of a combined analysis of all DERs since they can be managed in a way that peaks do not necessarily add up.

The more detailed investigations of EVs, including charging at work and public charging stations in addition to home charging, showed that shifting within the originally scheduled charging session already significantly reduces the necessary grid reinforcement. Furthermore, a rule-based reduced charging yields similar reduction potentials and might be a simple alternative for the centrally optimised charging with an easier real-world implementation not requiring any communication between the charging stations. Increasing the flexibility further by allowing shifting between parking times and V2G lead only to marginal improvements in grid reinforcement

costs but increased the available flexibility potential to overlying grids significantly. In the following Part III, we investigate in how far this flexibility can reduce national storage requirements on different time scales, which are defined to measure the temporal flexibility needs in renewable power systems.

## Part III

# TEMPORAL FLEXIBILITY NEEDS IN THE NATIONAL SYSTEM



## MOTIVATION AND RELATED WORK

---

*This part of the thesis is based on the working manuscript: A. Heider, M. Genena, B. Schachler, P. Blechinger and G. Hug, "Flexibility needs in a 100 % renewable German power system with growing shares of decentralised sector coupling technologies" [116].*

### 11.1 INTRODUCTION

The future German power system will rely heavily on the generation of variable renewable energy sources (VRES), namely photovoltaics (PV) and wind [178]. Unlike thermal power plants, which provide a dispatchable and continuous electricity supply, the power output from VRES is intermittent and more difficult to predict. Balancing supply and demand therefore becomes more challenging as now both demand and supply are uncertain, and need to be balanced. Consequently, there is a growing need for flexibility in the system [1].

Simultaneously, one of the primary source of flexibility, thermal power plants, are being replaced by VRES. With a growing need for flexibility and decreasing provision from the supply side, the changing power system requires a paradigm shift: from flexible generation following inflexible demand to flexible demand and storage consuming inflexible generation. Sector coupling technologies are one possible source of such flexible demand. More and more of these technologies, such as electric vehicles (EVs) and heat pumps (HPs), are introduced to the power system to electrify the transport and heating sectors. These new consumers increase the electricity demand, and are also likely to increase the need for flexibility when uncontrolled [38]. On the other hand, EVs and HPs can provide flexibility to the system as they can shift their demand within certain limits [2].

The key for a power system based on high shares of VRES is to provide enough flexibility. However, there is no clear and shared definition and means to quantify flexibility needs and availability. Yet, such an understanding is crucial for effectively incentivising and providing flexibility to

the system. Furthermore, it is equally important to quantify the flexibility potential of emerging technologies to estimate their possible contribution to cover future flexibility needs. In the scope of this study, we introduce a new flexibility quantification method based on linear optimisation to minimise energy shifts on different timescales<sup>1</sup>. It facilitates the determination of the system's requirements for load shifting and storage independent from specific technologies and the investigation of the contribution of individual flexibility options to supply these flexibility needs. With this approach, we evaluate the potential of new loads (EVs and HPs) to supply the flexibility needs in the system and showcase the utilisation of the new method to address the following questions:

- What temporal flexibility needs in terms of energy shifting are to be expected in a 100% renewable energy (RE) system in Germany?
- How do these flexibility needs change with the deployment of new consumers (EVs and HPs)?
- What potential do these new consumers offer to reduce the flexibility needs?

The remainder of this part is structured as follows: **Section 11.2** gives an overview over existing modelling approaches to determine the flexibility potential from the demand side and system flexibility needs. **Chapter 12** introduces the newly developed model and flexibility indicators considered in the evaluation. **Chapter 13** includes the case study setup in **Section 13.1** and introduces the investigated scenarios and results - including the influence of the generation mix in **Section 13.2**, the influence of decentralised flexibility options (DFOs) in **Section 13.3** and a combined analysis in **Section 13.4**. In **Section 13.5**, we investigate the sensitivities with respect to the most important model parameters and input data. **Chapter 14** discusses results and limitations. Finally, conclusions are drawn in **Chapter 15**.

## 11.2 BACKGROUND

In the literature, different approaches to quantify the flexibility potential from the demand side and flexibility needs have been introduced. In this section, we provide an overview of relevant works.

---

<sup>1</sup> The code is openly accessible online under <https://github.com/AnyHe/SEM.git>.

TABLE 11.1: Methodologies to quantify flexibility potential from the demand side

Flexibility Metric	Method	References
Change and duration of power increase or decrease	Energy flexibility envelopes from simulations or measurements	[114], [146], [180]
Maximum power, shiftable energy and recovery time	Simulations, detailed modelling of HPs	[143]
Storage capacity, storage efficiency and power shifting capacity	Simulations, detailed modelling of buildings	[181]
Storage formulation with time-varying power and energy constraints	Linear programming	[182], [183]
Demand shifting within delay time frame	Linear programming	[184]–[186]
Reduction in system flexibility needs	Energy and power flexibility envelopes from simulations, linear programming	This work

### 11.2.1 Flexibility Potential of the Demand Side

Table 11.1 summarises selected ways to quantify the flexibility potential of the demand side, their underlying methodology and relevant references for each. Generally, quantifying the flexibility potential of the demand side can be further subdivided into detailed modelling of specific technologies or buildings and the more aggregated representation for energy system modelling.

In a comparison of different approaches to quantify the flexibility of energy use in buildings, temporal flexibility, the amplitude of possible power change and the associated costs are identified as common aspects of energy flexibility [179]. As our work focuses on the technical aspect of flexibility, we omit the cost factor.

A concept of capturing the available flexibility is the determination of energy flexibility envelopes which are obtained from simulations or real measurements. The envelopes consist of the accumulated energy consumption of the flexible units for two extreme cases: the minimum represents the

minimum consumption and/or consumption as late as possible, and the maximum represents the maximum consumption and/or consumption as early as possible. In [180], only the feasible duration of forced operation at nominal capacity and the feasible delay time were extracted. In later applications, constant deviations from the undisturbed operation and the maximum duration during which these deviations can be sustained were evaluated [114], [146]. The concept was applied to combined heat and power (CHP) plants with thermal energy storage (TES) [180], residential appliances (washing machines, tumble dryers, dishwashers, domestic hot water buffers and electric vehicles) in a pilot project in Belgium [114] and to a building with different combinations of PV, EV, HP and TES [146].

The recovery time was added as a dimension of quantifying flexibility in addition to maximum power and shiftable energy by [143]. It describes the required time until the system returns to an undisturbed operation following a trigger signal. The authors simulated the reaction of a pool of heat pumps to different trigger signals to extract the values for the flexibility indicators.

Another concept to determine the flexibility potential for different residential building types is quantifying the available structural storage capacity, storage efficiency and power shifting capacity [181]. The structural storage capacity is the difference in heating energy consumption between flexible and undisturbed operations. The storage efficiency is defined as the share of the heat energy stored which can later be used for supplying the undisturbed heat demand with respect to the total heat energy stored during the demand response event. The shifting capacity is a measure of instantaneous energy flexibility. It describes the relation between the change in heating power and the possible duration to sustain the change.

Energy system modelling has also brought forward approaches to quantify and integrate demand side flexibility into the models. Large-scale energy system models require a higher level of abstraction as the inclusion of detailed building or appliance models significantly increases the complexity of the models. A possibility for such aggregation is to use a storage-like linear formulation for demand side management (DSM) [182]. This buffer storage has time variant minimum and maximum limits for shiftable power and energy consumption. The model was later extended using additional constraints for the flexible share of the load, restricting the shiftable amount to be within a minimum and maximum share of the total load capacity [183].

Another possibility is to directly model flexible demand with a linear formulation for DSM where the demand can be shifted within a specific time range  $L$ . To ensure that the overall consumption stays the same, one can either use an energy balance formulation [184] or link the down-regulation to time steps of up-regulation which can also account for the maximum shifting time [185]. A similar approach was used to study the influence of increased demand-side flexibility on the market and variable renewable energy integration in [186]. The authors introduced the fraction  $\Delta d$  of the load that can be shifted within the day as a flexibility metric. The daily consumption thereby stays constant.

### 11.2.2 Quantification of Flexibility Needs

In addition to the quantification of the flexibility potential of specific sources, there have also been studies to quantify the flexibility needs of a system. Table 11.3 summarises selected flexibility metrics and the relevant references.

TABLE 11.3: Methodologies to quantify flexibility needs

Flexibility Metric	Method	References
Storage energy capacity, balancing energy and power	Time series analysis	[187], [188]
Energy shifted by storage duration	Heuristics, time series analysis	[189], [190]
Storage energy and power capacity dependent on VRES penetration	Literature review	[3], [191]
Energy shifted by storage type	Linear programming	This work

Most approaches use simple time series analysis to evaluate the flexibility needs. In a study on the European energy system, the seasonal flexibility needs were assessed by calculating the required seasonal storage to balance monthly mismatches between supply and demand [187]. The seasonal flexibility needs were found to be highly dependent on the share of wind and PV feed-in and lowest for an optimal mix of 55 % wind and 45 % PV generation in a wind-plus-solar-only scenario. In a second study, the authors added the possibility for excess generation and assessed the flexibility needs to balance hourly and daily mismatches for different optimal mixes of wind

and PV generation [188]. They found that excess generation can significantly decrease the required storage energy capacity and balancing needs.

Another option is to model flexibility needs by determining the required equivalent storages for different storage durations. It was applied to different locations and varying penetrations of VRES and shares of wind in [189]. The authors investigated daily, weekly, monthly, and seasonal storage needs. Two dimensionless metrics were defined: the storage magnitude index and storage duration index. The storage magnitude index describes the percentage of total demand met by stored energy. The storage duration index provides an indication of the average time the energy needs to be stored. The authors found that seasonal balancing needs highly depend on the location and share of wind in the VRES mix.

Similarly, the storage needs of a fully renewable Austrian power system in 2030 were determined by summing the positive residual load unbalance on a daily, weekly, monthly and annual time scale [190]. It was found that flexibility needs increase compared to the current state of the system, with the highest increase in the annual flexibility needs. Furthermore, the flexibility provision from different flexibility options was investigated. The results show that the demand side can provide the flexibility to balance the short-term imbalances but cannot contribute to the seasonal balancing.

Two literature reviews summarised storage requirements in different systems to compare the flexibility needs as a function of the VRES penetration [3], [191]. Both studies found that the storage power capacity increases linearly with the VRES penetration and, in [191], the storage energy capacity increases exponentially. Furthermore, [191] examined the influence of the share of PV and wind in the mix of VRES on storage requirements and found that high PV scenarios required higher storage energy and power capacities compared to high wind scenarios in both Europe and the U.S..

In summary, there exist approaches to model both the flexibility potential from the demand side and the flexibility needs from a system perspective. However, they have not been brought together which is the focus of this chapter. In our work, we bridge the gap between the approaches from device and energy system modelling, which focus on the flexibility potential from the demand side, and the methods based on time series analysis, which focus on the system flexibility needs. This allows us to directly assess the influence of demand flexibility on the system flexibility needs. To this extent, we introduce a linear optimisation model based on the method introduced

by [189] but expand it by also including EV and HP models. Using linear optimisation allows leveraging existing formulations for different flexibility options used in energy system modelling and assessing their influence on the system flexibility needs.



## METHODOLOGY - STORAGE EQUIVALENT MODEL

---

The storage equivalent model uses the idea of quantifying the energy shifts on different timescales needed to balance electricity supply and demand as presented by [189]. The basic model is detailed in Section 12.1. We furthermore expand the model with flexibility from EVs and HPs. Lastly, Section 12.2 illustrates the evaluated flexibility indicators.

### 12.1 FORMULATION OF THE STORAGE EQUIVALENT MODEL

In the proposed model, we define a set of storage units  $S$  that operate on different time horizons  $h(s)$ . The idea is that each storage can only shift energy within the respective time horizon. For example, a daily storage can only perform shifting within the day, not to the next day.

The objective of the proposed model is to minimise the shifted energy, i.e. demand supplied by the storage units, by summing the discharging powers  $p_{s,t}^{dis}$  of the storage units over the different time scales  $s$  multiplied with weighting factors  $\delta_s$ :

$$\min \sum_{t \in T} \sum_{s \in S} \left( \delta_s \cdot \sum_{t \in T} p_{s,t}^{dis} \right). \quad (12.1)$$

The weighting factors should thereby be chosen in a way that prioritises the usage of short-term storage over long-term storage units. The discharging is determined by:

$$p_{s,t}^{dis} \geq -p_{s,t} \quad \forall s \in S, t \in T, \quad (12.2)$$

$$p_{s,t}^{dis} \geq 0 \quad \forall s \in S, t \in T, \quad (12.3)$$

where  $p_{s,t}$  is the (dis-)charging power of the storage unit  $s$ . Negative values of  $p_{s,t}$  imply discharging and positive values charging of the storage units.

The storage units are modelled as ideal storage units, i.e. with a round trip efficiency of 100%. The energy level  $el_{s,t}$  of each storage type  $s$  is thus calculated by:

$$el_{s,t} = el_{s,t-1} + p_{s,t} \cdot \Delta t \quad \forall s \in S, t \in T \setminus \{t = 0\}, \quad (12.4)$$

$$el_{s,t} = 0 \quad \forall s \in S, t = 0, \quad (12.5)$$

where  $\Delta t$  is the time increment of the input time series. The initial energy level is set to zero.

To allow only shifting within the defined time horizons  $h(s)$ , the energy level is fixed to zero at the beginning and end of each time interval equal to the horizon:

$$el_{s,t=n \cdot h(s)} = 0 \quad \forall s \in S, n \in \mathbb{N}. \quad (12.6)$$

In this way, the amount of charged energy equals the discharged energy within  $h(s)$  and no shifting exceeding  $h(s)$  is possible.

Further, the chosen time horizons have to be multiples of each other, i.e.

$$h(s_1) = m \cdot h(s_2) \quad \forall s_1, s_2 \in S : h(s_1) > h(s_2), m \in \mathbb{N}. \quad (12.7)$$

This constraint is added to avoid unintended shifting between different storage types. Consequently, when a storage unit has to be balanced at the end of its time horizon, it can only shift to or draw from a storage unit with a longer time horizon. The only exception to this rule is the storage unit with the longest time horizon. If the time horizon of this specific storage does not fulfil (12.7), it can be used to store excess generation or supply excess demand if supply and demand are not perfectly balanced.

As the capacities of the storage units are not known beforehand, the model allows negative values for the energy level, and the capacities of the storage units  $cap_s$  can be calculated by:

$$cap_s = \max(el_{s,t}) - \min(el_{s,t}) \quad \forall s \in S. \quad (12.8)$$

Finally, the sum of (dis-)charging of the different storage units has to meet the grid residual load:

$$\sum_{s \in S} p_{s,t} = p_{f,t} - p_{l,t} - p_{el,t}^{HP} - \sum_{c \in C} p_{c,t}^{EV} + \sum_{c \in C} p_{c,t}^{V2G} - p_{ch,t}^{BS} + p_{dis,t}^{BS} \quad (12.9)$$

$$\forall t \in T,$$

where  $p_{f,t}$  is the feed-in power,  $p_{l,t}$  the inflexible load,  $p_{el,t}^{HP}$  the electrical power consumption of HPs and  $p_{c,t}^{EV}$  and  $p_{c,t}^{V2G}$  the charging and discharging powers of EVs, respectively, for charging use case  $c$  (introduced in the next subsection). Variables  $p_{ch,t}^{BS}$  and  $p_{dis,t}^{BS}$  describe the charging and discharging of all battery energy storage systems (BESS) in the system.

### *Decentralised Flexibility Options*

Our goal is to measure the possible contribution of decentralised flexibility options to reduce the temporal flexibility needs. We therefore include the previously introduced model formulations of EVs, HPs and BESS. In the use case of inflexible charging, the charging of EVs is treated as an inflexible load. For flexible charging, we distinguish between different use cases, such as home and work charging, and introduce an equivalent aggregate model for each of these use cases using the formulation of flexibility envelopes introduced in Section 3.2.6. HPs are modelled including a TES, which can be used to shift the demand. All HPs in the system are modelled by a single aggregate component accumulating the nominal capacities and TES of individual HPs using the model formulation with lossy TES introduced in Section 3.3.5. Similarly, all BESS in the system are represented by a single aggregate model using the model formulation of lossy battery storage in Section 3.4.3.

## 12.2 FLEXIBILITY INDICATORS

In order to compare the results of different scenarios, we define indicators that quantify the flexibility needs. The first indicator is the shifted energy for different time scales. We call this indicator *shifted energy SE* and calculate it using:

$$SE_s = \sum_{t \in T} (p_{s,t}^{dis} \cdot \Delta t) \quad \forall s \in S, \quad (12.10)$$

where the energy discharged from each storage type  $p_{s,t}^{dis} \cdot \Delta t$  is summed over all time steps.

The second indicator is similar to the storage duration index  $SDI$  introduced in [189]. Specifically, we define the *mean storage duration*  $SD$  for each storage type, which indicates how long energy is stored on average in the storage units:

$$SD_s = \frac{\sum_{sh \in Sh_s} (\tau_{sh} \cdot E_{sh})}{\sum_{sh \in Sh_s} E_{sh}} \quad \forall s \in S, \quad (12.11)$$

where  $Sh_s$  are all shifting events for storage type  $s$ ,  $\tau_{sh}$  is the shifting time and  $E_{sh}$  the energy shifted for shifting event  $sh$ . The shifting events are determined in an iterative approach using the charging time series of the storage types, illustrated in Fig. 12.1.

Iterating through the time series, each time step with a charging power larger than zero is paired with the previous or next discharging event with a charging power lower than zero (and vice versa). The lower value between charged and discharged energy determines the shifted energy  $E_{sh}$ , and the difference of charging and discharging time steps determines the shifting time  $\tau_{sh}$ . Suppose in the described example, the energy of the charging event is higher than that of the discharging event (depicted on the left). In that case, the original value of charging is reduced by  $E_{sh}/\Delta t$  and the discharging event is removed from the time series. Then, the same procedure is followed with the remaining charged energy until it is fully paired with discharging events. Suppose the discharged energy exceeds the charged energy in the example (depicted on the right). In that case, the discharging at the time step of the discharging event is reduced by  $E_{sh}/\Delta t$ , and the iteration process moves ahead to the next time step after the charging event.

Since the obtained charging time series of the storage equivalents are not deterministic, the shifting times are obtained for ten optimisation runs with different solutions<sup>1</sup> and the mean values are used to quantify the mean storage duration  $SD_s$ .

<sup>1</sup> Different solutions are obtained by adding an additional constraint fixing the shifted energy on the different timescales and adapting the weights in the objective function.

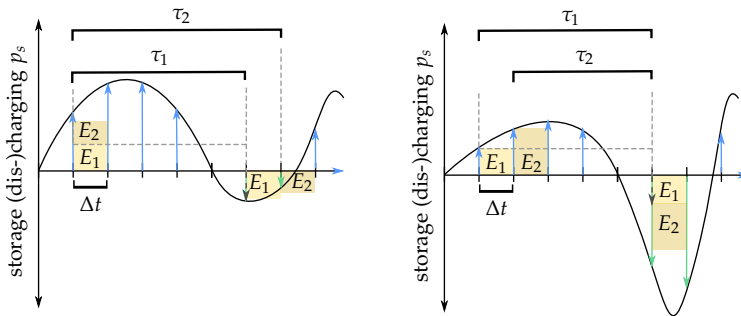


FIGURE 12.1: Concept of determining shifting times, displayed for the first two shifting events.



## CASE STUDIES

---

The goal of this study is to investigate the flexibility needs of highly renewable energy systems and the influence of increasing penetrations of sector coupling technologies. We therefore apply the proposed storage equivalent model to a case study of a 100% RE system in Germany and perform several scenario variations. **Section 13.1** explains the basic setup of the case studies. **Sections 13.2 and 13.3** include scenario variations for a varying generation mix, as well as varying penetration and level of flexibility of EVs, HPs and BESS. **Section 13.4** combines both analyses. In **Section 13.5**, sensitivities towards the most important model parameters and input data are investigated.

### 13.1 STUDY SETUP

The following sections describe the basic study setup. **Section 13.1.1** explains how the balance of generation and load is ensured in all test cases. Standard model parameters and inputs are introduced in **Section 13.1.2**.

#### 13.1.1 *Balancing of Generation and Load*

We assume that the total load can be met by a combined feed-in of PV and wind and scale the respective time series so that the energy provided equals the annual demand of conventional load and sector coupling technologies:

$$\sum_{t \in T} p_{f,t} = \sum_{t \in T} \left( p_{l,t} + p_{el,t}^{HP} + \sum_{c \in C} p_{c,t}^{EV} - \sum_{c \in C} p_{c,t}^{V2G} + p_{ch,t}^{BS} - p_{dis,t}^{BS} \right) = E. \quad (13.1)$$

If the flexibility of the sector coupling technologies is used, the total consumed electricity  $E$  can change. On the one hand, this is because there is additional electricity consumption through losses caused by the deployment of vehicle-to-grid (V2G) and TES. On the other hand, the utilisation of TES can shift the heat demand, which, in combination with a time-varying

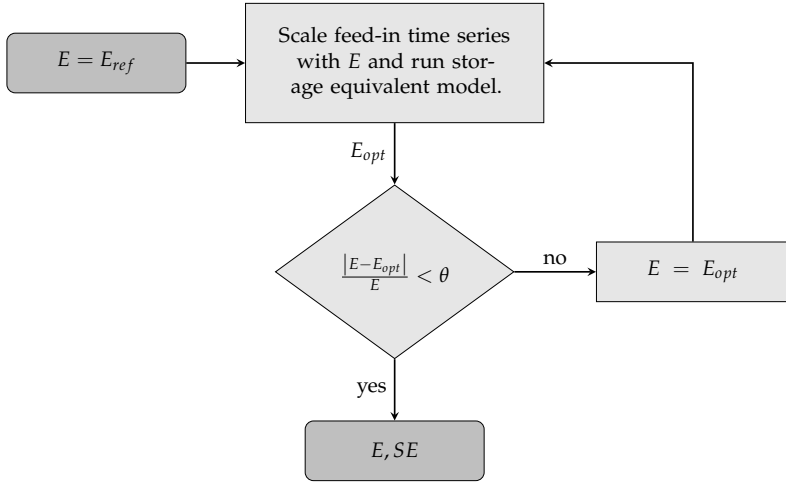


FIGURE 13.1: Iterative process to solve the storage equivalent model accounting for changes in electricity consumption by deployment of V2G and TES.

coefficient of performance (COP), alters the electricity consumption for heating. Since the total electricity consumption is thus dependent on the outcome of the optimisation, we choose the iterative approach displayed in Fig. 13.1 to determine storage equivalents.

The process starts with the electricity consumption in case of reference operation  $E = E_{ref}$ , which is used for the first scaling of the feed-in time series. Solving the storage equivalent model yields an updated total electricity consumption  $E_{opt}$ . The process terminates if the relative deviation of  $E_{opt}$  and the electricity consumption used for scaling  $E$  is smaller than a tolerance value, set to  $\theta = 1\%$ . If the tolerance value is exceeded, the scaling and model run is repeated with the updated electricity consumption  $E = E_{opt}$  until the tolerance value is reached. The according scaling of the feed-in time series ensures that feed-in and consumption are balanced.

### 13.1.2 Base Case

This section describes the basic study setup and input used for the *Base Case*. All mentioned values are also used in the following scenario variations if not mentioned otherwise.

TABLE 13.1: Default model parameters

Storage types ( $s$ )	Time horizons ( $h(s)$ )	Weightings ( $\delta_s$ )
short	24 h = 1 d	1.001
medium	4w = 28 d	$(1.001)^2$
long	1a = 365 d	$(1.001)^3$

### Model Parameters

The chosen model parameters are summarised in Table 13.1. We investigate short-, medium- and long-term flexibility needs and define daily, four-weekly and seasonal (365 days) storage as considered time horizons  $h(s)$ . These values are inspired by existing storage or load shifting time scales. As an example, residential battery storage is mainly operated on a daily basis, while EV driving predominantly follows a weekly pattern. In extreme cases, EV charging demand could be shifted for longer than a week, so we choose four weeks (i.e. approximately one month) for the medium-term storage. Large-scale heat storage or synthetic gases such as hydrogen can operate as seasonal storage, which we define as the long-term storage type.

For the weighting of the different storage types in the objective function, we use values of  $\delta_{short} = 1.001$ ,  $\delta_{medium} = (1.001)^2$  and  $\delta_{long} = (1.001)^3$ . The consequence is that shorter-term storage is chosen over longer-term storage if it leads to an increase of less than 0.1% in the overall shifted energy.

### Model Inputs

The *Base Case* describes a 100% RE system in Germany with a total served electrical load of 496.1 TWh<sup>1</sup> and generation from solar and wind only. The requirement that the VRES generation can fully cover the demand results in installed capacities of 185.9 GW solar and 157.95 GW wind, keeping the same proportion between solar and wind as for the current installed capacities [192]<sup>2</sup>.

The weather highly influences the feed-in of PV and wind. To investigate the general dynamics and average flexibility needs, we use data for a

<sup>1</sup> Using time series for 2019 from ENTSO-E [20].

<sup>2</sup> Using time series for 2019 from *renewables.ninja* [193], [194].

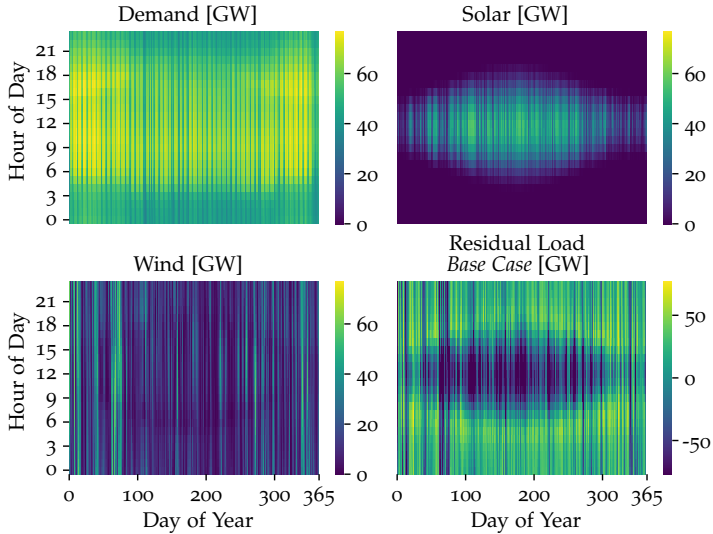


FIGURE 13.2: Heatmaps of input time series on electricity demand for conventional applications (upper left), solar (upper right) and wind (lower left) feed-in with current installed capacities and residual load in the *Base Case* (lower right) in GW.

representative medium weather year (see sensitivity analysis in 13.5.2), resulting in a share of 41.5% PV generation and 58.5% wind generation in terms of energy based on the above mentioned capacities. Fig. 13.2 shows the temporal characteristics of the input time series obtained from *ENTSO-E* [20] and *renewables.ninja* [193], [194]. Displayed are conventional demand (upper left), solar feed-in (upper right), wind feed-in (lower left) and residual load in the *Base Case* (lower right) over the day of the year and the hour of the day.

Both solar feed-in and demand show a strong daily and seasonal pattern. Naturally, solar feed-in shows high values during the day, especially around noon, and longer feed-in times in summer than in winter. The demand, on the other hand, shows its highest values during morning hours (07:00-12:00) and in the evenings (17:00-19:00) and a lower overall demand in summer than in winter. Wind feed-in shows less variation during single days but more between different days. On the seasonal scale, wind feed-in is higher in winter than in summer.

Consequently, the residual load shows both daily and seasonal patterns. On a daily scale, the highest positive residual loads, where load exceeds renewable feed-in, occur in the morning and evening. The highest negative residual load occurs around noon and in the night. A seasonal effect arises, where in summer the hours of negative residual load around noon increase and the hours of positive residual load shift to earlier morning and later in the evenings. During winter, the opposite occurs, and more days show strong wind feed-in.

In the *Base Case*, no sector coupling technologies, namely EVs and HPs, are present. The parameters and time series of these are described in Sections 13.3.1 and 13.3.2, which include the scenario variations investigating increasing penetrations of EVs and HPs.

All calculations are executed with an hourly resolution for 52 weeks (= 364 days). The period is chosen because it is a multiple of the short- and medium-term storage time horizons. This condition is necessary to ensure that the storage units are balanced at the end of the simulation period.

### 13.2 CASE STUDY I: GENERATION MIX

Flexibility needs are influenced by the feed-in pattern, which in turn depends on the types of generation units and their share in the generation mix. Therefore, we vary the generation mix in a first scenario variation. The simulated scenarios are summarised in Table 13.2.

#### 13.2.1 Scenario Variations

In *Gen. Base*, we compare the 100 % VRES feed-in (*VRES*) defined as the *Base Case* with a continuous generation (*Flat*), where all generators have a constant power output which, while not being very realistic, is assumed to be the preferred operational strategy of large conventional power plants.

To investigate the influence of the renewable generation mix, we vary the share of PV and wind in a second scenario *Gen. VRES*, where the share of energy provided by PV is varied from 0 % to 100 % in steps of 5 %. The total energy provided by the combined resources stays constant as defined in (13.1).

TABLE 13.2: Scenarios for the variation of the generation mix

Scenario	Profile	Share PV
Gen. Base Flat	Flat Gen.	None
Gen. Base VRES	100 % VRES	41.5 %
Gen. VRES	100 % VRES	{ 0 %, 5 %, ..., 100 % }

#### 13.2.2 Results

Here we present the results of the variation of the generation mix, providing values for the key indicators of flexibility needs for short-, medium- and long-term energy shifting. Figure 13.3 shows the energy shifted over the different time horizons for the reference scenario *Flat Gen.* of continuous generation and the *Base Case* of 100 % VRES (left) as well as for different shares of PV and wind generation in a 100 % VRES scenario (right). The *Flat Gen.* case requires shifting of 37.6 TWh, whereas the *Base Case* of 100 % VRES leads to the need of 138.1 TWh of energy shifting. This accounts for 7.6 % and 27.8 % of the total served load, respectively. There is an

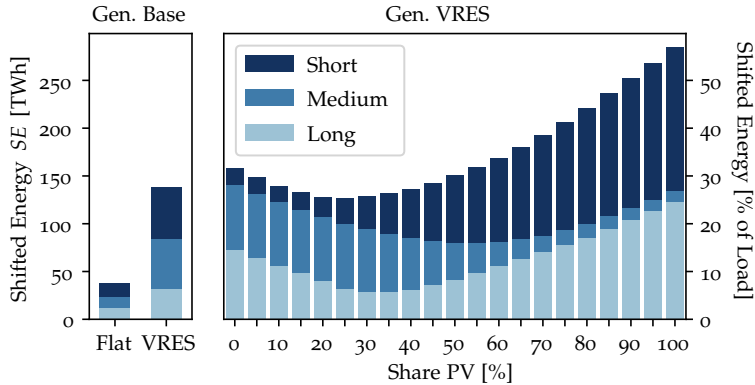


FIGURE 13.3: Flexibility needs for flat generation vs. the 100% RES scenario (left) and for a 100% RES with varying shares of PV and wind generation (right). The y-axes apply to both subplots.

increase of shifted energy for all three storage types. The short-term shifted energy increases from 2.8% to 11.0%, the medium-term shifted energy from 2.4% to 10.5% and the long-term shifted energy from 2.4% to 6.4% of the total served load in the *Base Case* of 100% renewable energy sources (RES) compared to the *Flat Gen.* case.

In case of the varying shares of PV and wind, a value of 0% signifies that the load is fully covered by wind generation and a value of 100% that the load is fully covered by PV generation. The shifted energy proves to be highly dependent on the generation mix. The lowest total shifted energy of 127.0 TWh (25.6% of the total served load) occurs at a share of 0.25, meaning that 25% of the energy is provided by PV and 75% by wind generation. The highest value of the total shifted energy with 284.5 TWh (57.3% of the total served load) occurs in the case of 100% PV generation. This represents more than double of the shifted energy compared to the optimal mix.

The influence of the generation mix on the three storage types differs. For all storage types, there is a minimum at a specific mix of PV and wind, but the specific mix differs depending on the storage type. The short-term energy shifting has a minimum of 16.7 TWh shifted energy (3.4% of the total load) at a share of 10% PV and increases with the share of PV up to 150.3 TWh (30.3% of the total demand). The medium-term energy shifting shows this minimum at a mix of 95% PV and 5% wind generation with 12.0 TWh shifted, equal to 2.4% of the total demand. The maximum medium-term

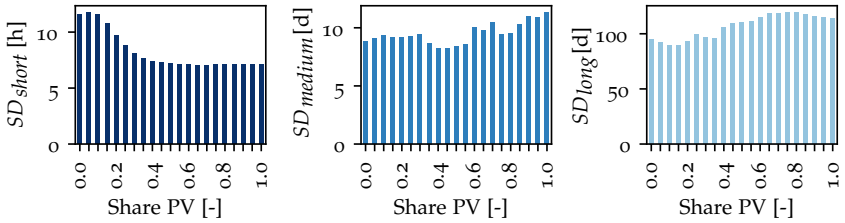


FIGURE 13.4: Storage durations for short- (left), medium- (middle) and long-term (right) storage in the 100% RES scenario with varying share of PV and wind generation.

energy shifting occurs at 75% wind generation with 68.5 TWh or 13.8% of the total demand shifted by medium-term storage, staying nearly constant at this value for a further increase in the share of wind generation. The long-term energy shifting is lowest for 35% PV and 65% wind generation with 27.8 TWh or 5.6% of the total demand shifted long-term. The highest amount of energy shifted by the long-term storage occurs at 100% PV generation with 24.6% of the total demand.

Fig. 13.4 displays the storage durations for short- (left), medium- (middle) and long-term (right) storage  $SD_s$  with a varying share of PV and wind feed-in in the 100% VRES scenario for varying levels of PV share. The storage duration of the short-term storage shows its maximum for 5% PV with 11.8 hours and decreases with increasing shares of PV to 7.0 hours at 65% PV. With a further increase of the PV penetration to 100%, the storage duration shows relatively stable values without further decrease. The medium-term storage duration decreases from 8.8 days for 0% PV to 8.2 days for 40% PV generation, to then increase with higher PV generation up to 11.3 days for 100% PV. The long-term storage duration ranges from 90 days to 119 days, with its minimum at 10% PV generation and an increasing trend for higher shares of PV. After reaching its maximum at 75% PV generation, the long-term storage duration slightly decreases with higher shares of PV to 114 days for 100% PV. The results imply that higher shares of PV decrease the short-term storage durations, but increase the medium- and long-term storage durations.

### 13.3 CASE STUDY II: DECENTRALISED FLEXIBILITY OPTIONS

Next, we investigate the influence of increasing shares of DFOs on the temporal flexibility needs. We thereby compare the uncoordinated operation with different levels of flexibility provision from EVs in **Section 13.3.1** and HPs in **Section 13.3.2**.

#### 13.3.1 *Electric Vehicles*

EVs, on the one hand, are likely to increase the flexibility needs due to the increasing system load. On the other hand, they can offer flexibility to the system. We therefore want to investigate the influence of the integration of EVs on the flexibility needs by varying the EV penetration and their level of flexibility in a second scenario variation.

##### *Scenario Variations*

To investigate the influence of increasing shares of EVs, we increase the EV penetration from 0% to 100% in steps of 10%. The case of 100% EV penetration translates to a total of 48.8 Mio. EVs, which is the current number of private cars in Germany [112]. We model different charging use cases: slow charging, divided into home, work and public charging, and fast charging at high power charging stations. The charging time series and flexibility bands associated with these use cases are based on the previous investigations in Part I of this thesis. There, we modelled a total of 26 880 EVs, divided into 16 597 battery electric vehicles (BEVs) and 10 283 plug-in hybrid electric vehicles (PHEVs), with a charging efficiency of  $\eta_{EV} = 0.9$  in six different distribution grids to cover various different driving profiles and charging infrastructure setups. The adopted time series for reference charging corresponds to a charging behaviour where the EVs charge at full power directly after plug-in until the charging demand of the charging session is met (see Section 3.2).

In this case study, we only consider BEVs since we assume that PHEVs will not play a significant role in a 100% renewable energy system [144]. Assuming that the number of  $nr_{EV,ref} = 16\,597$  BEV profiles is sufficiently high to account for statistical deviations, we sum the charging demands

of the different use cases and scale the obtained time series for reference charging  $p_{c,t}^{EV,ref}$  with the simulated number of BEVs  $nr_{EV}$ :

$$p_{c,t}^{EV} = p_{c,t}^{EV,ref} \cdot \frac{nr_{EV}}{nr_{EV,ref}} \quad \forall c \in C, t \in T. \quad (13.2)$$

The same scaling is done for the flexibility bands of flexible charging.

We further model the four flexibility scenarios for EVs with increasing levels of flexibility, as summarised in Tab. 3.10. For the lower levels of flexibility, shifting of charging demand within the originally scheduled session is allowed. In *EVs Flex*, only charging at home and work charging station is assumed to be flexible. In *EVs Flex+*, shifting is additionally allowed at public charging stations. For *EVs Flex++* and *EVs V2G*, shifting between standing times is possible for all three charging use cases, as long as charging infrastructure is available. *EVs V2G* furthermore allows to discharge the EVs, which is not possible in the other levels of flexibility. Further details on the underlying assumptions and their effects on the flexibility envelopes are detailed in Sections 3.2.4 and 3.2.6 for each level of flexibility.

## Results

In the following, we present the temporal flexibility needs with increasing shares of EVs. Figure 13.5 shows the shifted energy on the different time scales for the reference operation of EVs (left) and with maximum flexibility through V2G (right). With an increasing share of EVs integrated into the system, there is an increase in shifted energy in case of reference operation. For 100% EV penetration, this increase amounts to 29.0 TWh or 21.0% of overall shifted energy in the *Base Case*. The additional electricity consumption, in this case, equals 120.4 TWh, which is 24.2% of the original load.

For the *EVs V2G* scenario, the flexibility utilisation from EVs leads to a decrease in flexibility needs with increasing shares of EVs. Particularly the short-term energy shifting is almost entirely provided by EV flexibility with high penetrations of EVs. The medium-term energy shifting decreases by roughly half, while the long-term energy shifting shows no significant change. For 100% EV penetration, a reduction of 86.2 TWh or 62.4% of the total shifted energy in the *Base Case* can be achieved. The electricity consumption caused by additional losses with V2G amounts to 14.0 TWh,

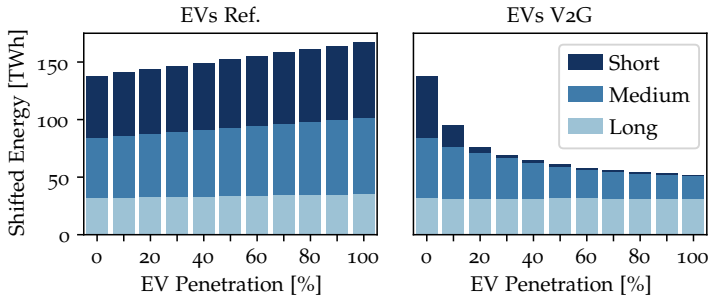


FIGURE 13.5: Flexibility needs for increasing penetrations of EVs with reference operation (left) and maximum flexibility (right) for the *Base Case* generation.

equal to 2.8% of the original load. With increasing penetrations of EVs, the additional consumption by V2G losses shows a saturation effect (not displayed), i.e. does not significantly increase any further.

Figure 13.6 shows the change in shifted energy with increasing penetration of EVs with reference operation (top) and flexible charging with different levels of flexibility (bottom) compared to the *Base Case*. All values are displayed in percent of the total shifted energy in the *Base Case* without EVs. The results show that the additional energy shifting with reference operation consists of mainly short- and medium-term energy shifting.

The change in additional flexibility needs differs for the investigated levels of EV flexibility. In the scenarios *EVs Flex* and *EVs Flex+*, we mainly observe a reduction in short-term flexibility needs. The net reduction of short-term energy shifting amounts to 3.8% and 9.5% for the integration of the 48.8 Mio. EVs (100% penetration), respectively for the two scenarios. The increase of medium-term shifting can be reduced from 10.6% with reference operation to 8.9% and 7.4% for 100% EV penetration. The long-term shifting shows a slight increase of 2.3% at 100% EV penetration in all three cases. Overall, the increase in total flexibility needs can be reduced from 21.0% with reference operation to 7.3% in the *EVs Flex* and 0.1% in the *EVs Flex+* scenario in case of a 100% EV penetration.

In the scenarios *EVs Flex++* and *EVs V2G*, there is a net reduction of flexibility needs with increasing penetrations of EVs. The total shifted energy can be decreased by 18.9% and 62.4% in the *EVs Flex++* and *EVs V2G* scenarios with 100% EV penetration compared to the *Base Case*. For *EVs*

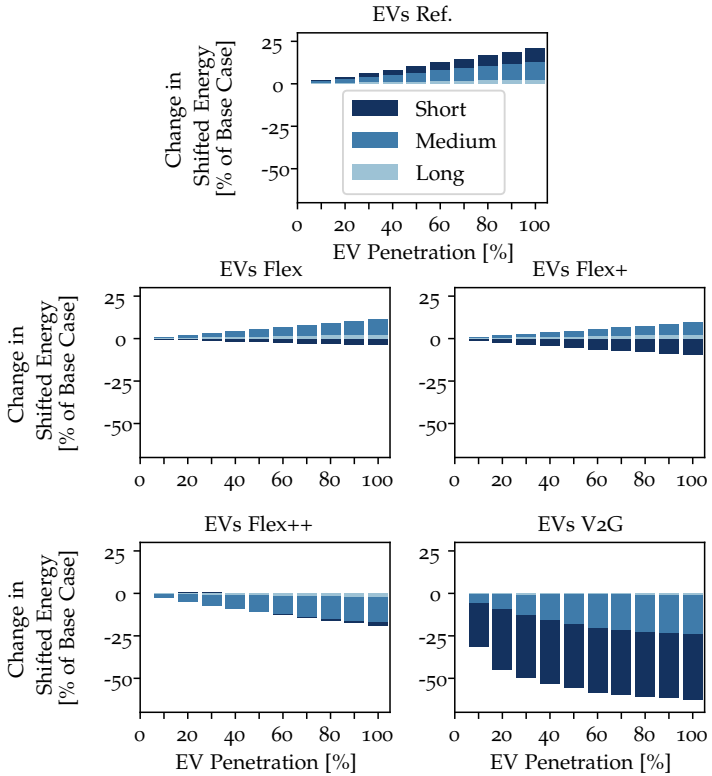


FIGURE 13.6: Change in energy shifting through the integration of EVs with reference operation (top) and flexible charging at different levels of flexibility compared to the *Base Case*. All values are displayed in percent of the overall shifted energy in the *Base Case* without EVs.

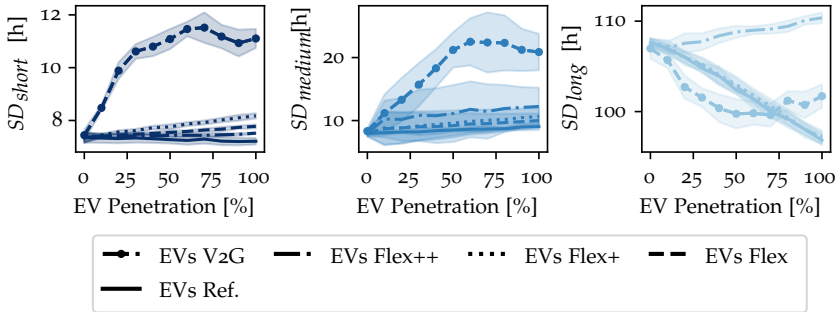


FIGURE 13.7: Storage durations for short- (left), medium- (middle) and long-term (right) storage with increasing shares of EVs in the simulated scenarios. The shaded areas indicate the standard deviation between the ten runs.

*Flex++*, the reduction is mainly in medium-term energy shifting, as the short- and long-term shifting stay nearly constant. For *EVs V2G*, both short- and medium-term energy shifting is significantly reduced. Long-term shifting again remains unchanged. While for all other flexibility scenarios, the change in flexibility needs follows a linear trend, the *EVs V2G* scenario shows a saturation with decreasing marginal reduction at higher EV penetrations.

Figure 13.7 displays the storage durations for the different storage types under increasing shares of EVs with reference operation and in the different flexible scenarios. The results show that in the *EVs Ref.* scenario, the storage durations stay relatively constant for short- and medium-term shifting and decrease for long-term shifting with increasing penetrations of EVs. Using EV flexibility to decrease a certain type of energy shifting generally increases the storage durations with increasing shares of EVs, notably in particular for short- and medium-term shifting in the *EVs V2G* scenario. This implies that the flexibility is mainly used to replace shorter shifting events for the respective storage type.

Figure 13.8 summarises the reduction potential of flexible EV charging compared to reference charging for different penetrations of EVs and levels of flexibility. We thereby examine the reduction of total shifted energy (left) and the reduction in shifted energy for individual storage types (right) relative to the flexibility needs in case of reference charging. The reduction of total shifted energy shows that the deployment of *V2G* shows the strongest

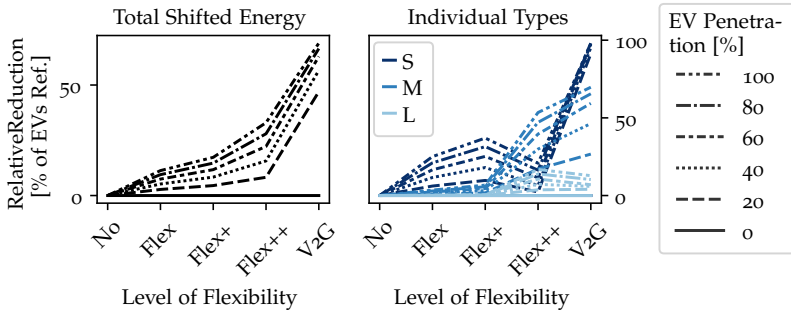


FIGURE 13.8: Overall reduction of total shifted energy (left) and reduction of individual storage types (right) for different levels of EV flexibility and different penetrations of EVs. A reduction of 100% thereby means that the flexibility needs in case of reference charging (*EVs Ref.*) can be fully met using EV flexibility.

increase in reduction of all flexibility measures (indicated by the gradient). Furthermore, the marginal reduction with increasing penetrations of EVs in general decreases for high penetrations. This effect is also visible in the reduction of shifted energy for individual storage types.

The reduction of shifted energy in individual storage types is different for short-, medium and long-term storage. A reduction of 100% thereby means that the required energy shifting in case of reference operation of EVs is fully covered by EV flexibility. This is for example almost reached for the reduction of short-term storage in the flexibility scenario *V2G* with EV penetrations of 20% or more. It has to be mentioned that the energy shifted short-term only amounts to 39.3-39.4% of the total shifted energy, and slightly decreases with the EV penetration. A 100% reduction in short-term energy shifting therefore means a reduction of 39.3-39.4% of the total shifted energy. The share of medium- and long-term energy shifting amount to 37.6-39.8% and 20.9-23.0% for the different scenarios, the medium-term share slightly increasing and the long-term share slightly decreasing with increasing EV penetrations.

Overall, the reduction in short-term energy shifting is highest for all levels of flexibility except for *EVs Flex++*. There, the flexibility is mainly used to reduce medium-term shifting. For medium- and long-term shifting, the reduction is low for *Flex* and *Flex+*, but increases with *Flex++* and *V2G*. The highest reduction values are obtained with 100% EV penetration with the

highest level of flexibility, being 98.1 % for short-term, 69.7 % for medium-term and 12.8 % for long-term energy shifting.

### 13.3.2 Heat Pumps

Similar to EVs, the integration of HPs increases the electricity demand but in combination with TES also offers the possibility to provide flexibility. In a third scenario variation, we therefore vary the penetration and level of flexibility of residential HPs.

#### Scenario Variations

In Germany, 19.4 Mio. residential buildings existed in 2021 [145]. For these, we analyse different heating scenarios, increasing the HP penetration from 0% to 100% in steps of 10%. A penetration of 100% means that every residential building is equipped with a HP. For the sizing of HPs and TES, we use mean values of 13.0 kW installed thermal capacities for the HPs and 21.5 MWh annual heat demand and we assume that we need 18.3 kWh of thermal storage to cover the heat demand for two consecutive hours [175]. The static and dynamic efficiencies are set to  $\eta_{stat}^{TES} = 0.99$  and  $\eta_{dyn}^{TES} = 0.95$  [195]. All average values for single HPs are scaled with the simulated number of HPs in the respective scenario variation. The time series for heat demand and COP for selected HP technologies are obtained from *When2Heat* [127].

Following a similar approach as introduced in [195], the overall COP time series is calculated as a weighted sum of the individual time series of air-source and ground-source HPs with floor and radiator heating:

$$COP_t = \sum_{\substack{src \in \\ \{air, \\ ground\}}} \sum_{\substack{snk \in \\ \{floor, \\ radiator\}}} \left( W_{src} \cdot W_{sk} \cdot COP_t^{src, snk} \right) \quad \forall t \in T. \quad (13.3)$$

The weights are set to  $W_{air} = 0.71$ ,  $W_{ground} = 0.29$ ,  $W_{floor} = 0.60$  and  $W_{radiator} = 0.40$  [195].

The normalised heat demand time series from *When2Heat* is scaled with the mean annual demand and multiplied by the number of HPs. Fig. 13.9 shows the resulting electricity demand for the 19.4 Mio. HPs in the case of reference operation (left) as well as the COP (right). Reference operation

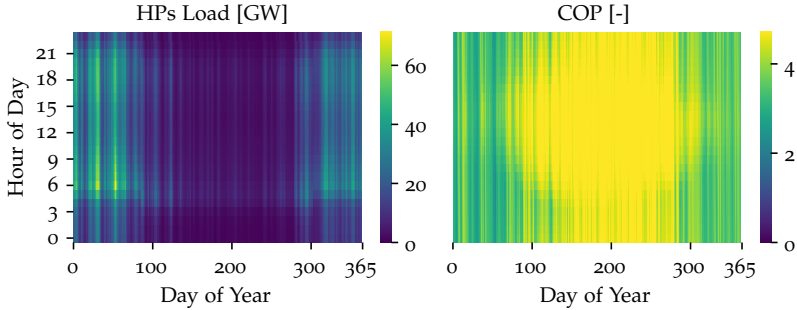


FIGURE 13.9: Heatmaps of HP reference operation (left) and mean COP (right) for 19.4 Mio. HPs.

assumes a direct supply of the requested heat demand by the HP without the usage of storage:

$$p_{el,t}^{HP,ref} = \frac{P_{th,t}^D}{COP_t} \quad \forall t \in T. \quad (13.4)$$

Furthermore, the level of flexibility is varied by adding differently sized TES according to Table 3.13. In *HPs Flex*, the TES is sized such that it can bridge the two hours of maximum thermal demand (see Section 3.3.4). In *HPs Flex+* and *HPs Flex++*, the size of TES is doubled and quadrupled, respectively.

### Results

In the following, we present the results for increasing penetrations of HPs at different levels of flexibility along the defined flexibility indicators. Figure 13.10 displays the shifted energy for increasing penetrations of heat pumps with reference operation (left) and maximum flexibility in the *HPs Flex++* scenario (right). Growing numbers of HPs cause a relatively linear increase in flexibility needs in both cases. In case of reference operation, with 100% HP penetration, the total shifted energy increases by 41.4 TWh or 30.0% compared to the *Base Case* without HPs, i.e. corresponding to the values at 0% in the figure. This amount can be reduced to 13.9 TWh or 10.1% with the highest level of flexibility. The additional electricity consumption for this number of integrated HPs amounts to 115.8 TWh, which is 23.3% of the original load. In the *HPs Flex++* scenario, losses from

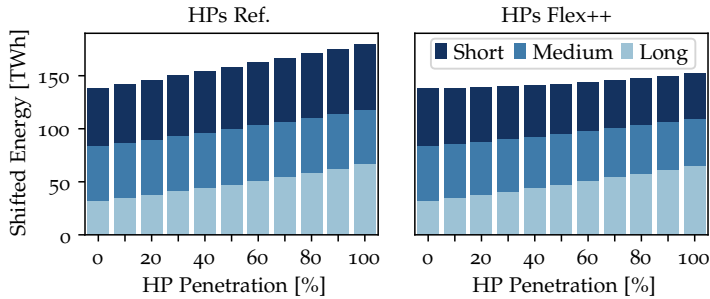


FIGURE 13.10: Flexibility needs for increasing penetrations of HPs with reference operation (left) and maximum flexibility (right) for the *Base Case* generation.

the TES cause an additional load of 7.3 TWh, which is 1.5 % of the original load.

Figure 13.11 displays the change in shifted energy when integrating HPs with reference operation (upper left) and flexible operation using TES of different sizes enabling a minimum of two (*Flex*: upper right), four (*Flex+*: lower left) and eight hours (*Flex++*: lower right) of shifting of the thermal load. All values are displayed compared to the *Base Case* without HPs and in percent of total shifted energy in this case. The increase in shifted energy shows a strong increase in long-term shifting with increasing HP penetration and a smaller increase in short-term shifting for the reference operation. For 100 % HP penetration, the increase of short-term energy shifting amounts to 5.2 % and the long-term to 24.8 %. The medium-term energy shifting stays nearly constant.

For all levels of flexibility, the highest reduction can be seen in short-term energy shifting. The reduction is higher than the original increase with reference operation in all cases such that a net reduction of short-term energy shifting is achieved with increasing numbers of HPs. At the same time, there is almost no reduction in long-term energy shifting for all the flexibility scenarios. The reduction of medium-term energy shifting, on the other hand, increases with increasing level of flexibility. However, the total shifted energy still increases with increasing numbers of HPs since the potential to decrease long-term energy shifting is limited, and the decrease in short- or medium-term energy shifting does not outweigh the increase in long-term energy shifting.

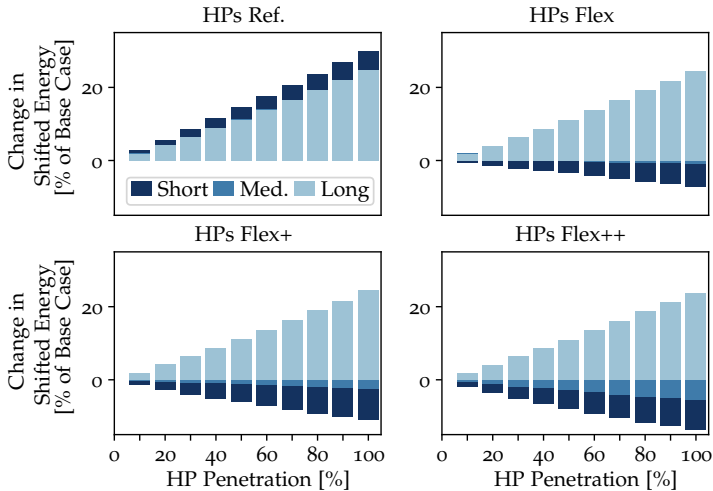


FIGURE 13.11: Change in shifted energy through the integration of HPs with reference operation (upper left) and with flexible charging at different levels of flexibility compared to the *Base Case*. All values are displayed in percent of overall shifted energy in the *Base Case* without HPs.

Overall, in case of 100% HP penetration, the increase in the total shifted energy can be reduced from 30.0% with reference operation to 17.5% in the *Flex*, 13.4% in the *Flex+* and 10.1% in the *Flex++* scenario.

Fig. 13.12 shows the storage durations of short-, medium- and long-term storage for increasing penetrations of HPs in the simulated scenarios. The short-term storage duration stays nearly constant for increasing HP penetrations with reference operation. Using flexibility increases the short-term storage durations with rising HP penetrations for all three flexible scenarios. This implies that mainly short shifts are covered by HP flexibility. For the medium-term energy shifting, no clear trend can be identified for the storage durations. The long-term storage durations first decrease for increasing HP penetrations. However, for penetrations higher than 60%, the storage durations start to increase again with increasing HP penetrations, with larger slopes for higher levels of flexibility.

Fig. 13.13 summarises the overall reduction of total shifted energy (left) and the reduction of the shifted energy by storage types (right) for different levels of HP penetration and flexibility compared to the reference operation.

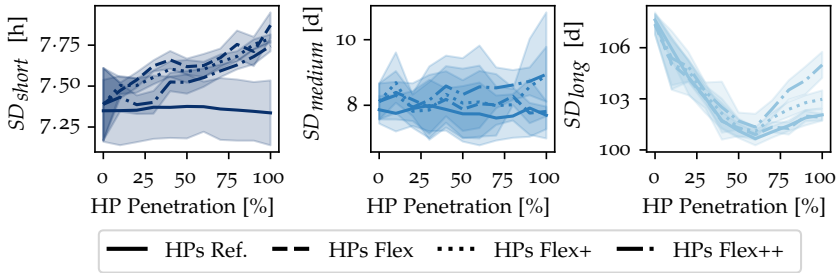


FIGURE 13.12: Storage durations for short- (left), medium- (middle) and long-term (right) storage with increasing shares of HPs in the simulated scenarios. The shaded areas indicate the standard deviation between the ten runs.

The reduction of total shifted energy shows a maximum of 15.3 % compared to flexibility needs with reference operation. Similar to EVs, the marginal reduction potential decreases with increasing numbers of HPs. Another effect is that the efficacy of additional TES capacity to reduce the total and short-term flexibility needs decreases with a growing size of TES. For short-term energy shifting, there is thus a saturation effect for increasing sizes of the TES indicated by the small differences between the different flexibility cases.

The reduction in shifted energy of individual storage types is highest for short-term shifting, followed by medium- and long-term shifting. The highest values are obtained for 100 % HP penetration in the *Flex++* scenario with the reduction amounting to 30.1 % for short-term, 14.4 % for medium-term and 2.2 % for long-term flexibility needs. The shares of short- and medium-term energy shifting with respect to total shifted energy amount to 34.3-39.4 % and 28.9-37.6 %, both showing a decreasing trend with an increasing HP penetration. The distribution of the flexibility needs across the different time scales is shifted to higher percentages of long-term storage needs with increasing HP penetration, taking values between 23.0-36.8 %.

### 13.3.3 Battery Storage

Battery storage is increasingly installed together with residential PV [18]. Unlike EVs and HPs, BESS do not significantly increase the electricity consumption (only through losses), but flexibility provision is their primary

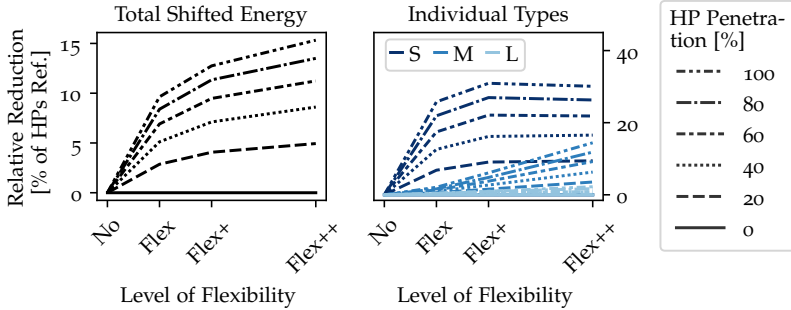


FIGURE 13.13: Reduction of total shifted energy (left) and of individual storage types (right) for different levels of HP flexibility and different numbers of HPs. A reduction of 100% thereby means that the flexibility needs in case of reference charging ( $HPs\ Ref.$ ) can be fully met using HP flexibility.

goal. We therefore investigate the effects of residential BESS with reference operation, i.e. maximising PV self consumption, and an optimised operation on the system temporal flexibility needs.

### Scenario Variations

Similar to the integration of HPs, we assume that every residential building owns a BESS in the case of 100% BESS penetration. The penetration is increased from 0% to 100% in steps of 10%, until every of the 19.4 Mio. residential buildings is equipped with a battery storage. The BESS are sized according to Section 3.4.1, resulting in a mean power capacity of 5.2 kW and a mean energy capacity of 8.7 kWh. The charging and discharging efficiencies are set to  $\eta_{bs}^{BS,ch} = 0.93$  and  $\eta_{bs}^{BS,dis} = 0.94$  [156].

The reference operation assumes a charging at excess generation until the storage energy capacity is reached and a discharging at excess demand until the storage is empty (see Section 3.4.2). The reference time series is scaled with the number of BESS for the reference operation. For the optimised operation, the model formulation of a lossy battery storage introduced in Section 3.4.3 is used. Therefore, the mean values for power and energy capacities are scaled with the number of simulated BESS in the respective scenario variation.

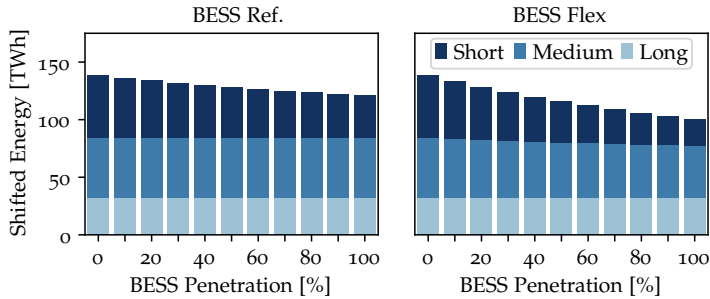


FIGURE 13.14: Storage equivalents for increasing penetrations of BESS with reference (left) and optimised operation (right) for the *Base Case* generation.

### Results

The following section summarises the results for the integration of BESS with reference and optimised operation along the defined flexibility indicators. Figure 13.14 displays the shifted energy, divided into short-, medium- and long-term shifts, for the reference operation of BESS (left) and an optimised operation (right). In both cases, the shifted energy is reduced with increasing shares of BESS. With the reference operation, the total shifted energy is reduced by 17.1 TWh, which is 12.3 % of the shifted energy in the *Base Case*. This reduction can be increased to 38.1 TWh by the optimised operation, i.e. 27.6 % of the total shifted energy in the *Base Case*.

Figure 13.15 displays the change in shifted energy caused by the integration of BESS with reference (left) and optimised operation (right). The values are displayed in percent of total shifted energy in the *Base Case*. The results show that with the reference operation, only the short-term energy shifting is reduced. When optimised to reduce the necessary energy shifting, additionally to an increased reduction of short-term energy shifting, the energy shifted medium-term can also be reduced to a smaller extent. The short-term shifting can be reduced by 22.7 % and the medium-term shifting by 4.8 % of total shifted energy in the *Base Case* for 100 % BESS penetration.

In Fig. 13.16, the mean storage durations for the different storage type and the integration of BESS with reference and optimised operation are displayed. The storage duration for short-term energy shifting increases for increasing BESS penetration in both cases. The increase is thereby stronger

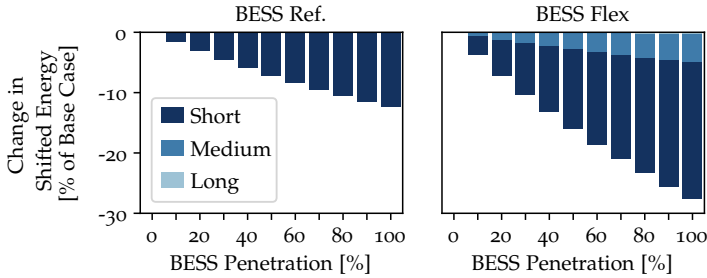


FIGURE 13.15: Change in shifted energy through the integration of BESS with reference (left) and optimised operation (right) compared to the *Base Case*. The values are displayed in percent of total shifted energy in the *Base Case* without BESS.

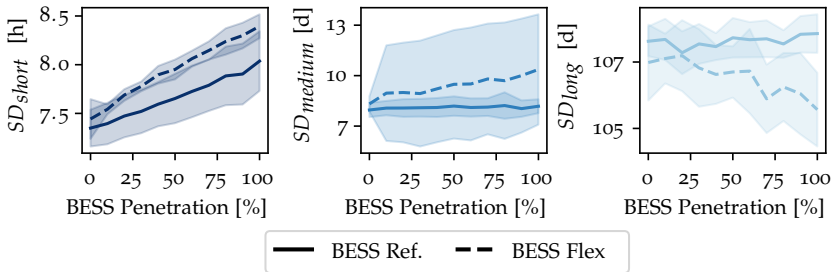


FIGURE 13.16: Storage durations for short- (left), medium- (middle) and long-term (right) storage with increasing shares of BESS in the simulated scenarios. The shaded areas indicate the standard deviation between the ten runs.

for the flexible operation ranging from 7.4 hours to 9.3 hours than the reference operation rising from 7.4 hours to 8.0 hours. The medium-term storage duration in case of reference operation stays nearly constant around 8.0 days while it increases for the flexible operation with increasing shares of BESS from 8.1 to 10.0 days. The long-term storage duration shows now clear trend for increasing shares of BESS and ranges between 107 and 108 days. For the optimised operation of BESS, the storage durations decrease with increasing shares of BESS.

The relative reduction of total shifted energy (left) and for individual storage types (right) is displayed in Fig. 13.17. Since BESS do not consume energy except for charging and discharging losses, the results are displayed in percent of total shifted energy in the *Base Case*. The reduction of total shifted

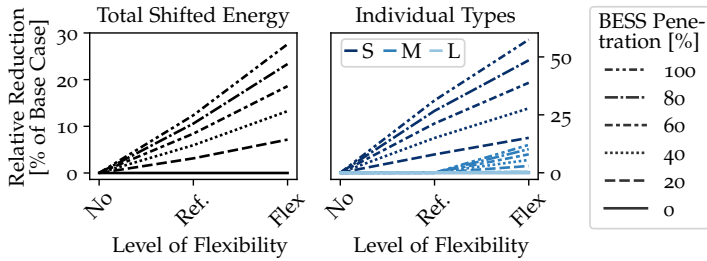


FIGURE 13.17: Storage durations for short- (left), medium- (middle) and long-term (right) storage with increasing shares of BESS in the simulated scenarios.

energy can be more than doubled with the optimised operation compared to the reference operation. The marginal reduction thereby decreases with increasing BESS penetrations. This effect also occurs for the reduction of individual storage types. At 100 % BESS penetration, the short-term energy shifting can be decreased by 57.5 % and the medium-term shifting by 12.1 % with the optimised BESS operation. The reference operation reduces the short-term energy shifting by 31.2 %, largely leaving the energy shifted medium- and long-term unchanged.

### 13.4 CASE STUDY III: COMBINED ANALYSIS

The uptake of DFOs influences the optimal generation mix. In a combined analysis, we therefore investigate the interplay of DFOs and generation mix.

#### *Scenario Variations*

We vary the generation mix from 0 % PV to 100 % PV in steps of five percent for 100 % penetration of EVs, HPs and BESS. After investigating the influence of individual DFOs, we also look at the combination of all in case of reference operation (*Combined Ref.*) and for maximum levels of flexibility (*Combined Max. Flex.*), i.e. *EVs V2G*, *HPs Flex++* and *BESS Flex.*

#### *Results*

In the following, we present the results of the combined analysis with regards to the shifted energy on different time scales. Figure 13.18 shows

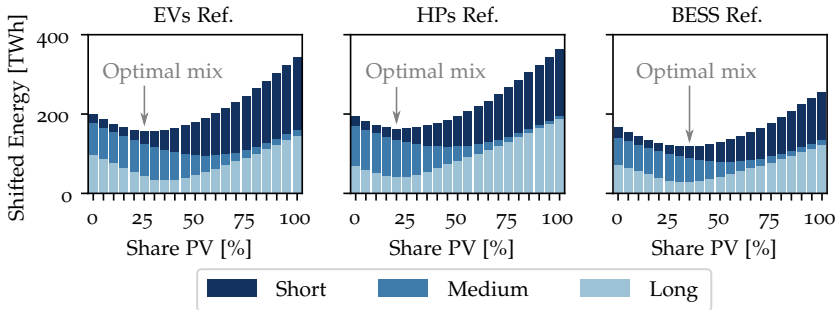


FIGURE 13.18: Flexibility needs for varying shares of PV and wind generation with 100% EVs (left), HPs (middle) and BESS (right) under reference operation.

the temporal flexibility needs for 100% EV (left), HP (middle) and BESS (right) penetrations under reference operation. The DFOs change the absolute amount of shifted energy and the division into short-, medium- and long-term shifting. Furthermore, the optimal mix is altered in case of HPs and BESS. While the total shifted energy shows its minimum at 25% PV generation with only conventional load (*Gen. VRES*) and for the integration of EVs, it shifts to 20% with the integration of HPs and to 35% PV generation for the integration of BESS. Furthermore, the minimum of long-term flexibility needs shifts to 20% PV generation, while it stays unchanged at 35% PV generation for the integration of EVs and BESS.

Figure 13.19 displays the change in shifted energy caused by the integration of the respective DFO, i.e. in comparison to the shifting needs with only conventional load in *Gen. VRES*. It shows that EVs lead to an increase in shifted energy on all time scales for all generation mixes. The total increase is lowest with 28.6 TWh for a mix of 35% PV and 65% wind generation. The smallest increase in short-term shifting occurs at 15% PV, for medium-term shifting at 95% PV and for long-term shifting at 40% PV. For HPs, the minimum increase is caused for a mix of 10% PV and 90% wind generation, amounting to 33.3 TWh. The smallest increase in short-term shifting is caused at 5% PV. For medium- and long-term energy shifting, there is even a small reduction at certain generation mixes. The largest reduction of medium-term shifting of 5.0 TWh occurs at 80% PV and of long-term shifting of 5.6 TWh at 5% PV. BESS only show a significant influence on short-term storage, increasing it by a maximum of 8.2 TWh for

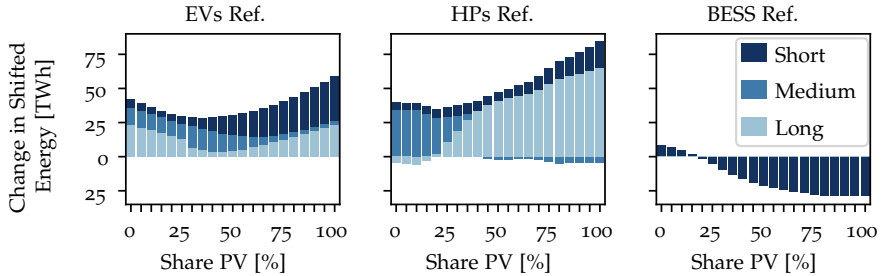


FIGURE 13.19: Change in shifted energy compared to *Gen. VRES* for varying shares of PV and wind generation with 100 % EVs (left), HPs (middle) and BESS (right) under reference operation.

100 % wind generation and decreasing it by a maximum of 28.7 TWh for 100 % PV generation.

The results of a combined integration of EVs, HPs and BESS are presented in Fig. 13.20. We thereby compare the integration under reference operation (left) and when using the flexibility of the DFOs in an optimised operation (right). For the reference operation, the lowest total shifted of 182.3 TWh energy occurs at 30 % PV and 70 % wind generation. The optimal mix with the combined integration of EVs, HPs and BESS thus increases the necessary shifting by 43.6 % compared to the optimal mix in *Gen. VRES*. The minimum short-term shifting in the combined integration of DFOs with reference operation occurs at 15 % PV, the medium-term at 100 % PV and the long-term at 25 % PV. When the DFOs are optimised to minimise the required energy shifting, the minimum total energy shifting amounts to 82.2 TWh and occurs at a generation mix of 40 % PV and 60 % wind. This signifies a reduction of 35.3 % compared to the optimal mix in *Gen. VRES*. For all generation mixes, the short-term shifting is reduced to nearly zero by DFO flexibility. The medium-term energy shifting shows the same effect for high shares of PV larger than 65 %. The long-term shifting shows its minimum at a mix of 25 % PV and 75 % wind.

The change in shifted energy compared to *Gen. VRES* caused by the combined integration of EVs, HPs and BESS is displayed in Fig. 13.21. The change with reference operation is shown on the left and the change with optimised operation on the right. The minimum increase in total shifted energy with reference operation occurs with 51.3 TWh at a generation mix of 40 % PV and 60 % wind. The short-term shifting stays nearly constant

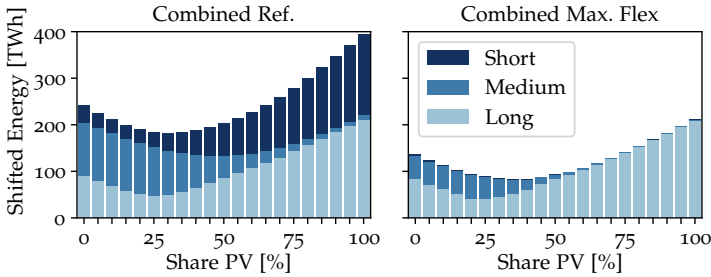


FIGURE 13.20: Flexibility needs for varying shares of PV and wind generation with the combination of 100 % EVs, HPs and BESS under reference (left) and optimised (right) operation.

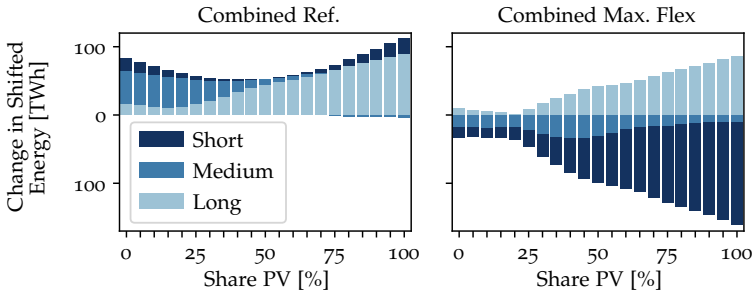


FIGURE 13.21: Change in shifted energy compared to *Gen. VRES* for varying shares of PV and wind generation with the combination of 100 % EVs, HPs and BESS under reference (left) and optimised (right) operation.

with a balanced mix of PV and wind generation but shows an increase for high shares of one or the other. The medium-term shifting is even slightly reduced for high shares of PV generation. It increases with higher wind generation. The long-term shifting is least increased at a mix of 15 % PV. For the optimised operation of DFOs, we see a net decrease in energy shifting for all generation mixes. The highest decrease of total energy shifting occurs at 100 % PV. However, it comes with a high increase in long-term shifting, which is compensated by an even higher decrease in short-term shifting. The reduction in short-term shifting shows its maximum for 100 % PV generation. The medium-term shifting is also decreased over all generation mixes, showing its maximum decrease at 40 % PV. The increase in long-term shifting is close to zero at 20 % PV and increases with high shares of PV.

### 13.5 SENSITIVITIES

Modelling results depend on underlying assumptions, model parameters and input data. We therefore run sensitivity analyses to investigate and showcase the sensitivity of the displayed results towards the most important model parameters and input data, namely the weighting of the storage types in the objective function and the input time series for feed-in and demand.

The flexibility needs on different time scales depend on the weighting of the storage types relative to each other. In a first sensitivity analysis, we therefore vary the weighting of storage types in the objective function to identify ranges of appropriate values for these weightings.

Furthermore, it was shown that the weather year greatly influences overall flexibility needs [190], [196]. In a second analysis, we therefore investigate the influence of demand and generation time series of different years to estimate the sensitivity of the resulting flexibility needs towards the weather year.

#### 13.5.1 Weighting of Storage Types

To investigate the influence of the relative weights, we vary the weights of the different storage types in the objective function. Values of relative weights  $\delta^{rel}$  are defined as:

$$\delta^{rel} = \delta^{rel*} + \epsilon = \frac{\delta_{long}}{\delta_{medium}} = \frac{\delta_{medium}}{\delta_{short}} \quad (13.5)$$

and varied in a sensitivity analysis with values of  $\delta^{rel*} = \{10^{-1}, 1, 10^1, 10^2\}$  and  $\epsilon = 1e - 3$ . The small value of  $\epsilon$  is added to avoid that all values are exactly equal for  $\delta^{rel*} = 1$ . The weights are chosen as  $\delta_{short} = \delta^{rel}$ , and consequently  $\delta_{medium} = (\delta^{rel})^2$  and  $\delta_{long} = (\delta^{rel})^3$ .

The influence of the relative weights on the shifted energy may differ with and without flexibility from EVs and HPs. We therefore investigate the *Base Case* and the scenarios of maximum flexibility (*EVs V2G* and *HPs Flex++*) with 100 % EV and 100 % HP penetration, respectively. The scenarios of maximum flexibility are chosen as they show the strongest effects of different relative weights on the shifted energy.

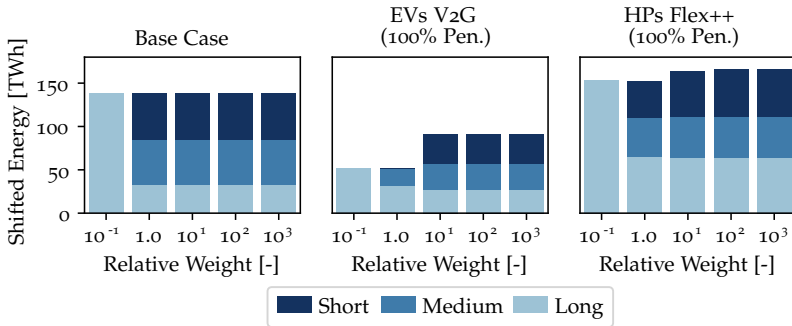


FIGURE 13.22: Flexibility needs for different relative weights in the base case (left) with 100 % flexible EVs (middle) and 100 % flexible HPs (right).

Figure 13.22 shows the resulting shifted energy for varying relative weights in the *Base Case* (left), with 100 % flexible EVs (middle) and with 100 % flexible HPs (right). The results show that the shares of the different storage types and the overall shifted energy vary with different relative weights. In all investigated cases, long-term storage covers the whole shifting for a value of  $\delta^{rel*} = 10^{-1}$  as it is the "cheapest" and offers the highest flexibility.

In the *Base Case* without flexibility, the total amount of shifted energy is only dependent on the mismatch of supply and demand and therefore is the same for all investigated relative weights. For values of  $\delta^{rel*} \geq 1.0$ , the short- and medium-term storage are used additionally to the long-term storage, and there is no further change for increasing relative weights.

When flexible units are included, both the distribution of the shifted energy across the three storage types and the total shifted energy change with different relative weights. For both EVs and HPs, the total shifted energy increases with relative weights of  $\delta^{rel*} > 1.0$ . In these cases, the long-term energy shifting slightly decreases while the medium-term storage shifting shows a slight and the short-term energy shifting a significant increase. For large relative weights, both the shares of storage types and the total shifted energy stay constant.

The reason for the increase in the overall shifted energy with higher relative weights is that higher amounts of short-term energy shifts are traded for a decrease of longer energy shifts, as these are more expensive in the objective function. In this case, flexibility is used to decrease long-term or medium-

term energy shifting, even though it could have been utilised to reduce short-term shifting to a larger extent.

In the case of EVs, a high relative weight leads to limited utilisation of V2G as this causes additional losses, which partially have to be stored long-term. For significantly higher weights on long-term compared to short-term shifting needs, this additional long-term shifting is not accepted even though it would result in a significant decrease in short-term shifting. For the same reason, the utilisation of TES is limited for HPs for high relative weights. Furthermore, the usage of the flexibility and the resulting needs for energy shifting in the HP scenario are impacted by the time-varying COP. For high relative weights, the optimisation schedules demand of HPs that originally coincided with renewable energy supply into times with high COP, thus reducing the overall electricity demand and seasonal shifting but requiring more shifting within the day. The higher the relative weights, the more additional short-term shifting is accepted for decreasing long-term flexibility needs.

In summary, the sensitivity analysis shows that both the total flexibility needs as well as the shares of the different storage types highly depend on the relative weighting. The results furthermore indicate that the choice of a relative weight of  $\delta^{rel} = 1.001$  is a reasonable trade-off, leading to a sensible utilisation of the short- and medium-term storage types without increasing the overall shifted energy as there is no strong preference to reduce long-term shifting.

### 13.5.2 Input Time Series

To investigate the influence of different load and feed-in patterns, we run a sensitivity analysis with different years as inputs and compare them to the simulated *Base Case*. For the conventional load profiles, we use the annual electricity demand for the years 2015-2022 provided by ENTSO-E [20]. The renewable feed-in is taken from *renewables.ninja*, which provides nationwide data for the years 1980-2019 [193], [194].

Figure 13.23 shows the data for the years 2015-2019 for demand (top) and VRES feed-in (bottom). The feed-in time series are scaled such that the total generated energy is the same as the load in the *Base Case*. They show different peaks, which are highly dependent on the weather conditions, but similar general characteristics. The demand displays a similar pattern in all investigated years.

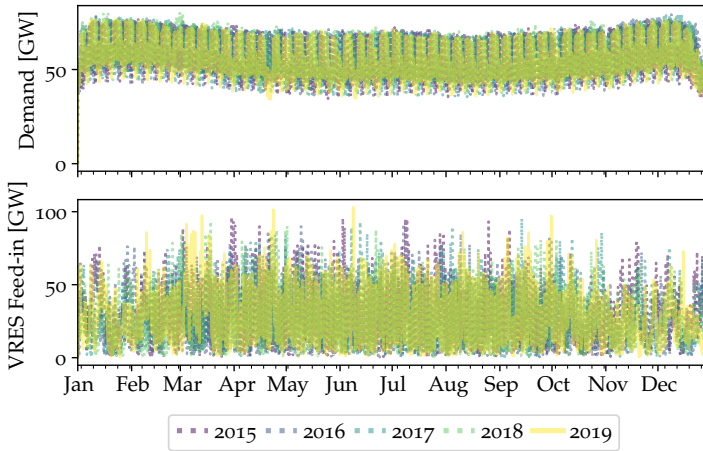


FIGURE 13.23: Load (top) and feed-in (bottom) time series for the years 2015-2019.

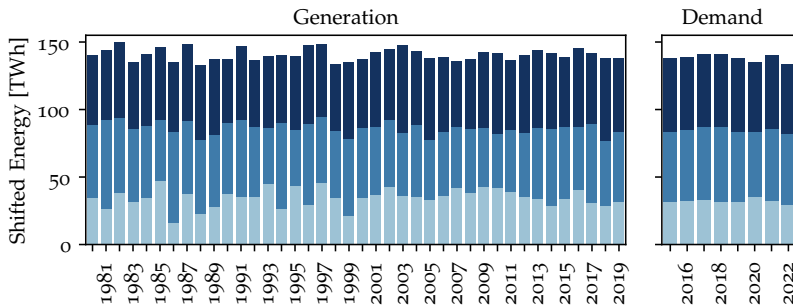


FIGURE 13.24: Flexibility needs with varying generation and demand time series.

Figure 13.24 shows the shifted energy for different simulated years for the variation of the generation time series (left) and the variation of the demand time series (right). For the variation of generation time series, the overall shifted energy varies between 96.2 % and 108.6 % of the total shifted energy in the reference case (2019). The shares of the different storage types in the reference case is 39.4 % of energy shifted by the short-term, 37.6 % shifted by the medium-term and 23.0 % shifted by the long-term storage unit. For the other years, the share of energy shifted by the short-term storage varies between 34.4 % and 44.6 %, the share of energy shifted by the medium-term storage between 28.4 % and 49.4 % and the share shifted by long-term storage between 12.0 % and 32.2 %.

Two factors lead to differences in flexibility needs for the investigated years. The first is that the share of PV and wind generation varies between the years. In the investigated data set, the share of PV varies between 37.3 % and 46.8 %. This share influences the total shifted energy and the shares of the different storage types as the scenario with a varying generation mix shows. However, the years deviating most from the mean of all years (e.g. 1997 and 1999) have generation mixes similar to the mean value of all years (1997: 43.0 %, 1999: 40.7 %, mean: 41.2 % PV). They should thus not deviate significantly from the mean distribution if this was the main factor for these differences which is not the case. Therefore, the second influencing factor, the time series patterns, seems to have a stronger influence on the outcome than the generation mix.

The differences in shifted energy and shares of the different storage types are smaller for the variation of the demand (Fig. 13.24, right) than for the variation of feed-in (Fig. 13.24, left). However, a smaller sample size was used for the demand time series. Nevertheless, the demand also shows less deviations between the years in Fig. 13.23 than the feed-in time series. The total amount of shifted energy ranges from 96.9 % to 102.4 % of the total shifted energy in the reference case. The share of short-term shifted energy ranges between 38.1 % and 39.4 %, where the reference case is at the upper limit. The share of energy shifted medium-term ranges between 35.7 % and 39.4 %, where the reference case is close to the mean with 37.6 %. The long-term storage ranges between 21.8 % and 26.3 % and the reference case is at 23.0 %. Therefore, overall, the results are relatively stable for the variation of the demand time series.

In summary, the sensitivity analysis with input data from different weather years shows some influence on the total shifted energy and shares of the different storage types by both the variation of feed-in and demand time series. However, the sensitivity analyses also show that while there are dependencies on the weather year, the results are still relatively robust, and the chosen weather year (2019) represents the other years reasonably well. A certain influence of the weather year is expected as previously mentioned [190], [196].

It should be noted that the starting time of the simulation also impacts the results. Varying the starting time for the *Base Case* within the day (i.e. shifting by zero to 23 hours) impacts the shares of short-, medium- and long-term storage. The shares range between 39.3 - 41.1 %, 35.7 - 37.6 % and 23.0 - 23.4 %, respectively. Furthermore, the storage durations differ, with

the largest difference in short-term storage durations (7.8 - 12.9 hours). A variation of the starting time within a month (i.e. shifting by zero to 28 days) does not affect the short-term shifting, but the shares of medium- and long-term shifting within the total shifted energy. They vary from 34.7 - 40.8 % for medium-term and from 19.8 - 25.9 % for long-term shifting. The storage durations range from 6.8 to 17.9 days and 96 to 113 days, respectively. The storage durations can therefore only be compared for a given study setup as they are sensitive towards the starting times. The reason is that there are border cases that are, in some cases, covered by medium-term storage, while other starting times require long-term storage to cover the imbalance. If the medium-term storage covers the border case, it will be a comparably long shift, increasing the mean storage duration.



## DISCUSSION

---

In this chapter, we critically reflect on the model and our results, put them into perspective with previous work from the literature and point out directions for future research. **Sections 14.1 and 14.2** discuss the influence of the generation mix and decentralised flexibility options on temporal flexibility needs. **Section 14.3** reflects on the limitations.

### 14.1 INFLUENCE OF THE GENERATION MIX

The results show that the required storage is highly dependent on the generation mix. The short-term flexibility need increases with the share of PV, which can be explained by the diurnal generation pattern of PV. It only produces electricity during the day, reaching its peak around noon (see Fig. 13.2). While the load is also higher during the day, it spreads over a longer period over the day, and the values are non-zero over the night. Therefore, the higher the share of the load supplied by PV, the higher the daily flexibility needs, as the PV generation needs to be shifted from day to night. Wind generation seems to have a stronger influence on the medium-term flexibility need. This can also be explained by the feed-in pattern displayed in Fig. 13.2. Wind generation shows higher variations between days than within a day. Therefore, the modelled short-term storage cannot compensate for such fluctuations, and medium-term storage is needed instead. The long-term flexibility need is lowest for a mix of 35% PV and 65% wind. Our results are comparable to [187], who found the optimal mix to be between 40-50% PV and 50-60% wind to minimise the seasonal storage needs (i.e. imbalances in a monthly resolution) in the European power system. A possible reason for the small difference is most likely that they cover the whole of Europe and the wind and PV time series therefore differ. The presence of an optimal mix can be explained by the partly complementing feed-in patterns of PV and wind. While PV shows lower feed-in values in winter, wind generation tends to be higher at these times. Therefore, combining both decreases the seasonal flexibility needs by smoothing the feed-in. Similarly, wind generation tends to be slightly

higher at night while PV only produces electricity during the day, reducing the short-term flexibility needs at a certain mix of both.

The total shifted energy shows a minimum at a share of 25 % PV and 75 % wind generation. This is relatively close to the optimum that was found for the European system in [188], where in terms of balancing energy, they found an optimal mix of 20 % PV and 80 % wind generation. Regarding absolute values, our results only differ by  $\sim 2\%$  from the ones in [196] when adjusted to the same modelling assumptions. In a comparison of different 100 % RE studies for Germany, the ratio of PV and wind generation was mainly found to be between 1:5 and 1:3 [197]. Our results with 1:4 lie precisely within that range. So overall, our results are in line with existing literature.

While in literature, either the total or individual storage needs or a specific mix of generation have been investigated, our study adds information on the influence of the mix of VRES generation on flexibility needs on different time scales. Depending on which needs to minimise, different mixes of PV and wind generation are optimal. The investigated short-, medium- and long-term shifting each show a minimum at a specific mix of PV and wind generation, implying that on all these timescales, the feed-in patterns are to some extent complementary. Depending on which time scales the energy shifting should be minimised, a carefully chosen generation mix can reduce these flexibility needs.

#### 14.2 INFLUENCE OF DECENTRALISED FLEXIBILITY OPTIONS

Another contribution of our work is the analysis of the impact of EVs, HPs and BESS on flexibility needs. In our investigations, EVs show a lower absolute and relative increase in flexibility needs and higher absolute and relative flexibility potential than HPs at the current mix of PV and wind generation. The increase in energy shifting is thereby smaller than the increase in electricity consumption, implying lower relative flexibility needs for EV charging than for the conventional load. Nevertheless, with higher penetrations, the share of shifted load increases. This is also observed for HPs. The additionally required energy shifting mainly consists of short- and medium-term storage for EVs. The uptake of HPs, on the other hand, shows a specifically high increase in long-term energy shifting due to the seasonality of the heat demand. This is caused by the fact that the seasonal pattern of the heat demand is opposite to PV feed-in, with higher

generation in summer. Furthermore, the relative increase in flexibility needs is significantly higher than the relative increase in electricity consumption, implying that a higher share of HP consumption has to be shifted than of conventional load. BESS cause a net reduction in flexibility needs, mainly in short-term energy shifting. The reference operation already yields reduction potential, which is doubled with an optimised operation.

It has to be mentioned that the additional flexibility needs caused by EVs and HPs and the influence of BESS also depend on the mix of generation as shown in the last case study. For the investigation of the influence of DFOs, we used the current mix of 41.5 % PV and 58.5 % wind generation. For HPs, where the seasonal pattern is opposite to PV and more in line with wind generation, higher shares of wind generation lead to lower additional energy shifting. The effect is especially pronounced for medium- and long-term shifting. They show large differences, with a reduction of long-term shifting but significant increase in medium-term shifting for high shares of wind generation and the exact opposite for high shares of PV generation. The influence of BESS also highly depends on the generation mix. With low shares of PV, BESS lead to an increase of short-term energy shifting since they are operated following PV generation. However, these edge cases are not realistic, since residential BESS are mainly installed alongside PV-systems and consequently no BESS would be present in the 0 % PV case in the real system. EVs, HPs and BESS mainly show the potential to decrease short- and medium-term energy shifting. Including a flexible operation of all DFOs therefore leads to an optimal generation mix with higher shares of PV closer to the minimum of long- and medium-term shifting.

Overall, the potential to decrease energy shifting by EV, HP and BESS flexibility is higher for short-term shifting, which was also found in [190]. For most of the investigated flexibility scenarios, a net decrease in short-term shifting can be achieved by the flexible units. This means that part of the short-term shifting caused by conventional load is also reduced by integrating sector coupling technologies. The reason for this effect is that part of the additionally required generation coincides with the conventional load. The share of the conventional load that has to be covered by the storage equivalents therefore decreases, allowing a net reduction of flexibility needs with the smart operation of EVs and HPs, even if discharging (e.g. by V2G or BESS) is not enabled.

Considering medium-term shifting, these flexibility needs are only significantly reduced by shifting EV charging over different parking events. This

would require an adjusted user behaviour and therefore stronger incentives than shifting within standing times. Additional utilisation of V2G allows for a simultaneous decrease of short- and medium-term energy shifting and reduces the initial flexibility needs in the *Base Case* by 62%. However, the scenarios with higher EV flexibility are also the only ones where users might experience any change in service quality. The TES and BESS allow for a reduction of flexibility needs without a change of consumption behaviour from the customer side. Similarly, in the lower flexibility scenarios of EVs, the charging demand is still covered in the originally scheduled session. Shifting between standing times, on the other hand, might require a higher tolerance of lower EV battery state of charges.

The decrease in long-term flexibility needs is limited for the investigated technologies and can mainly be influenced by choosing the right generation mix. The remaining long-term energy shifting would have to be covered by other technologies, such as large-scale heat storage, synthetic fuels or hydrogen. The reduction of long-term storage is possible to a small extent with the investigated technologies mainly due to the discrete formulation of the different time horizons, i.e. suppose a flexible unit can shift demand between two following medium-term periods, thereby equaling out opposite imbalances. In that case, this will be valued as the reduction of long-term shifting even though the shift performed by the flexible unit is not longer than two weeks (the time horizon of medium-term storage). Indeed, the storage durations increase with increasing levels of flexibility, implying that the flexibility is primarily used for shorter shifts. These shorter shifts are easier to substitute than longer shifts.

Another effect of the utilisation of flexible units is an increase in demand through additional losses. These amount to 2.8% and 1.5% of the original load for EVs and HPs, respectively. It has to be mentioned that real storage units would also cause additional losses, unlike the modelled ideal storage equivalents. Interestingly, the total incurred losses by V2G saturate at a certain level, meaning that even with higher potential to use V2G, this potential is not fully exploited. This effect implies that only a certain level of V2G is necessary to reduce the required shifting. Additional capabilities show only marginal benefits.

Between the DFOs, EVs show the highest reduction potential for total flexibility needs, followed by BESS and lastly HPs. The ability for discharging with V2G thereby leads to a significant increase in flexibility supply for EVs compared to *EVs Flex++*, where the flexible energy is the same as for *EVs*

V2G but discharging is not allowed. Comparing the observed reductions in total flexibility needs with the estimated flexibility potential in Chapter 4, both show the highest values for EVs at higher flexibility levels. However, the effects for HPs and BESS differ. HPs display higher values for flexible energy in *HPs Flex++* than BESS (see Section 4.3). However, their reduction potential for temporal flexibility needs prove to be lower. The reason might be the reduced temporal availability of HPs (see Fig. 4.5), especially in summer when shifting needs for PV are high. Furthermore, BESS display higher available power and have the ability to discharge, while HPs can only shift their electricity demand in time. The results thus stress the importance of accounting for the temporal availability of the DFOs. They furthermore show that the ability to discharge (BESS or EVs) can effectively increase the ability to supply temporal flexibility needs.

### 14.3 LIMITATIONS

We use a basic linear optimisation model to evaluate the flexibility needs for energy shifting on different time scales. Even though these are modelled as storage units, it has to be pointed out that the flexibility needs assessed in this study simply reflect the need to shift energy which may not be equivalent to the need for energy storage like in some other studies (e.g. [3], [191]). While storage units could cover these flexibility needs, the chosen interpretation is closer to the flexibility provided by DSM since we measure the shifted energy instead of storage energy and power capacities. It would be straightforward to adapt the introduced model to minimise the storage energy or power capacity of the storage equivalents. However, our study focuses on the potential of DSM from EVs and HPs, which is why we use the minimisation of shifted energy as our flexibility measure. In future work, it might nevertheless be interesting to investigate the influence of DFOs on the required energy and power storage capacities as well as the interaction with other flexibility options, like curtailment of excess VRES generation or dispatchable back-up generation.

In our case study, we showcase the use of the newly introduced model. Our goal was to approximate flexibility needs and the influence and reduction potential of residential EVs, HPs and BESS. We chose a model that is sufficiently simple but provides insights into the raised questions. However, we would also like to acknowledge the assumptions and simplifications which might have some impact onto the results. The model does not directly consider the degradation, losses or ramping limits of any of the storage

types. This is because our goal was to measure the theoretical minimum in required energy shifting. In reality, however, such inefficiencies would require higher generation as well as more shifting of energy. Further, we assume that the electricity supply and demand as well as EVs and HPs are perfectly known at every point in time (perfect foresight of future energy generation and load). This is not the case in reality, as there are always uncertainties in demand and supply forecasting. These uncertainties would lead to higher overall flexibility needs.

Moreover, the model uses the copper plate approach, not accounting for grid constraints. Grid constraints can restrict the energy exchange between different regions at certain times and thus require more local balancing of supply and demand. This effect would likely increase the total flexibility needs in the system. In future work, it would be interesting to investigate the interplay of grid and flexibility needs on the different timescales.

Furthermore, we model all EVs of one charging use case in an aggregated fashion and all HPs and BESS as one single unit. While this is a common approach in energy system modelling, it can yield inaccuracies and overestimate the flexibility potential [198]. However, the effects should be rather small and our model proved to be insensitive to different levels of aggregation in respective sensitivity model runs.

When integrating EVs and HPs, both technologies lead to an increase in shifted energy with reference operation. One simple reason is that more electricity is consumed with higher numbers of EVs and HPs. The assumed electricity consumption per EV and HP therefore influences the additional energy shifting. We compared our values to other studies in the modelling section of DFOs (see Fig. 3.12 and 3.17). The electricity consumption assumed for EVs in this thesis is on the lower end while the electricity consumption for HPs is comparably high. Similarly, we compared the energy and power capacities of BESS with the values chosen in other studies in Fig. 3.20. It shows that both values are within the range of literature values but on the higher end. However, all chosen values of EVs, HPs and BESS still lie within assumed literature values and therefore show a reasonable order of magnitude. Overall, projections of technology uptakes are always subject to uncertainty. The results should therefore not be interpreted as absolute values but the observed trends and tendencies are important.

## SUMMARY AND CONCLUSIONS

---

We developed a new model to quantify the flexibility needs in a 100 % renewable power system. The model uses linear optimisation and storage units operating at different time scales. These storage equivalents can help to analyse the energy-shifting needs in highly renewable power systems. We used the model to investigate the influence of the generation mix, increased penetrations of EVs, HPs and BESS as well as the utilisation of their flexibility potential on flexibility needs in terms of short- (daily), medium- (monthly) and long-term (seasonal) energy shifting.

The results show that the flexibility needs in a power system supplied by only PV and wind highly depend on the generation mix. Compared to a continuous generation (representing a stable base load power supply by thermal generation units) even the optimal mix of 25 % PV and 75 % wind generation increases the total flexibility needs from 37.6 TWh to 127.0 TWh, which amounts to 7.6 % to 25.6 % of the served load. The extreme cases of 100 % PV and 100 % wind feed-in lead to flexibility needs of 284.5 TWh and 158.6 TWh, an increase of 111.4 % and 24.9 % compared to the optimal mix. Choosing the optimal mix of PV and wind generation can therefore contribute to minimising the flexibility needs of a 100 % RE system.

Increasing penetrations of private EVs and residential HPs lead to flexibility needs of 167.1 TWh and 179.5 TWh in the German system for 100 % penetrations in case of reference operation in which no flexibility is provided by these devices. This signifies an increase of 21.0 % and 30.0 % of total flexibility needs compared to the base case without EVs and HPs. The additional energy shifting caused by EVs is mainly short- and medium-term. HPs, on the other hand, mainly increase the long-term flexibility needs. BESS under reference operation decrease the total flexibility needs by 12.3 % for 100 % penetration, thereby only influencing the short-term energy shifting.

EV flexibility proves to be more effective in reducing the flexibility needs than small-scale TES added to the HPs. Allowing shifting over standing times and the deployment of V2G even lead to a net reduction of total shifted energy with increasing penetrations of flexible EVs. With the highest

level of flexibility using V2G, the total shifted energy can be decreased to 51.9 TWh for a 100 % EV penetration, which corresponds to a reduction of 62.4 % compared to the base case. The EV flexibility can cover the entire short-term and large shares of medium-term flexibility needs. The potential to reduce long-term flexibility needs is comparably small. For the maximum flexibility of HPs equipped with a TES that allows shifting of the heat demand by at least eight hours, a net increase in total shifted energy can be observed with increasing penetrations of flexible HPs. The total flexibility needs amount to 152.0 TWh for the German system in this case. This means the increase in total flexibility needs can be reduced to 10.1 % compared to the base case. The reduction potential thereby primarily lies in the short- and medium-term energy shifting, where a net reduction can be achieved. However, this is outweighed by the increase in long-term shifting needs. An optimised operation of BESS at 100 % penetration can more than double their reduction of flexibility needs compared to the reference operation to 27.6 % compared to the base case, thereby still mainly reducing short-term energy shifting but also slightly decreasing medium-term shifting.

The combined integration 100 % penetration of the three decentralised flexibility options shifts the optimal generation mix to 40 % PV and 60 % wind for a flexible operation of the DFOs. Compared to the optimal generation mix without EVs, HPs and BESS, the total flexibility needs can be decreased by 35.3 %, covering nearly all short- and large shares of the medium-term energy shifting. This means that even though the total electricity consumption increases significantly with increasing shares of EVs and HPs, the amount of energy that has to be shifted to balance generation and demand decreases with the deployment of decentralised flexibility.

In summary, our model facilitates a comparison of the effectiveness of different flexibility options and measures to reduce flexibility needs on different time scales. The results show that a carefully chosen mix of PV and wind generation can reduce the flexibility needs of a 100 % RE system and that decentralised flexibility options have a large potential to decrease short- and medium-term flexibility needs. Flexibility provision from privately owned EVs, HPs and BESS should therefore be incentivised to untap this potential. One possibility is to forward time-varying price signals to consumers to alter their consumption behaviour. The following part of the thesis therefore investigates the influence of different price structures on the consumption behaviour of residential consumers and the influence on temporal and geographic flexibility needs.

Part IV

ECONOMIC INCENTIVES - ELECTRICITY  
TARIFFS



## MOTIVATION AND RELATED WORK

---

The power system is transitioning towards a cleaner and more efficient energy generation, causing numerous changes in the power system [148]. One of the most important changes is the increasing use of renewable generation. Renewable energy sources are often connected directly to the distribution grid. This distributed generation may cause reverse power flows, new congestion and voltage issues, which need to be addressed by the distribution system operator (DSO) [148]. Additionally, the distributed generation is intermittent, which increases the importance of flexibility in the grid [199]. If supply and demand cannot be balanced, this will cause stability issues and might even lead to blackouts or brownouts.

Another challenge is the increasing electricity demand caused by electric vehicles (EVs) and heat pumps (HPs), whose numbers are increasing. However, these new consumers also offer the possibility to operate them flexibly, which can reduce the additional stress on the grids. Similarly, battery energy storage systems (BESS) could be used in a system-friendly way when incentivised correctly. So far, few such incentives exist for households to adapt their behaviour according to system needs. However, with the increasing penetration of decentralised flexibility options, finding the right incentive systems is gaining in importance. One possible solution is to adapt electricity tariffs, combining suppliers' costs, taxes and network tariffs. Designing future tariffs in a way that effectively incentivises system-friendly consumption behaviour is therefore an important challenge.

Various studies analyse network tariffs and how they can efficiently prevent congestion and fulfil the new requirements of the changing power system. The most commonly discussed tariffs are different forms of energy-based and capacity-based tariffs. However, fixed tariffs and flexibility markets are often discussed as well. In [199], energy tariffs, capacity tariffs and a flexibility market were simulated and compared using centralised optimisation as a benchmark. Different penetrations of EVs were analysed as flexibility options, and the authors showed that, except for energy tariffs, all cost

structures could prevent congestion. However, there was no clear winner. Under different circumstances, different options were beneficial.

While most literature has focused on cost-reflectivity (e.g. [200], [201]) and congestion management (e.g. [199], [201]), the first study in **Chapter 17** focuses on the geographic flexibility needs, i.e. grid reinforcement and resulting costs, and the temporal flexibility needs, i.e. required energy shifting on different time scales. Additionally, the flexibility option considered is most often solely EV charging (e.g. [199], [100]). In contrast, this study includes heat pumps with thermal storage, battery household storage and photovoltaics (PV) curtailment as additional flexibilities.

The second study in **Chapter 18** focuses on network tariffs, as one important price component of electricity tariffs. Traditional network tariff structures were established when electricity generation and demand were, in the aggregate, easily predictable and the demand relatively inflexible [202]. In recent years, however, these conditions have changed due to the energy transition and the associated increasing integration of distributed energy resources (DERs) [203], [204]. DERs are assets such as rooftop PV systems, batteries, EVs, heat pumps, and other resources connected to the distribution grid. These resources challenge the grid's traditional structure, which was not originally designed for their volatility and level of penetration [202]. On the other hand, with the right incentives, flexible loads and decentralised storage offer the possibility to be part of the solution, for example, to resolve grid congestion [205]. The question arises as to whether the prevalent tariff structures can still fulfil the new requirements leading to appropriate incentives under these changes [206].

Recently, network tariff design has been subject to much debate, e.g. in Switzerland, with the revision of the energy supply act [206]. Considering the number of stakeholders involved in the discussion, e.g. DSOs and regulators, finding a suitable tariff structure that satisfies the needs of everyone is difficult. However, what are the needs and motivations of stakeholders regarding network tariff structures, and what are the resulting requirements with respect to these tariffs? Identifying network tariff requirements under increased integration of DERs has received limited attention in the literature and practice. Most studies focus on proposing new tariff structures that are suitable considering one or more specific criteria, e.g. reducing network stress and necessary reinforcement (e.g. [19], [207]), cost recovery (e.g. [208]–[210]) or ensuring fairness (e.g. [211]–[213]). Other works only investigate specific tariff types (e.g. [214]–[216]).

There have also been approaches to evaluate several different tariff structures based on various criteria. Abdelmottaleb, Gómez, and Reneses assessed the performance of different network tariffs based on four criteria: network cost recovery, deferral of network reinforcements, efficient consumer response and recognition of side-effects on consumers [201]. They used the analytic hierarchy process (AHP) to rank the network tariffs, putting equal weight on all criteria. They found that the cost-reflective design outperforms the traditional tariff structures. Brown, Faruqui, and Lessem determined five criteria for network tariff design in a stakeholder process: simplicity, economic efficiency, adaptability, affordability and equity [57]. They provided a simplified comparison of different network tariffs based on these criteria and assessed if they show a weak, medium or strong performance towards the respective criterion.

Hennig *et al.* proposed quantitative indicators for commonly used objectives for distribution network tariffs and discuss their interdependence [202]. They showcased that some of the objectives contradict each other leading to trade-offs between different tariff options. Since there is no one-size fits all solution, they proposed that relevant stakeholders agree on a set of objectives and their weighting with respect to each other. Our work contributes to filling this gap and proposes a process that includes identifying and weighting relevant criteria by stakeholder involvement. Vaughan, Doumen, and Kok also used stakeholder weighting to determine the relative importance of relevant criteria [217]. However, their set of criteria was determined by a literature review without further involvement of the stakeholders. Nair and Nair compared network tariffs along four main criteria (economic efficiency, revenue model, non-discriminatory design and customer satisfaction) and relevant sub-criteria determined from the literature using a Benefits-Opportunity-Costs-Risks model [218]. Between the investigated tariffs, they found the hybrid tariff of energy and capacity charges with coincident peak pricing to be the best alternative.

So far, the proposed frameworks either work with commonly used criteria from the literature [201], [202], [217], [218] or use a simplified evaluation method without quantitative performance indicators [57]. Furthermore, most of the works introduced so far use an equal weighting of the criteria [57], [201], [202], [218] and do not assess their importance relative to each other. We expand the existing literature by proposing a process that includes identifying relevant criteria, their weighting against each other and a quantitative assessment of the level of fulfilment by different network tariffs. We showcase the applicability of the proposed process by applying

it in a Swiss environment. In our work, we extract the relevant criteria from stakeholder interviews and determine the weights by expert weighting. These are combined with quantitative performance indicators using multi-criteria decision analysis (MCDA), which includes methods for decision making in complex, multi-dimensional problem settings and is therefore widely used in the field of sustainable energy [219].

We apply the framework to a case study and find that the best tariff depends on the expert weightings. However, in the scenario with high flexibility, capacity-based tariffs on average perform better than the standard volumetric tariff. Our results therefore emphasise the necessity for adapted network tariffs in future grids with high penetrations of DERs. Our proposed process and the open source evaluation framework can provide an informed decision process to determine the most suitable network tariff considering the most critical design criteria.

In summary, the main contributions of this part of the thesis (Chapters 17 and 18) are:

- Development of a consumer-based model to investigate the influence of different electricity tariffs on consumption profiles of households. Investigation of their influence on temporal and geographic flexibility needs.
- Introduction of a coherent process to identify and weigh relevant decision criteria for network tariff design. Translation of identified criteria into quantitative performance indicators to measure the diverse criteria.
- Synthesis into an open-source evaluation framework for network tariffs. The framework is modular, easily adaptable and can be applied to a wide range of tariff structures to allow for a better comparison and informed decision support.

## INFLUENCE ON FLEXIBILITY NEEDS

---

*The content of this chapter is extended from the published paper: L. Kundert, A. Heider and G. Hug, "The Influence of Different Network Tariffs on Distribution Grid Reinforcement Costs", 2023 IEEE Belgrade PowerTech, Belgrade, Serbia, 2023 [19], Copyright ©2023, IEEE. Compared to the original paper, we investigate additional tariffs, vary the penetration of distributed energy resources and determine the temporal flexibility needs in addition to the distribution grid reinforcement.*

The transition towards a renewable power grid raises various challenges in distribution grids, potentially leading to significant future geographic and temporal flexibility needs. This chapter analyses how different electricity tariffs can reduce these needs by steering the use of decentralised flexibility options, namely curtailment of photovoltaic generation, battery storage systems, smart charging, and usage of thermal energy storage to shift heat demand. Therefore, the reaction of prosumers with different combinations of these flexibility options is modelled by a cost-minimising consumer-based optimisation<sup>1</sup>. With these, a case study for six different grids in Germany is conducted for various combinations of different energy- and capacity-based tariff components.

The remainder of the chapter is structured as follows. **Section 17.1** introduces the developed consumer model. **Section 17.2** presents the case study, including the simulated customers, DER penetrations and investigated tariff structures. In **Section 17.3**, the results are presented and discussed. Finally, conclusions are drawn in **Section 17.4**.

### 17.1 METHODOLOGY - CONSUMER OPTIMISATION

If the electricity tariff is designed well, it can incentivise the consumers to shift their flexible demand to times when the grid has free capacity, thus mitigating the need for distribution grid reinforcement. On the other hand, it can give incentives to consume at times of high renewable feed-in, thus helping the integration of variable renewable energy sources (VRES). In

---

<sup>1</sup> The developed model is available open source under <https://github.com/AnyHe/NeTS.git>.

order to simulate the consumers' reaction to different tariffs, we carry out a consumer-based optimisation where the consumers' objective is to minimise their costs. It is assumed that every consumer has an energy management system (EMS) that manages their flexibility potential in this cost-optimal way. The total electricity consumption of the residential consumers and their EVs and the heat consumption provided by HPs are assumed to be fixed and cannot be reduced by the EMS.

Depending on the flexibility options available to the consumer, the optimisation problems differ. Here, the complete optimisation problem for a prosumer with all flexibility options is displayed. If other consumers do not own a specific flexibility option, the respective variables and constraints can be omitted. For simplicity, we do not account for taxes, levies and surcharges but focus on different combinations of network tariffs and suppliers' costs.

The objective is to minimise the total costs of the consumer  $\pi_{total}$  and a penalty term  $pen_{ev}$  for discomfort caused by late EV charging:

$$\min \pi_{total} + \delta^{ev} \cdot pen^{ev}, \quad (17.1)$$

where  $\delta^{ev}$  is the weighting factor for the penalty term for late EV charging. These terms and their meaning are further described in the respective paragraph about EVs. The costs of a consumer  $\pi_{total}$  are the sum of electricity purchase costs and network tariff minus their revenues from PV feed-in:

$$\begin{aligned} \pi_{total} = & \sum_{t \in T} \left( (\pi_t^p + \pi_t^e) \cdot p_t^L \right) + \pi^{cl} \cdot \bar{p}^L + \pi^{cf} \cdot \bar{p}^F \\ & + \sum_{sg \in SG} \left( \pi_{sg}^s \cdot p_{sg,t}^{SG} \right) - \sum_{t \in T} \left( \pi_t^{pv} \cdot p_t^F \right), \end{aligned} \quad (17.2)$$

where  $\pi_t^p$  is the suppliers' cost,  $\pi_t^e$  the energy-based component,  $\pi^{cl}$  and  $\pi^{cf}$  the capacity-based components on peak load and peak feed-in of the network tariff and  $\pi^{pv}$  the feed-in tariff. Price components  $\pi_{sg}^s$  describe a segmented tariff where the price for power consumption is dependent on the power drawn from the grid. Therefore, different segments  $SG$  are defined, within which the price for the power is constant. If the maximum power  $P_{sg}^{SG,max}$  of one specific segment  $sg$  is reached, the additionally required power is billed with the next more expensive segment. The sum of

power  $p_{sg,t}^{SG}$  within all segments thereby has to cover the load drawn from the grid:

$$0 \leq p_{sg,t}^{SG} \leq P_{sg}^{SG,max} \quad \forall sg \in SG, t \in T \quad (17.3)$$

$$\sum_{sg \in SG} p_{sg,t}^{SG} = p_t^L \quad \forall t \in T. \quad (17.4)$$

Variable  $p_t^L$  is the power drawn from the grid, i.e. equal to the residual load (ResL) when the load exceeds the feed-in and zero otherwise, and the maximum is denoted by  $\bar{p}^L$ . Analogously,  $p_t^F$  is power fed back to the grid, equal to the negative residual load when the feed-in exceeds the load and zero otherwise. The maximum is denoted by  $\bar{p}^F$ . Both variables result from the power balance of the household:

$$p_t^L - p_t^F = P_t^D + p_t^{HP} + p_t^{EV} - p_t^{PV} + p_t^{BS} \quad \forall t \in T, \quad (17.5)$$

$$p_t^L, p_t^F \geq 0 \quad \forall t \in T, \quad (17.6)$$

where  $P_t^D$  is the inflexible household load,  $p_t^{HP}$  and  $p_t^{EV}$  the flexible load of HPs and EVs,  $p_t^{PV}$  the PV feed-in and  $p_t^{BS}$  the battery (dis)charging.

Heat pumps are modelled with an ideal thermal energy storage (TES) that provides flexibility to shift their demand according to Section 3.3.6. It is assumed that  $soe_t^{TES}$  at the end and right before the start of the simulation period are equal to  $\frac{1}{2}C_{hp}^{TES}$ , i.e. half of the thermal energy capacity of the thermal energy storage  $C_{hp}^{TES}$ .

EVs are modelled analogously to Section 3.2.6 with the flexibility to shift their charging demand within their standing time. It is furthermore assumed that the preferred charging strategy is to charge as early as possible. To model growing user discomfort with deviation from this preferred charging, we introduce the penalty term  $pen^{ev}$ , adding the following constraint:

$$pen^{ev} = \sum_{t \in T} (\bar{E}_t - e_t)^2, \quad (17.7)$$

where  $e_t$  is the cumulative electricity consumption at the home charging station and  $\bar{E}_t$  the upper energy bound, which is obtained with the reference charging as early as possible. It is assumed that the energy level at the end and right before the start of the simulation period are equal to  $\frac{1}{2}(\underline{E}_t + \bar{E}_t)$ , i.e. the middle of lower and upper energy bounds  $\underline{E}_t$  and  $\bar{E}_t$ .

PV-systems are modelled in a way that they can be curtailed, i.e.:

$$0 \leq p_t^{PV} \leq \bar{P}_t^{PV} \quad \forall t \in T, \quad (17.8)$$

where  $\bar{P}_t^{PV}$  is the PV feed-in without curtailment and  $p_t^{PV}$  is the actual feed-in after curtailment.

BESS are modelled as ideal batteries according to Section 3.4.4. The state of charge at the end and right before the simulation period are fixed to  $\frac{1}{2}C_{bs}^{BS}$ , i.e. half of the energy capacity of the battery  $C_{bs}^{BS}$ .

## 17.2 DATA / CASE STUDY

The following section explains the setup of the simulated case study. Figure 17.1 displays the general structure of the study. Different electricity tariffs, i.e. combinations of suppliers' costs and network tariffs, serve as input for the introduced consumer optimisation. The obtained operation time series are then used to examine the effect on geographic and temporal flexibility needs.

The simulated consumer groups and characterisation of DERs are summarised in **Section 17.2.1**. The simulated scenarios regarding DER penetration are explained in **Section 17.2.2**. **Section 17.2.3** includes the investigated electricity tariffs and **Section 17.2.4** the indicators used to measure geographic and temporal flexibility needs.

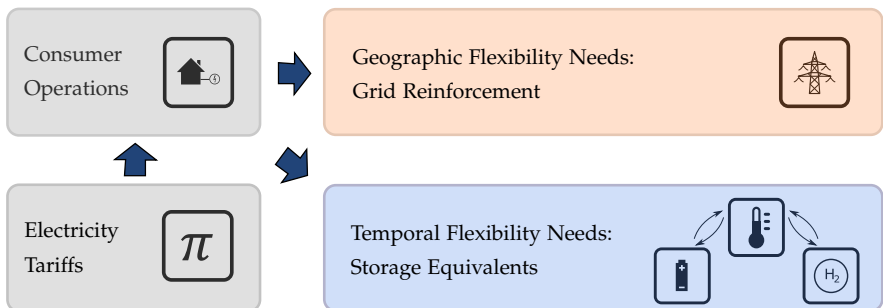


FIGURE 17.1: Research design of study.

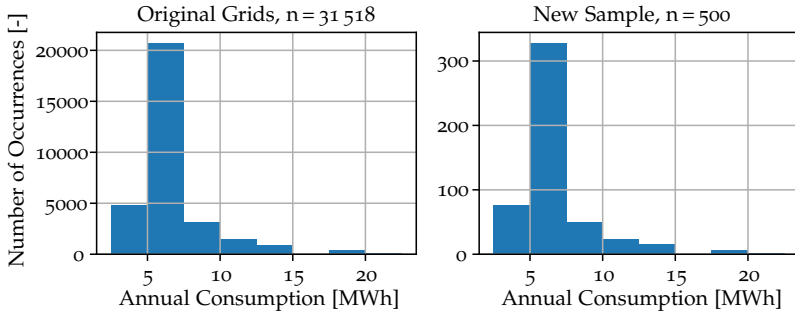


FIGURE 17.2: Distribution of annual consumption of residential loads in the original grids (left) and the new sample (right).

### 17.2.1 Consumers

We evaluate the electricity tariffs for 500 different consumer profiles in hourly resolution. For these, we use a subset of profiles from [220]. The profiles are chosen such that the distribution of annual consumption matches the distribution within the distribution grids introduced in Section 3.1.5 (see Fig. 17.2). We use updated profiles to capture better the variation of individual consumption profiles and higher individual peaks of consumers than the standard load profiles of the original grids.

Similarly, 500 of each DER are modelled using the sizing and technical values described in the respective sections of Chapter 3. For clarity, the underlying assumptions are briefly summarised below.

**PV-SYSTEMS** - The size of PV is drawn from a gamma distribution fitted to recent sales statistics. The mean size of the obtained sample is 8.4 kW. More details can be found in Section 3.4.1.

**BATTERY STORAGE** - It is assumed that batteries are only purchased in combination with a PV-system and sized accordingly. Consequently, the battery capacities are sized with a ratio of  $1 \frac{\text{kWh}}{\text{kW}}$  to the nominal power of the PV-system, which was found to be an economic ratio by [221]. The maximum charging power of the battery is chosen as a  $0.6 \frac{\text{kW}}{\text{kWh}}$  ratio to the battery capacity [140] and the battery is assumed to have a 100% charging and discharging efficiency. The mean battery capacity and charging power of the sample are thus 8.4 kWh and 5.0 kW.

**HEAT PUMPS WITH THERMAL ENERGY STORAGE** - The thermal capacity of HPs is drawn from a gamma distribution fitted to recent sales statistics. The mean of the obtained distribution is 13 kW of thermal capacity. The electric power of the heat pump is obtained with the minimum coefficient of performance (COP) (see more details in Section 3.3), and the mean of the obtained sample amounts to 7 kW. The TES is sized to cover the highest heat demand of two consecutive hours. The sample has a mean TES capacity of 19 kWh and consists of 81 % air-sourced and 19 % ground-sourced HPs. We assume an ideal TES, i.e. efficiencies of 100 %.

**ELECTRIC VEHICLES** - Regarding EVs, home charging stations modelled according to Section 3.2.2 are used. It has to be mentioned that it is still assumed that a significant share of the total charging demand occurs at other charging opportunities, i.e. at work or public charging points. The charging efficiency is assumed to be 90 % [115], and the weight for the penalty term is set to  $\delta_{ev} = 0.001$ .

### 17.2.2 Scenarios

In order to determine the effect of different network tariffs on consumer behaviour and flexibility needs under different local conditions, we study the six distribution grids introduced in Section 3.1.5 under varying penetrations of DERs. Four scenarios are compared. In the first, we randomly choose respectively 10 % of the households to distribute EVs, HPs and PV systems. The loads are drawn independently for the three technologies, meaning that certain households own a combination of them. For simplicity, we assume that every PV unit has a BESS installed alongside since already nowadays,  $\sim 80$  % of residential PV is installed together with battery storage [18]. In the second scenario, respectively 50 % of the residential loads are chosen to own EVs, HPs and PV with BESS. In scenarios three and four, 90 % and 100 % of the residential loads are chosen. The resulting shares of different household groups are displayed in Fig. 17.3. Note that, for clarity, percentages  $p \leq 1$  % are not labelled and that the values in the individual grids can slightly differ because of the random choice.

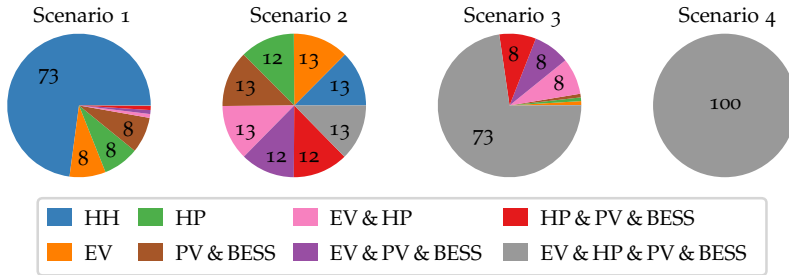


FIGURE 17.3: Distribution of consumer groups in the simulated scenarios. The displayed values are percent of total consumers in all six grids.

### 17.2.3 Electricity Tariffs

All investigated combinations of the electricity tariffs used in this study are summarised in Table 17.1. The electricity price comprises network tariff costs, suppliers' costs, different taxes, levies and surcharges. In our investigations, the taxes, levies and surcharges are omitted since they are not the focus of this study and assumed to be constant, thus not giving incentives to adapt the consumption behaviour. In the first tariffs, we focus on the network tariff. The suppliers' cost is fixed at 8 ct/kWh in these cases, which is the rounded value of the year 2021 in Germany [222]. In the last two tariffs, the suppliers' costs are varied, investigating the interaction of time-dependent suppliers' costs with selected network tariff structures. The PV feed-in tariff is the same for all cases except for the variation of suppliers' cost (explained later in this section), and it amounts to 6.24 ct/kWh, which is the feed-in tariff of Germany in July 2022 [223].

This study distinguishes two network tariff components: energy- and capacity-based. The *energy-based component* was chosen because it is the most commonly used one [224]. We simulate three different types, a constant value, a day/night charge with two different values for day times (d: 07:00-21:00) and night times (n: 21:00-07:00) and a charge depending on the residual load (ResL) of the grid. If it is one constant value, the case name contains  $E_c$  whereas an energy-based day/night component is denoted with  $E_{d/n}$ . The implemented energy-based day/night component  $E_{d/n}$  is similarly used in some countries such as the Netherlands [225], Switzerland and Italy [226]. The grid-dependent residual load based component is denoted by  $E_r$  and investigated in two variations. One uses the residual load at the medium voltage (MV)/low voltage (LV)-transformers ( $E_r$ ) and

TABLE 17.1: Investigated electricity tariffs

Tariff ID	Energy component [ct/kWh]	Capacity load component [€/kW]	Capacity generation component [€/kW]	Suppliers' cost [ct/kWh]
$E_c$	8.0	0	0	8.0
$E_{d/n}$	d: 8.5, n: 5.0	0	0	8.0
$E_r$	Grid-based	0	0	8.0
$E_{r-mv}$	Grid-based (MV)	0	0	8.0
$C_L$	0	122.8	0	8.0
$C_{SG}$	0	1: 60, 2: 90, 3: 140	0	8.0
$C_{LF}$	0	122.8	12.3	8.0
$E_r C_{LF}$	Grid-based	61.4	12.3	8.0
$E_c S_r$	4.0	0	0	ResL-based
$C_{LF} S_r$	0	122.8	12.3	ResL-based

one the residual load at the high voltage (HV)/MV-transformer ( $E_{r-mv}$ ). To calculate the residual load, the household load is updated with the resulting consumer profiles of the constant energy-based tariff  $E_c$ , which is the reference in the following investigations as it does not provide time- or power-dependent incentives to change the consumption behaviour.

The *capacity-based components* are a promising means to help with grid issues by reducing peaks, which cause grid reinforcement needs [202]. Capacity-based components tend to be charged only for peak demand. However, with a growing share of decentralised generation, feed-in peaks might become a driver of necessary grid reinforcement. We therefore also analyse a capacity component based on feed-in peaks in this work. The constant capacity components are implemented as an annual tariff and levied on the maximum demand or feed-in of the year. If the tariff has a capacity charge on peak consumption, the case name includes  $C_L$ , and a capacity charge raised on peak consumption and peak feed-in is denoted with  $C_{LF}$ . Additionally, we investigate a segmented tariff, where the charge on the current power consumption depends on the power drawn from the grid. We choose three segments, depending on the load time series of the investigated consumers. The maximum of the first segment is set to the mean of all 50 % quantiles of the customer load profiles. The second

one is set such that the maximum of the first and second is equal to the mean of all 90 % quantiles. For the investigated load profiles, this results to  $P_1^{SG,max} = 0.51 \text{ kW}$  and  $P_2^{SG,max} = 1.15 \text{ kW}$ . The maximum power of the third segment is set to a sufficiently high value  $P_3^{SG,max} = 1 \text{ MW}$  such that it covers all peak values. If the segmented tariff component is included, the tariff name comprises  $C_{SG}$ .

All network tariffs are designed so that inflexible consumers pay the same price. The constant energy-based component is fixed to  $\pi_t^e = 8 \text{ ct/kWh}$  (rounded value of the year 2021 in Germany [222]). The day and night tariff is composed of  $\pi_d^e = 8.5 \text{ ct/kWh}$  and  $\pi_n^e = 5 \text{ ct/kWh}$ . The resulting load capacity component equals  $\pi^{cl} = 122.8 \text{ €/kW}$ . The capacity component for feed-in is set to 10 % of the capacity load component, i.e.  $\pi^{cf} = 12.3 \text{ €/kW}$ . The prices for the segmented tariff are set to  $\pi_1^s = 6 \text{ ct/kW}$ ,  $\pi_2^s = 9 \text{ ct/kW}$  and  $\pi_3^s = 14 \text{ ct/kW}$ . If the tariff simultaneously contains energy and capacity components for load, both values are adjusted to half the original values. This way, inflexible consumers also pay the same in the combined cases.

For the energy components depending on the residual load of the grids, the residual load time series are shifted so that all values are positive. Furthermore, the shifted time series is scaled to ensure that inflexible consumers pay the same as for the constant energy tariff. To limit computational complexity, we cluster the six MV and 1052 LV grids depending on their technological composition and use the mean residual load of all grids within that cluster. Figure 17.4 displays the mean technological composition within the five simulated clusters, and Fig. 17.5 the price time series which are all scaled to a mean of 8 ct / kWh for easier comparison. Note that the mean prices used in the simulations differ to achieve the same price for inflexible consumers (1: 6.3 ct / kWh, 2: 7.2 ct / kWh, 3: 6.6 ct / kWh, 4: 7.1 ct / kWh, 5: 5.8 ct / kWh).

The number of customers being exposed to the time series of a certain cluster with tariff  $E_r$  changes between the scenarios, but all customers at the same MV/LV-transformer get the same tariff in any case. Figure 17.6 displays the number of customers assigned to the different clusters in the investigated grids and scenarios. In *Scenario 1*, the customers are distributed between the different clusters with high shares of Clusters 2 and 3. With increasing shares of DERs, more customers are assigned to Cluster 3, which shows high relative shares of DERs (see Fig. 17.4). For the tariff based on the residual load of the MV grid  $E_{r-mv}$ , the assignment to the clusters

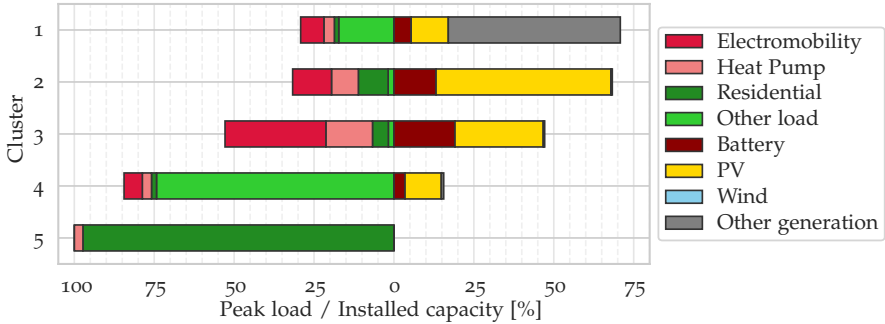


FIGURE 17.4: Mean technological composition of simulated clusters.

TABLE 17.2: Assigned clusters for different grids and scenarios under tariff  $E_{r-mv}$ .

	Load-1	Load-2	PV-1	PV-2	Wind-1	Wind-2
<b>Scenario 1</b>	4	4	2	2	3	3
<b>Scenario 2</b>	3	4	2	3	3	3
<b>Scenario 3</b>	3	3	3	3	3	3
<b>Scenario 4</b>	3	3	3	3	3	3

is summarised in Table 17.2. In *Scenario 1*, the load-dominated grids are assigned to Cluster 4, the PV-dominated grids to Cluster 2, and the wind-dominated grids to Cluster 3. Again, with increasing shares of DERs in the other scenarios, more grids are assigned to Cluster 3. In *Scenario 2*, four of the six grids and in the other two scenarios, all are assigned to the same Cluster 3.

To investigate the interplay of different incentive schemes, we simulate a scenario variation with time-varying *suppliers' cost*. Therefore, a price based on the residual load a 100 % VRES German system (see *Base Case* in Section 13.1.2) is used. The residual load is shifted such that only positive values occur. For a comparable price scenario, we scale the time series by dividing it by its average and multiplying it with the constant suppliers' cost of 8 ct/kWh used in the other cases. Figure 17.7 shows the resulting time series and, as a comparison, the day-ahead prices in Germany for 2019 (also scaled to a mean of 8 ct/kWh). They show the same characteristics, but the real price time series displays higher fluctuations and negative prices. The scenario variations including the ResL-based suppliers' costs are indicated

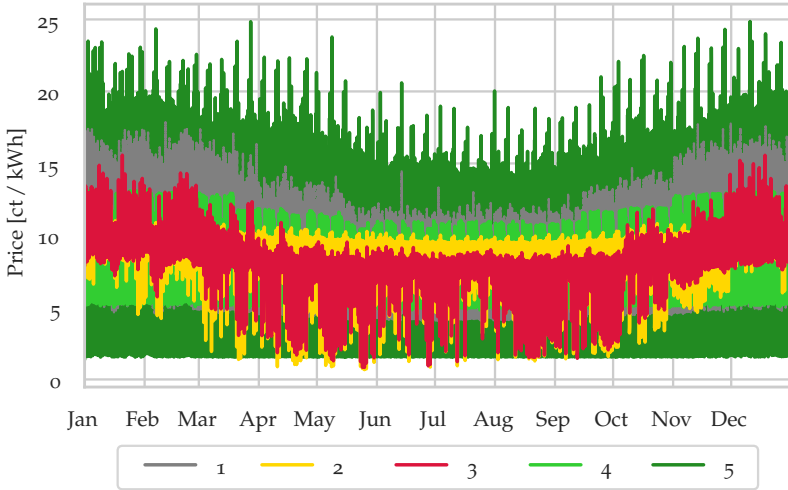


FIGURE 17.5: Annual price time series for the simulated clusters. The displayed time series are scaled to a mean of 8 ct / kWh.

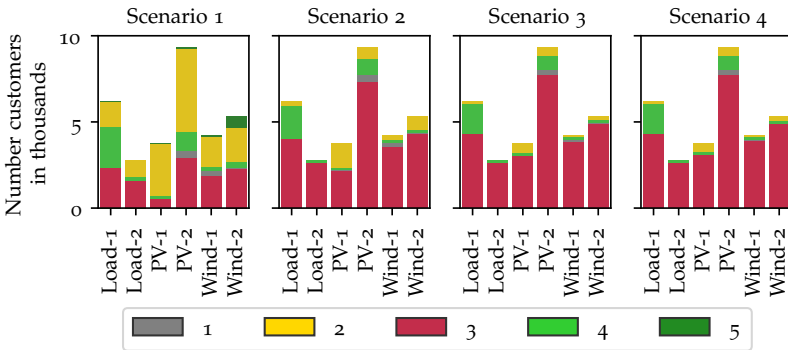


FIGURE 17.6: Number of customers assigned to the different clusters in the simulated scenarios under tariff  $E_r$ .

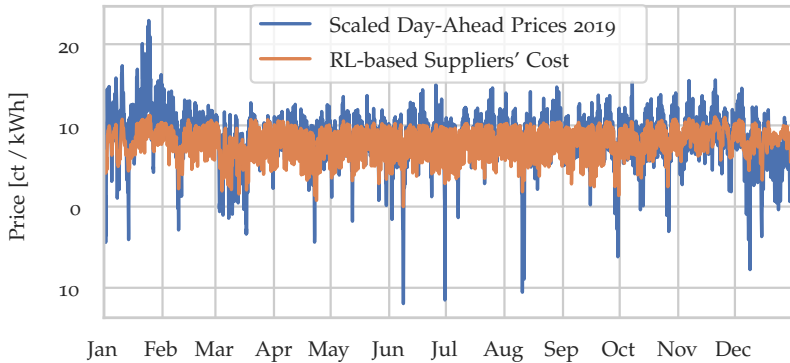


FIGURE 17.7: Annual price time series of the residual load-based suppliers' cost and day-ahead prices in the German bidding zone for the year 2019. The displayed time series are scaled to a mean of 8 ct / kWh.

with the suffix  $S_r$ . We also assume time-varying PV revenues for this tariff. We therefore use the same price time series as for the load but scale it to a mean of 6.24 ct/kWh to be in line with the other tariffs. With the obtained price time series, consumers pay more in times of high residual load, and PV feed-in achieves high revenues in these times. The opposite is the case in times of low or negative residual load. Prices for consumption are thereby still always higher than the revenues from PV feed-in.

#### 17.2.4 Flexibility Needs

After the consumer behaviour is determined, we compare the effects of the different electricity tariffs on geographic and temporal flexibility needs and their supply.

As a measure of geographic flexibility needs, the necessary grid reinforcement costs are calculated with the open-source model  $\epsilon$ DisGo [75]. Therefore, the consumers' time series are updated according to the results of the optimisation problems, and an AC power flow is conducted with the resulting grid to obtain bus voltages and component loading. If the calculated values exceed the predefined limits, parallel lines and transformers are installed in an iterative process until all voltage violations and overloading issues are resolved. We refer to Section 3.1.3 for a more detailed description. We use the predefined limits under normal operation for the voltage with a minimum of 0.9 p.u. and a maximum of 1.1 p.u. whereas the maximum

component loading is limited to 1.0 p.u. (see Section 3.1.2). To keep the simulation time sensible, we only run calculations for two critical weeks of the year: the week with the highest and lowest residual load of the respective grid and scenario.

The temporal flexibility needs are determined with the storage equivalent model introduced in Section 12. It measures the required energy shifts on a short, medium and long time scale. The acquired time series of the consumers are therefore scaled to the total number of residential buildings in Germany and integrated into the *Base Case* of the model, representing a 100% VRES German power system with 41.5% PV and 58.5% wind generation. To do so, the scaled time series of residential consumers without DERs is subtracted and replaced by the new aggregated time series with the respective tariff and DER penetration of the current scenario.

## 17.3 RESULTS AND DISCUSSION

In the following, the effects of the different tariff options on consumers' profiles, flexibility needs and cost implications are presented and discussed. **Section 17.3.1** showcases the influence of the investigated tariffs on the grid residual load. **Section 17.3.2** displays and discusses the influence of individual price components on consumer profiles and flexibility needs. **Sections 17.3.3 and 17.3.4** display the change in geographic and temporal flexibility needs for all investigated tariffs. The implications for the costs paid by the consumers are presented in **Section 17.3.5**. **Section 17.3.6** finally discusses limitations and avenues for future research. In all investigations, the tariff with only a constant energy-based component  $E_c$  serves as the base case as it is the most commonly used tariff in Germany and does not give temporally resolved incentives.

### 17.3.1 Grid Residual Load

The effects on geographic and temporal flexibility needs depend on the consumer profiles and how they interact with existing generation and load in the grids. Therefore, we present the effects of the different electricity tariffs on the grid residual load. The results are displayed for a selected load- and PV-dominated grid. These two grids are chosen as they best reflect the different effects of the tariff components. Similar effects can be observed in all other grids but to a smaller extent. For the load-dominated

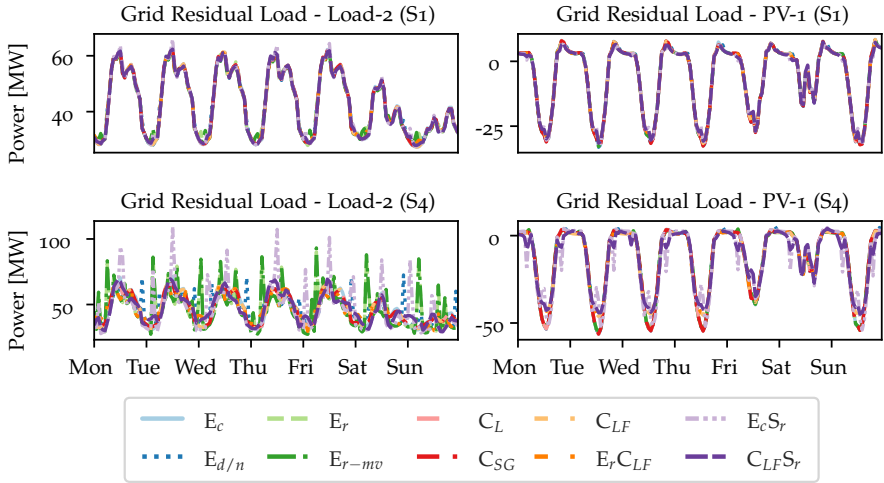


FIGURE 17.8: Residual load with different electricity tariffs.

grid, we showcase the week of highest residual load in *Scenario 2* and for the PV-dominated grid the week of the lowest residual load in *Scenario 2*. This scenario is chosen as the intermediate scenario, and we will use the same weeks in the following visualisations for a clearer comparison. All changes between the scenarios and tariffs are thus caused by increasing shares and different operations of DERs. Note that the weeks of actual highest and lowest residual load can differ between the scenarios.

Figure 17.8 displays the residual load of both grids with all investigated tariffs in *Scenario 1* (S1) on the top and *Scenario 4* (S4) below. The results show that with low penetration of DERs in *Scenario 1*, the effects of the different tariffs are limited in both grids. In the load-dominated grid (upper left), the peaks around noon are slightly increased by tariff  $E_c S_r$  as it gives incentives to consume around noon to use PV generation. The tariffs based on the grid residual load ( $E_r$  and  $E_{r-mv}$ ) shift demand to the night valleys since the conventional load and consequently the prices are low in these times. In the PV-dominated grid (upper right), the tariffs with capacity components slightly decrease both load- and feed-in-driven peaks. Other than that, the profiles look similar with all investigated tariffs.

In *Scenario 4* with 100% DER penetration, the difference between the investigated electricity tariffs is higher. In the week of high load in the load-dominated grid (lower left), tariffs with only energy-based incentives

( $E_{d/n}$ ,  $E_r$ ,  $E_{r-mv}$ ,  $E_c S_r$ ) lead to new, partly significantly higher, peaks than the other tariff options. No such new peaks are visible in the week of high feed-in in the PV-dominated grid (upper right). On the contrary, some tariffs lead to lower negative peaks in the residual load. The tariffs with a capacity feed-in component ( $C_{LF}$ ,  $E_r C_{LF}$ ,  $C_{LF} S_r$ ) are especially effective in doing so but also suppliers' costs based on the residual load ( $E_c S_r$ ) reduces the feed-in peaks to a small extent. In general, the effect of the different tariffs on load peaks is higher than on feed-in peaks.

### 17.3.2 Influence of Individual Price Components

To showcase the effects of the different tariffs in more detail, the consumption profiles of residential loads are discussed along the different tariff components in the following. They are presented for the same setup (displayed grids, scenarios and weeks) as explained in the previous section. Additionally, their effects on temporal and geographic flexibility needs are presented and discussed.

#### *Energy-based Tariff Component*

Fig. 17.9 shows the residual load of residential consumers for the four purely energy-based tariffs. The results are displayed for *Scenario 1* (S1) with low DER penetration and *Scenario 4* (S4) with high DER penetration. For the consumption profile in the load-dominated grid with low DER penetration (upper left), we see a smoothing effect due to the  $E_{d/n}$ ,  $E_r$  and  $E_{r-mv}$  tariffs compared to the base case. Especially the peaks in the evening hours are reduced by shifting demand into the night. On the other hand, focusing on feed-in peaks in the PV-dominated grid (upper right), only the tariffs based on the grid residual load  $E_r$  and  $E_{r-mv}$  have a positive effect on these peaks. The reason is that shifting demand into the night with  $E_{d/n}$  conflicts with the local situation in the grid where a high feed-in excess is present on sunny days. Load peaks, on the other hand, are still reduced in this case.

With high DER penetration in *Scenario 4*, the time-varying energy-based tariffs introduce new load peaks in the load-dominated grid (bottom left). The day and night tariff  $E_{d/n}$  causes peaks in the evening when the low-price period starts through synchronisation of EV charging. Another peak occurs in the early morning when the low-price period ends through a synchronisation of HPs. For the tariffs based on the grid residual load

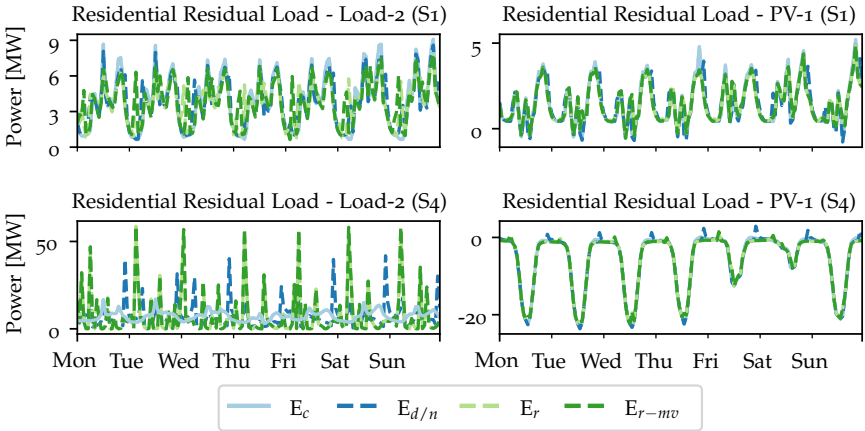


FIGURE 17.9: Residual load of residential consumers for representative load-dominated grid in the week of high residual load (left) and for representative PV-dominated grid in the week of low residual load (right). The time series are displayed for the energy-based tariffs in a scenario of low (top) and high DER penetration (bottom).

$E_r$  and  $E_{r-mv}$ , even higher new peaks occur during the night and early morning. In these times, the conventional load is low and consequently the prices as well. Additionally, smaller load peaks occur around midday during high PV feed-in. The influence of the tariffs is less pronounced in the PV-dominated grid in the week of highest feed-in (bottom right). Again, the tariffs based on grid residual load  $E_r$  and  $E_{r-mv}$  slightly decrease the feed-in peaks. The newly introduced peaks of all tariffs are comparably low in this case.

Table 17.3 summarises the effects of the energy-based tariffs on the total geographic and temporal flexibility needs in all investigated grids. The values are displayed relative to the flexibility needs in the base case ( $E_c$ ) of the respective scenario. The results show that over the different tariffs and scenarios, only  $E_{d/n}$  achieves a slight decrease in reinforcement costs with low penetrations of DERs. In all other scenario combinations, the flexibility needs either stay nearly unchanged or increase significantly.

For 100% DERs in *Scenario 4*, the increase in costs reaches up to 261% compared to the base case for  $E_{r-mv}$ . Tariff  $E_r$  reaches similarly high values. The day and night tariff  $E_{d/n}$  increases the reinforcement costs by 88% compared to the base case in the same scenario. The less significant increase,

TABLE 17.3: Geographic and temporal flexibility needs with energy-based tariffs relative to flexibility needs in the base case.

	Reinforcement costs [%]				Shifted energy [%]			
	S1	S2	S3	S4	S1	S2	S3	S4
$E_{d/n}$	98.6	147.8	160.4	188.0	101.5	107.3	110.6	110.9
$E_r$	107.4	206.2	260.9	341.4	99.9	103.2	108.5	109.8
$E_{r-mv}$	138.8	204.3	340.2	361.2	100.1	103.1	109.1	110.6

which is in line with the lower load peaks displayed in Fig. 17.9, is likely because there are longer time periods with the same price. This way, the flexible load can be shifted into a longer interval. In contrast, for the temporally resolved tariffs, the flexible load is concentrated on individual time steps with low prices. In *Scenario 3*, tariff  $E_r$  also shows a lower increase in costs than  $E_{r-mv}$ , most likely because consumers in different LV grids follow different price time series and their peaks therefore do not necessarily coincide, which is the case when all consumers follow the same price signal.

The increase in temporal flexibility needs is similar for the three tariffs. The day and night and grid-based tariffs ( $E_{d/n}$ ,  $E_r$ ,  $E_{r-mv}$ ) increase the total shifted energy by 10-11% with the highest penetration of DERs in *Scenario 4*. With lower penetrations of DERs, the difference between these three tariffs is higher, and  $E_r$  even slightly reduces the total shifted energy compared to the base case in *Scenario 1*. However, with increasing DER penetrations, the effects of these three tariffs align.

Summarising, purely energy-based tariffs can give good incentives at low DER penetrations but lead to high load peaks at high DER penetrations, increasing geographic and temporal flexibility needs. The results imply that longer periods with the same price and varying price time series for different consumers can partly reduce the increase of flexibility needs caused by time-varying energy-based cost components. However, there is still a significant increase of flexibility needs in the scenarios with high DER penetrations. Pure time-varying energy-based tariffs should therefore be avoided in this case.

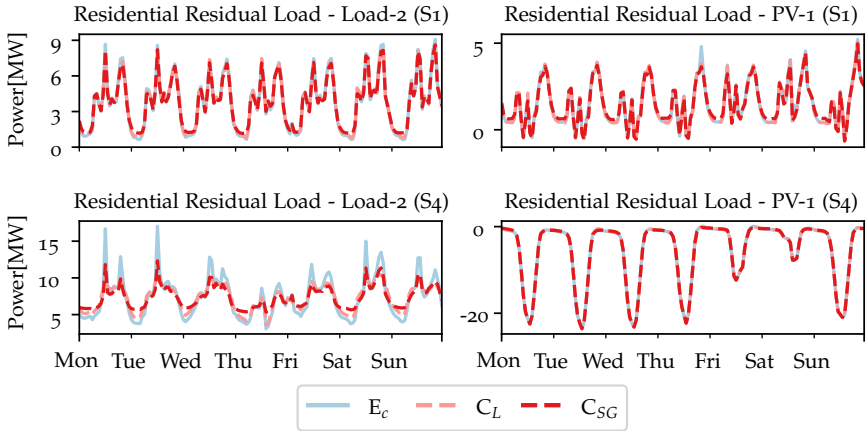


FIGURE 17.10: Residual load of residential consumers for representative load-dominated grid in the week of high residual load (left) and for representative PV-dominated grid in the week of low residual load (right). The time series are displayed for the capacity load tariffs in a scenario of low (top) and high DER penetration (bottom).

### Load Capacity Component

Fig. 17.10 shows residential consumers' residual load, including their PV-generation and flexibility options for both grids when applying a capacity component on the load. The results are displayed for a peak component on the load ( $C_L$ ) and the segmented tariff ( $C_{SG}$ ). In the low DER penetration scenario (top), the effects are small, but the load peaks are slightly reduced in both grids.

The effects become more pronounced in the high DER penetration scenario at high residual load (bottom left). While the pure capacity component on peak load  $C_L$  effectively reduces the peak, the segmented tariff  $C_{SG}$  additionally smoothens the time series in the remaining times, filling the valleys in the early morning. This effect can be explained by the additional incentive given by the three segments. Consumers will shift their flexible demand into times of low inflexible demand to benefit from the lower prices of the cheapest segment. However, the peak reduction is lower for the segmented tariff than for the peak load tariff. The reason is that load reduction is only economically attractive when the consumer can reduce the load to the extent that it is billed with a cheaper segment. If the peak is too high to achieve that, there is no incentive to reduce the load.

TABLE 17.4: Geographic and temporal flexibility needs with capacity load tariffs relative to flexibility needs in the base case.

	Reinforcement costs [%]				Shifted energy [%]			
	S1	S2	S3	S4	S1	S2	S3	S4
$C_L$	9.5	75.0	94.4	96.6	100.0	99.7	99.9	100.0
$C_{SG}$	67.2	91.0	96.4	97.2	100.5	101.2	100.3	99.8

In the PV-dominated grid in the week of low residual load (bottom right), we see little effect of the capacity load tariffs. In these times, the feed-in exceeds the demand, and no incentives are given to alter the feed-in of the residential loads.

Table 17.4 summarises the effects of the capacity load tariffs on geographic and temporal flexibility needs. The values are presented relative to the flexibility needs in the base case ( $E_c$ ) of the respective scenario. There is nearly no difference in temporal flexibility needs with the capacity load tariffs. Even though load peaks are reduced, the influence on the shifted energy is small.

On the other hand, the effect on the geographic flexibility needs depends on the DER penetration. In *Scenario 1* with low DER penetration, the reinforcement costs can be significantly reduced, by 90.5% with tariff  $C_L$  and by 32.8% with the segmented tariff  $C_{SG}$ . The higher reduction of reinforcement costs by  $C_L$  is in line with the stronger peak reduction observed in the consumption profiles in Fig. 17.10. With increasing penetrations of DERs, both the reduction potential and the difference between both capacity load tariffs decrease. In *Scenario 4* with 100% DER penetration, the reduction of both tariffs only amounts to 3.4% and 2.8%, which implies that a large share of the remaining reinforcement needs are feed-in driven.

Summarising, pure capacity load tariffs can effectively reduce load-driven grid reinforcement but have little influence on temporal flexibility needs. The importance of this price component depends on whether distributed PV or new loads such as EVs and HPs are the main driver of future grid reinforcement costs.

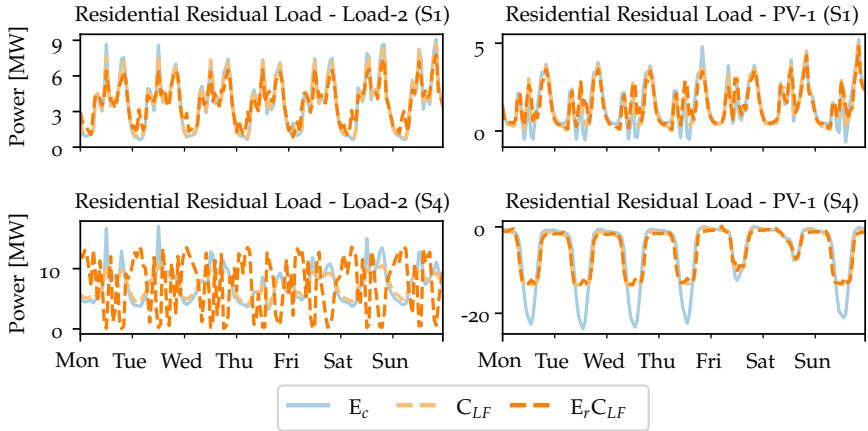


FIGURE 17.11: Residual load of residential consumers for representative load-dominated grid in the week of high residual load (left) and for representative PV-dominated grid in the week of low residual load (right). The time series are displayed for tariffs including a capacity feed-in price component in a scenario of low (top) and high DER penetration (bottom).

### *Feed-in Capacity Component*

In case of high shares of distributed PV, an additional feed-in capacity component can reduce feed-in peaks. Fig. 17.11 shows the residual load of residential loads, including their PV-generation and flexibility options, in the week of high residual load for a representative load-dominated grid (left) and in the week of low residual load for a representative PV-dominated grid (right). The time series are displayed for the pure capacity-based tariff comprising peak prices on load and feed-in  $C_{LF}$  and a combination of the energy price component based on the grid residual load and capacity component on peak load and feed-in  $E_r C_{LF}$ .

In the load-dominated grid with low penetration of DERs (upper left), both tariffs decrease the peak load. The combination of energy- and capacity-based price components  $E_r C_{LF}$  proves to be more effective in smoothing the load than the capacity components on their own in tariff  $C_{LF}$ . The reason is that, in addition to the incentive to decrease the highest occurring peak, the energy price component based on the grid residual load gives incentives to shift into times of low residual load, which seems to coincide well with the residential load. In the scenario of high DER penetration (lower left),

TABLE 17.5: Geographic and temporal flexibility needs with capacity feed-in tariffs relative to flexibility needs in the base case.

	Reinforcement costs [%]				Shifted energy [%]			
	S <sub>1</sub>	S <sub>2</sub>	S <sub>3</sub>	S <sub>4</sub>	S <sub>1</sub>	S <sub>2</sub>	S <sub>3</sub>	S <sub>4</sub>
$C_{LF}$	8.1	48.8	55.8	52.3	98.9	96.9	98.2	98.8
$E_r C_{LF}$	0.0	46.7	56.5	55.8	98.9	98.2	102.6	103.9

the time series of both tariffs differ significantly. The combined tariff  $E_r C_{LF}$  shows higher fluctuations and shifts more load into the early morning when the conventional load is low. The capacity-based peak components prevent new high peaks caused by the energy-based component on its own  $E_r$ . With the combination of time-resolved energy-based and peak capacity components, it is thus possible to give temporal incentives without causing new peaks through synchronisation.

The difference between both tariffs is smaller in the PV-dominated grid in the week of low residual load (right). Both significantly reduce the feed-in peaks in the displayed scenarios.

Table 17.5 summarises the influences of the tariffs comprising capacity components pricing peak load and feed-in on geographic and temporal flexibility needs. The values are displayed relative to the flexibility needs in the base case ( $E_c$ ) in the respective scenario. With low penetrations of DERs, both tariffs effectively reduce the geographic flexibility needs. The pure tariff  $C_{LF}$  reduces the reinforcement costs by 91.9% in *Scenario 1*, the combined tariff  $E_r C_{LF}$  even completely avoids grid reinforcements in this case. With increasing penetrations of DERs, the reduction potential decreases but stays relatively high at 47.7% for  $C_{LF}$  and 44.2% for  $E_r C_{LF}$  in *Scenario 4* with 100% DERs.

The effects on the temporal flexibility needs are smaller. The pure capacity-based tariff  $C_{LF}$  slightly reduces the temporal flexibility needs in all scenarios. The combined tariff  $E_r C_{LF}$ , on the other hand, decreases the flexibility needs for low to intermediate DER penetrations but increases the shifted energy for high DER penetrations up to 3.9% in *Scenario 4*. This still signifies a reduction compared to the pure energy-based tariff  $E_r$ , which increases the temporal flexibility needs by 9.8%.

Summarising, capacity price components on load and feed-in reduce the geographic and temporal flexibility needs. They are especially effective in reducing feed-in peaks and therefore gain importance with high shares of distributed PV. Similar to the capacity tariffs on load only, synchronisation effects caused by temporally resolved incentives at high DER penetrations can be effectively prevented. Capacity price components on load and feed-in should therefore be included for high DER penetrations.

### *Time-varying Suppliers' Cost*

Time-varying suppliers' costs can be a means to forward market prices to end consumers and thus give temporal incentives to consume at times of high renewable feed-in. We therefore investigate the effect of tariffs including time-varying suppliers' cost based on the residual load in a 100 % VRES system in Germany. The resulting consumer time series are displayed in Fig. 17.12. Generally, similar effects as for the time-varying energy-based price components can be observed for tariff  $E_c S_r$ . However, this tariff already increases load peaks for low penetrations of DERs (top). These become more significant with increasing penetrations of DERs, especially in the load-dominated grid in the week of high residual load (bottom left). The new peaks occur around noon during high PV feed-in and at night during low conventional load. An additional capacity component on peak load and feed-in in tariff  $C_{LF} S_r$  effectively reduces both load and feed-in peaks.

Table 17.6 summarises the influence of the tariffs with time-varying suppliers' costs on geographic and temporal flexibility needs. These are displayed relative to the flexibility needs in the base case ( $E_c$ ) of the respective scenario. The new peaks through synchronisation lead to a massive increase in reinforcement costs for tariff  $E_c S_r$  in all investigated scenarios, with a relative increase between 128.2 - 493.6 % compared to the base case. The additional capacity price component on load and feed-in in  $C_{LF} S_r$  can significantly reduce the costs. With low DER penetration, a reduction of 89.3 % compared to the base case can be achieved this way. With increasing DER penetrations, the reduction decreases to 43.7 % in *Scenario 4*.

The temporal flexibility needs are reduced by 4.4 % with both tariffs in *Scenario 1* with low DER penetration. With increasing penetrations of DERs, the two tariffs perform differently. The reduction decreases for  $E_c S_r$  with high penetrations of DERs. With 100 % DERs in *Scenario 4*, there is even a slight increase in temporal flexibility needs of 0.4 %. With a capacity

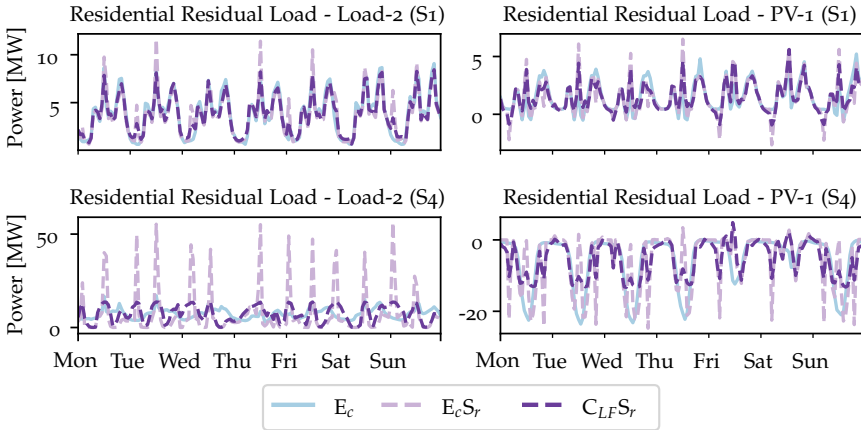


FIGURE 17.12: Residual load of prosumers with time-varying suppliers' costs in the week of high feed-in.

TABLE 17.6: Geographic and temporal flexibility needs with tariffs including time-varying suppliers' costs relative to flexibility needs in the base case.

	Reinforcement costs [%]				Shifted energy [%]			
	S1	S2	S3	S4	S1	S2	S3	S4
$E_c S_r$	593.6	228.2	352.4	354.9	95.6	92.2	98.6	100.4
$C_{LF} S_r$	10.7	50.6	57.1	56.3	95.6	86.1	86.8	87.8

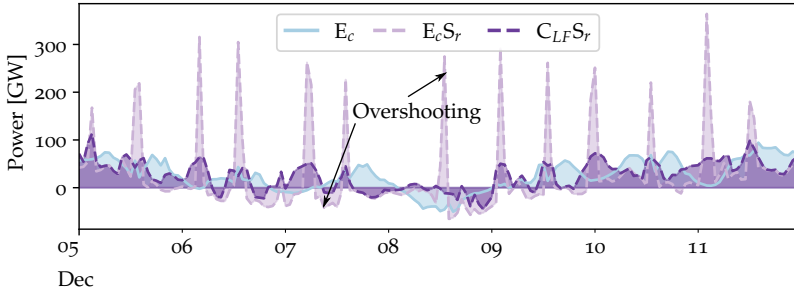


FIGURE 17.13: National residual load in week of high load with time-varying suppliers' costs compared to the reference tariff  $E_c$  in *Scenario 4*.

price component on both load and feed-in in  $C_{LF}S_r$ , on the other hand, the reduction of temporal flexibility needs is higher with high DER penetrations than in *Scenario 1* with low DER penetration, amounting to 12.2 % in *Scenario 4* with 100 % DERs. Tariff  $C_{LF}S_r$  thus proves to be the most effective in reducing both geographic and temporal flexibility needs.

The decreasing performance for  $E_c S_r$  with high penetrations of DERs can be explained by overshooting, which is showcased in Fig. 17.13. If DER penetrations and their flexibility are high, reacting to predefined price time series can lead to load peaks exceeding the excess feed-in (that caused the low prices), possibly resulting in new high load periods. Similarly, if too much feed-in is shifted into times of originally high load, it can create new times of excess feed-in, which then has to be stored and shifted to later times.

With peak prices on both load and feed-in in tariff  $C_{LF}S_r$ , the overshooting can be reduced, and reduction potentials stay high also with high penetrations of DERs. However, Fig. 17.13 shows that situations still occur where the consumer reaction overcompensates the original imbalance. Therefore, the DERs still do not unfold their full potential to reduce temporal flexibility needs, even with the most effective tariff  $C_{LF}S_r$ . Therefore, it might be worth to consider including decentralised flexibility directly in the market in these situations with high flexibility since they can influence the residual load significantly and should consequently not act as price takers.

Summarising, time-varying suppliers' costs can reduce the temporal flexibility needs at low DER penetrations, but significantly increase geographic flexibility needs. At high DER penetrations, overshooting leads to an increase in temporal flexibility needs as well. Capacity-based price compo-

nents can counteract this effect, but overshooting still occurs. For high DER penetrations, direct integration of decentralised flexibility to the market might therefore be preferable to a fixed price time series.

### 17.3.3 Geographic Flexibility Needs

In the following, we present and discuss the influence of different tariff options on the geographic flexibility needs in the distribution grids, measured by the required distribution grid reinforcement and resulting costs. Fig. 17.14 shows the total grid reinforcement costs for the different tariffs and scenarios summed over the six distribution grids and divided into the different voltage levels.

The absolute grid reinforcement costs vary with the investigated tariffs and penetration of DERs. In *Scenario 1* with low penetrations of DERs, the reinforcement costs are low, and the differences between the network tariffs are small. Only the time-varying suppliers' cost in  $E_c S_r$  lead to a significant increase in reinforcement costs. Tariffs  $C_L$ ,  $C_{LF}$ ,  $E_r C_{LF}$  and  $C_{LF} S_r$  can nearly completely avoid reinforcement needs. On the other hand, the results differ significantly in the other scenarios with higher penetrations of DERs and the total reinforcement costs increase significantly. The total costs in the base case ( $E_c$ ) increase from 0.7 Mio. € in *Scenario 1* to 15.7 Mio. €, 26.5 Mio. € and 28.7 Mio. € in the other three scenarios. With 100% DER penetration in *Scenario 4*, the prices between all investigated scenarios range between 15.0 Mio. € with tariff  $C_{LF}$  and 103.8 Mio. € with tariff  $E_r - mv$ .

In all investigated scenarios, there is a high share of the reinforcement costs in the LV. In the base case of *Scenario 4*, 86% of the costs occur in the LV, 13% for MV/LV-transformers and 1% in the MV within all six grids. The reduction potential with capacity-based tariffs thus mainly lies in the LV. With increasing costs for other tariffs, the share of costs in the higher grid levels increases, reaching up to 32% of costs in the MV and 21% for MV/LV-transformers with tariff  $E_c S_r$  in *Scenario 4*. The previously mentioned difference in reinforcement costs for tariffs  $E_r$  and  $E_r - mv$  in *Scenario 3* mainly stems from the MV, supporting the hypothesis that the different price time series in  $E_r$  limit the synchronisation of loads to a certain extent.

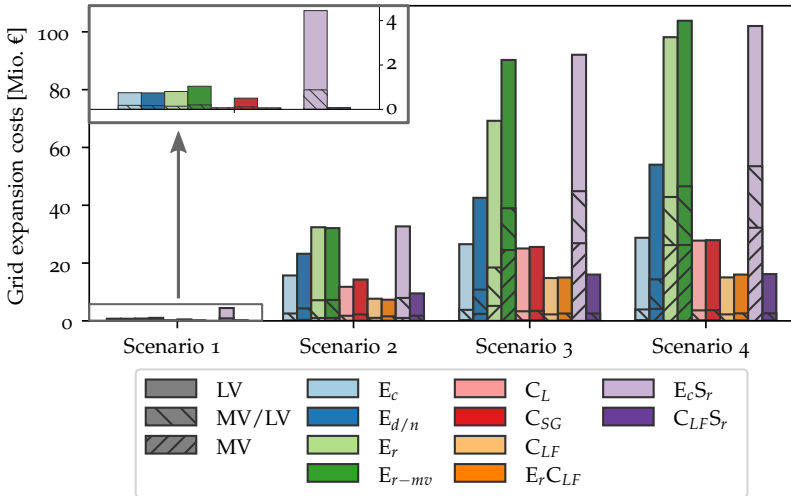


FIGURE 17.14: Grid reinforcement costs in investigated grids and scenarios with different tariff structures.

### 17.3.4 Temporal Flexibility Needs

Next, we investigate the influence of the different tariff options on the temporal flexibility needs of a fully renewable German energy system powered by PV and wind only. Fig. 17.15 displays the temporal flexibility needs in terms of energy shifting on different time scales for the investigated tariffs and scenarios for entire Germany. Again, the difference is small in *Scenario 1* with low penetrations of DERs, ranging from -4.4 % for  $E_c S_r$  and  $C_{LF} S_r$  to 1.5 % for tariff  $E_{d/n}$ . Negative values thereby indicate a reduction, and positive values indicate an increase in total shifted energy. Changes mainly occur in short-term shifting and, to a small extent, in medium-term shifting. The long-term flexibility needs remain constant over all simulated tariffs and scenarios. The differences between the tariffs increase with growing shares of DERs. In the extreme *Scenario 4*, where all residential loads are equipped with all investigated DERs, the change in total shifted energy compared to the base case ranges between -12.2 % for tariff  $C_{LF} S_r$  and 10.9 % for  $E_{d/n}$ .

The total shifted energy increases with increasing penetrations of DERs, from 143.4 TWh in *Scenario 1* to 164.5 TWh, 184.1 TWh and 189.3 TWh in *Scenarios 2 to 4*, which can be explained by the additional load by EVs and

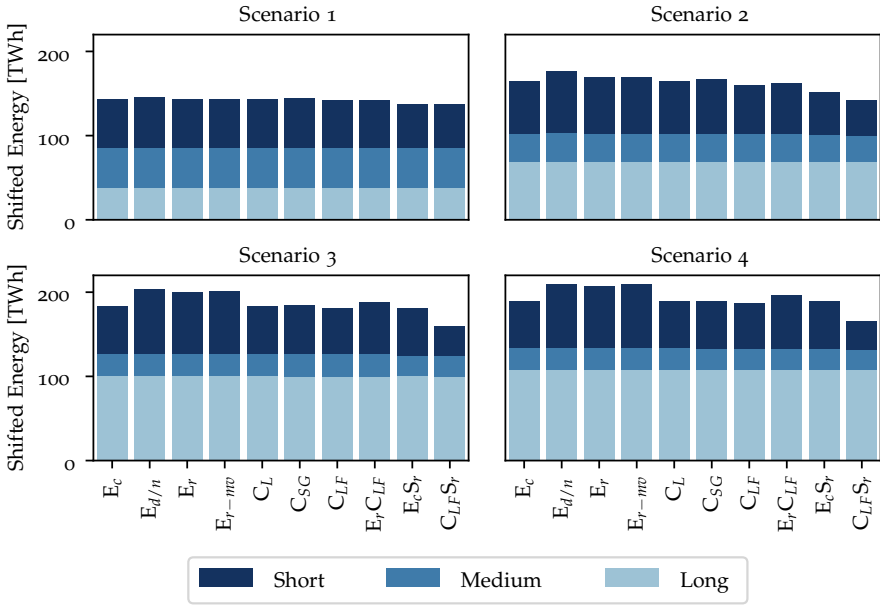


FIGURE 17.15: Storage equivalents in investigated grids and scenarios with different tariff structures.

HPs and additional PV feed-in which needs to be shifted. Furthermore, the share of energy shifted long-term increases between the scenarios. This effect can be explained by the increasing shares of HPs, which lead to additional long-term shifting with the current mix of PV and wind (see Section 13.3.2). The reduction potential being mainly in the short-term shifting is in line with the previous investigations where DFO could only significantly reduce medium-term shifting when shifting between standing times was allowed for EV charging (see Section 13.3), which is not the case in the given setup.

### 17.3.5 Implications for Consumer Costs

Lastly, we want to showcase the effects of the investigated electricity tariffs on costs paid by the different consumer groups. In the following, we therefore investigate the network tariff costs and the suppliers' cost paid by the different consumer groups in the four scenarios with increasing penetrations of DERs. The results show that the total costs paid by all

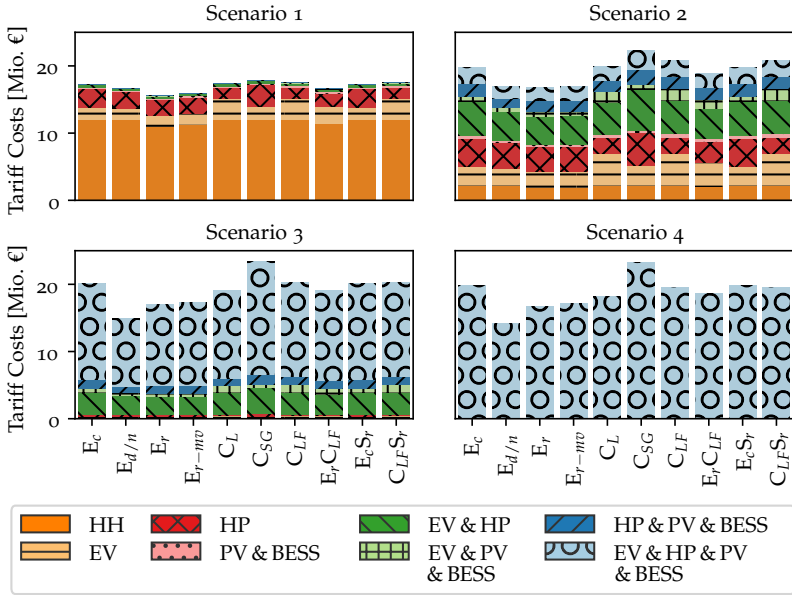


FIGURE 17.16: Network tariff costs paid by different consumer groups in the simulated scenarios.

consumers and the division of costs covered by the different consumer groups differ between the investigated tariff options and scenarios.

### Network Tariff Costs

We first focus on the costs for the network tariffs in Fig. 17.16. In *Scenario 1* (upper left), a large share of the network tariff costs is paid by inflexible households (HH), which are also the largest group in this scenario with 73 % of all residential consumers (see Fig. 17.3). For all tariffs, the inflexible consumers pay less relative to their group share, covering between 66.5 % and 71.2 % of the total network tariff costs. Even though the tariffs are designed in a way that the inflexible customers should pay the same, the costs for this group are lower for the tariffs based on the grid residual load  $E_r$  and  $E_{r-mv}$ . The reason is that the costs were scaled individually for each cluster, accounting for all simulated consumers. In the scenarios, the consumers are assigned to different clusters, which does not necessarily result in the same distribution of customer profiles for each cluster and thus leads to the observed deviations. In reality, the tariffs would need to

be scaled to recover the costs in any case. As tariffs  $E_r$  and  $E_{r-mv}$  lead to relatively high reinforcement needs, inflexible consumers would also have to pay more to cover these costs than with other tariffs that lead to lower reinforcement needs.

In *Scenario 1* and *Scenario 2*, the tariffs with time-varying energy-based tariff components lead to a reduction of total network tariff costs paid by the consumers compared to the base case of the constant energy-based tariff  $E_c$ . On the other hand, capacity-based tariffs lead to an increase in total paid costs. With higher flexibility in *Scenario 3* and *Scenario 4*, the total paid costs also slightly decrease for the capacity-based tariffs except for the segmented tariff  $C_{SG}$ , which still leads to a significant increase in total paid tariff costs. The cost reduction is still higher for the time-varying energy-based tariffs than capacity-based ones, implying that flexible consumers can better optimise against the simulated energy-based tariffs than the capacity-based ones. These trends are exactly opposite to the influence of the tariffs on the grid reinforcement costs, which would have to be covered by the paid network tariffs. Capacity-based tariffs lead to a reduction, while energy-based tariffs lead to an increase in the grid reinforcement costs. The resulting costs for inflexible consumers would therefore increase for the time-varying energy-based tariffs and decrease for tariffs with capacity-based components. This customer group is specifically interesting since they do not contribute to increasing grid reinforcement costs. They should therefore not be burdened excessively with any of the tariffs, which could be the case for time-varying energy-based tariffs.

The higher paid costs for the segmented tariff  $C_{SG}$  are mainly caused by the deployment of HPs. These lead to higher consumption, especially in winter when less PV generation occurs for self-consumption. In these times, reducing the total household consumption to the cheaper segments is often impossible, causing higher total costs. This tariff should therefore be adapted in future investigations to maintain accurate incentives for consumer groups owning HPs. A seasonal variation could thereby also be considered.

The effects of the tariffs on the different consumer groups are best visible in *Scenario 2*, where all consumer groups are equally large (see Fig. 17.3). Differences in costs paid by the consumer groups in Fig. 17.16 (upper right) can therefore be directly attributed to the tariffs. One effect is that consumers owning PV and BESS (also in combination with other DERs) pay significantly less than the other groups with all the simulated tariffs.

Other effects are higher costs for the group of EV owners with the capacity price component on load, and higher costs for the group of HP owners under the segmented tariff.

The simulated consumers and DERs display different consumption profiles, and the observed effects might not be homogeneous for the whole group. Furthermore, in the future, consumers might choose between different tariff options. Therefore, we investigate which share of the simulated pool of consumers would choose which tariff option, assuming an economically rational choice. Figure 17.17 displays the share of the 500 simulated consumer profiles that would choose a certain tariff option with the investigated tariff designs (excluding the variations with time-varying suppliers' costs since the focus is on the network tariff price component). The values are displayed for inflexible households (HH) and households equipped with different combinations of DERs.

While inflexible consumers (HH) are divided between the residual load based energy tariff  $E_r$ , the segmented tariff  $C_{SG}$ , the capacity tariff on peak load  $C_L$  and a small share of the constant energy-based tariff  $E_c$ , most combinations with DERs show only one or two predominantly chosen tariff options. One reason is that the tariffs are designed so that inflexible consumers (HH) pay the same. If equipped with one or more DERs, their characteristics change, making certain tariff options more attractive than others. For example, EVs show a relatively high peak-to-energy ratio, thus leading to the preferred choice of an energy-based tariff  $E_r$ . On the other side, HPs have comparably low peak-to-energy-ratio, leading to a strong preference towards the capacity-based tariff on load peaks  $C_L$ . With the combination of both (EV & HP), the economical choice seems to depend on the sizing of both technologies with similarly large shares choosing the energy-based tariff  $E_r$  and the capacity-based tariff on peak load  $C_L$ . Additionally, a smaller share prefers the day and night tariff  $E_{d/n}$ .

Households only equipped with a PV system (without BESS) largely prefer the segmented tariff  $C_{SG}$  with two-thirds of the households. The remaining third chooses the day and night tariff  $E_{d/n}$ . PV produces electricity during the day, thereby naturally reducing daytime demand, which causes higher costs for the day and night tariff. Similarly, for residential loads, the consumption is usually higher during the day, causing higher costs for the segmented tariff, which PV can effectively reduce. The day and night tariff seems to become more attractive for the combination of different DERs. This effect implies that even when given the choice between different tariff

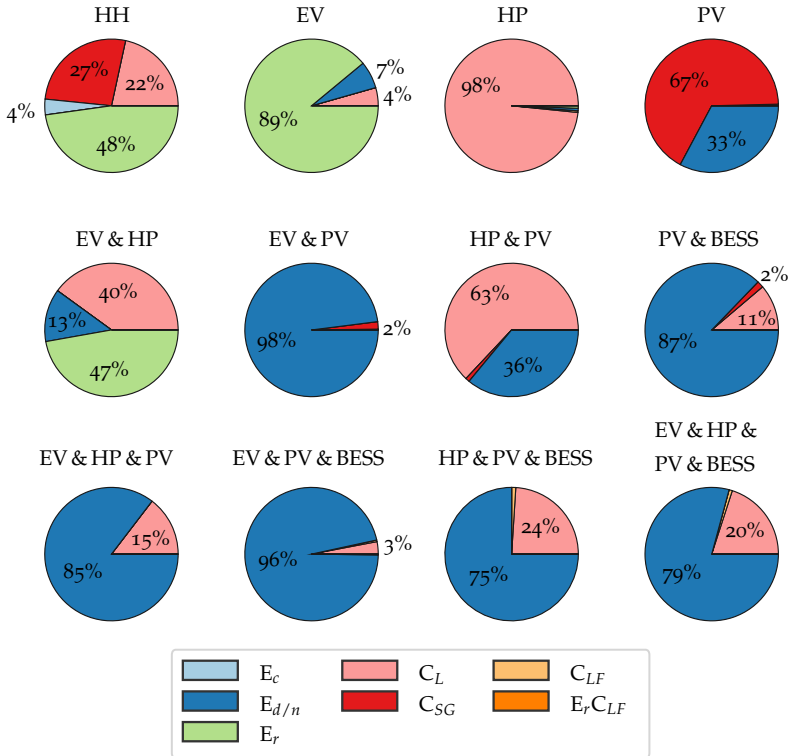


FIGURE 17.17: Share of economically optimal network tariffs for simulated 500 customers equipped with different combinations of DERs. For clarity, shares of  $\leq 1\%$  are not displayed.

options, consumers of the same type might choose a similar tariff. With the day and night tariff, a tariff is preferred for high penetrations of DERs that increases both geographic and temporal flexibility needs (see Table 17.3).

Naturally, the economical choice of a network tariff depends on the specific configuration and price values chosen for the different tariffs. In our study, they are chosen so that, over all 500 simulated consumers, the mean costs for inflexible consumers are constant. The observed tendencies therefore only apply in this case. If consumers with DERs were given different tariff options than inflexible consumers, the observed effects are no longer valid. However, we would argue that DSOs will try to offer the same

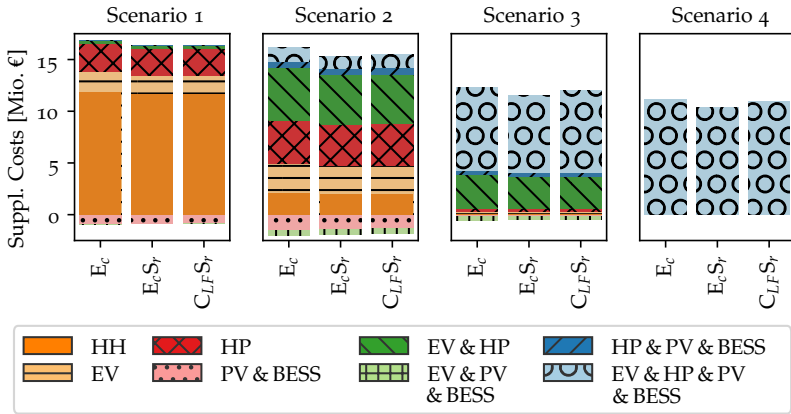


FIGURE 17.18: Suppliers' cost paid by different consumer groups in the simulated scenarios.

tariff to consumers. Therefore, the discussed results still show interesting tendencies and highlight the risk that consumers with similar characteristics tend to choose the same tariff option, which might lead to synchronised consumption behaviour.

### Suppliers' Costs

For suppliers' cost in Fig. 17.18, only the constant energy-based tariff  $E_c$  and the tariffs with time-varying suppliers' cost are displayed since the results of the other investigated tariffs largely resemble the ones of tariff  $E_c$ . The results show that owners of PV systems with BESS partly show negative values. This means that they produce more electricity than they consume, selling the excess electricity and thus displaying net revenues. It implies that the PV systems are oversized for households without HPs. If these are included, the suppliers' costs show positive values. With increasing penetrations of DERs in the different scenarios, the total suppliers' cost paid by the consumers decreases even though the electricity consumption by EVs and HPs increases. At the same time, PV deployment increases, leading to higher self-consumption and, thus, less electricity drawn from the grid. With time-varying suppliers' costs, flexible consumers generally seem to pay less since they optimise for low prices.

Lastly, we investigate the economically rational choice of electricity tariffs including the investigated network tariffs and suppliers' cost in Fig. 17.19.

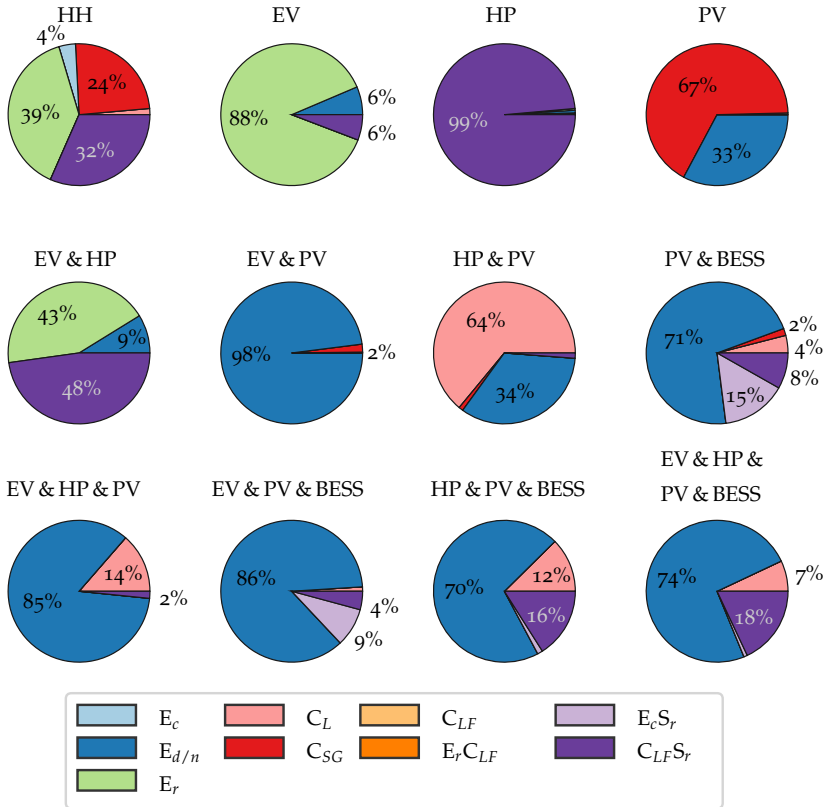


FIGURE 17.19: Share of economically optimal electricity tariffs for simulated 500 customers equipped with different combinations of DERs. For clarity, shares of  $\leq 1\%$  are not displayed.

The results show that for most investigated groups, a certain share of the simulated 500 consumers prefers the electricity tariffs with time-varying suppliers' costs  $E_c S_r$  and  $C_{LF} S_r$ . Exceptions are groups that own a PV-system without BESS (PV, EV & PV, HP & PV, EV & HP & PV), for which either no consumers choose these tariffs or a very small share  $\leq 2\%$ . The tendency is that the consumers that would choose the capacity-based tariff on peak load as a network tariff (see Fig. 17.17) switch to the combination of time-varying suppliers' costs and capacity network tariff on peak load and feed-in  $C_{LF} S_r$ . For example, tariff  $C_{LF} S_r$  is the cheapest option for almost the entire group of HP owners. This effect implies that the time-varying

suppliers' cost is more attractive than the constant cost with the same mean value. When HP owners additionally own a PV system without BESS, they stick with the capacity-based network tariff on load peaks with constant suppliers' costs  $C_L$ . The reason is that the PV remuneration also follows the time-varying suppliers' cost, and prices are lower in times of high PV feed-in. The losses of PV revenues thus seem to be higher than the savings potential by lower costs for consumption. For consumers owning PV with BESS, the largely preferred option is still the day and night tariff with constant suppliers' costs  $E_{d/n}$  with  $\geq 70\%$  for all these groups. However, it has to be mentioned that we did not consider combinations of time-varying energy-based network tariffs and suppliers' costs. It can be assumed that in this case, consumers opting for  $E_{d/n}$  would change to  $E_{d/n}S_r$ .

### 17.3.6 *Limitations and Future Research*

While we cover a wide range of tariffs and investigate various aspects of electricity tariffs and their effects on consumption profiles, we use simplifying assumptions that might impact the results. In the following, we want to discuss these and provide areas for future research.

In our model formulation, late EV charging is penalised to mimic the range anxiety of EV owners. This formulation might overestimate the synchronisation of EV charging and lead to excessively high peaks. The height of the peaks highly depends on the user preference represented by the penalty term  $pen_{ev}$  and the length of the low-price period. The longer the times of low prices and the lower the user's discomfort in charging later, the less pronounced the synchronisation effect will be. Similarly, all HPs of the same technology share the same COP time series and have a similar heat demand in our investigations. These result in similar consumption profiles and peaks at high COP values and low prices. In reality, the heat demand would differ, and simultaneities might be lower. Nevertheless, the synchronisation of flexible demand with time-varying prices poses a realistic threat of increased stress on the grid and has been reported and discussed in various previous studies and trials (e.g. [227]–[229]). The underlying trends of our results are therefore still valid, even though the increase in peak load and grid reinforcement might be overestimated.

On the other hand, the observed synchronisation effects will likely increase with increasing flexibility, e.g. by allowing vehicle-to-grid (V2G). To estimate the effects of network tariffs in real-world applications, it is therefore

crucial to determine the willingness of users to adapt their behaviour. Digitisation and the widespread use of intelligent EMSs, as we assume in our study, will likely increase the willingness to participate in such schemes. A situation where the penetration of flexibility options is still low in the distribution grids (DGs) would offer the opportunity to learn about consumers' reactions to different incentive schemes without risking severe negative effects from undesired synchronisation. Field trials evaluating the effects of the investigated tariff options in a real-world setting would therefore be an interesting extension of this work.

Furthermore, we model the extreme cases where all consumers adopt the same tariff. While this is an interesting edge case to estimate the maximum effect of different electricity tariffs, it is unrealistic. In the real world, consumers can choose between different tariff options, resulting in a diversification of consumer responses. It was shown that the free choice between different dynamic (energy-based) electricity tariffs lead to a release of stress in a LV distribution grid [230]. However, only an intermediate penetration of DERs was modelled, and our results imply that with increasing flexibility, the rational choice of electricity tariff might be similar for a large share of the flexible consumers. The effect of mixed tariff choices should therefore be further examined in future investigations.

We do not account for a mix of time-varying suppliers' costs and time-varying energy-based network tariffs in the investigated electricity tariffs. It was shown that the positive effects of different network tariffs were reduced when consumers were reacting to spot prices and that energy-based network tariffs were influenced more than capacity-based charges [231]. We therefore do not expect such tariffs to perform well. Similarly, we did not account for critical peak pricing. In a recent study, this design was shown to have little effect [232], stressing the complexity of setting incentives right with this approach. It would nevertheless be interesting to expand the investigation on this concept as it is widely discussed. Furthermore, the grid-based energy charges could be improved. The investigated number of clusters was too low to adequately reflect the situation in the LV grids. Higher differentiation might improve the effect of this price component, and a combination with capacity charges might further decrease the necessary reinforcement and smoothen the system's residual load. Similarly, the segmented tariff was not adjusted to increasing load with EVs and HPs, which is why this tariff did not perform well for high DER penetrations. Furthermore, the segmented tariff could be expanded to also apply to local PV feed-in, giving incentives to smooth the feed-in in addition to the load.

The efficacy of capacity-based price components on load and feed-in to reduce grid reinforcement costs proved to be dependent on whether load or feed-in peaks are the main driver for grid reinforcement. In the investigated scenarios, all DERs were adopted at the same rate. In future investigations, it would be interesting to vary the rates between EVs, HPs, PV and BESS to get a better understanding of the interplay of the tariff options with the different DERs and their uptake.

Lastly, we do not account for costs associated with using flexibility. While it can be argued that the marginal costs for flexibility utilisation are low, the investment costs for the EMS would have to be recovered by the cost savings achieved by flexibility procurement. In a recent study, it was shown that a majority of users opted for the investment in an EMS with most tariffs [232]. However, not all investigated tariffs were covered in that study. So, in future investigations, the influence of the tariffs on investment decisions on EMSs and DERs could be included.

#### 17.4 CONCLUSION

We investigated the influence of different electricity tariff components on the consumption behaviour of prosumers and resulting geographic and temporal flexibility needs by applying these to six differently composed grids. The geographic flexibility needs were determined regarding the required distribution grid reinforcement and the resulting costs. Temporal flexibility needs were measured by required energy shifting in a fully renewable German power system. Prosumers with different combinations of PV-systems, BESS, EVs and HPs were modelled by a cost-minimising optimisation to model their reaction to the investigated tariffs. Flexibility options available to them were PV curtailment, BESS and smart operation of EVs and HPs.

Our results show that using the modelled flexibility options decreases the need for grid reinforcement if network tariffs are set efficiently. However, network tariffs can also have the opposite effect. Time-varying energy-based tariffs led to a synchronisation effect, drastically increasing grid reinforcement costs in scenarios with high DER penetrations. On the other hand, a capacity charge on peak load encourages consumers to decrease their peak loads, and thus, the grid-straining peaks are reduced. This price component can also effectively counteract the synchronisation effects observed for time-varying energy-based prices. With increasing penetrations of de-

centralised PV, capacity components on peak feed-in become increasingly important. Together with a capacity component on load, they can reduce the grid reinforcement costs by 47.7% in the extreme scenario where every household owns a PV system with BESS, HP and EV.

The temporal flexibility needs depend more on energy-based than on capacity-based price components. On their own, the capacity-based price components show little effect on the required energy shifting. The time-varying energy-based price components depend on their design and the penetration of DERs. If not aligned with the residual load, such prices increase temporal flexibility needs. For low to intermediate penetrations of DERs, prices based on the residual load can reduce the required energy shifting. However, with high DER penetrations, there is an overshoot effect, and the temporal flexibility needs increase. In this case, the peak load and feed-in capacity components can positively counteract the high peaks. For the scenario with the highest DER penetration, the combination of residual load based suppliers' costs and capacity prices on peak load and feed-in achieves the highest reduction of temporal flexibility needs with 12.2%. Overall, this tariff proved to be the most promising one, reducing both temporal and geographic flexibility needs.

Our investigations showed that incentives given by electricity tariffs can reduce geographic and temporal flexibility needs and thus contribute to their supply. However, purely energy-based tariffs with temporally resolved incentives bear the danger of high new peaks and thus increase flexibility needs, especially at high DER penetrations. Therefore, we recommend including capacity-based price components in future electricity tariffs to counteract these effects. In future investigations, the effects of consumers choosing different tariff options should be included since that might reduce the simultaneity and, thus, newly created peaks. Furthermore, our results imply that with increasing flexibility, it might be beneficial that end customers directly participate in the market instead of acting as price takers. The interplay of concepts allowing this, e.g. through aggregators, with different price components would be an interesting path for future research. Lastly, the choice for a good electricity tariff depends not only on their effects on geographic and temporal flexibility needs but also on various other factors, e.g. fairness aspects. In the next chapter, we therefore develop and apply an evaluation framework for tariffs, where such other goals are also included in the final decision.



EVALUATION OF TARIFF DESIGNS

---

*The content of this chapter is based on the published paper: A. Heider, J. Huber, Y. Farhat, Y. Hertig and G. Hug, "How to choose a suitable network tariff? - Evaluating network tariffs under increasing integration of distributed energy resources", Energy Policy, Vol. 188, 2024, DOI: 10.1016/j.enpol.2024.114050 [233].*

©2024 The Authors. Published by Elsevier Ltd.

*The interviews, criteria identification and weighting were conducted by Jill Huber in her master thesis [234] that was supervised during this PhD research. For completeness, the interviews, criteria identification and weighting are still included in the following chapter but were not the contribution of the author. The original case study is replaced with more realistic input data from the previous chapter, investigating more complex tariffs, including flexibility from heat pumps and electric vehicles and providing data for individual consumers instead of customer groups.*

In a changing power system with increasing penetrations of distributed energy resources, traditional network tariffs might not be able to meet the underlying requirements. Therefore, it is necessary to assess suitable alternatives. We propose a new two-stage process and evaluation framework to support an informed decision process and test them in a Swiss environment. In the first stage, stakeholder interviews determine the relevant design criteria. In the second step, these are translated into a quantitative evaluation framework. The single indicators are weighted by expert weighting, following the analytic hierarchy process, to arrive at the final ranking. The application in a case study shows that the final ranking of the examined tariff structures depends on expert weighting. It is therefore vital to work on a shared understanding of the importance of the different criteria. Moreover, in a scenario with high shares of distributed energy resources, tariffs including capacity-based price components on average outperform the standard volumetric tariff. This result stresses the importance of adapting network tariffs for a future power system with high penetrations of

distributed energy sources. Our open-source evaluation tool<sup>1</sup> can help with an informed and transparent decision process.

The remainder of the chapter is structured as follows: **Section 18.1** presents the proposed two-stage process with the identification of relevant criteria in **Section 18.1.1** and the translation into a multi-criteria decision analysis (MCDA) evaluation framework in **Section 18.1.2**. In **Section 18.2**, we apply the proposed framework to a case study and present and discuss the results in **Section 18.3**. **Section 18.4** translates the findings into conclusions and policy recommendations.

## 18.1 RESEARCH DESIGN

Fig. 18.1 gives an overview over the two-stage process proposed in this work. In the first step, the relevant criteria are extracted from stakeholder interviews. In the second step, we define quantitative evaluation indices for the extracted criteria in an iterative process. In both stages, relevant stakeholders are involved. As the second stage depends on the outcome of the first stage, the results of stakeholder interviews are presented as part of this section. All mathematical symbols relevant to this chapter are summarised in Tab. B.3 and Tab. B.5 in the appendix.

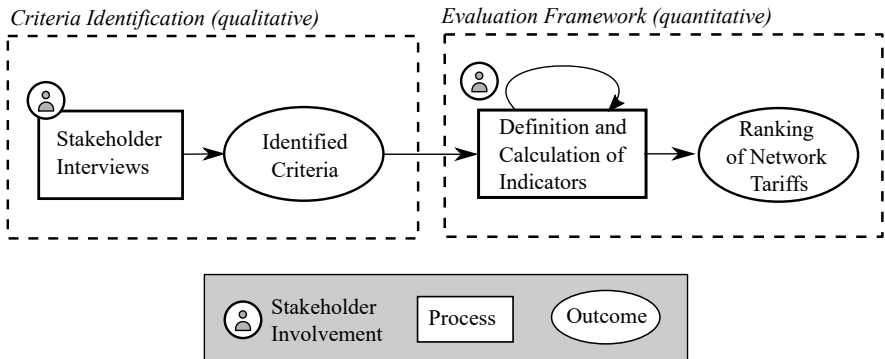


FIGURE 18.1: Two-stage process to define evaluation framework for network tariffs.

<sup>1</sup> Available at: <https://github.com/AnyHe/EFf-NeTs>

### 18.1.1 *Identification of Relevant Criteria*

In the following, the first stage of the proposed process is introduced. The first part describes the applied method of stakeholder interviews, followed by a discussion of the extracted design criteria for network tariffs.

#### *Stakeholder Interviews*

As many different stakeholder groups are involved in the design of network tariffs, capturing their different perspectives and objectives is crucial. Therefore, we choose semi-structured interviews with representatives of relevant stakeholder groups, which allows the interview partner to address unexpectedly relevant topics [235]. Semi-structured interviews are characterised by following an interview guide. The guide consists of questions and topics to be addressed but leaves room to address further topics based on the interviewee's answers.

In our work, we conducted five online interviews with stakeholder representatives from Swiss entities. The interviews were conducted in March and April 2022, each lasting one hour. The interview guide consisted of the following questions:

1. In your view, what is the task of network tariffs?
2. What incentives should be set with network tariffs? Is there any prioritisation?
3. What conditions need to be considered when designing network tariffs? What are the regulatory framework conditions for network tariff design? How would you assess customer requirements?
4. To what extent are the conditions and requirements for network tariffs changing under the increased integration of distributed energy resources?
5. Are there differences between the requirements for tariffs for consumers and (distributed) producers or storage systems?

To cover different aspects of the requirements of network tariffs, we choose respectively one representative of each of the following stakeholder groups as interview partners:

THE AUTHORITY defines all the legal requirements for the network tariff design.

**POLITICS** gives input within this process of formulating network design principles.

**THIRD PARTY**, analogue to politics, provides opinions and remarks in defining legal requirements.

**DSOS** are responsible for setting and eventually charging the network tariffs.

**THE REGULATOR** is responsible for checking the costs charged by network tariffs on their conformity with the legal requirements.

The stakeholder group of end consumers is not chosen as an interview partner as we focus on stakeholders involved in the definition and implementation of new network tariff structures. Still, end consumers who pay the network tariffs are an important group when it comes to the design of network tariffs. Therefore, the motivation and needs of end consumers are addressed in the interviews conducted with the other stakeholders.

After conducting the interviews, the relevant design criteria for network tariffs must be extracted. Therefore, we transcribe, code and interpret the interviews. Intelligent verbatim transcription is used, as presented by Dresing and Pehl [236]. It is transcribed verbatim, but filler words, pauses or stuttering are omitted or smoothed out. Dialects, such as different variations of Swiss German, are translated into High German.

For coding and condensation, the statements of the interview partners are categorised by assigning keywords to text segments [237]. The keywords assigned to text segments consist of critical statements made by the interview partners on evaluation criteria and network tariff structures, such as “customer acceptance” or “cost reflection”. These coded transcripts are then summarised following the lead questions of the interview guide. Each summary includes a sketch of general conditions and objectives of network tariffs mentioned by the interview partner. To ensure that the statements are summarised correctly, the interview partners were asked to proofread the interview summaries. Their feedback was then integrated into the final summaries.

Last, the statements given in the interviews are interpreted to identify relevant network tariff requirements. Interpreting the statements consists of structuring the apparent meaning of what was said and a deeper and applied interpretation concerning the research question [237]. The most

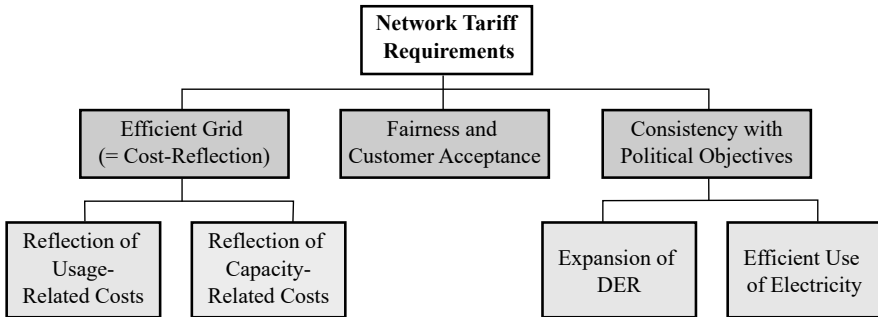


FIGURE 18.2: Identified criteria through stakeholder interviews.

addressed and highlighted network tariff requirements are summarised and defined from all statements.

Since five interviews might not be enough to capture the full variety of perspectives in network tariff design, we compare the outcomes of the interviews with previous literature in the field and current regulations. Additionally, a preliminary framework of criteria obtained by a literature review was discussed at the end of the interview process to converge towards one coherent framework. Furthermore, this study mainly aims to prove the applicability of the proposed process and showcase a possible application. The developed framework should therefore be seen as a basis for further development and refinement since the criteria and their importance can also differ depending on the local application.

### *Identified Criteria*

Figure 18.2 shows the most prominent network tariff requirements to be considered as criteria in network tariff design, which result from the interviews conducted with the representatives of the relevant stakeholders. These criteria are described in more detail below. In addition to these criteria, technical and regulatory feasibility are also relevant for implementing a tariff structure. However, both are more prerequisites than design criteria and therefore not included in the evaluation framework but considered in the discussion of the results.

The representatives interviewed agreed that the main task of network tariffs is covering the costs of the electricity grid. This is also generally stated in the literature [201], [202]. Literature has proposed indicators to measure the

expected deviation between costs and revenues [201], [202] as well as its variance [202]. However, every tariff structure can be designed to recover the costs by adjusting the price components. Over- and under-recoveries are compensated and balanced out in subsequent years [238]. The fulfilment of cost-recovery is thus assumed as an underlying condition for network tariff design and not a decision criterion. However, the stability of income and the influence of uncertainties in terms of costs and revenues can still differ with the type of tariff. Depending on the size and cash flow availability of the distribution system operator (DSO), it might become a relevant criterion. This factor is not included in this work but could be added as an extension in future work (e.g. as proposed in [202]).

### *Efficient Grid (= Cost-Reflection)*

While covering the costs incurred, network tariffs should provide incentives for an efficient grid. All representatives of the different stakeholders agreed that an efficient grid is to be achieved with the signals through network tariffs, avoiding unnecessary costs and minimising the grid cost incurred. Therefore, network tariffs should incentivise grid-supportive behaviour by the end customers. To achieve this, the tariffs that end customers pay should reflect the cost they impose on the system. According to all the stakeholders, it is the most important criterion that network tariffs are cost-reflective. Further, it is mandated by Swiss and EU law [239], [240] and thus taken into account by various studies on network tariff design (e.g. [202], [241]). Especially with the increased integration of distributed energy resources (DERs), the reflection of the costs is of high relevance, as resources such as electric vehicles (EVs), heat pumps (HPs) and photovoltaics (PV) systems can cause large load peaks, driving the grid costs [241], [242].

The difficulty lies in establishing the cost contribution of a consumer [202]. The conducted interviews with the relevant stakeholders show that there are differing opinions on how to design network tariffs in order to be cost-reflective. While some state that tariffs should account for the costs imposed on the system through aggregated load peaks and therefore real-time usage, others state that tariffs should primarily reflect the fixed costs for providing the available capacity at the grid connection point. The aggregated load peaks are thereby relevant for the costs in the higher grid levels while the contracted capacity is the main cost driver in lower grid levels. Therefore, this criterion is divided into two sub-criteria, the reflection of usage-related costs and the reflection of capacity-related costs. Both reflect long-term

marginal costs, i.e. the costs for operating, maintaining and expanding the network infrastructure. Other cost factors are short-term marginal costs, like losses [202], and fixed costs. In the interviews, they were not seen as relevant design criteria and the share of short-term marginal costs in the overall costs is rather low [206], [243]. However, in the future, if electricity costs are rising, these costs might increase and become a more relevant factor. In this case, the short-term marginal costs could be included as an additional criterion in future work.

### *Fairness and Customer Acceptance*

From the interviews with the representatives of the stakeholders, it can be noted that the fairness of network tariffs and their customer acceptance are essential criteria that need to be taken into account when designing network tariffs. Network tariffs should not favour or discriminate against anyone. The understandability and comprehensibility of network tariffs should be guaranteed for everyone, irrespective of their level of education and expertise, one reason being that good comprehensibility of the tariff can increase customer acceptance. Customers should also not be disadvantaged because of their financial resources; therefore, network tariffs should be affordable. Particularly with the trend towards the increased integration of DERs, customer groups with assets to meet their own electricity demand are growing, enabling them to optimise their consumption from the grid and thus save on grid costs. Network tariffs should consider that people who do not have these possibilities due to their living situation or financial resources are not disadvantaged.

Fairness and customer acceptance were mentioned in relation to each other in the interviews. Similar to the criterion of an efficient grid, they could also be further divided into two different sub-criteria. However, both factors are highly interconnected and influence each other. It has been shown that policies are more accepted if they are perceived to be fair [244], [245] and that fairness is an important factor in public engagement [245]. With the criterion, we mainly want to measure how likely customers are going to participate in a new tariff scheme. For these reasons, fairness and customer acceptance are defined as a single criterion in the following.

Again, this criterion is mandated by the Swiss and EU law [239], [240] and widely discussed in the literature. It is immensely subjective and difficult to quantify. Nevertheless, also in the literature, it is generally agreed that

fairness and customer acceptance are relevant criteria for the design of network tariffs [201], [241], [242].

### *Consistency with Political Objectives*

From the interviews, network tariffs should be consistent with political energy objectives. While they do not have to facilitate these political objectives, they should also not hinder them. In addition to the phase-out of nuclear energy, the expansion of renewable energies and the increase in energy efficiency are the most important measures of the Swiss Energy Strategy 2050 [246], approved by the Swiss population in 2017. Energy efficiency includes not only the reduction of energy consumption but also the electrification of the heating and transport sectors and thus an increase in DERs such as heat pumps and residential batteries.

Article 14, paragraph 3 and letter e of the Electricity Supply Act states that “network tariffs must take into account the objective of efficient [...] use of electricity” [239]. Furthermore, the Electricity Supply Ordinance stipulates the corresponding implementation with the aid of a non-degressive volumetric component (in Rp./kWh) of at least 70 % of the total network tariff costs [247]. The regulatory framework for network tariffs shows that, already nowadays, political objectives are taken into consideration within the design of network tariffs. Therefore, we define consistency with political energy objectives as a relevant criterion for network tariff design. A distinction is made between two sub-criteria when it comes to political objectives: the expansion of DERs, such as PV systems, heat pumps and batteries, and the efficient use of electricity.

#### *18.1.2 Evaluation of Network Tariff Structures*

In the first stage, we determined relevant design criteria for network tariffs. To find the most suitable tariff option based on these criteria, we translate them into a coherent evaluation framework. For this, we propose the use of a MCDA based on the weighted sum method [219]. The proposed framework thereby combines weights determined with the analytic hierarchy process (AHP) [248] with newly defined performance indicators. Overall, the proposed MCDA is inspired by the AHP, which is based on a linear hierarchical structure of the problem, including criteria, sub-criteria and alternatives. Fig. 18.3 shows the hierarchical structure of the proposed framework. In contrast to the AHP, the lowest level of the hierarchy is

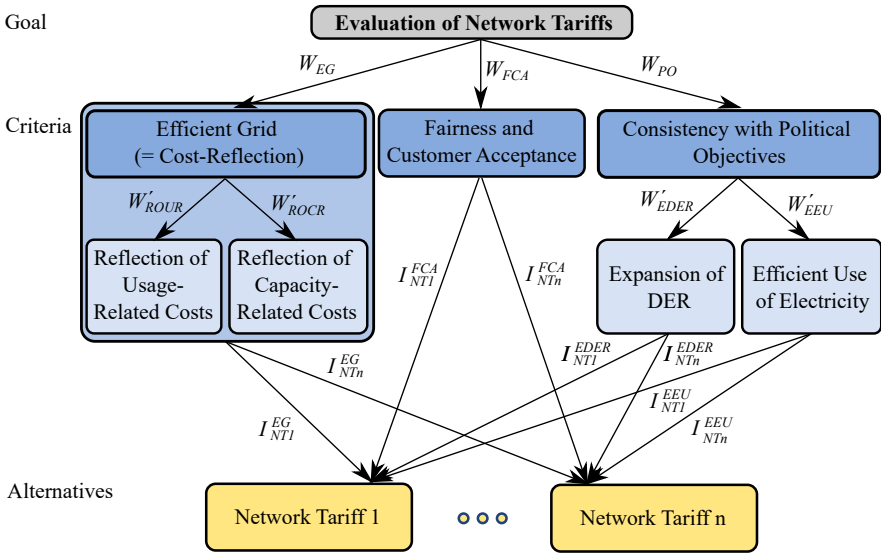


FIGURE 18.3: Hierarchical structure of the evaluation of network tariff structures as basis for the MCDA.

replaced with quantitative performance indicators instead of pairwise comparisons.

The criteria of an efficient grid ( $EG$ ), fairness and customer acceptance ( $FAC$ ) and consistency with political goals ( $PO$ ) are treated as independent criteria. For the efficient grid, the sub-criteria for the reduction of usage- and capacity-related costs are defined as sub-criteria but integrated into the criterion of an efficient grid  $EG$  as both are closely related. For the criterion of consistency with political goals ( $PO$ ), on the other hand, the sub-criteria for the expansion of DERs ( $EDER$ ) and efficient use of electricity ( $EEU$ ) are independent of each other and therefore treated as separate sub-criteria.

To conduct the overall ranking  $I_{NT}$  of the tariff structures, the weights and performance indicators towards all evaluation criteria  $EC = \{EG, FAC, EDER, EEU\}$  are combined according to:

$$I_{NT} = \sum_{i \in EC} W_i * I_{NT}^i, \tag{18.1}$$

where  $W_i$  is the importance of criterion  $i$  on the first level of the hierarchy and  $I_{NT}^i$  is the alternative's performance towards the criterion  $i$  on the second level of the hierarchy. The higher the overall importance  $I_{NT}$ , the higher the tariff structure  $NT$  in the final ranking.

### *Level I: Weighting of Criteria*

The weighting of the criteria is used to indicate the importance of the respective criterion to the overarching goal, in this case, the evaluation of network tariffs. Since there are no quantitative measurements of the criteria's importance regarding the overall goal, their priorities are assessed with the help of subjective judgements of experts [249]. First, a **pairwise comparison matrix** denoting the relative importance of the criteria relative to each other is constructed [248]. To then analyse the pairwise comparisons and determine the importance of each element at each level of the hierarchy, the AHP suggests using the **eigenvalue method** [248]. Filling out an entire matrix of pairwise comparisons can improve the validity of people's judgements that tend to be inconsistent [250]. Applying the eigenvalue method therefore encourages consistency, and we additionally calculate a consistency ratio (CR) that guarantees a certain consistency of the expert's judgement [251].

Similar to the main criteria, there is also no quantitative measurement for the relative importance of the sub-criteria of consistency with political objectives. We therefore propose to fill out two pairwise comparison matrices for the comparison of the main criteria (efficient grid, fairness and customer acceptance, consistency with political objectives) and sub-criteria of consistency with political objectives (expansion of DER, efficient use of electricity). An example of the pairwise comparison matrices filled out by the DSO representative can be found in Tab. 18.1 and 18.2.

The weights of the sub-criteria of expansion of DERs  $W_{EDER}$  and efficient electricity usage  $W_{EEU}$  are calculated by multiplying the weight of the main criterion of consistency with political objectives  $PO$  with the weights of the sub-criteria:

$$W_j = W_{PO} \cdot W_j' \quad \forall j \in \{EDER, EEU\}. \quad (18.2)$$

The AHP enables the decision maker to combine subjective opinions and the quantitative assessment of criteria [249]. For the sub-criteria of an efficient grid, we choose the quantitative approach since the relative importance can

TABLE 18.1: Pairwise comparison matrix of the main criteria with respect to the goal based on the judgement of the DSO's representative, where  $CR = 0.077$

	Incentives for Efficient Grid	Fairness and Customer Accept.	Consistency with Polit. Objectives	<i>Importances</i> $W_i$
Incentives for Efficient Grid	1	7	9	0.79
Fairness and Customer Accept.	1/7	1	3	0.15
Consistency with Polit. Objectives	1/9	1/3	1	0.07

TABLE 18.2: Pairwise comparison matrix for the sub-criteria with respect to consistency with political objectives based on the judgement of the DSO's representative.

	Expansion of DER	Eff. Electri- city Usage	<i>Importances</i> $W'_i$	<i>Global</i> <i>Importances</i> $W_i$
Expansion of DER	1	1	0.50	0.03
Eff. Electri- city Usage	1	1	0.50	0.03

TABLE 18.3: Overview of the criteria indicators.

Criterion	Sub-criterion	Indicator
Efficient Grid	Reduction of Costs	<ul style="list-style-type: none"> <li>• Reduction of Usage-Related Costs (<math>UCR</math>)</li> <li>• Reduction of Capacity-Related Costs (<math>CCR</math>)</li> </ul>
	Reflection of Costs	<ul style="list-style-type: none"> <li>• Reflection of Cost Drivers in Costs (<math>ROC</math>)</li> </ul>
Fairness and Customer Acceptance		<ul style="list-style-type: none"> <li>• Cost Change for Inflex. Consumers (<math>I^{FAC}</math>)</li> </ul>
Consistency with Political Objectives	Expansion of DERs	<ul style="list-style-type: none"> <li>• Cost Change for DER Owners (<math>I^{EDER}</math>)</li> </ul>
	Efficient Electricity Usage	<ul style="list-style-type: none"> <li>• Reduction in Shifted Energy (<math>SER</math>)</li> <li>• Reflection of Electricity Usage in Costs (<math>ROE</math>)</li> </ul>

be measured by the share of usage-related  $c_{NT}^{UR}$  and capacity-related costs  $c_{NT}^{CR}$  within the overall costs  $C_{NT}$ :

$$W'_{ROUR} = \frac{C_{NT}^{UR}}{C_{NT}} = c_{NT}^{UR}; \quad W'_{ROCR} = \frac{C_{NT}^{CR}}{C_{NT}} = c_{NT}^{CR}, \quad (18.3)$$

where  $C_{NT}^{UR}$  and  $C_{NT}^{CR}$  are the absolute usage-related and capacity related costs. Note that the assumption here is that the overall costs only consist of usage- and capacity-related costs.

The weights of all main criteria and the sub-criteria  $SC$  of a single criterion need to sum up to 1:

$$\sum_{i \in EC} W_i = 1; \quad \sum_{j \in SC} W'_j = 1. \quad (18.4)$$

*Level II: Performance Indicators*

In the second level, we develop performance indicators for the criteria fulfilment by different network tariff structures. Each criterion or sub-criterion is associated with one or two indicators. Tab. 18.3 gives an overview of the proposed indicators, further detailed below.

The indicators can be divided into two groups: indicators measuring the correlation between a specific aspect and the paid costs and indicators measuring the reduction of a parameter. The structure and obtainable values are the same for all indicators of the same group.

The first group consists of the reflection of costs drivers in costs (*ROC*) and the reflection of electricity usage in costs (*ROE*). For both, we use the Pearson correlation between tariff costs and costs incurred by the customer or electricity consumption of the consumer, and the slope of a linear regression function as proposed in [202]. The Pearson correlation takes values between -1 and 1. The absolute value thereby indicates the strength of the correlation and the algebraic sign whether the parameters are positively or negatively correlated. The slope indicator takes values between 0 and 1. The final indicators, which are the product of Pearson correlation and slope, therefore also range between -1 and 1. Generally, we expect a positive correlation. Therefore values between 0 and 1 are more realistic.

The remaining indicators form the second group. For them, the reduction of a certain parameter compared to a reference value is measured. The general structure of the indicators is thereby:

$$I_{NT} = 1.5 - \frac{X_{NT}}{X_{ref}}, \quad (18.5)$$

where  $X_{NT}$  is the parameter value under tariff  $NT$  and  $X_{ref}$  the reference value. The parameter is designed such that the indicator obtains a value of  $I_{NT} = 0.5$  if  $X_{NT} = X_{ref}$  since this is the middle of the expected range of the first indicator group. The maximum possible value is  $I_{NT} = 1.5$  for the case where the parameter is reduced to  $X_{NT} = 0$ , which is however unrealistic. If the parameter value is higher than the reference value, the indicator value is  $I_{NT} < 0.5$  and can obtain negative values if  $X_{NT}$  is more than 50% higher than the reference value.

### *Efficient Grid*

The goal of an efficient grid is to reduce unnecessary costs. We therefore propose the reduction of costs achieved by a network tariff  $NT$  as an indicator for an efficient grid. It can be further subdivided into the reduction of usage-related costs  $UCR_{NT}$  and capacity-related costs  $CCR_{NT}$ . Usage-related costs thereby reflect the long-term marginal costs that are influenced

by how and when a consumer draws electricity from the grid. The capacity-related costs, on the contrary, do not depend on the time of use but only on the amount of contracted capacity. These costs are prevalent in the lower grid levels, as grid operators have to account for high simultaneities and therefore plan with the full contracted capacity of a user. In higher grid levels, on the other hand, a higher number of consumers allows to use lower simultaneity factors and plan with the aggregated peak of a larger group of consumers instead. Since an actual calculation of the costs might be difficult, we propose proxies for both values as well.

If cost-driving factors are reflected well in the tariff, and customers are price responsive, customer behaviour is expected to be network-friendly and lower long-term investment are needed. The reflection of cost-driving factors  $ROC_{NT}$  is therefore a third indicator for an efficient grid.

The overall indicator for an efficient grid is calculated by:

$$I_{NT}^{EG} = \frac{1}{2} \cdot (W'_{ROUR} \cdot UCR_{NT} + W'_{ROCR} \cdot CCR_{NT} + ROC_{NT}), \quad (18.6)$$

where  $W'_{ROUR}$  and  $W'_{ROCR}$  are the relative weights of the reflection of usage- and capacity-related costs.

### *Reduction of Usage-Related Costs*

The first indicator is the reduction of usage-related costs. Therefore, the usage-related costs  $C_{NT}^{UR}$  under the tariff structures  $NT$  are compared with those of undisturbed operation. As the constant energy-based tariff does not provide time-dependent incentives, we use its value  $C_{VT}^{UR}$  as a reference.

If the costs cannot be directly obtained, we propose the reduction of aggregated power peaks as a proxy for the reflection of usage-related costs, as presented in [252]. The aggregated simultaneous power peak within a network is assumed to be the driving factor of usage-related costs. Therefore, a percentage of the highest aggregated power peaks within the simulated network, where  $Q(p)$  is the lowest peak, is used as a proxy for the usage-related costs. The 10 % highest aggregated power peaks for all time intervals are considered, hence  $p = 0.9$ . The aggregated power peak  $P_{NT}^{peak}$  is calcu-

lated by summing the power drawn from all consumers  $P(t)$  of a subset of all time steps  $T^{peak} = \{t \in T : P(t) > Q(p)\}$ :

$$P_{NT}^{peak} = \sum_{t \in T^{peak}} P(t). \quad (18.7)$$

The indicator for the reduction of usage-related costs  $UCR_{NT}$  can be calculated and approximated by:

$$UCR_{NT} = 1.5 - \frac{C_{NT}^{UR}}{C_{VT}^{UR}} \approx 1.5 - \frac{P_{NT}^{peak}}{P_{VT}^{peak}}. \quad (18.8)$$

### *Reduction of Capacity-Related Costs*

To quantify the ability of a tariff structure to set incentives to reduce capacity-related costs, we again compare the capacity-related costs  $C_{NT}^{CR}$  under network tariff  $NT$  to the reference value of the volumetric tariff  $C_{VT}^{CR}$ . If these costs are not available, the reduction in aggregated contracted capacity  $CC_{NT}$  can serve as a proxy. Customers are thereby assumed to fall into a lower contracted capacity category when they reduce their local power peak on a permanent basis. The indicator for the reduction of capacity-related costs can therefore be calculated and approximated by:

$$CCR_{NT} = 1.5 - \frac{C_{NT}^{CR}}{C_{VT}^{CR}} \approx 1.5 - \frac{CC_{NT}}{CC_{VT}}. \quad (18.9)$$

### *Cost Reflection*

For the reflection of cost-driving factors in the costs, we use the Pearson correlation between tariff costs and costs incurred by the customer in combination with the slope of the correlation as proposed in [202]. Since the reduction in cost-driving factors is already measured with the previous two indicators  $UCR_{NT}$  and  $CCR_{NT}$ , we use relative values to measure the correlation. The idea is that users should pay more – if they have a high share of aggregated power peak and contracted capacity. Therefore, the cost share

$c_{u,NT}$ , the share of aggregated peaks  $p_{u,NT}$  and share of contracted capacity  $cc_{u,NT}$  of a user  $u$  under tariff  $NT$  are defined:

$$c_{u,NT} = \frac{C_{u,NT}}{C_{NT}}, \quad p_{u,NT} = \frac{P_{u,NT}^{peak}}{P_{NT}^{peak}}, \quad cc_{u,NT} = \frac{CC_{u,NT}}{CC_{NT}}, \quad (18.10)$$

To define the correlation, the share of aggregated peaks and contracted capacity must be scaled with the share of costs both factors incur. We therefore define adjusted parameters  $p'_{u,NT}$  and  $cc'_{u,NT}$  as follows:

$$p'_{u,NT} = p_{u,NT} \cdot c_{NT}^{UR}, \quad (18.11)$$

$$cc'_{u,NT} = cc_{u,NT} \cdot c_{NT}^{CR}, \quad (18.12)$$

where  $c_{NT}^{UR}$  is the share of usage-related costs and  $c_{NT}^{CR}$  the share of capacity-related costs under network tariff  $NT$ .

The defined indicator for the reflection of costs  $ROC_{NT}$  equals to:

$$ROC_{NT} = ROC_{NT}^{corr} \cdot ROC_{NT}^{slope}, \quad (18.13)$$

$$ROC_{NT}^{corr} = \text{corr}(c_{u,NT}, p'_{u,NT} + cc'_{u,NT}), \quad (18.14)$$

$$ROC_{NT}^{slope} = \min\left(|\beta_1|, \frac{1}{|\beta_1|}\right), \quad (18.15)$$

where  $\beta_1$  is the slope of a linear regression function

$$c_{u,NT} = \beta_0 + \beta_1 \cdot (p'_{u,NT} + cc'_{u,NT}). \quad (18.16)$$

### *Fairness and Customer Acceptance*

As mentioned, the criterion of fairness and customer acceptance is difficult to measure. To really understand customer acceptance for different network tariffs, a survey would have to be conducted, which is out of the scope of this study. Hence, we focus more on fairness and that user groups with low financial means should be protected. Therefore, the change in the relative cost share of users defined as a vulnerable group  $VU$  compared to their current relative cost share is assessed. The proposed indicator  $I_{NT}^{FAC}$  considers the fraction of the relative cost share of vulnerable consumers

under the considered network tariff  $NT$  and the relative cost share of customers of that vulnerable group in the status quo (SQ):

$$I_{NT}^{FAC} = 1.5 - \frac{rc_{VU,NT}}{rc_{VU,SQ}} \quad (18.17)$$

$$rc_{VU,NT} = \frac{\sum_{v \in VU} c_{v,NT}}{g_{VU}} \quad (18.18)$$

$$g_{VU} = \frac{|VU|}{|U|}, \quad (18.19)$$

where  $g_{VU}$  is the group share of vulnerable consumers compared to all consumers and  $rc_{VU,NT}$  is the cost share of the vulnerable customers divided by the group share.

#### *Expansion of DERs*

To assess the consistency with the political objective of expanding DERs, we compare the costs before and after purchasing a DER ( $C_{NT}^{before}$  and  $C_{NT}^{after}$ ):

$$I_{NT}^{EDER} = 1.5 - \frac{C_{NT}^{after}}{C_{NT}^{before}}. \quad (18.20)$$

If the costs cannot be calculated, the cost drivers can be used instead. Cost drivers for exemplary network tariffs are the purchased electricity for the volumetric tariff, the monthly or yearly power peaks for peak tariffs and the contracted capacity for capacity tariffs.

#### *Efficient Electricity Usage*

To evaluate whether a tariff structure fosters efficient electricity usage, we define two indicators: the reduction in shifted energy in a 100 % renewable system  $SER$  and the reflection of purchased electricity in the costs  $ROE$ . Both values are combined to obtain the overall rating:

$$I_{NT}^{EEU} = \frac{1}{2} \cdot (SER_{NT} + ROE_{NT}). \quad (18.21)$$

### *Reduction in Shifted Energy*

In future systems with high shares of renewable energy, it becomes more important when electricity is consumed. A consumption at times of high variable renewable energy sources (VRES) feed-in can help their integration and reduce the overall system costs. We therefore measure the change in shifted energy, determined with the storage equivalent model described in Chapter 12, as the ability of a tariff structure to set incentives to reduce the temporal flexibility needs in renewable power systems. For this, the total shifted energy  $SE_{NT}$  under the tariff structures  $NT$  is normalised compared to a base value under the volumetric tariff  $SE_{VT}$ :

$$SER_{NT} = 1.5 - \frac{SE_{NT}}{SE_{VT}}. \quad (18.22)$$

### *Reflection of Purchased Electricity*

If the purchased electricity is reflected well in the costs, consumers have an incentive to reduce their electricity consumption. We therefore define a new indicator measuring the correlation between a customer  $u$ 's electricity share  $pe_{u,NT}$  and its cost share of the total paid costs  $c_{u,NT}$  under a given tariff:

$$ROE_{NT} = ROE_{NT}^{corr} \cdot ROE_{NT}^{slope}, \quad (18.23)$$

$$ROE_{NT}^{corr} = \text{corr}(c_{u,NT}, pe_{u,NT}), \quad (18.24)$$

$$pe_{u,NT} = \frac{PE_{u,NT}}{PE_{NT}}, \quad (18.25)$$

$$ROE_{NT}^{slope} = \min\left(|\beta_3|, \frac{1}{|\beta_3|}\right), \quad (18.26)$$

where  $\beta_3$  is the slope of a linear regression function

$$c_{u,NT} = \beta_2 + \beta_3 \cdot pe_{u,NT}. \quad (18.27)$$

## 18.2 CASE STUDY - APPLICATION OF THE PROPOSED FRAMEWORK

In this section, we showcase the application of the proposed framework to prove its applicability. Therefore, we use the consumers' reaction modelled in the previous chapter to evaluate the effects on the distribution grids. The results are then used to calculate the proposed indicators and the final

ranking of the different electricity tariffs. The values of the relative weights in the first level of the process are obtained from pairwise comparison matrices filled out by the interviewed stakeholders. We want to emphasise that the case study is mainly meant to prove the applicability of the proposed framework and therefore uses some simplifications, like the limited number of expert weightings.

### 18.2.1 *Simulation Setup*

We use the data obtained in the previous chapter to apply the second level in the proposed framework. Even though the framework is originally intended to evaluate network tariffs, we expand the application to all investigated electricity tariffs, i.e. the combination of network tariff and suppliers' costs. The same assumptions for consumers and DER penetrations as in the previous chapter (see Sections 17.2.1 and 17.2.2) are used for the following investigations. The constant energy-based tariff is used as a reference, i.e.  $VT = E_c$ . For clarity, the investigated tariffs are shortly summarised in the following. A more detailed description and the used values are summarised in Section 17.2.3 and Table 17.1. The tariffs can be divided into three groups:

**PURELY ENERGY-BASED TARIFFS:** As already mentioned, the constant energy-based tariff  $E_c$  serves as the reference. Furthermore, the day and night tariff  $E_{d/n}$  with high prices during the day and low prices at night is investigated. The last two purely energy-based tariffs  $E_r$  and  $E_{r-mv}$  are based on the grid residual load. The prices of  $E_r$  thereby follow the residual load at the medium voltage (MV)/low voltage (LV)-transformers, and the prices of  $E_{r-mv}$  follow the residual load at the high voltage (HV)/MV-transformers.

**PURELY CAPACITY-BASED TARIFFS:** We consider three purely capacity-based tariffs, two of which are solely applied to load and one additionally pricing feed-in peaks. Tariff  $C_L$  prices the annual peak load of consumers. The segmented tariff  $C_{SG}$  prices the power consumption in segments, with increasing prices for higher power segments. The capacity-based tariff for load and feed-in  $C_{LF}$  prices the annual peaks of load and feed-in.

**MIXED TARIFFS:** Three mixed tariffs are investigated. The first ( $E_r C_{LF}$ ) is the combination of the grid residual load based energy component and the capacity peak components on load and feed-in. The second

( $\mathbf{E}_c\mathbf{S}_r$ ) is the combination of the constant energy-based network tariff with time-varying suppliers' costs. Finally, the last ( $\mathbf{C}_{LF}\mathbf{S}_r$ ) is the combination of the capacity-based network tariff on load and feed-in peaks with time-varying suppliers' costs.

### 18.2.2 Simplifications and Adaptions of Indicators

The overlying grid levels are not modelled. Therefore, we use the proposed proxy of aggregated power peaks  $P_{NT}^{peak}$  to estimate the reduction of usage-related costs. For the reduction of capacity-related costs, we use the reduction of grid reinforcement costs determined in the previous chapter.

For the share of usage- and capacity-related costs, we use values from the literature, where 41 % of the costs were linked to consumption and 59 % to gross asset value [243]. We use these values for the status quo (SQ) without DERs:

$$c_{SQ}^{UR} = 0.41, \quad c_{SQ}^{CR} = 0.59. \quad (18.28)$$

For the simulated electricity tariffs  $ET$  and scenarios, the values are adjusted according to the respective aggregated power peaks and contracted capacities (as assumed drivers of usage- and capacity-related costs) and normalised such that they sum up to 1:

$$c_{ET}^{UR'} = c_{SQ}^{UR} \cdot \frac{P_{ET}^{peak}}{P_{SQ}^{peak}}, \quad (18.29)$$

$$c_{ET}^{CR'} = c_{SQ}^{CR} \cdot \frac{CC_{ET}}{CC_{SQ}}, \quad (18.30)$$

$$c_{ET}^{UR} = \frac{c_{ET}^{UR'}}{c_{ET}^{UR'} + c_{ET}^{CR'}}, \quad (18.31)$$

$$c_{ET}^{CR} = \frac{c_{ET}^{CR'}}{c_{ET}^{UR'} + c_{ET}^{CR'}}. \quad (18.32)$$

For the correlation indicators, we use different cost values. For the reflection of costs in the criterion of an *efficient grid*, only the costs for the network tariff  $C_{NT}$  are used to determine the correlation. The idea is that this criterion is

primarily targeted at network tariffs, which should incentivise the efficient use of the grid. For the correlation indicators in the criterion on the *efficient use of electricity*, on the other hand, we use the total cost for electricity  $C_{ET}$ , i.e. the sum of network tariff and suppliers' costs. The political objective of efficient use of electricity is thus seen as an overarching goal, not primarily targeted at the network tariffs but the electricity price.

For fairness and customer acceptance, we define the vulnerable group as consumers who do not own DERs in the first two scenarios and whose annual electricity consumption is below the mean of all investigated consumers. In *Scenario 3* and *4*, (almost) all consumers own DERs. These are therefore not accounted for when determining vulnerable consumers. The underlying assumption using consumers that do not own DERs in *Scenarios 1* and *2* is that DERs are more affordable for higher-income customers, and only low-income customers will stay without DERs. Within the six grids, the so-obtained share of vulnerable consumers ranges between 3.9-4.7%.

For the criterion of expansion of DERs, we evaluate the cost change when purchasing a PV system with or without battery for all consumers not owning a PV system yet, namely inflexible consumers (HH), EV owners (EV), heat pump owners (HP) and consumers owning both EV and heat pump (EV & HP). For simplicity, the cost change for all 500 modelled consumers is determined and then weighted with the share of the respective customer group within all consumers without PV system  $CG_{EDER} = \{HH, EV, HP, EV\&HP\}$  in the evaluation process:

$$\frac{C_{NT}^{after}}{C_{NT}^{before}} = \sum_{u \in CG_{EDER}} \left( \frac{|u|}{|CG_{EDER}|} \cdot cr_{u,NT}^{DERs} \right), \quad (18.33)$$

$$cr_{u,NT}^{DERs} = \frac{1}{2} \left( cr_{u,NT}^{PV} + cr_{u,NT}^{u+PV\&Bat.} \right) \quad (18.34)$$

$$cr_{u,NT}^{der} = \frac{C_{u,NT}^{der}}{C_{u,NT}}, \quad der \in \{PV, PV\&Bat.\}. \quad (18.35)$$

The reduction  $cr$  achieved by a PV system on its own ( $cr_{u,NT}^{PV}$ ) and in combination with a battery system ( $cr_{u,NT}^{PV\&Bat.}$ ) are thereby weighted as equally important.

### 18.3 RESULTS AND DISCUSSION

While the goal of the case study is mainly to showcase the applicability of the proposed framework, it still yields some interesting findings that are presented and discussed in the following. For clarity, the results are only presented for grid *PV-2* and *Scenarios 1* and *4* in the following, if not mentioned otherwise. The grid is chosen because it is the most balanced one, comprising similar shares of load and (mainly PV) feed-in. Differences between the grids are additionally discussed where present.

#### 18.3.1 *Weighting of Requirements*

Fig. 18.4 shows the resulting weights of the different requirements provided by the interviewed stakeholders<sup>2</sup>. The results show that the perception of the most important objectives of network tariffs is highly dependent on the interviewed expert. While the representatives of the authority, DSO and regulator clearly see an efficient grid as the most important criterion, the politics and third-party representatives do not show such a high preference for this criterion. The representative of politics puts a high weight on fairness and customer acceptance and expansion of DERs. The third-party representative still sees a high importance of an efficient grid, closely followed by efficient electricity usage.

So overall, there is no shared understanding of the most important criteria. Visualising the different weightings can be a helpful step in defining a suitable tariff candidate. For future development of the process, we suggest including a step to combine the weightings of the different stakeholder groups to arrive at a shared understanding of the relative importance of the determined criteria. It would also be interesting to confront experts with the results of the quantitative framework and assess whether this alters their perception of the importance of the criteria but this was outside the scope of this study. Furthermore, a larger pool of experts would be preferable to gain more robust insights and to investigate whether the differences mainly depend on the field of expertise and position or also vary significantly within the stakeholder groups.

<sup>2</sup> The actual values can be found in Table B.1 in the appendix.

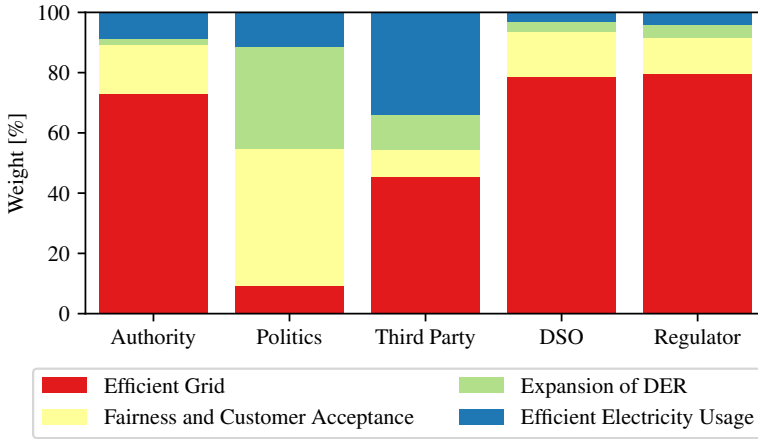


FIGURE 18.4: Criteria's importance evaluating network tariffs based on experts' judgements.

### 18.3.2 Performance Indicators

Fig. 18.5 shows the resulting performance indicators for the different network tariffs under varying levels of penetration of DERs<sup>3</sup>. The performance of the network tariffs obviously depends on the level of DER penetration.

For the indicator of an *efficient grid*, the performance of the tariffs is differently influenced by the penetration of DERs in the scenarios. Some show similar values in both scenarios, namely  $E_c$ ,  $C_{LF}$ ,  $E_r C_{LF}$  and  $C_{LF} S_r$ . Next to the reference constant energy-based tariff  $E_c$ , these are all tariffs with a capacity component on both load and feed-in ( $C_{LF}$ ) which show high indicator values in both scenarios. Other values change significantly between the scenarios, e.g. the performance of  $E_{d/n}$ ,  $E_r$ ,  $E_{r-mv}$ ,  $C_L$ ,  $C_{SG}$  and  $E_c S_r$ . The performance of the first tariffs decreases, while the indicator value of  $E_c S_r$  increases (but still shows negative values). The decrease in performance of the time-dependent energy-based tariffs  $E_{d/n}$ ,  $E_r$  and  $E_{r-mv}$  can be explained by the increasing simultaneity and newly created peaks and resulting increased reinforcement costs that were observed in the last chapter (see Sections 17.3.1 and 17.3.3). On the other hand, the lower values of the load capacity-based tariffs  $C_L$  and  $C_{SG}$  are mainly caused by the fact

<sup>3</sup> The concrete values are summarised in Table B.2 in the appendix.

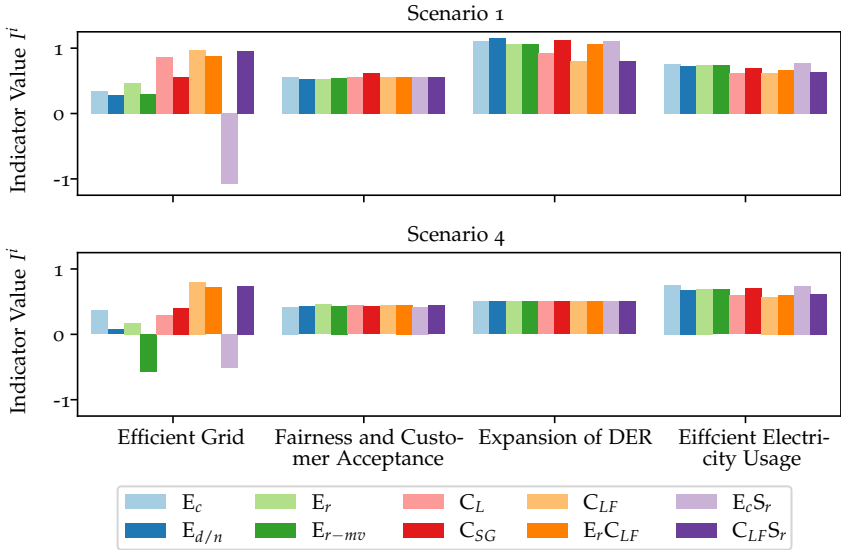


FIGURE 18.5: Results for the indicators of each criterion by scenario and alternative.

that with increasing DER penetrations, the reinforcement becomes more feed-in driven, and cost components applying to only load do not give incentives to reduce feed-in peaks.

In the displayed grid, the purely capacity-based tariff on both load and feed-in peaks  $C_{LF}$  performs best in both scenarios for the indicator of an efficient grid. In some of the other grids,  $C_{LF} S_r$  is the best-performing tariff in part of the scenarios. The general tendency in the high DER scenarios is that the combinations with a capacity price component on load and feed-in ( $C_{LF}$ ) perform significantly better than the other tariffs. On the other hand, time-varying energy-based tariffs perform worst, even showcasing negative indicator values. In the displayed grid,  $E_c S_r$  performs worst in *Scenario 1* with low DER penetration and  $E_{r-mv}$  in *Scenario 4* with high DER penetration. The same tendency can be observed in most other grids as well. In all grids, either  $E_c S_r$  or  $E_{r-mv}$  are the worst-performing tariffs in all scenarios.

The indicator of *fairness and customer acceptance* shows little variation in the displayed grid for both scenarios. In *Scenario 1*, the segmented tariff  $C_{SG}$  performs best. In *Scenario 4*, the grid residual load energy-based tariff  $E_r$

performs slightly better than the others. The low variation between the tariffs can be partly explained by the fact that, in this scenario, all consumers own all DER options. The difference in costs for the customers therefore decreases compared to the case where some own only peak- or energy-intensive technologies (without PV and battery energy storage systems (BESS) to optimised self-consumption) and thus pay more (see Section 17.3.5). The effect can also be observed in the other feed-in-dominated grids.

On the other hand, the difference between the tariffs is higher in the scenarios with high DER penetrations in the load-dominated grids. In these grids and scenarios, the capacity-based tariffs (except for the segmented tariff) perform significantly worse than the other tariff options. The segmented tariff  $C_{SG}$  performs best for low to intermediate DER penetrations in all the grids. The best tariff for high DER penetrations varies between the grids within the options  $E_{d/n}$ ,  $E_r$ ,  $E_{r-mv}$ ,  $C_{SG}$  and  $C_{LF}$ . The worst-performing options vary between the grids and scenarios, with a tendency of the day and night tariff  $E_{d/n}$  performing worst for low to intermediate DER penetrations and capacity-based tariffs for high DER penetrations. In the previous chapter, the day and night tariff  $E_{d/n}$  was the preferred option for households with several DERs (see Section 17.3.5), indicating that they can best optimise against this tariff. This leaves inflexible consumers with a higher share of the costs, leading to a low indicator value. However, overall, there are not as clear trends for this indicator as for the other criteria.

The criterion for the *expansion of DERs* shows higher differences but only for the low DER penetration scenario. In *Scenario 4*, every consumer already owns all DERs and the indicator consequently is constant for all tariffs. In all other scenarios, the energy-based day and night tariff  $E_{d/n}$  performs best and the capacity-based tariff on peak load and feed-in  $C_{LF}$  worst. These tendencies are consistent over all investigated grids. Generally, tariffs comprising peak-based price components perform worse than the other tariffs for this criterion.

For the *efficient electricity usage*, the performance of the different tariff options is similar between the scenarios and grids. In low to intermediate DER penetrations, the combination of constant energy-based network tariff and time-varying suppliers' costs  $E_c S_r$  performs best. For high DER penetrations, the purely constant energy-based tariff  $E_c$  outperforms the others. The capacity-based tariff on peak load and feed-in  $C_{LF}$  performs worst in all investigated grids and scenarios. In general, similarly to the last criterion,

the tariffs with peak-based price components perform worse than the other options.

In summary, for every criterion, different tariffs perform best. The performance can furthermore vary between the different grids. These results confirm that no single network tariff consistently outperforms the others, which was also highlighted in [202]. On the contrary, different criteria lead to different rankings of the alternatives, and the final rating will depend on the relative importance of the different criteria. The detailed results for the single criteria and sub-criteria are discussed in the following sections.

### *Efficient Grid*

Fig. 18.6 shows the indicators for the sub-criteria of the criterion of an efficient grid in grid *PV-2*. It should be mentioned that the set of indicators related to an efficient grid is most dependent on the type of grid within all indicators. The differences thereby mainly occur along the line of the relation of load and feed-in within the grids. Grids with high shares of load (*PV-2*, *Load-1* and *Load-2*) show different tendencies than the highly feed-in-dominated grids (*Wind-1*, *Wind-2* and *PV-1*). The results are therefore discussed for both groups of grids.

The reflection of usage-related costs (upper left) with the indicator *reduction of usage-related costs UCR* shows relatively similar values for all tariffs in *Scenario 1* but increasing variations in *Scenario 4*. In *Scenario 1*, the tariffs comprising time-dependent energy-based network tariffs (i.e.  $E_{d/n}$ ,  $E_r$ ,  $E_{r-mv}$  and  $E_r C_{LF}$ ) perform better than the other options in grids with relatively high shares of load (*PV-2*, *Load-1* and *Load-2*). In the highly feed-in-dominated grids (*Wind-1*, *Wind-2* and *PV-1*), tariffs  $E_r C_{LF}$ ,  $E_c S_r$  and  $C_{LF} S_r$  show slightly higher values than the other tariff options. For these grids, the suppliers' costs based on the system residual load seem to correlate well with the local situation in the grids, reducing the aggregated peaks.

For high penetrations of DERs in *Scenario 4*, the differences between the tariffs and the differences between the grids increase. The reason is that the ten per cent highest peaks highly depend on the technological composition within the grid and the resulting grid residual load. The effects in the displayed grid *PV-2* are strongest, but the trends are also visible in most other grids. The exception is grid *Wind-1*, where little variation is visible between the tariff options. The grid is strongly dominated by wind generation, and most peaks therefore likely depend on the wind feed-in, with little effect on

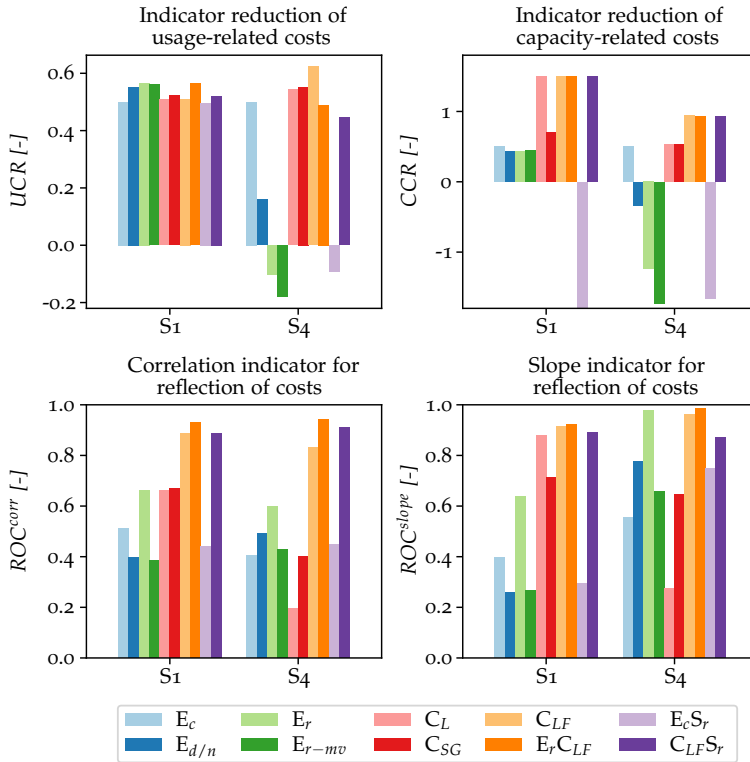


FIGURE 18.6: Results for the indicators of the sub-criteria of the criterion efficient grid by scenario and alternative. For clarity, the values for the reduction of capacity-related costs are capped at -1.8.

the consumption pattern of residential loads. In all other grids, the purely energy-based time-varying incentives in tariffs  $E_{d/n}$ ,  $E_r$ ,  $E_{r-mv}$  and  $E_c S_r$  lead to low indicator values. In the displayed grid, the last three tariffs even lead to negative indicator values, which means that the sum of the ten per cent highest peaks increases by more than 50% compared to the volumetric tariff  $E_c$ . These results are in line with the investigations of the previous chapter, where these tariffs lead to high new load peaks.

The best-performing tariff depends on the grid. In the displayed grid *PV-2*, the pure capacity-based tariff on peak load and feed-in  $C_{LF}$  performs best. In grids *Wind-1* and *Wind-2*, the tariff with additional time-varying suppliers' costs  $C_{LF} S_r$  shows the highest indicator values. For grids *Load-1* and *Load-2*,

tariff  $E_r C_{LF}$  shows the highest value. The results indicate that combining a capacity-based price component with time-varying energy-based prices can reduce the ten per cent highest peaks if the time-varying prices are set well. The chosen clusters for the grid residual load based tariffs might not represent the grids well, especially the wind-dominated grids, where the system residual load in the time-varying suppliers' costs perform better. Future investigations should evaluate more clusters or even separate time series for the individual grids. This might further reduce the ten per cent highest peaks as an indicator for usage-related costs.

The *reduction in capacity-related costs*  $CCR$  (upper right), on the other hand, shows similar trends for all investigated grids except for the grid residual load based tariffs  $E_r$  and  $E_{r-mv}$  in *Scenario 1*. They perform well (with indicator values close to 1.5) in *PV-1* and *Load-2* but very poorly in *Wind-2*. Again, this shows that the representative time series of the clusters work well in some grids but not in others. On the other hand, the scenarios with higher DER penetrations show negative values in all investigated grids, indicating a robust trend. Analogue to the aggregated peaks, the purely energy-based tariffs  $E_{d/n}$ ,  $E_r$ ,  $E_{r-mv}$  and  $E_c S_r$  show poor performance with high DER penetrations (for all investigated grids) for the reduction of capacity-related costs. On the other hand, the tariffs including a capacity-based price component on peak load and feed-in  $C_{LF}$ ,  $E_r C_{LF}$  and  $C_{LF} S_r$  perform well in all grids and scenarios. Capacity-based price components only on load in  $C_L$  and  $C_{SG}$  achieve a reduction if there is load-induced grid reinforcement which can be effectively reduced. For higher DER penetrations and in grid *PV-1* (with high PV penetration from the start), these tariffs become less effective, indicating that the reinforcement becomes more feed-in-driven in these cases.

The correlation between paid cost share and contribution to cost-driving factors  $ROC^{corr}$  (lower left) differs for grids with relatively high load (*PV-2*, *Load-1* and *Load-2*) and highly feed-in-dominated grids (*Wind-1*, *Wind-2* and *PV-1*). To showcase the different effects, we display cost share versus cost contribution of all consumers under the different tariff options in *Scenario 2* for grid *PV-2* (representing grids with high shares of load) in Fig. 18.7 and for grid *PV-1* (representing highly feed-in-dominated grids) in Fig. 18.8. The cost contribution thereby indicates the contribution of the consumer to cost driving factors ( $p'_{u,NT} + cc'_{u,NT}$ ) as defined in (18.14). The cost share ( $c_{u,NT}$ ) refers to the cost share an individual consumer pays for network tariff *NT* relative to the total paid network tariff costs. *Scenario 2* is chosen because, in this scenario, all consumer groups are equally represented, which better

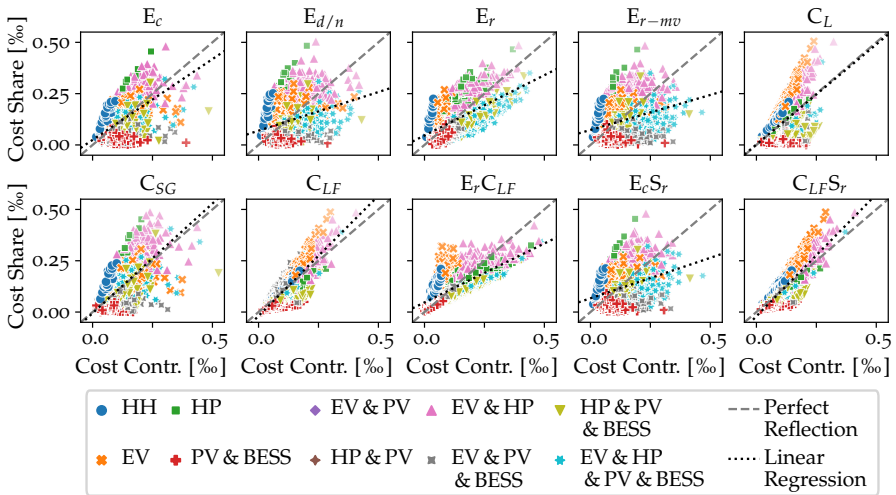


FIGURE 18.7: Cost share vs. cost contribution of the different customer-groups by tariff in grid *PV-2* in *Scenario 2*. Each customer is thereby represented by one data point.

allows the analysis of the effects of the investigated tariffs on the different consumer types.

The difference between the two groups of grids is that for *PV-2*, *Load-1* and *Load-2*, a significant share of the ten per cent highest peaks is load-driven. Consumers thus increase the peaks when consuming in these times. Consequently, we see a positive correlation between cost share and cost contribution for all electricity tariff options in Fig. 18.7. The dashed lines display a perfect reflection of costs, and the dotted lines are the linear regressions as described in (18.16). Consumer points above the dashed line pay too much relative to their contribution to cost-driving factors, and consumer points below too little. The energy-based tariffs tend to underestimate the costs ( $\beta_1 < 1$ ). One reason could be the change in cost-driving factors, as shown in Fig. 18.9. The increase in aggregated contracted capacity  $CC$  is higher than in aggregated peaks  $p^{peak}$  between the two scenarios. Therefore, the correct representation of contracted capacity becomes more important with growing flexibility. The energy-based tariffs do not price contracted capacity and lead to a high increase in this capacity (because of missing incentives to reduce it).

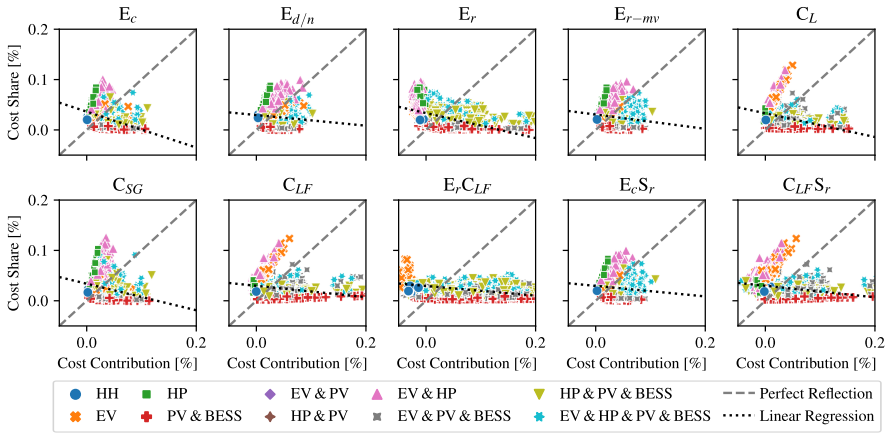


FIGURE 18.8: Cost share vs. cost contribution of the different customer-groups by tariff in grid *PV-1* in *Scenario 2*. Each customer is thereby represented by one data point. For clarity, only consumers with cost share and contribution between  $-0.05$  and  $0.2$  % are displayed.

For these tariffs, customers owning PV and BESS tend to pay too little and customers without too much, especially inflexible households (HH) and HP owners (HP). The data points are relatively spread out, resulting in low correlation indicators in Fig. 18.6 (bottom left). Capacity-based tariffs, on the other hand, lead to data points more closely aligned with the linear regression and, consequently, higher correlation indicators. In these cases, the group of EV owners (EV) pays more relative to their contribution to the cost-driving factors instead of HP owners (HP). Generally, the slope is closer to  $\beta_1 = 1$  for the capacity-based tariffs, leading to higher slope indicators in Fig. 18.6 (bottom right). It has to be mentioned that the capacity load tariff  $C_L$  loses efficacy in the scenarios with high DER penetration. In these scenarios, feed-in peaks become more important, and they are not priced by tariff  $C_L$ .

Most of the ten per cent highest peaks are feed-in driven for the highly feed-in dominated grids. Consumption in these times therefore reduces peaks. All tariffs positively price electricity consumption, leading to negative correlations between cost share and contribution for the highly feed-in dominated grid *PV-1* in Fig. 18.8. The case that it can benefit the grid to consume electricity at certain times is not accounted for in the tariffs and indicators, leading to poor performance of all tariffs in the highly feed-in

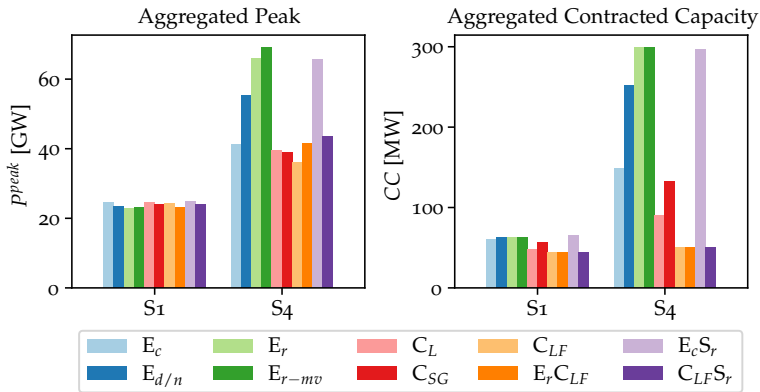


FIGURE 18.9: Development of cost-driving factors by scenario and alternative.

dominated grids (*Wind-1*, *Wind-2* and *PV-1*) in the correlation indicators for cost reflection at high DER penetrations. Note that while all tariffs show a negative correlation between cost share and contribution in *Scenario 2* in Fig. 18.8, some of the tariffs perform better at higher DER penetrations. This effect highlights the difficulty of designing suitable tariffs that are simultaneously applicable to all customer groups. With increasing shares of DERs, the share of customers owning all DERs increases, and the customers become more uniform again. Furthermore, the results show that none of the tariffs effectively accounts for the positive effect of consumption in highly feed-in-dominated grids. The indicators are not designed for these grids, which needs to be improved in future versions of the evaluation framework.

It has to be noted that we measure the correlation between paid costs and contribution to cost-driving factors since it is hard to assess the contribution to the absolute costs directly. These cost-driving factors are easier to approximate than the real costs and might therefore overestimate the correlation.

#### *Fairness and Customer Acceptance*

In all the grids, the highest indicator value for the criterion of *fairness and customer acceptance* occurs for the segmented tariff  $C_{SG}$  in scenarios with low to intermediate DER penetrations (see Fig. 18.5). With increasing DER penetrations, different tariffs perform best. However, the variation is small in most grids. Only in the grids *Load-1* and *Load-2* do the tariffs show sig-

nificant differences for these scenarios with low indicator values for tariffs with peak price components. It has to be mentioned that the distribution of DERs in *Scenarios 3* and *4* does not consider any statistical deviations between vulnerable and other consumers that might occur in reality (e.g. that vulnerable consumers might tend to buy smaller appliances). The results in these scenarios should therefore be interpreted with care.

To compare the costs paid by the vulnerable consumers compared to the other customers, the cost contribution and paid cost shares of both groups are displayed in Fig. 18.10. It shows that for  $C_{SG}$ , the other consumers pay relatively more, explaining the higher indicator value. However, the displayed linear regression for vulnerable consumers shows that the cost increase relative to the increase in cost contribution is higher than the perfect reflection (indicated by the slope of the regression). Furthermore, the slope of the linear regression for the vulnerable consumers in Fig. 18.10 is steeper than that for all consumers in Fig. 18.7. This means that the vulnerable consumers pay more with increasing cost contributions than the mean of all consumers. In the current version of the indicator, the reflection of costs for vulnerable consumers is not accounted for, only the paid costs relative to their group share. In future versions, the correlation could be included as an additional sub-indicator to factor in the higher costs for increasing cost contributions.

Our results furthermore show that inflexible consumers generally pay less relative to their group size in *Scenarios 1* and *2* than in the status quo with a volumetric tariff  $E_c$  (indicator values  $> 0.5$ ). In the other scenarios, the costs are higher. However, the overall costs that have to be covered might increase in *Scenarios 1* and *2*, potentially leading to higher absolute costs for the vulnerable consumers in these scenarios as well. For future investigations, the framework could be expanded with the absolute change in costs paid by the vulnerable consumers if DSOs have to recover their costs, i.e. taking into consideration the changes in usage- and capacity-related costs.

As already mentioned in [202], fairness is hard to measure, and the perception of what is fair might depend on the perspective. One possible interpretation is that those who cause high costs should also pay relative to that. In the proposed framework, this aspect is already covered in the indicator for an efficient grid. We therefore focus on vulnerable customer groups and ensure that no network tariffs disadvantage this group. In the case study, we choose the inflexible consumer group to represent vulnerable consumers. The idea behind that is that in a situation with high penetration of

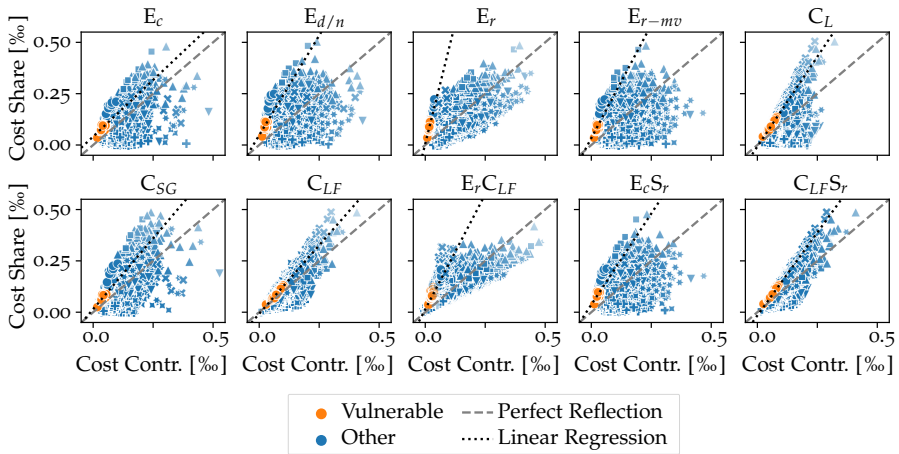


FIGURE 18.10: Cost share vs. cost contribution of vulnerable and other consumers by tariff in grid PV-2 in *Scenario 2*. Each customer is thereby represented by one data point. The linear regression is performed only for the vulnerable consumers.

DERs, such as *Scenario 2*, it must be favourable to purchase DERs and every consumer with the economic means would do so. In reality, wealthy consumers might choose not to purchase DERs despite their economic ability to do so. In this case, the results could be distorted, and the indicator value could be lower than it should be. Therefore, a second factor, the consumed electricity, was used to define vulnerable consumers. However, in real applications, the vulnerable consumers should be defined by economic factors which may not correlate perfectly with electricity consumption.

The current work assumes that customer acceptance will be high if the tariff is fair. However, it was shown that the perception of the fairness of specific tariff options is heterogeneous and that social tariffs are not necessarily perceived as fair [213]. We therefore propose to conduct surveys in future work to estimate the perception of fairness and the customer acceptance of specific network tariffs, similar to [213]. This way, the influence of simplicity, predictability and understandability of network tariffs, which were introduced as additional factors influencing customer acceptance in the literature [57], [202], [211], could also be considered. It was shown previously that the perception of how fair a tariff option changes when additional arguments for the tariff are provided [211]. This effect shows that customer acceptance is not a fixed value but can be influenced by providing

additional information on the tariff options. It should therefore also be the goal to educate customers and provide a transparent decision process to increase customer acceptance.

### *Consistency with Political Objectives*

In the interviews, it was expressed that the tariffs should not contradict certain political objectives, namely the expansion of DERs and efficient usage of electricity. However, political objectives can be subject to change. For the efficient use of electricity, it can be discussed whether the availability of clean energy resources reduces the importance of this sub-criterion. As an example, there has been a debate about reducing the obligatory energy-related component of network tariffs and increasing power-related price components in Switzerland [253]. For the expansion of DERs, there is an ongoing debate about whether central larger assets are more efficient or a more decentralised energy system is preferable (e.g. [254]). Similarly, new political objectives might evolve. This criterion and its sub-criteria should therefore be adapted according to the political developments and the region under investigation. However, here we discuss the sub-criteria identified by the stakeholders and presented in Section 18.1.1.

### *Expansion of DERs*

This indicator measures the cost reduction by purchasing a PV system with or without a battery. Fig. 18.11 shows the costs after purchasing a PV system with or without battery relative to the costs before the purchase. The displayed values include the change in network tariff and suppliers' costs, considering the revenues of selling to the grid. Our investigations do not account for the investment costs. Note that for the displayed indicators, low values are preferable since they represent low costs after purchasing PV systems with and without BESS, thus increasing their attractiveness for investments into these technologies.

The results show that the day and night tariff  $E_{d/n}$  leads to the highest cost reduction when purchasing PV systems with and without batteries for all displayed consumer groups. The lowest reduction is observed for tariff  $C_{LF}S_r$  in all cases. The reason is twofold. First, peak-based network tariffs show lower reduction potential than energy-based tariffs. This is somewhat contrary to the results of our original case study [233] and other work in the literature (e.g. [230]), where PV-systems with battery were found to be more economical with capacity-based than energy-based tariffs.

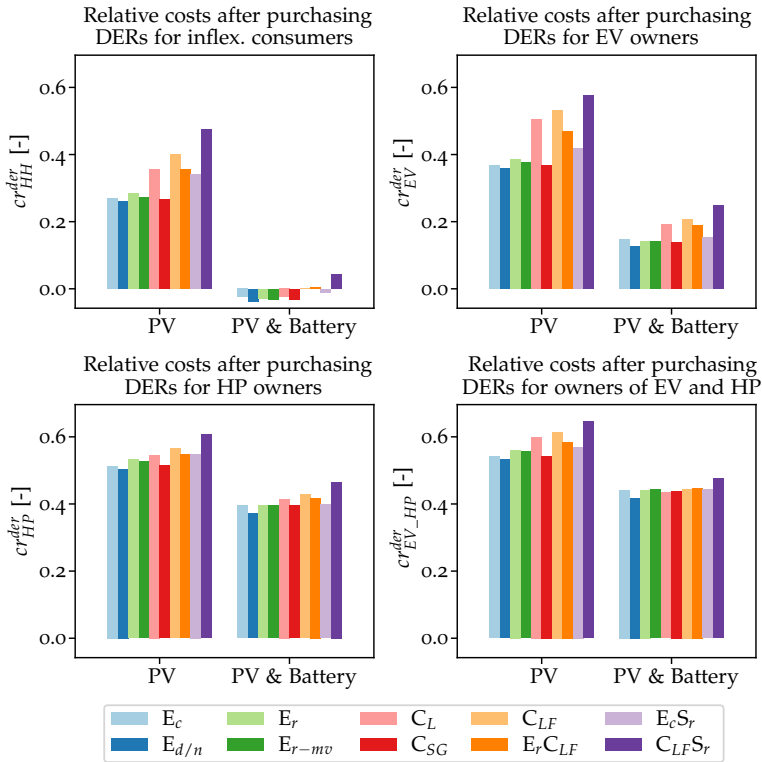


FIGURE 18.11: Costs for inflexible consumers (left) and EV owners (right) after purchasing a PV system with and without battery relative to the costs before the purchase.

However, in [233], it depended on the time scale of the tariff, and a monthly peak price achieved a higher reduction than an annual one. Thus, peak-based prices on shorter periods might perform better and could be an interesting extension of this work. Furthermore, EVs were not assumed flexible in the previous study, leading to high peak values that could be effectively reduced by PV-BESS-systems. The second factor is the time-varying suppliers' cost, which has lower prices in times of high PV feed-in, leading to lower revenues.

For PV systems with a battery, the possible cost reduction is generally higher than for a PV system without a battery. The highest reduction can be achieved for inflexible customers, where even negative values occur for most

investigated electricity tariffs. This means that the revenues by selling PV feed-in to the grid exceed the costs of electricity purchase and network tariff costs. However, we omit taxes, surcharges and levies. Consumers might therefore still pay despite the negative values. Still, the negative values indicate that the PV-battery systems are oversized relative to the household loads without EV or HP. In future studies, the size of PV systems (and other DERs) could be chosen more specific to the individual households and depending on existing household load and other connected DERs.

We see in our results that the reduction of tariff costs by purchasing DERs differs with the type of tariff. For example, the day and night tariff leads to a higher cost reduction for PV-battery systems than the other tariffs. This effect consequently influences the investment of consumers in PV and batteries. In future work, the composition of customers within the scenarios could be adjusted accordingly, or the resulting investments could be directly assessed.

### *Efficient Use of Electricity*

Fig. 18.12 shows the indicators for the sub-criteria of the criterion efficient use of electricity. The *reduction of shifted energy SER* (Fig. 18.12 top) is similar for all tariffs in the low flexibility scenario, showing the highest values for the tariffs with time-varying suppliers' costs  $E_c S_r$  and  $C_{LF} S_r$ . In the high flexibility scenario, on the other hand, the differences are more pronounced, and the combined scenario with capacity-based prices on load and feed-in and time-varying suppliers' costs  $C_{LF} S_r$  clearly outperforms the other tariffs. For a more detailed discussion of the required shifted energy with the different tariff options, we refer to the previous chapter 17.3.4.

The correlation of the share of electricity usage and cost share  $ROE^{corr}$  (Fig. 18.12 bottom left) is relatively high for all alternatives in both scenarios. The gradient  $ROE^{slope}$  (Fig. 18.12 bottom right), in contrast, shows more significant variations but the same tendency of high values for the energy-based tariffs and lower values for tariffs including capacity-based price components. The energy-based tariffs (and the segmented tariff) naturally perform best regarding the reflection of purchased electricity in the costs as they essentially price the electricity consumption. With the peak-based tariffs, consumers with higher peaks pay relatively more than consumers with lower peaks but with the same electricity consumption. With increasing penetrations of DERs, the variation of consumption profiles increases, especially with high peak consumption from EVs. With more

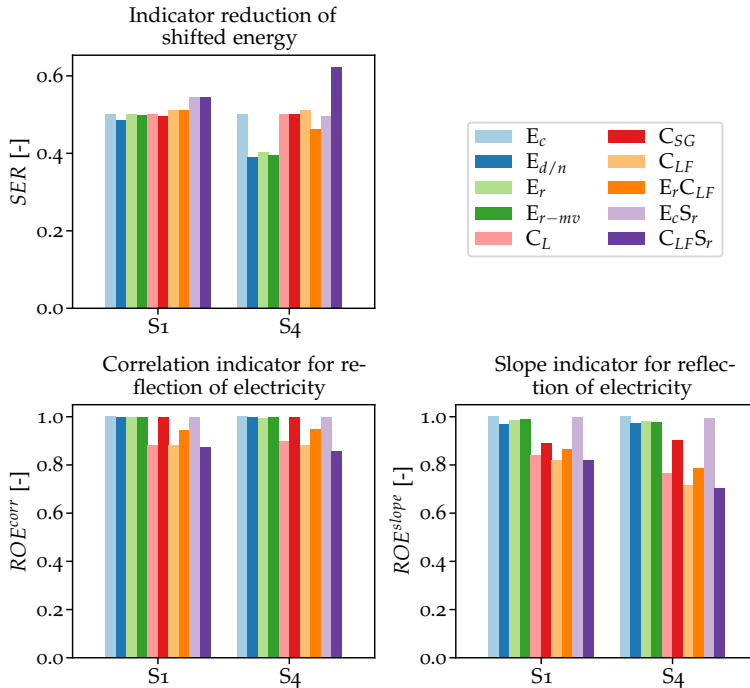


FIGURE 18.12: Results for the indicators of the sub-criteria of the criterion efficient usage of electricity by scenario and alternative.

varying peak-to-energy ratios, the reflection of purchased electricity by peak- or capacity-based tariffs decreases.

### Other Relevant Factors

As mentioned earlier, regulatory feasibility is crucial for implementing a network tariff, which depends on the regulatory framework within a country. The regulatory feasibility is not necessarily a factor to consider when evaluating the general suitability of a tariff structure. However, it has to be considered when it comes to implementing a new tariff structure. Furthermore, the regulatory framework is not fixed but can be adapted to a changing situation. The results of a more general evaluation of different network tariff types against each other could therefore provide arguments for or against certain aspects of the regulatory framework.

Like regulatory feasibility, technical feasibility is crucial for implementing a tariff structure but not relevant for a statement on its theoretical suitability. Some tariff structures do not require any technical conditions for their implementation. However, there are also some, such as dynamic tariffs or static power tariffs, which depend on infrastructure for measuring the network status. This data must be available for tariff structures based on the real-time electricity consumption or the network status. Today, the distribution network is not yet measured across the board, especially at the low-voltage level. However, with the increased equipment of end customers with smart meters, the technical requirements for specific tariff structures can be provided [242].

### 18.3.3 Overall Ranking

Fig. 18.13 shows the overall ranking of the analysed tariffs with equal weights and expert weightings. The results are normalised, i.e. the scoring of all alternatives with a specific set of weights (e.g. equal weights) is multiplied with a constant factor such that  $I_{E_c} = 0.5$ . The conducted case study uses several simplifications. The results should therefore not be taken as the ground truth but more to raise awareness about some underlying tendencies.

First, the "optimal" tariff depends on the weighting of criteria, the grid and the penetration of DERs. In *Scenario 1* of the displayed grid, the capacity-based tariff pricing peak load and feed-in  $C_{LF}$  scores the highest rating for the expert weighting of the representatives of authority, DSO and regulator. For the third party representative and equal weighting of all criteria, the mixed tariff with grid residual load based energy-based price component and capacity-based price component on peak load and feed-in  $E_r C_{LF}$  is rated best. The weighting of the politics representative leads to the segmented tariff  $C_{SG}$  being rated best. Independent of the rating, the tariff with constant energy-based network tariff and time-varying suppliers' costs  $E_c S_r$  performs worst in this scenario and grid.

In *Scenario 4* with 100% DER penetration of the displayed grid, the time-varying energy-based tariff based on the residual load at the HV/MV-transformer  $E_{r-mv}$  scores the lowest rating for all weightings, and the capacity-based tariff pricing peak load and feed-in  $C_{LF}$  scores the highest rating for all investigated weightings. It has to be mentioned that in

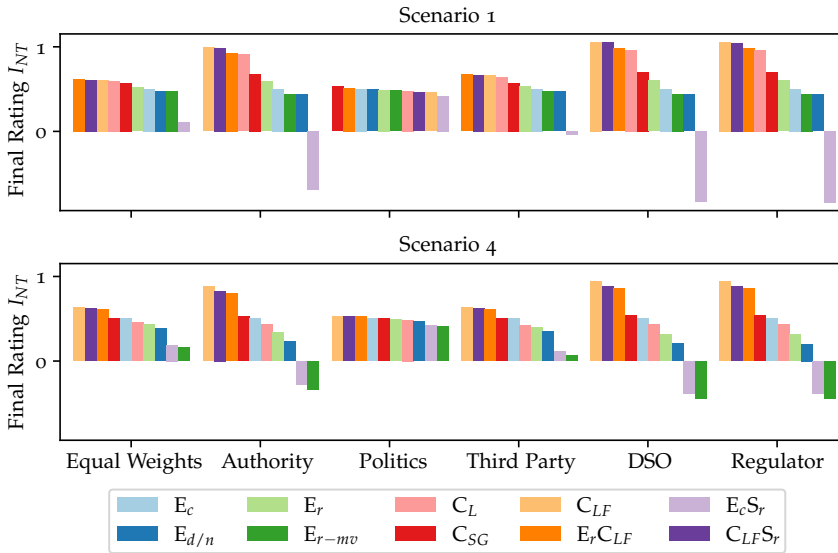


FIGURE 18.13: Overall ratings of investigated tariffs with equal weights and expert weighting for the two scenarios. Results are normalised such that  $I_{E_c} = 0.5$  for every set of weights.

the other grids, there is more variation for the best-performing tariff in *Scenario 4*.

Figure 18.14 therefore displays the share of tariff options that score best (top) and worst (bottom) for the different combinations of expert weighting and grid in the four simulated scenarios. In *Scenario 1* ( $S_1$ ), the best-performing tariffs are divided between various options. The segmented tariff  $C_{SG}$  displays the highest share, followed by the pure capacity-based tariff pricing peak load and feed-in  $C_{LF}$  and its combination with time-varying suppliers' costs  $C_{LFS_r}$ . With increasing shares of DERs, the share of the segmented tariff  $C_{SG}$  in the best-performing tariffs decreases. On the other hand, the share of the pure capacity-based tariff pricing peak load and feed-in  $C_{LF}$  slightly and its combination with time-varying suppliers' costs  $C_{LFS_r}$  in the best-performing tariffs significantly increase with increasing shares of DERs. Generally, the share of purely energy-based tariffs in the best-performing tariffs is comparably low in all investigated scenarios, reaching a maximum of 12 % in *Scenario 4* (comprising 6 % constant energy-based  $E_c$  and 6 % grid residual load based tariff  $E_r$ ).

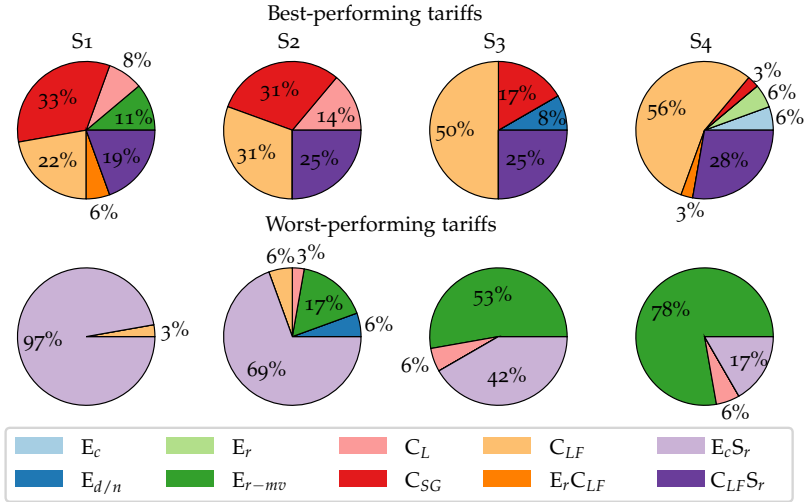


FIGURE 18.14: Share of best (top) and worst (bottom) rated tariff options in the different scenarios.

On the other hand, the largest share of worst-performing tariffs in all scenarios comprises time-varying purely energy-based tariffs, ranging from 91 - 97%. In *Scenario 1*, the combination of constant energy-based network tariff with time-varying suppliers' costs  $E_cS_r$  performs worst in almost all cases. Its share decreases with increasing shares of DERs, while the share of the tariff based on the grid residual load at the HV/MV-transformer  $E_r$  increases.

The weighting of the different criteria influences the final rating. Figure 18.15 therefore displays the influence of the weighting on best-performing (left) and worst-performing (right) tariffs. The division of worst-performing tariffs is relatively stable between the different weightings with  $\sim 60\%$   $E_cS_r$  and  $\sim 40\%$   $E_r-mv$ . The only significant deviation can be observed for the weighting of the politics representative. There, other tariffs, i.e.  $C_L$ ,  $C_{LF}$  and  $E_{d/n}$ , occur additionally to  $E_cS_r$  and  $E_r-mv$ .

The best-performing tariff proves to be more sensitive towards the weighting. For weightings strongly prioritising the criterion of an efficient grid, like the representatives of the authority, DSO and regulator chose, the capacity-based tariff on peak load and feed-in  $C_{LF}$  and its combination with time-varying suppliers' costs  $C_{LF}S_r$  show the highest scores in most cases.

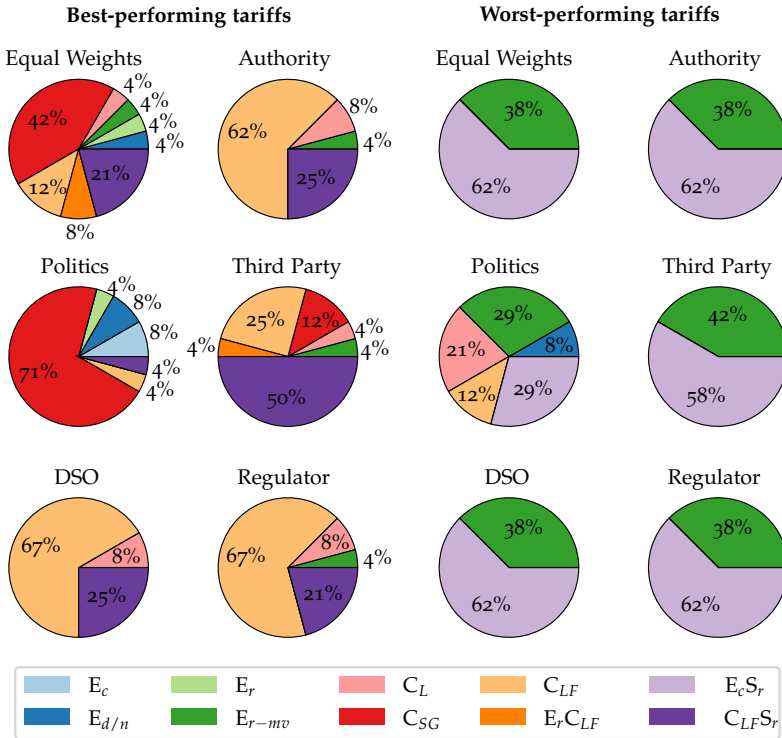


FIGURE 18.15: Share of best (left) and worst (right) rated tariff options with different weightings.

For the weighting of the third party representative, where the efficient use of electricity is rated as similarly important as an efficient grid, the combined tariff  $C_{LFSr}$  makes up a higher share than the pure capacity-based tariff  $C_{LF}$ . The politics representative with a higher preference for fairness and customer acceptance leads to a different division of best-performing tariffs, strongly dominated by the segmented tariff  $C_{SG}$ , which performs best in that criterion. The equal weighting of criteria leads to a more diverse distribution of best-performing tariffs. The segmented tariff  $C_{SG}$  also makes up the highest share in this case, followed by the combined capacity-based tariff with time-varying suppliers' costs  $C_{LFSr}$ .

While the best- and worst-performing tariffs can indicate trends between the different scenarios and criteria weightings, the difference between the first- and second-best tariff options is partly very small (see Fig. 18.13),

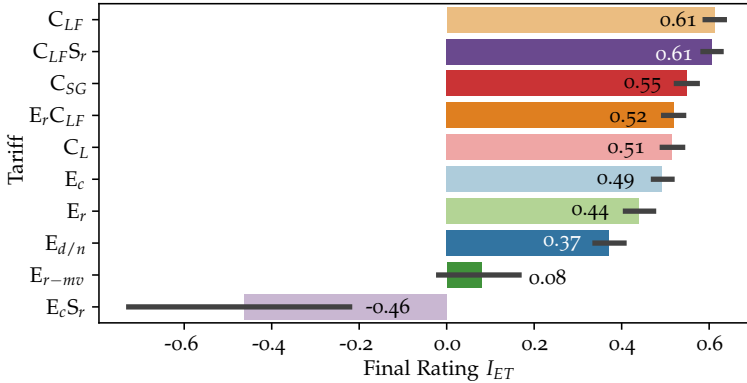


FIGURE 18.16: Mean final rating for investigated tariffs. The black bars indicate the 95 % confidence intervals.

which is not accounted for in these considerations. Figure 18.16 therefore displays the mean rating over all investigated scenarios, criteria weightings and grids. The black bars thereby indicate the 95 % confidence intervals. The results show that the first- and second-best options show very similar values, i.e. the capacity-based tariff on peak load and feed-in  $C_{LF}$  and its combination with time-varying suppliers' costs  $C_{LFS_r}$ . Other tariffs including capacity-based price components follow. These are the segmented tariff  $C_{SG}$ , the combination of peak prices on feed-in and load with a grid residual load based energy component  $E_r C_{LF}$  and the peak price on load only  $C_L$ . They all perform better than the reference tariff of constant energy-based prices  $E_c$ . In contrast, all time-varying purely energy-based tariff options perform worse, namely the tariff based on the grid residual load at MV/LV-transformers  $E_r$ , the day and night tariff  $E_{d/n}$ , the tariff based on the grid residual load at HV/MV-transformer  $E_{r-mv}$  and the combination of constant energy-based network tariff with time-varying suppliers' costs  $E_c S_r$ . The last two tariffs show high variations between the scenario variations (indicated by the large confidence intervals) while the other tariffs show relatively stable values in comparison. It indicates that the performance of  $E_{r-mv}$  and  $E_c S_r$  is more dependent on the scenario and grid than that of the other tariffs.

It should be noted that three of the six investigated combinations of criteria weightings strongly prioritise the criterion of an *efficient grid* (see Fig. 18.4), which is best met by tariffs with a peak component on both capacity and load (see Fig. 18.5). For a different set of weights, the order of tariffs

could thus change. On the other hand, higher grid reinforcement needs also lead to increased costs that the DSOs has to cover. We did not account for this fact in our investigations, where all tariffs were designed so that inflexible consumers pay the same. In reality, the tariff options would be scaled to guarantee cost recovery. Therefore, inflexible consumers would end up paying more for options that lead to high reinforcement costs and the criterion of *fairness and customer acceptance* would change accordingly. If the absolute costs for vulnerable consumers were additionally included, the capacity-based tariffs would likely perform even better compared to the other options. However, to estimate the cost change, it would be necessary to know the exact cost structure of the respective DSO, which is not openly accessible and the reason why we did not include this aspect in our investigations.

The segmented tariff  $C_{SG}$  performs relatively well even though it is only applied to the load and not the feed-in and was not scaled to increasing consumption by HPs and EVs. We therefore recommend adjusting both in future investigations and additionally considering a combination of the segmented tariff and peak price components, which might combine the advantages of both options. Lastly, all mixed tariffs assume the same magnitude of capacity- and energy-based price components. A different mix with higher values for one or the other might increase the performance and a possible extension is to optimise a mixed tariff for the overall weighted ranking of the proposed framework.

Since the framework is very flexible and can be applied to any time series data, it could also be used to evaluate other economic incentive schemes, like billing energy communities or consumer groups instead of single customers and market-based flexibility procurement. However, it would have to be assessed first whether the defined criteria are all relevant for the investigated schemes and if additional requirements should be considered. For these, new indicators would have to be defined and integrated into the framework. The combination of market-based consumption and feed-in with different network tariff options would be specifically interesting to investigate since the investigations in the previous chapter proved that fixed price time series can lead to overshooting at high DER penetrations and a market-based approach might therefore be the better option.

## 18.4 CONCLUSIONS AND POLICY IMPLICATIONS

We propose a new process with stakeholder involvement to extract and measure the requirements of network tariffs, which we applied to a Swiss use case. The relevant criteria for evaluating network tariffs were identified through stakeholder interviews and translated to an open-source evaluation framework using a MCDA approach based on the AHP. Lastly, we applied the new framework to ten different electricity tariffs to showcase its usability.

According to the stakeholders interviewed, network tariffs should fulfil the criteria of an *efficient grid*, *fairness and customer acceptance* and *consistency with political objectives*. An efficient grid requires the reduction of usage- and capacity-related costs as well as cost reflection. Furthermore, two relevant objectives were mentioned for consistency with political objectives: the *expansion of DERs* and *efficient use of electricity*.

Regarding the relative importance of the criteria, there is no common understanding of which criterion is the most important among the interviewed experts. While the representatives of the authority, DSO and regulator weigh an efficient grid as the most important criterion, the representatives of politics and third party choose fairness and customer acceptance and consistency with political objectives, respectively. Converging to a common understanding of the relative importance of the different criteria should therefore be a focus in defining a suitable future network tariff.

We translated the identified design criteria to a quantitative evaluation framework, which is modular, easily adaptable and available open source. It can thus be adapted to the local situation for specific DSOs and further refined in future work. The framework facilitates the comparison of different tariff designs and can be applied to various scenarios and tariff options. For the case study, we expanded it to cover electricity tariffs, i.e. the combination of network tariffs and suppliers' costs.

We compared ten tariffs (different energy- and capacity-based network tariffs in combination with constant or time-varying suppliers' costs) in scenarios with low and high penetration of DERs. The results show that tariffs including capacity-based price components on average perform better than the reference constant energy-based tariff over all investigated scenario combinations. On the other hand, time-dependent energy-based prices perform worse than the reference, supporting the political process to move away from a purely energy-based network tariff. However, the performance

also depends on the chosen criteria weighting, the grid and penetration of DERs. With increasing DERs penetrations, the tariffs with capacity-based price components increasingly outperform the purely energy-based options, stressing the importance of adapting network tariffs to a changing environment.

We showed that the optimal tariff highly depends on the local situation in the grids and the weighting of criteria. The choice of adapted tariffs should therefore always be subject to the negotiation of different stakeholder groups. Our open-source evaluation tool can be a first step towards a more informed and transparent decision process. It can help visualising the complex interplay between the different, partly contradicting goals of network tariffs and simplify the choice of a suitable tariff option for future electricity systems with high penetrations of DERs.



## CONCLUSION

---

### 19.1 MAIN FINDINGS

Energy systems worldwide are transitioning towards a more sustainable energy supply, largely depending on renewable energy sources. In Germany, photovoltaics (PV) and wind generation most likely dominate a fully renewable energy system. To ensure a secure power system operation with high shares of such variable renewable energy sources (VRES), power system flexibility is a key enabler, and flexibility needs are increasing. This thesis investigated the possible contribution of decentralised flexibility options, namely electric vehicles (EVs), residential heat pumps (HPs) and battery energy storage systems (BESS) in terms of meeting geographic and temporal flexibility needs and what are good economic incentives to untap their flexibility potential.

In order to quantify these flexibility needs and their supply, a range of tools and models have been developed in the framework of this thesis (further detailed in the following Section 19.2). The tools and investigations of this work thereby focused on the temporal flexibility needs of the German system and geographic flexibility needs within typical German distribution grids. Geographic flexibility needs were measured by required grid reinforcement and the resulting costs, and temporal flexibility needs by required energy shifting on different time scales. The time scales considered in this work were short-term shifting on a daily scale, medium-term shifting up to a month and long-term shifting covering anything longer than that. The main insights and key findings gained with the help of these concepts are summarised along the research questions (RQs) posed in the introduction of this thesis in the following.

**RQ1:** *What is the flexibility need in a renewable German power system?*

- Variable renewable energy sources lead to an increase in temporal and geographic flexibility needs. Additionally, the uptake of decen-

tralised sector coupling technologies, i.e. residential EVs and HPs, increases geographic and temporal flexibility needs if uncoordinated. The impact of HPs is thereby higher than that of EVs.

- Under the current load and mix of PV and wind generation, the temporal flexibility needs increase between two- to three-fold for a system powered by PV and wind only compared to a continuous power generation (representing the preferred operation of conventional base load power plants). Increasing shares of decentralised flexibility options further change the flexibility needs in this renewable German power system. Introducing 100% EVs and HPs, i.e. every private car is replaced by an EV and every residential building owns a HP, increases the temporal flexibility needs by up to 21% and 30% when uncoordinated. EVs thereby mainly increase short- and medium-term flexibility needs, while HPs primarily cause an increase in long-term energy shifting. Integrating 100% BESS under reference operation, i.e. every residential building owns a BESS, decreases the flexibility needs by 12%, thereby mainly supplying short-term flexibility needs.
- The generation mix influences the temporal flexibility needs in a 100% renewable German system powered by PV and wind only. The resulting temporal flexibility needs furthermore depend on the interplay of generation and demand. With the current demand, a mix of 25% PV and 75% wind generation minimises the total temporal flexibility needs. While EVs do not change the optimal mix, it shifts to 20% PV and 80% wind generation for 100% HP penetration and to 35% PV and 65% wind for 100% BESS. The total change in flexibility needs and the division into short-, medium- and long-term flexibility needs caused by the integration of EVs, HPs and BESS also change with the generation mix. Choosing the right generation mix for the expected uptake of distributed energy resources (DERs) can therefore limit the additional temporal flexibility needs.
- The geographic flexibility needs caused by the integration of distributed energy resources depend on the technology and penetration. Residential PV lead to mean costs of 74€/kW in the investigated grids. Whether or not the PV system is equipped with a BESS thereby does not significantly change the costs. This result showcases that the currently dominant operational strategy maximising self consumption does not benefit the grid. Home charging stations for EVs and residential HPs lead to mean costs of 19€/kW and 185€/kW in the

investigated grids. For a simultaneous integration of EVs, HPs and PVs with BESS, HPs prove to be the main driver of reinforcement costs. With increasing shares of DERs, the marginal costs for their integration increase since larger parts of the grids reach their limits.

**RQ2:** *What share of this flexibility need can be supplied by decentralised flexibility options?*

- Using the flexibility of decentralised flexibility options offers a large potential to decrease geographic and temporal flexibility needs.
- The temporal flexibility needs and reduction potential of decentralised flexibility in a 100 % renewable German power system with generation only from PV and wind again depend on the generation mix. The flexibility needs at the optimal mix of PV and wind can be reduced by 54.9 % for an optimised operation of EVs, HPs and BESS compared to the reference operation if every private car is replaced an EV and every residential building is equipped with a HP and BESS. Compared to the optimal generation mix and the current demand (i.e. without the integration of EVs, HPs and BESS) this signifies a reduction of 35.3 %. The flexibility of EVs, HPs and BESS can thereby mainly supply the short-term flexibility needs (shifting within one day). When shifting between different charging sessions is possible for EVs, they can additionally reduce medium-term shifting (shifting up to one month). The long-term shifting cannot be reduced and would have to be supplied by other sources.
- The geographic flexibility needs in terms of distribution grid reinforcement increase with increasing shares of DERs even if their flexibility is utilised for a grid-friendly operation. The total costs can be decreased by roughly 40 % for the combined integration of DERs if the assets are operated grid-optimised. For a separate investigation of smart EV charging, a rule-based reduced charging achieved similar reduction in grid reinforcement costs as the optimised operation. This approach could therefore pose a simple but effective alternative to the centrally optimised charging.

**RQ3:** Which economic incentive systems are most suitable to stimulate a system-friendly operation of decentralised flexibility options?

- Economic incentives can have positive and negative effects on flexibility needs and supply. Time-varying energy-based prices can lead to higher simultaneities and increase temporal and geographic flexibility needs. Peak-based prices, on the other hand, can counteract this effect and reduce new peaks and resulting grid reinforcement. On their own, these price components do not largely influence the temporal flexibility needs but can prevent overshooting for high penetrations of decentralised flexibility, which occurs for time-varying purely energy-based tariffs. Summarising, economic incentives should be carefully designed to account for geographic and temporal flexibility needs. The combination of time-varying energy-based prices and capacity-based peak prices on load and feed-in pose a promising option to reduce temporal and geographic flexibility needs, especially at low DER penetrations. At high penetrations of decentralised flexibility, a direct market integration instead of the energy-based price component should be considered to prevent overshooting.
- Electricity tariffs, as one specific economic incentive, follow many different, partly contradicting goals. The most important design criteria to meet these goals (determined by expert interviews) are an *efficient grid*, *fairness and customer acceptance* and *consistency with other political objectives*. These criteria are met differently well by the investigated tariff options and a different tariff option performs best for each criterion. Therefore, the best performing tariff also depends on the weighting of criteria. Overall, tariffs purely based on time-varying energy-based price components perform worse than tariffs including capacity-based price components in our investigations. Capacity-based pricing should therefore be included in future tariff designs, especially at high penetrations of DERs.

## 19.2 SUMMARY OF TOOLS

In the course of this PhD research, several tools were developed or expanded to investigate the role of decentralised flexibility in renewable power systems. Figure 19.1 displays the tools, which are all available open source and can serve as the basis for future investigations. Their scope and functionalities are briefly summarised in the following.

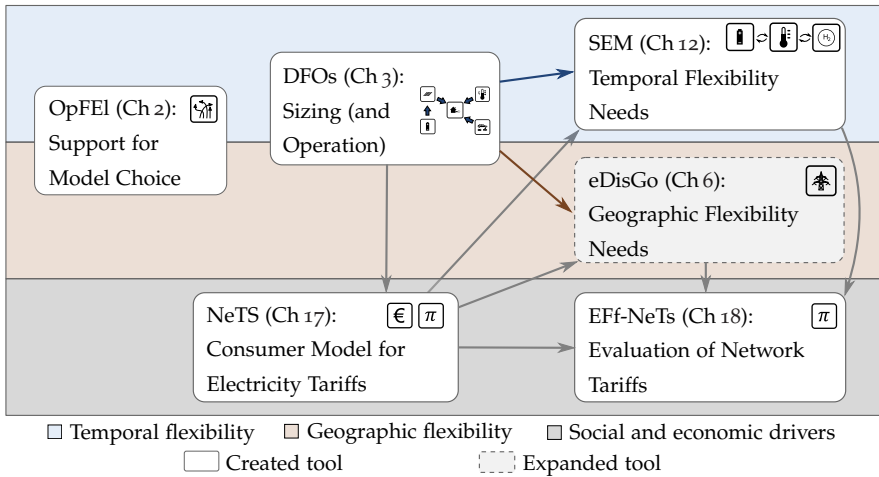


FIGURE 19.1: Open source tools created or expanded in the course of this dissertation.

OpFEL is a tool for decision support for the right existing model. It focuses on the representation of different flexibility options and relevant aspects for investigations concerning flexibility assessments. Since flexibility is relevant on a wide range of geographic and temporal scales, and many technologies can supply flexibility needs, the model choice highly depends on the research question at hand and the focus of the study. Therefore, OpFEL allows the definition of relevant criteria and examines to which extent these aspects defined by the user are covered in the investigated models. Lastly, it returns a final ranking based on a weighted sum. It was used in Part I of this thesis to choose the model for distribution grids.

DFOs is a tool for the sizing and reference operation of DERs, namely EV home charging stations, HPs and PV systems with BESS. The so-obtained pool of DERs served as the basis for all further investigations of the PhD research. The tool is closely linked to the existing tool eDisGo, which was expanded with the implementation of a grid-optimised operation of decentralised flexibility options based on a linear optimal power flow formulation. Together, both tools can be used to estimate the required grid reinforcement costs under reference and optimised operation for increasing shares of DERs (using the previously existing grid reinforcement methodology implemented in eDisGo). Both were used in Part II of this thesis to estimate

the geographic flexibility needs in representative German distribution grids and their supply by decentralised flexibility options.

A model for temporal flexibility quantification is provided with SEM. It measures the required energy shifting on different time scales to balance electricity generation and demand as a measure for temporal flexibility needs. It furthermore allows to assess the flexibility supply by decentralised flexibility options. This model (with input data obtained from the tool DFOs) was used in Part III of this thesis to estimate the flexibility needs in a fully renewable German power system and the influence of increasing shares of decentralised flexibility options on temporal flexibility needs and supply.

Well designed electricity tariffs can help to leverage the flexibility potential of decentralised flexibility options. The developed consumer model NETS allows to investigate the influence of different electricity tariff designs on residential consumption patterns. It economically optimises the operation of residential consumers with different combinations of DERs and was used in Part IV of this thesis to compare different combinations of suppliers' costs and network tariffs. The resulting consumption patterns were therefore used as input for EDISGo and SEM to measure the effect on geographic and temporal flexibility needs and supply.

Choosing a suitable tariff does not solely depend on their effect on flexibility needs but on a variety of decision criteria. To this end, the tool EFF-NETS provides decision support for choosing network or electricity tariffs under increasing penetrations of DERs. It combines the most important decision criteria obtained from stakeholder interviews in a quantitative evaluation framework, namely the criteria of an *efficient grid*, *fairness and customer acceptance* and *consistency with other political goals*. The tool was used in Part IV of this thesis to rank the investigated tariffs. Therefore, expert weightings of the decision criteria, the consumer profiles and costs provided by NETS, and resulting flexibility needs obtained with EDISGo and SEM were used as input to obtain a final ranking of the investigated tariffs.

### 19.3 FURTHER RESEARCH NEEDS

Although this thesis tries to touch on the most critical aspects of decentralised flexibility in renewable power systems, several aspects need further investigation and provide avenues for future research:

- The investigations focused on residential consumers, largely omitting flexibility from other sources. In future investigations, the interplay with industrial demand side management, large-scale HPs or storage and other flexibility options should be included. Furthermore, the flexibility provided by the thermal inertia of the building itself was not accounted for in this thesis. Incorporating a more accurate building model which leverages building flexibility would be an interesting extension of this work.
- In the grid studies, only rural and sub-urban grids were investigated since they were found to be affected stronger by the integration of DERs in the literature. However, including urban grids and expanding the carried-out investigations to a representative study for the whole of Germany would be an interesting use case and could further increase the robustness of the results.
- Geographic and temporal flexibility needs were investigated independently in this thesis. However, in reality, both are highly interconnected and influence each other. Furthermore, both compete against each other in terms of utilisation of available flexibility. A combined investigation of both would help find an optimal balance between geographic and temporal flexibility needs. First investigations showed little influence of distribution grid constraints on the possible reduction of energy shifting. However, further investigation is required to draw final conclusions.
- The study on electricity tariffs showed that, in some cases, incentives for individual consumers counteract local synergies between different consumers. It would be interesting to study concepts that incentivise groups of consumers like energy communities to leverage these local synergies. Furthermore, the market integration of decentralised flexibility should be investigated since it was shown that at high DER penetrations, purely price-based incentives lead to overshooting.
- This thesis mainly focused on the technical potential of decentralised flexibility to decrease geographic and temporal flexibility needs. Estimating the maximum potential naturally comes with many simplifications and is far from the realisable potential. Therefore, it would be interesting to include aspects like customer response, willingness to participate, uncertainties in demand and VRES generation into further investigations.

- Lastly, changes in consumer behaviour are not accounted for in this thesis. However, there are many efforts to achieve sufficient behaviour, and a changing world will likely change how electricity is consumed. As an example, increasing temperatures might make the use of air conditioning more common in future scenarios. Such developments should be included in future investigations.

### *Recommendations*

Despite these alleys for future research, this thesis provides valuable insights and a set of open source tools that can be used for further investigations on decentralised flexibility in renewable power systems. From these, the following recommendations are derived.

- Decentralised flexibility options offer a large potential to supply geographic and temporal flexibility needs. This potential should be used and future research and implementation should focus on how to untap it.
- Adapted electricity tariffs are one possible measure to leverage the flexibility potential of decentralised flexibility options if designed well. However, they can also have the opposite effect. While pure energy-based tariffs can lead to unwanted synchronisation and increase in geographic and temporal flexibility needs, a simple additional peak-based component on both load and feed-in can largely avoid these negative effects. We therefore recommend to use a combination of energy- and power-based price components to limit the risk of synchronisation.
- Furthermore, the negative effects seem manageable at lower penetrations of distributed energy resources. An early adoption of different tariff designs could therefore allow to gather data and learn about consumer reaction and acceptance at a low risk for the distribution grids and should therefore be pushed.
- Lastly, the results imply that for high penetrations of distributed energy resources and high levels of flexibility, passive price incentives might not be the right measure of choice. A direct integration into the market through aggregators might be the preferable option in this case and should be further investigated.

Summarising, the next step should be to translate the developed insights and recommendations into the real world and to start to leverage decentralised flexibility from an early stage.



## APPENDIX



---

 MODELLING OF FLEXIBILITY OPTIONS
 

---

## A.1 OVERVIEW OF MODELS AND THEIR EVALUATION

TABLE A.1: Overview of models (m) and frameworks (f) under consideration

Name (m/f)	Modelling language	Short description
BACKBONE (f)	GAMS	BACKBONE is an adaptable energy systems modelling framework. It is an optimisation framework, based on mixed-integer programming. [255]
BALMOREL (m)	GAMS	BALMOREL is a partial equilibrium model for optimising and analysing energy systems focusing on the international electricity and combined heat and power sector. [256]
CALLIOPE (f)	Python	CALLIOPE is an energy systems modelling framework with a high temporal and spatial resolution. The framework is based on scale-agnostic formulation. [257]
DIETER (m)	GAMS	DIETER stands for <i>dispatch and investment evaluation tool with endogenous renewables</i> . The model was developed to study the role of storage and further flexibility options. It identifies cost-minimising combinations of power production, demand-side-management and storage capacities, taking into consideration reserve and wholesale markets. [258]
DISPA-SET (m)	GAMS & Python	DISPA-SET is an optimisation model for unit-commitment and dispatch. It focuses on flexibility and balancing problems. [259]
eGo (m)	Python	eGo stands for <i>electricity grid optimisation</i> . The model is an intersection for the high- and medium voltage layer. It is used to simulate grid and storage development costs for all voltage layers. The two tools eTRaGo and eDisGo, parts of the eGo project, focus on the simulation of transmission and distribution grids, respectively. [74]
EMMA (m)	GAMS	EMMA stands for <i>European electricity market model</i> . It is a partial equilibrium optimisation model, which models prices, capacities, output, profits and deal flows in the electricity market. [260]

Continued on next page

Table A.1 – Continued from previous page

Name (m/f)	Modelling language	Short description
ENERGYPLAN (m)	Delphi & Pascal	ENERGYPLAN is a model for the design of energy planning strategies. It simulates the operation of national energy systems and is based on economic and technical analyses of different implementations of energy systems and investments. [261]
ENERGYSCOPE (m)	GLPK & GLPSOL	ENERGYSCOPE is a linear optimisation model for planning urban and regional energy systems for the purpose of optimising investment and operating strategies. [262]
FLEXIGIS (m)	Python	FLEXIGIS stands for <i>Flexibilisation in Geographic Information Systems</i> . It is a modelling platform for energy systems and flexibility options in urban areas. FLEXIGIS uses geo-referenced urban energy infrastructure for simulating local electricity consumption, power generation and the distribution to decentralised storage in urban settings. [263]
FRIGG (m)	Python	FRIGG is the soft-linking of frameworks to model demand flexibility through a set of differential equations and a dynamic price-making algorithm to minimise system costs. The physical side of the energy system can be modelled by well-established frameworks such as TIMES, BALMOREL or CALLIOPE. The model uses data from these frameworks, generates hourly prices and simulates the demand side. The flexibility of the demand side can be implemented by calculating energy system equilibria by returning a changed demand level to the energy system model. [264]
GRIDCAL (m)	Python	GRIDCAL is an optimisation tool for modelling transmission as well as distribution grids. It allows an extension by building or reusing parts of other models. [265]
IRENA FLEX- TOOL (m)	GLPK	IRENA FLEXTOOL stands for <i>International Renewable Energy Agency Flexibility Tool</i> . It is a detailed tool for analysing the flexibility of energy systems and their optimal costs, including innovative technologies that provide new flexibility options. [266]
OEMOF (f)	Python	OEMOF stands for <i>open energy modelling framework</i> . It is a modular open source framework for cross-sectoral, multi-regional and time-step-flexible energy system modelling, based on a linear optimisation library. [267]
OMEGALPES (m)	Python	OMEGALPES stands for <i>Generation of Optimisation Models As Linear Programming for Energy Systems</i> . It is an energy systems modelling tool for linear optimisation. OMEGALPES is based on the linear programming (LP) modeller PuLP, which is written in Python. [268]

Continued on next page

Table A.1 – *Continued from previous page*

Name (m/f)	Modelling language	Short description
OSEMOSYS (f)	GLPK & Python	OSEMOSYS stands for <i>Open Source Energy modelling System</i> . The framework enables powerful energy systems analysis and prototyping of new energy model formulations focusing on medium and long-term time scopes. It is based on linear optimisation. [269]
PANDAPOWER (m)	Python	PANDAPOWER is a simulation tool for the detailed modelling of power systems. The tool, based on the Python data analysis library pandas and the power system analysis toolbox PYPOWER is a simple network calculation program. [270]
PyPSA (m)	Python	PyPSA stands for <i>Python for Power System Analysis</i> . It is a simulation and optimisation toolbox for energy systems, especially for modelling long time-series and large-scale networks. [271]
REGION4FLEX (m)	Python	REGION4FLEX is an optimisation model for load shifting potentials in the German high voltage network, which includes the electricity and heat sector. [272]
RTTESTPSM (m)	Python	The test case renewable power system models were developed in the <i>Calliope</i> framework and are an easy way to approach energy system modelling. The models, which can be run in different optimisation modes, provide generation and transmission expansion planning, economic dispatch and unit commitment-type power system models. [273]
TIMES (f)	GAMS	TIMES stands for <i>The Integrated MARKAL-EFOM System</i> . TIMES is a energy system model generator that combines a technical engineering approach with an economic approach on energy modelling. It is based on linear programming [274]
TRANSIENT (m)	Modelica	TRANSIENT is a dynamic system simulation model library that simulates integrated energy networks in different scenarios with a high share of renewable energies. Simulations are based on differential algebraic equations. [275]
URBS (f)	Python	URBS is an optimisation model generator for capacity expansion planning and unit commitment for distributed energy systems. It is based on linear programming, and focuses on the optimisation of storage sizing and use. [276]

*Continued on next page*

Table A.1 – Continued from previous page

Name (m/f)	Modelling language	Short description
XEONA (m)	UML & C++	XEONA stands for <i>extensible entity-oriented optimisation-based network-mediated analysis</i> . XEONA is an object-oriented simulation environment designed to facilitate sustainability policies taking into account uncertainties. The model combines multi-agent simulation with high-resolution system optimisation modelling. [277]

TABLE A.2: Model rating methodology

Category	Specification	Rating
General	Geographic scope	Local (NUTS3); used, local (NUTS3) /possible, regional; used, regional; possible, national; used, national; possible, international; used, international; possible
	Temporal scope	Very short; used, very short; possible, short; used, short; possible, intermediate; used, intermediate; possible, long; used, long; possible
	Temporal resolution	<Hourly; used, <hourly; possible, hourly used; hourly; possible, intermediate; used, intermediate; possible, annual; used, annual; possible
	Probability	Yes: 1; no: 0
	Decision making	Perfect foresight & rolling horizon; myopic foresight & decision- / agent based = 1; rolling horizon; myopic foresight & decision-; agent based = 0.8, perfect foresight & rolling horizon; myopic foresight <b>or</b> perfect foresight & decision-; agent based = 0.6, rolling horizon; myopic foresight <b>or</b> decision-; agent based = 0.4, perfect foresight = 0.2, else = 0
	Social factors	Yes: 1; no: 0
Characteristics	Efficiency	Function: 1; fixed value: 0.5; ∈ operational characteristics
	Ramping	Yes: 1; no: 0; ∈ operational characteristics
	Response time	Yes: 1; no: 0; ∈ operational characteristics
	Recovery time	Yes: 1; no: 0; ∈ operational characteristics

Continued on next page

Table A.2 – *Continued from previous page*

Category	Specification	Rating
Network	Distribution grid	Defined: 1; possible: 0.5
	Transmission grid	Defined: 1; possible: 0.5
	Network extensions	Defined: 1; possible: 0.5
	Switches	Defined: 1; possible: 0.5
	Grid representation	alternating current (AC) power flow (PF) & direct current (DC) PF & inter-connectors & transfer capacity = 1; AC PF & DC PF & inter-connectors = 0.86; AC PF & DC PF & transfer capacity = 0.71; AC PF & DC PF = 0.57; AC PF & transfer capacity <b>or</b> DC PF & transfer capacity = 0.43; AC PF <b>or</b> DC PF = 0.28; else: 0
	Grid ancillary services	Spinning reserve, balancing energy, sheddable loads, feed-in management, redispatch, power factor corrections, curtailment, black start
	Import	Flow based: 1; simplified: 0.5
Supply	Coal	defined: 1; possible: 0.5
	Lignite	defined: 1; possible: 0.5
	Oil	defined: 1; possible: 0.5
	Natural gas	defined: 1; possible: 0.5
	Combined heat and power (CHP)	defined: 1; possible: 0.5
	Combined cycle gas turbine (CCGT)	defined: 1; possible: 0.5
	Open-cycle gas turbine (OCGT)	defined: 1; possible: 0.5
	Bio energy	defined: 1; possible: 0.5
	Hydro reservoirs	defined: 1; possible: 0.5
	Geothermal energy	defined: 1; possible: 0.5
Concentrated solar power	defined: 1; possible: 0.5	

*Continued on next page*

Table A.2 – Continued from previous page

Category	Specification	Rating
	PV	defined: 1; possible: 0.5
	Wind onshore	defined: 1; possible: 0.5
	Wind offshore	defined: 1; possible: 0.5
	River hydro	defined: 1; possible: 0.5
	Wave power	defined: 1; possible: 0.5
	Tidal power	defined: 1; possible: 0.5
	Proton exchange membrane fuel cell (PEMFC)	defined: 1; possible: 0.5
	Solid oxide fuel cell (SOFC)	defined: 1; possible: 0.5
	Nuclear	defined: 1; possible: 0.5
	Curtailed operation	yes: 1; no: 0; $\in$ Technology Specifications
	Minimum load	yes: 1; no: 0; $\in$ Technology Specifications
	Discrete capacity expansion	yes: 1; no: 0
Demand	Households	Defined: 1; possible: 0.5
	Industrial load	Defined: 1; possible: 0.5
	Service sector	Defined: 1; possible: 0.5
	Maximum deferrable load	Time- & type dependent = 1; Type dependent or time dependent = $\frac{2}{3}$ ; Fixed value = $\frac{1}{3}$ ; $\in$ technology specifications
	Shifting time	Yes: 1; no: 0; $\in$ technology specifications
	Price elasticity	Yes: 1; no: 0
Storage	Batteries	Defined: 1; possible: 0.5
	Storage implementation	Dynamic: 1; static: 0.5
	Ageing	Cycle ageing; calendrical ageing; $\in$ technology specifications
	Self-discharge	Yes: 1; no: 0; $\in$ technology specifications

Continued on next page

Table A.2 – *Continued from previous page*

Category	Specification	Rating
	pumped hydro storage (PHS)	Defined: 1; possible: 0.5
	compressed air energy storage (CAES)	Defined: 1; possible: 0.5
	Capacitors	Defined: 1; possible: 0.5
	Flywheels	Defined: 1; possible: 0.5
	Power-to-gas	Defined: 1; possible: 0.5
	Power-to-hydrogen	Defined: 1; possible: 0.5
Sector coupling	Heat pumps	Defined: 1; possible: 0.5
	Electric vehicles	Defined: 1; possible: 0.5
	Synthetic fuels	Defined: 1; possible: 0.5
	Heat storage	Defined: 1; possible: 0.5
	Vehicle-to-grid	Defined: 1; possible: 0.5
	Heat sector	Endogenous disaggregated technology & endogenous disaggregated demand = 1; Endogenous disaggregated technology <b>or</b> endogenous disaggregated demand = $\frac{2}{3}$ ; Exogenous aggregated demand = $\frac{1}{3}$ ; Heat sector excluded or not specified = 0
	Transport sector	Endogenous disaggregated technology & endogenous disaggregated demand = 1; Endogenous disaggregated technology <b>or</b> endogenous disaggregated demand = $\frac{2}{3}$ ; Exogenous aggregated demand = $\frac{1}{3}$ ; Transport sector excluded or not specified = 0
	Sector coupling demand	If power-to-gas <b>or</b> power-to-hydrogen <b>or</b> heat pumps <b>or</b> electric vehicles was ticked as defined <b>or</b> possible: Shifting time: yes = $\frac{1}{3}$ ; Price elasticity: yes = $\frac{1}{3}$ ; Rating of maximum deferrable load derived by 3; $\in$ technology specifications
	Sector coupling supply	If CHP was ticked as defined <b>or</b> possible: Minimum load: yes = 0.5; Discrete power expansion: yes = 0.5; $\in$ technology specifications

*Continued on next page*

Table A.2 – Continued from previous page

Category	Specification	Rating
	Sector coupling storage	If synthetic fuels <b>or</b> heat storage <b>or</b> vehicle-to-grid was ticked as defined <b>or</b> possible: Self-discharge: yes = $\frac{1}{3}$ ; Cycle ageing: yes = $\frac{1}{6}$ ; Calendrical ageing: yes = $\frac{1}{6}$ ; Storage implementation: dynamic = $\frac{1}{3}$ ; Storage implementation: fixed; static = $\frac{1}{6}$ ; $\in$ technology specifications

## A.2 ADDITIONAL RESULTS FOR INDIVIDUAL FLEXIBILITY CATEGORIES

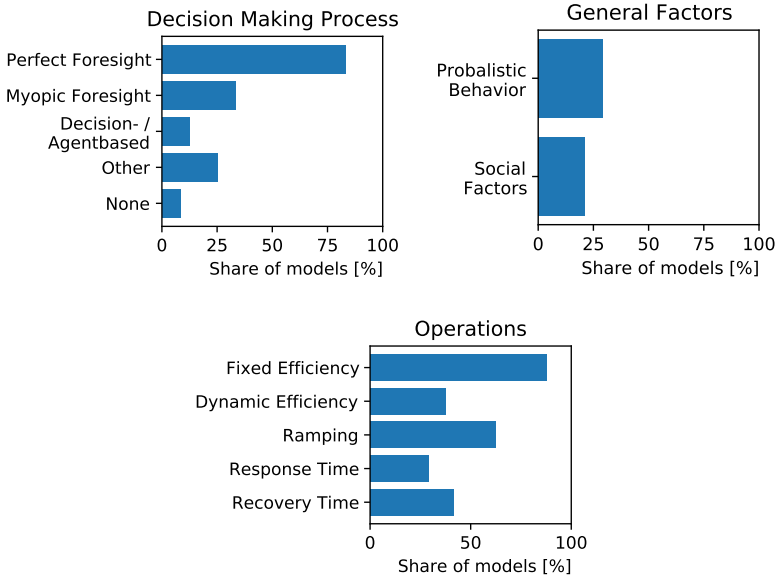


FIGURE A.1: Representation of decision-making processes (upper left), probabilistic behaviour and social factors (upper right) and operational characteristics (bottom)

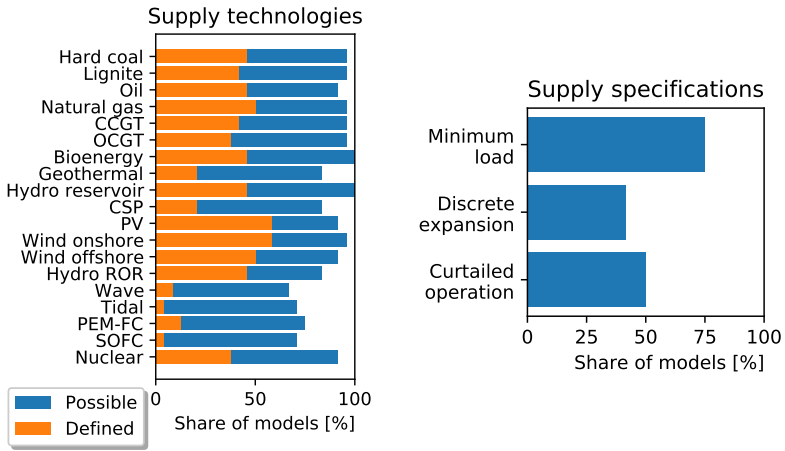


FIGURE A.2: Representation of supply-side technologies (left) and specifications (right)

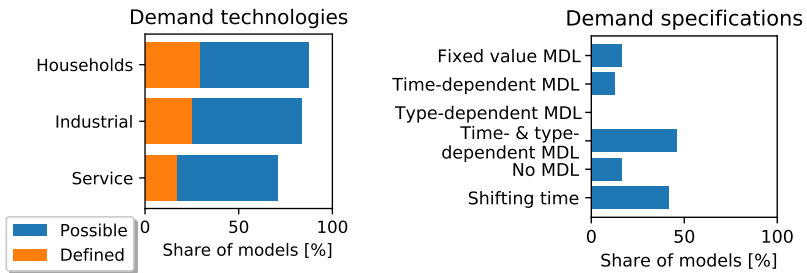


FIGURE A.3: Representation of demand-side technologies (left) and specifications (right)

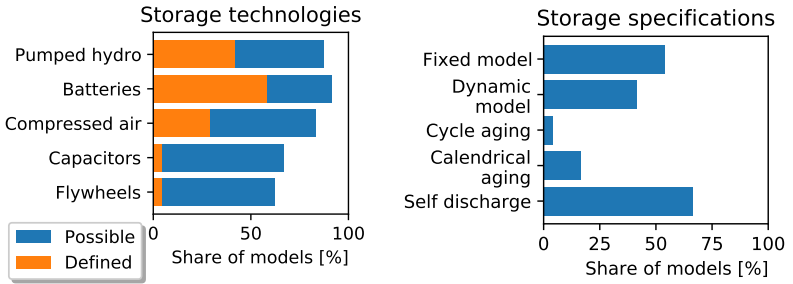


FIGURE A.4: Representation of storage technologies (left) and specifications (right)

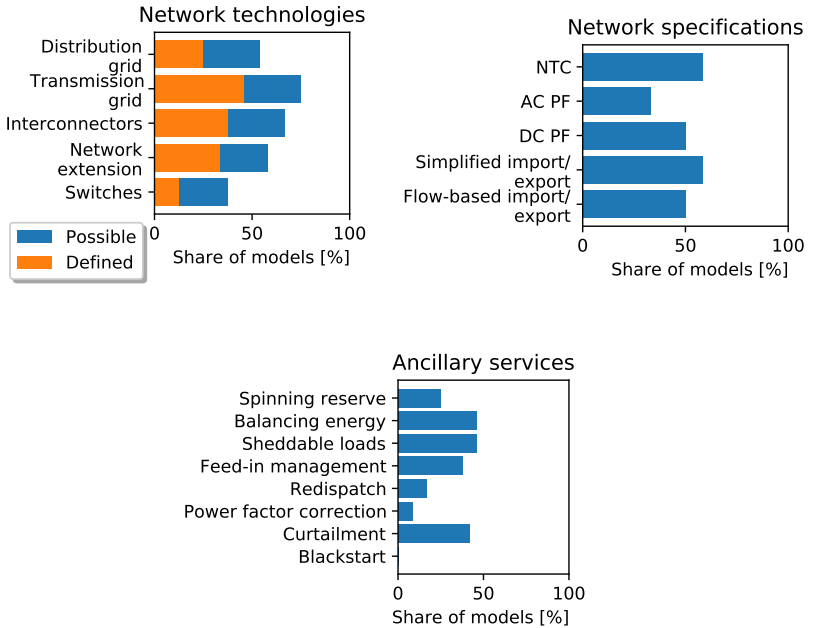


FIGURE A.5: Representation of network technologies (upper left), specifications (upper right) and ancillary services (bottom)

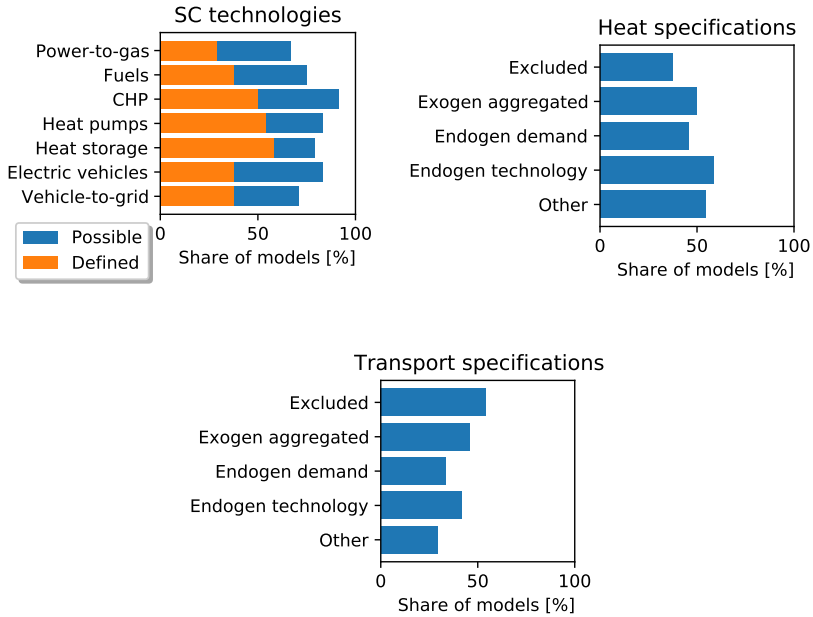


FIGURE A.6: Representation of sector coupling technologies (upper left), heat (upper right) and transport sectors (bottom)

### A.3 MODELLING OF DISTRIBUTION GRIDS

The traditional planning of grids is based on worst case analysis using simultaneity factors [22]. To compare our time series based approach with the traditional grid planning, we calculate the reinforcement costs for both cases (see Fig. 3.8). We use the standard simultaneity factors defined in eDISGo, which are summarised in Tab. A.3. The simultaneity factors are defined for the load and feed-in case and are differentiated for the medium voltage (MV) and the low voltage (LV). The values are inspired by other technical reports [85], [278].

TABLE A.3: Standard simultaneity factors as defined in eDISGo

Technology	Load Case		Feed-in Case	
	MV	LV	MV	LV
Conventional load	1.0	1.0	0.15	0.1
Heat pumps	0.8	1.0	0.0	0.0
Private charging points	0.2	1.0	0.0	0.0
Public charging points	1.0	1.0	0.0	0.0
Photovoltaic	0.0		0.85	
Wind	0.0		1.0	
Other generation	0.0		1.0	

# B

## ADDITIONAL MATERIAL ON THE EVALUATION OF TARIFF DESIGNS

---

The values for the relative weights chosen by the interviewed experts are presented in Tab. B.1, and indicator values for the low and high flexibility scenarios in Tab. B.2.

All mathematical symbols are summarised in Tab. B.3 and Tab. B.5. Table B.3 includes the sets used in the sub- and super-scripts and Tab. B.5 the indicators and relevant parameters.

TABLE B.1: Weights in percent for the investigated criteria determined by the interviewed experts.

<b>Weights [%]</b>	<b>DSO</b>	<b>Authority</b>	<b>Regulator</b>	<b>Politics</b>	<b>Third Party</b>
$W_{EG}$	78.5	72.9	79.6	9.1	45.5
$W_{FAC}$	14.9	16.3	12.1	45.5	9.1
$W_{EDER}$	3.3	2.2	4.1	34.1	11.4
$W_{EEU}$	3.3	8.7	4.1	11.4	34.1

TABLE B.2: Indicator values for investigated tariffs in Scenario 1 (low flexibility) and Scenario 4 (full flexibility) of grid PV-2.

	Scenario 1									
	$E_c$	$E_{d/n}$	$E_r$	$E_{r-mv}$	$C_L$	$C_{SG}$	$C_{LF}$	$E_r C_{LF}$	$E_c S_r$	$C_{LF} S_r$
Efficient Grid - $I_{NT}^{EG}$	0.35	0.29	0.47	0.29	0.86	0.56	0.97	0.87	-1.08	0.96
Fairness and Customer Acceptance - $I_{NT}^{FCA}$	0.56	0.53	0.53	0.55	0.56	0.62	0.56	0.55	0.56	0.56
Expansion of DERs - $I_{NT}^{EDER}$	1.10	1.15	1.07	1.07	0.92	1.12	0.80	1.07	1.10	0.80
Efficient Use of Electricity - $I_{NT}^{EEU}$	0.75	0.73	0.74	0.74	0.62	0.69	0.62	0.66	0.77	0.63
	Scenario 4									
	$E_c$	$E_{d/n}$	$E_r$	$E_{r-mv}$	$C_L$	$C_{SG}$	$C_{LF}$	$E_r C_{LF}$	$E_c S_r$	$C_{LF} S_r$
Efficient Grid - $I_{NT}^{EG}$	0.36	0.07	0.18	-0.57	0.30	0.40	0.80	0.72	-0.51	0.74
Fairness and Customer Acceptance - $I_{NT}^{FCA}$	0.42	0.43	0.46	0.43	0.44	0.42	0.44	0.45	0.42	0.44
Expansion of DERs - $I_{NT}^{EDER}$	0.50	0.50	0.50	0.50	0.50	0.50	0.50	0.50	0.50	0.50
Efficient Use of Electricity - $I_{NT}^{EEU}$	0.75	0.68	0.69	0.69	0.59	0.70	0.57	0.60	0.74	0.61

TABLE B.3: Sets used in sub- and superscripts.

<b>Name</b>	<b>Description</b>
<i>EC</i>	<b>Evaluation Criteria</b>
<i>EG</i>	Criterion of an efficient grid (= cost-reflection)
<i>FAC</i>	Criterion of fairness and customer acceptance
<i>PO</i>	Criterion of other political objectives
<i>SC</i>	<b>Sub-Criteria</b>
<i>EDER</i>	Sub-criterion of expansion of distributed energy resources
<i>EEU</i>	Sub-criterion of efficient use of electricity
<i>ROCR</i>	Sub-criterion of reflection of capacity-related costs
<i>ROUR</i>	Sub-criterion of reflection of usage-related costs
<i>NT</i>	<b>Network Tariffs</b>
<i>VT</i>	Volumetric tariff, used as the reference; equivalent to $E_c$
<i>S</i>	<b>Scenarios</b>
<i>S1- S4</i>	Scenarios with respectively 10% ( <i>S1</i> ), 50% ( <i>S2</i> ), 90% ( <i>S3</i> ) and 100% ( <i>S4</i> ) of residential loads owning HPs, EVs and PV-battery-systems
<i>SQ</i>	Status quo
<i>CG</i>	<b>Customer Groups</b>
<i>HH</i>	Inflexible consumers
<i>EV</i>	EV owners
<i>HP</i>	HP owners
<i>PV</i>	PV owners
<i>PV &amp; BESS</i>	Owners of PV-battery-systems
<i>U</i>	All users
<i>VU</i>	Vulnerable users
<i>T</i>	<b>Time Steps</b>
<i>T<sup>peak</sup></i>	Subset of time steps when 10% highest aggregated power peaks occur

TABLE B.5: Indicators and parameters used in the evaluation framework.

Name	Description	Unit
$C_{NT}$	Total costs under network tariff $NT$	[CHF]
$C_{u,NT}$	Costs paid by user $u$ under network tariff $NT$	[CHF]
$c_{u,NT}$	Share of costs paid by user $u$ in overall costs under network tariff $NT$	[-]
$C_{NT}^{after}$	Costs paid after purchasing a DER under network tariff $NT$	[CHF]
$C_{NT}^{before}$	Costs paid before purchasing a DER under network tariff $NT$	[CHF]
$C_{NT}^{CR}$	Capacity-related costs under network tariff $NT$	[CHF]
$c_{NT}^{CR}$	Share of usage-related costs in overall costs under network tariff $NT$	[-]
$C_{NT}^{UR}$	Usage-related costs under network tariff $NT$	[CHF]
$c_{NT}^{UR}$	Share of usage-related costs in overall costs under network tariff $NT$	[-]
$CC_{NT}$	Aggregated contracted capacity under network tariff $NT$	[kW]
$cc_{u,NT}$	Share of capacity contracted by user $u$ in aggregated contracted capacity under network tariff $NT$	[-]
$cc'_{u,NT}$	Adjusted share of capacity contracted by user $u$ in aggregated contracted capacity under network tariff $NT$	[-]
$CCR_{NT}$	Indicator for the reduction of capacity-related costs under network tariff $NT$	[-]
$cr_{u,NT}^{DERs}$	Costs for user or user group $u$ after purchasing DERs (PV and PV-battery-system) under network tariff $NT$ relative to the costs before purchasing the DERs	[-]
$cr_{u,NT}^{der}$	Costs for user or user group $u$ by purchasing DER $der$ (PV or PV-battery-system) under network tariff $NT$ relative to the costs before purchasing the DER	[-]
$g_u$	Group share of user or user group $u$ in total number of users	[-]
$I_{NT}$	Overall ranking of network tariff $NT$	[-]
$I_{NT}^i$	Indicator for the (sub-)criterion $i$ under network tariff $NT$ , $i \in \{EG, FAC, EDER, EEU\}$	[-]
$P_{NT}^{peak}$	Aggregated power peak under network tariff $NT$	[kW]
$P_{u,NT}^{peak}$	Contribution of user $u$ to aggregated power peak under network tariff $NT$	[kW]
$p_{u,NT}$	Share of aggregated power peak caused by user $u$ under network tariff $NT$	[-]

<b>Name</b>	<b>Description</b>	<b>Unit</b>
$p'_{u,NT}$	Adjusted share of aggregated power peak caused by user $u$ under network tariff $NT$	[-]
$P(t)$	Aggregated power drawn from overlying grid at time step $t$	[kW]
$PE_{NT}$	Aggregated purchased electricity under network tariff $NT$	[kWh]
$PE_{u,NT}$	Purchased electricity of user or user group $u$ under network tariff $NT$	[kWh]
$pe_{u,NT}$	Share of purchased electricity of user or user group $u$ in aggregated purchased electricity under network tariff $NT$	[-]
$Q(p)$	Lowest power value within share of $p$ highest aggregated power peaks	[kW]
$rc_{u,NT}$	Relative cost share paid by user or user group $u$ (in relation to their group share) under network tariff $NT$	[-]
$ROC_{NT}$	Indicator for the reflection of costs under network tariff $NT$	[-]
$ROC_{NT}^{corr}$	Indicator for the correlation between cost contribution and paid costs under network tariff $NT$	[-]
$ROC_{NT}^{slope}$	Indicator for the slope of a linear regression between cost contribution and paid costs under network tariff $NT$	[-]
$ROE_{NT}$	Indicator for the reflection of purchased electricity under network tariff $NT$	[-]
$ROE_{NT}^{corr}$	Indicator for the correlation between purchased electricity and paid costs under network tariff $NT$	[-]
$ROE_{NT}^{slope}$	Indicator for the slope of a linear regression between purchased electricity and paid costs under network tariff $NT$	[-]
$SER_{NT}$	Indicator of the reduction in total shifted energy under network tariff $NT$	[-]
$UCR_{NT}$	Indicator for the reduction of usage-related costs under network tariff $NT$	[-]
$W_i$	Relative importance of evaluation criterion $i$ on first level of hierarchy	[-]
$W'_j$	Relative importance of sub-criterion $j$ on the second level of hierarchy	[-]
$X_{NT}$	Placeholder for parameter value under network tariff $NT$	
$X_{ref}$	Placeholder for reference value of a certain parameter	

<b>Name</b>	<b>Description</b>	<b>Unit</b>
$\beta_0, \beta_1$	Y-interception and slope of a linear regression function between paid cost share and cost contribution	[-]
$\beta_2, \beta_3$	Y-interception and slope of a linear regression function between paid cost share and purchased electricity	[-]
$\pi_{buy}$	Price for electricity purchased from the grid	[CHF/kWh]
$\pi_{NT}$	Price values under network tariff <i>NT</i>	[CHF/kW(h)]
$\pi_{sell}$	Price for electricity sold to the grid	[CHF/kWh]

## BIBLIOGRAPHY

---

- [1] D. Gielen, F. Boshell, D. Saygin, M. D. Bazilian, N. Wagner, and R. Gorini, "The role of renewable energy in the global energy transformation", *Energy Strategy Reviews*, vol. 24, 38, 2019.
- [2] P. D. Lund, J. Lindgren, J. Mikkola, and J. Salpakari, "Review of energy system flexibility measures to enable high levels of variable renewable electricity", *Renewable and Sustainable Energy Reviews*, vol. 45, 785, 2015.
- [3] H. Kondziella and T. Bruckner, "Flexibility requirements of renewable energy based electricity systems – a review of research results and methodologies", *Renewable and Sustainable Energy Reviews*, vol. 53, 10, 2016.
- [4] A. Ulbig and G. Andersson, "Analyzing operational flexibility of electric power systems", *International Journal of Electrical Power & Energy Systems*, vol. 72, 155, 2015.
- [5] I. Batas Bjelić, N. Rajaković, G. Krajačić, and N. Duić, "Two methods for decreasing the flexibility gap in national energy systems", *Energy*, vol. 115, 1701, 2016.
- [6] International Energy Agency (IEA), *Will pumped storage hydropower expand more quickly than stationary battery storage?*, 2019. Available: <https://prod.iea.org/articles/will-pumped-storage-hydropower-expand-more-quickly-than-stationary-battery-storage>.
- [7] J. Rosenow, D. Gibb, T. Nowak, and R. Lowes, "Heating up the global heat pump market", *Nature Energy*, vol. 7, no. 10, 901, 2022.
- [8] International Energy Agency (IEA), *Global heat pump sales continue double-digit growth*, 2023. Available: <https://www.iea.org/commentaries/global-heat-pump-sales-continue-double-digit-growth>.
- [9] International Energy Agency (IEA), *Global EV Outlook 2023*, 2023. Available: <https://www.iea.org/reports/global-ev-outlook-2023>.

- [10] A. Pena-Bello, P. Schuetz, M. Berger, J. Worlitschek, M. K. Patel, and D. Parra, "Decarbonizing heat with PV-coupled heat pumps supported by electricity and heat storage: Impacts and trade-offs for prosumers and the grid", *Energy Conversion and Management*, vol. 240, 114220, 2021.
- [11] K.-P. Kairies, J. Figgener, D. Haberschusz, O. Wessels, B. Tepe, and D. U. Sauer, "Market and technology development of PV home storage systems in Germany", *Journal of Energy Storage*, vol. 23, 416, 2019.
- [12] U. Datta, A. Kalam, and J. Shi, "A review of key functionalities of battery energy storage system in renewable energy integrated power systems", *Energy Storage*, vol. 3, no. 5, e224, 2021.
- [13] A. Ajanovic, A. Hiesl, and R. Haas, "On the role of storage for electricity in smart energy systems", *Energy*, vol. 200, 117473, 2020.
- [14] Kraftfahrt-Bundesamt (KBA), *Anzahl der Elektroautos in Deutschland von 2006 bis Januar 2024 [Graph]*, 2024. Available: <https://de.statista.com/statistik/daten/studie/265995/umfrage/anzahl-der-elektroautos-in-deutschland/>.
- [15] Bundesverband der Energie- und Wasserwirtschaft (BDEW), *Statusreport: Wärme*, 2024. Available: <https://www.bdew.de/service/publikationen/statusreport-waerme/>.
- [16] Bundesverband Solarwirtschaft e.V. (BSW), "Solarstromspeicher - Anzahl in Deutschland bis 2023 [Graph]", *Statista*, 2024. Available: <https://de.statista.com/statistik/daten/studie/1078876/umfrage/anzahl-installierter-solarstromspeichern-in-deutschland/>.
- [17] 50Hertz, Amprion, TenneT, TransnetBW, "Netzentwicklungsplan Strom 2035, Version 2021, zweiter Entwurf", 2021.
- [18] J. Weniger, N. Orth, L. Meissner, C. Schlüter, and J. von Rautenkranz, "Stromspeicher Inspektion 2024", Hochschule für Technik und Wirtschaft Berlin, 2024. Available: <https://solar.htw-berlin.de/studien/stromspeicher-inspektion-2024/>.
- [19] L. Kundert, A. Heider, and G. Hug, "The Influence of Different Network Tariffs on Distribution Grid Reinforcement Costs", in *2023 IEEE Belgrade PowerTech*, IEEE, 2023, 1.
- [20] ENTSO-E, *ENTSO-E Transparency Platform*. Available: <https://transparency.entsoe.eu/>, (accessed: 18.08.2022).

- [21] Federal Ministry for Economic Affairs and Climate Action (BMWK), *Electricity Storage Strategy*, 2023. Available: [https://www.bmwk.de/Redaktion/DE/Publikationen/Energie/electricity-storage-strategy.pdf?\\_\\_blob=publicationFile&v=4](https://www.bmwk.de/Redaktion/DE/Publikationen/Energie/electricity-storage-strategy.pdf?__blob=publicationFile&v=4).
- [22] S. Kippelt, C. Wagner, and C. Rehtanz, "Consideration of New Electricity Applications in Distribution Grid Expansion Planning and the Role of Flexibility", in *International ETG Congress 2017*, 2017, 1.
- [23] B. Schachler, A. Heider, T. Röpke, F. Reinke, and C. Bakker, "Assessing the Impacts of Market-Oriented Electric Vehicle Charging on German Distribution Grids", in *5th E-Mobility Power System Integration Symposium (EMOB 2021)*, vol. 2021, 2021, 128.
- [24] A. Heider, R. Reibsch, P. Blechinger, A. Linke, and G. Hug, "Flexibility options and their representation in open energy modelling tools", *Energy Strategy Reviews*, vol. 38, 100737, 2021.
- [25] United Nations, *Paris Agreement*, 2015. Available: [https://unfccc.int/files/essential\\_background/convention/application/pdf/english\\_paris\\_agreement.pdf](https://unfccc.int/files/essential_background/convention/application/pdf/english_paris_agreement.pdf).
- [26] S. Pfenninger, A. Hawkes, and J. Keirstead, "Energy systems modeling for twenty-first century energy challenges", *Renewable and Sustainable Energy Reviews*, vol. 33, 74, 2014.
- [27] S. Jebaraj and S. Iniyan, "A review of energy models", *Renewable and Sustainable Energy Reviews*, vol. 10, no. 4, 281, 2006.
- [28] L. M. Hall and A. R. Buckley, "A review of energy systems models in the UK: Prevalent usage and categorisation", *Applied Energy*, vol. 169, 607, 2016.
- [29] P. Lopion, P. Markewitz, M. Robinius, and D. Stolten, "A review of current challenges and trends in energy systems modeling", *Renewable and Sustainable Energy Reviews*, vol. 96, 156, 2018.
- [30] International Energy Agency, *Harnessing Variable Renewables*. 2011, 200. DOI: 10.1787/9789264111394-en. Available: <https://www.oecd-ilibrary.org/content/publication/9789264111394-en>.
- [31] S. Ø. Jensen, A. Marszal-Pomianowska, R. Lollini, W. Pasut, A. Knotzer, P. Engelmann, A. Stafford, and G. Reynders, "IEA EBC Annex 67 Energy Flexible Buildings", *Energy and Buildings*, vol. 155, 25, 2017.

- [32] J. Cochran, M. Miller, O. Zinaman, M. Milligan, D. Arent, B. Palmintier, M. O'Malley, S. Mueller, E. Lannoye, A. Tuohy, B. Kujala, M. Sommer, H. Holttinen, J. Kiviluoma, and S. K. Soonee, "Flexibility in 21st Century Power Systems", 2014. DOI: 10.2172/1130630.
- [33] M. Alizadeh, M. P. Moghaddam, N. Amjady, P. Siano, and M. Sheikh-El-Eslami, "Flexibility in future power systems with high renewable penetration: A review", *Renewable and Sustainable Energy Reviews*, vol. 57, 1186, 2016. DOI: 10.1016/j.rser.2015.12.200.
- [34] H. Auer and R. Haas, "On integrating large shares of variable renewables into the electricity system", *Energy*, vol. 115, 1592, 2016. DOI: 10.1016/j.energy.2016.05.067.
- [35] G. Papaefthymiou and K. Dragoon, "Towards 100% renewable energy systems: Uncapping power system flexibility", *Energy Policy*, vol. 92, 69, 2016. DOI: 10.1016/j.enpol.2016.01.025.
- [36] M. R. Cruz, D. Z. Fitiwi, S. F. Santos, and J. P. Catalão, "A comprehensive survey of flexibility options for supporting the low-carbon energy future", *Renewable and Sustainable Energy Reviews*, vol. 97, 338, 2018.
- [37] G. Papaefthymiou, E. Haesen, and T. Sach, "Power System Flexibility Tracker: Indicators to track flexibility progress towards high-RES systems", *Renewable Energy*, vol. 127, 1026, 2018.
- [38] H. Jabir, J. Teh, D. Ishak, and H. Abunima, "Impacts of Demand-Side Management on Electrical Power Systems: A Review", *Energies*, vol. 11, no. 5, 1050, 2018.
- [39] R. Verzijlbergh, L. D. Vries, G. Dijkema, and P. Herder, "Institutional challenges caused by the integration of renewable energy sources in the european electricity sector", *Renewable and Sustainable Energy Reviews*, vol. 75, 660, 2017.
- [40] P. L. Joskow, "Creating a Smarter U.S. Electricity Grid", *Journal of Economic Perspectives*, vol. 26, no. 1, 29, 2012.
- [41] S. Minniti, N. Haque, P. Nguyen, and G. Pemen, "Local Markets for Flexibility Trading: Key Stages and Enablers", *Energies*, vol. 11, no. 11, 2018. DOI: 10.3390/en11113074.
- [42] S. M. Nosratabadi, R.-A. Hooshmand, and E. Gholipour, "A comprehensive review on microgrid and virtual power plant concepts employed for distributed energy resources scheduling in power systems", *Renewable and Sustainable Energy Reviews*, vol. 67, 341, 2017.

- [43] N. Good, K. A. Ellis, and P. Mancarella, "Review and classification of barriers and enablers of demand response in the smart grid", *Renewable and Sustainable Energy Reviews*, vol. 72, 57, 2017.
- [44] D. Connolly, H. Lund, B. Mathiesen, and M. Leahy, "A review of computer tools for analysing the integration of renewable energy into various energy systems", *Applied Energy*, vol. 87, no. 4, 1059, 2010.
- [45] M. Gargiulo and B. O. Gallachóir, "Long-term energy models: Principles, characteristics, focus, and limitations", *WIREs Energy and Environment*, vol. 2, no. 2, 158, 2013.
- [46] P. G. Machado, D. Mouette, L. D. Villanueva, A. R. Esparta, B. Mendes Leite, and E. Moutinho dos Santos, "Energy systems modeling: Trends in research publication", *WIREs Energy and Environment*, vol. 8, no. 4, e333, 2019.
- [47] B. Müller, F. Gardumi, and L. Hülk, "Comprehensive representation of models for energy system analyses: Insights from the Energy Modelling Platform for Europe (EMP-E) 2017", *Energy Strategy Reviews*, vol. 21, 82, 2018.
- [48] H.-K. Ringkjøb, P. M. Haugan, and I. M. Solbrekke, "A review of modelling tools for energy and electricity systems with large shares of variable renewables", *Renewable and Sustainable Energy Reviews*, vol. 96, 440, 2018.
- [49] G. Savvidis, K. Siala, C. Weissbart, L. Schmidt, F. Borggreffe, S. Kumar, K. Pittel, R. Madlener, and K. Hufendiek, "The gap between energy policy challenges and model capabilities", *Energy Policy*, vol. 125, 503, 2019.
- [50] M. Groissböck, "Are open source energy system optimization tools mature enough for serious use?", *Renewable and Sustainable Energy Reviews*, vol. 102, 234, 2019.
- [51] X. Deng and T. Lv, "Power system planning with increasing variable renewable energy: A review of optimization models", *Journal of Cleaner Production*, vol. 246, 118962, 2020.
- [52] A. Krumm, D. Süsser, and P. Blechinger, "Modelling social aspects of the energy transition: What is the current representation of social factors in energy models?", *Energy*, vol. 239, 121706, 2022.
- [53] OpenEnergy family, *OpenEnergy Platform (OEP)*. Available: <https://openenergy-platform.org/factsheets/frameworks/>.

- [54] Open Energy Modelling Initiative, *openmod* — *Open Energy Modelling Initiative*. Available: [https://wiki.openmod-initiative.org/wiki/Open\\_Models](https://wiki.openmod-initiative.org/wiki/Open_Models).
- [55] S. Pfenninger, L. Hirth, I. Schlecht, E. Schmid, F. Wiese, T. Brown, C. Davis, M. Gidden, H. Heinrichs, C. Heuberger, S. Hilpert, U. Krien, C. Matke, A. Nebel, R. Morrison, B. Müller, G. Pleßmann, M. Reeg, J. C. Richstein, A. Shivakumar, I. Staffell, T. Tröndle, and C. Wingenbach, "Opening the black box of energy modelling: Strategies and lessons learned", *Energy Strategy Reviews*, vol. 19, 63, 2018.
- [56] M. Chang, J. Z. Thellufsen, B. Zakeri, B. Pickering, S. Pfenninger, H. Lund, and P. A. Østergaard, "Trends in tools and approaches for modelling the energy transition", *Applied Energy*, vol. 290, 116731, 2021.
- [57] T. Brown, A. Faruqui, and N. Lessem, *Electricity Distribution Network Tariffs. Principles and analysis of options. Technical Report*, 2018. Available: [https://www.brattle.com/wp-content/uploads/2021/05/14255\\_electricity\\_distribution\\_network\\_tariffs\\_-\\_the\\_brattle\\_group.pdf](https://www.brattle.com/wp-content/uploads/2021/05/14255_electricity_distribution_network_tariffs_-_the_brattle_group.pdf).
- [58] G. Pleßmann, M. Erdmann, M. Hlusiak, and C. Breyer, "Global Energy Storage Demand for a 100 % Renewable Electricity Supply", *Energy Procedia*, vol. 46, 22, 2014.
- [59] S. Schiebahn, T. Grube, M. Robinius, V. Tietze, B. Kumar, and D. Stolten, "Power to gas: Technological overview, systems analysis and economic assessment for a case study in Germany", *International Journal of Hydrogen Energy*, vol. 40, no. 12, 4285, 2015.
- [60] G. Venturini, J. Tattini, E. Mulholland, and B. Ó. Gallachóir, "Improvements in the representation of behavior in integrated energy and transport models", *International Journal of Sustainable Transportation*, vol. 13, no. 4, 294, 2018.
- [61] S. Yeh, G. S. Mishra, L. Fulton, P. Kyle, D. L. McCollum, J. Miller, P. Cazzola, and J. Teter, "Detailed assessment of global transport-energy models' structures and projections", *Transportation Research Part D: Transport and Environment*, vol. 55, 294, 2017.
- [62] B. Tranberg, M. Schäfer, T. Brown, J. Hörsch, and M. Greiner, "Flow-Based Analysis of Storage Usage in a Low-Carbon European Electricity Scenario", in *2018 15th International Conference on the European Energy Market (EEM)*, 2018, 1.

- [63] J.-P. Heckel and C. Becker, "Advanced Modeling of Electric Components in Integrated Energy Systems with the TransiEnt Library", *13th International Modelica Conference*, 2019.
- [64] J. Bistline, W. Cole, G. Damato, J. DeCarolis, W. Frazier, V. Linga, CaraMarcy, C. Namovicz, K. Podkaminer, R. Sims, M. Sukunta, and D. Young, "Energy storage in long-term system models: A review of considerations, best practices, and research needs", *Progress in Energy*, 2020.
- [65] B.-J. Jesse, S. Morgenthaler, B. Gillessen, S. Burges, and W. Kuckshinrichs, "Potential for Optimization in European Power Plant Fleet Operation", *Energies*, vol. 13, 2020.
- [66] S. KSV, A. Vinayagam, S. yang Khoo, and A. Stojcevski, "Impacts of Integration of Wind and Solar PV in a Typical Power Network", in *Proceedings of the 2015 International Conference on Sustainable Energy and Environmental Engineering*, Atlantis Press, 2015, 21.
- [67] B. Weise, A. Korai, and A. Constantin, "Comparison of Selected Grid-Forming Converter Control Strategies for Use in Power Electronic Dominated Power Systems", *18th Wind Integration Workshop*, 2019.
- [68] DIGSILENT, *Power Factory application brochures*, 2021. Available: <https://www.digsilent.de/en/downloads.html>.
- [69] Siemens, *Sincal application*, 2021. Available: <https://assets.new.siemens.com/siemens/assets/api/uuid:31ece3a2-e9cc-4528-b9f9-6bf61b613de2/ref-no-69-ps-c-pss-sincal-brochure-hires-intl-sept2018.pdf>.
- [70] S. Allard, V. Debusschere, S. Mima, T. T. Quoc, N. Hadjsaid, and P. Criqui, "Considering distribution grids and local flexibilities in the prospective development of the European power system by 2050", *Applied Energy*, vol. 270, 114958, 2020.
- [71] R. Likert, "A technique for the measurement of attitudes", *Archives of Psychology*, vol. 22 140, no. 55, 1932.
- [72] J. Hörsch, F. Hofmann, D. Schlachtberger, and T. Brown, "Pypsa-eur: An open optimisation model of the european transmission system", *Energy Strategy Reviews*, vol. 22, 207, 2018.
- [73] A. Senkel, C. Bode, J.-P. Heckel, O. Schülting, G. Schmitz, C. Becker, and A. Kather, "Status of the TransiEnt Library: Transient Simulation of Complex Integrated Energy Systems", in *Modelica Conferences*, 2021, 187.

- [74] U. P. Müller, B. Schachler, M. Scharf, W.-D. Bunke, S. Günther, J. Bartels, and G. Pleßmann, “Integrated Techno-Economic Power System Planning of Transmission and Distribution Grids”, *Energies*, vol. 12, no. 11, 2019. DOI: 10.3390/en12112091.
- [75] Reiner Lemoine Institut gGmbH, *eDisGo - Electricity distribution grid optimization*, <https://github.com/openego/eDisGo>, 2021.
- [76] J. Amme, G. Pleßmann, J. Bühler, L. Hülk, E. Kötter, and P. Schwägerl, *Distribution grid data generated by DINGO*, 2017. DOI: <http://doi.org/10.5281/zenodo.890479>.
- [77] *eGo<sup>n</sup>-Open and cross-sectoral planning of transmission and distribution grids*, <https://ego-n.org/>.
- [78] PyPSA Developers, *PyPSA - Python for Power System Analysis*, <https://github.com/PyPSA/PyPSA>, 2021.
- [79] DIN EN 50160/A1:2016-02, “Voltage characteristics of electricity supplied by public electricity networks; German version EN 50160:2010/A1:2015”, *German Institute for Standardisation: Berlin, Germany*, 2016.
- [80] BDEW, „*technische richtlinie erzeugungsanlagen am mittelspannungsnetz*“ richtlinie für den anschluss und parallelbetrieb von erzeugungsanlagen am mittelspannungsnetz; stand: Ausgabe juni 2008; hrsg.: BdeW, 2008.
- [81] VDE Verband der Elektrotechnik Elektronik Informationstechnik e.V., “Erzeugungsanlagen am Niederspannungsnetz Technische Mindestanforderungen für Anschluss und Parallelbetrieb von Erzeugungsanlagen am Niederspannungsnetz–Draft of 07-08-2010”, *Berlin www.vde.com/de/fnn/dokumente/documents*, 2010.
- [82] IEA, “Strengthening Power System Security in Kyrgyzstan: A Roadmap”, *IEA, Paris*, 2022. Available: <https://www.iaea.org/reports/strengthening-power-system-security-in-kyrgyzstan-a-roadmap>.
- [83] C. Rehtanz, M. Greve, U. Häger, Z. Hagemann, S. Kippelt, C. Kittl, M.-L. Kloubert, O. Pohl, F. Rewald, and C. Wagner, *Verteilnetzstudie für das Land Baden-Württemberg*, 2017.
- [84] Consentec, IAEW and RZVN, Frontier Economics, “Untersuchung der Voraussetzungen und möglicher Anwendung analytischer Kostenmodelle in der deutschen Energiewirtschaft”, *Untersuchung im Auftrag der Bundesnetzagentur, Abschlussbericht vom 20.11*, 2006.

- [85] A. C. Agricola, B. Höflich, and P. e. Richard, "Ausbau- und Innovationsbedarf der Stromverteilnetze in Deutschland bis 2030 (kurz: dena-Verteilnetzstudie)", Deutsche Energie-Agentur GmbH (dena), Final report, 2012.
- [86] R. Gupta, A. Pena-Bello, K. N. Streicher, C. Roduner, Y. Farhat, D. Thöni, M. K. Patel, and D. Parra, "Spatial analysis of distribution grid capacity and costs to enable massive deployment of PV, electric mobility and electric heating", *Applied Energy*, vol. 287, 116504, 2021.
- [87] U. P. Müller, B. Schachler, W.-D. Bunke et al., "Netzebenenübergreifendes Planungsinstrument - zur Bestimmung des optimalen Netz- und Speicherausbaus in Deutschland - integriert in einer OpenEnergy-Plattform", 2019.
- [88] oemof-Team, *Demandlib*, 2016. Available: <https://github.com/oemof/demandlib>.
- [89] Elia Group, "Accelerating to net-zero: redefining energy and mobility", 2020.
- [90] Kraftfahrt-Bundesamt. "Bestand an Kraftfahrzeugen und Kraftfahrzeuganhängern nach Zulassungsbezirken". (2020).
- [91] J. Amme, G. Pleßmann, J. Bühler, L. Hülk, E. Kötter, and P. Schwaegerl, "The eGo grid model: An open-source and open-data based synthetic medium-voltage grid model for distribution power supply systems", *Journal of Physics: Conference Series*, vol. 977, no. 1, 012007, 2018.
- [92] S. Tews, "Vergleich von synthetischen dingo-Netzen mit realen und synthetischen Netzen durch die Simulation von Speichern auf der Mittelspannungsebene", *Master Thesis, Fachgebiet Elektrische Energiespeichertechnik, Technische Universität Berlin*, 2021.
- [93] S. Meinecke, D. Sarajlić, S. R. Drauz, A. Klettke, L.-P. Lauven, C. Rehtanz, A. Moser, and M. Braun, "Simbench—a benchmark dataset of electric power systems to compare innovative solutions based on power flow analysis", *Energies*, vol. 13, no. 12, 3290, 2020.
- [94] S. Meinecke, N. Bornhorst, and M. Braun, "Power System Benchmark Generation Methodology", in *NEIS 2018; Conference on Sustainable Energy Supply and Energy Storage Systems*, 2018, 1.

- [95] C. Matrose, T. Helmschrott, M. Gödde, E. Szczechowicz, and A. Schnettler, "Impact of Different Electric Vehicle Charging Strategies onto Required Distribution Grid Reinforcement", in *2012 IEEE Transportation Electrification Conference and Expo (ITEC)*, 2012, 1. DOI: 10.1109/ITEC.2012.6243435.
- [96] J. Gemassmer, C. Daam, and R. Reibsch, "Challenges in Grid Integration of Electric Vehicles in Urban and Rural Areas", *World Electric Vehicle Journal*, vol. 12, no. 4, 2021.
- [97] S. Karagiannopoulos, *Data-driven and Optimization-based Methods for Active Distribution Grids*. ETH Zurich, 2019.
- [98] Flensburg University of Applied Sciences and University of Flensburg and Reiner Lemoine Institute and Otto-von-Guericke University Magdeburg and German Aerospace Center Institute of Networked Energy Systems, *Ein offenes netzebenen- und sektorenübergreifendes Planungsinstrument zur Bestimmung des optimalen Einsatzes und Ausbaus von Flexibilitätsoptionen in Deutschland - Projektabschlussbericht*, 2024. DOI: 10.5281/zenodo.10677901. Available: <https://doi.org/10.5281/zenodo.10677901>.
- [99] L. Pieltain Fernández, T. Gomez San Roman, R. Cossent, C. Mateo Domingo, and P. Frías, "Assessment of the Impact of Plug-in Electric Vehicles on Distribution Networks", *IEEE Transactions on Power Systems*, vol. 26, no. 1, 206, 2011. DOI: 10.1109/TPWRS.2010.2049133.
- [100] F. Gonzalez Venegas, M. Petit, and Y. Perez, "Active integration of electric vehicles into distribution grids: Barriers and frameworks for flexibility services", *Renewable and Sustainable Energy Reviews*, vol. 145, 111060, 2021.
- [101] F. Mwasilu, J. J. Justo, E.-K. Kim, T. D. Do, and J.-W. Jung, "Electric vehicles and smart grid interaction: A review on vehicle to grid and renewable energy sources integration", *Renewable and Sustainable Energy Reviews*, vol. 34, 501, 2014. DOI: <https://doi.org/10.1016/j.rser.2014.03.031>. Available: <https://www.sciencedirect.com/science/article/pii/S1364032114001920>.
- [102] P. A. Gunkel, C. Bergaentzlé, I. Græsted Jensen, and F. Scheller, "From passive to active: Flexibility from electric vehicles in the context of transmission system development", *Applied Energy*, vol. 277, 115526, 2020.

- [103] Y. Mu, J. Wu, N. Jenkins, H. Jia, and C. Wang, "A spatial-temporal model for grid impact analysis of plug-in electric vehicles", *Applied Energy*, vol. 114, 456, 2014.
- [104] Reiner Lemoine Institut gGmbH, *SimBEV*, 2021. Available: <https://github.com/rl-institut/simbev>.
- [105] Institut für angewandte Sozialwissenschaft GmbH, *Mobilität in Deutschland*, 2017.
- [106] Bundesministerium für Digitales und Verkehr (BMVI), *Regional-statistische Raumtypologie (RegioStaR)*, 2021. Available: <https://bmdv.bund.de/SharedDocs/DE/Artikel/G/regionalstatistische-raumtypologie.html>.
- [107] D. Kucevic, B. Tepe, B. Schachler, T. Röpcke, K. Helfenbein, and P. Dotzauer, "Abschlussbericht open\_BEa-03ET4072 Open Battery Models for Electrical Grid Applications", Technische Universität München, 2022. DOI: <https://doi.org/10.2314/KXP:1798888513>.
- [108] K. Helfenbein. "Analyse des Einflusses netzdienlicher Ladestrategien auf Verteilnetze aufgrund der zunehmenden Netzintegration von Elektrofahrzeugen". (2021).
- [109] Reiner Lemoine Institut gGmbH, *TracBEV*, 2022. Available: <https://github.com/rl-institut/tracbev>.
- [110] Statistisches Bundesamt. "Ergebnisse des zensus 2011". (2011).
- [111] OpenStreetMap Foundation (OSMF). "Openstreetmap". (), Available: <https://www.openstreetmap.org/>.
- [112] Kraftfahrt Bundesamt (KBA), *Pressemitteilung Nr. 08/2023 - Der Fahrzeugbestand am 1. Januar 2023*, [https://www.kba.de/SharedDocs/Downloads/DE/Pressemitteilungen/DE/2023/pm\\_08\\_2023\\_bestand\\_01\\_23.pdf;jsessionid=E7ED6362F09D4E8B0F18C0986659D64A.live21322?\\_\\_blob=publicationFile&v=7](https://www.kba.de/SharedDocs/Downloads/DE/Pressemitteilungen/DE/2023/pm_08_2023_bestand_01_23.pdf;jsessionid=E7ED6362F09D4E8B0F18C0986659D64A.live21322?__blob=publicationFile&v=7), 2023.
- [113] F. Moors, "The Influence of Smart Charging and V2G on the Flexibility Potential and Grid Expansion Needs of German Distribution Grids", *Master Thesis, Power Systems Laboratory, ETH Zurich*, 2022.
- [114] R. D'hulst, W. Labeeuw, B. Beusen, S. Claessens, G. Deconinck, and K. Vanthournout, "Demand response flexibility and flexibility potential of residential smart appliances: Experiences from large pilot test in Belgium", *Applied Energy*, vol. 155, 79, 2015.

- [115] A. Heider, K. Helfenbein, B. Schachler, T. Röpcke, and G. Hug, "On the Integration of Electric Vehicles into German Distribution Grids through Smart Charging", in *2022 International Conference on Smart Energy Systems and Technologies (SEST)*, 2022, 1.
- [116] A. Heider, M. Genena, B. Schachler, P. Blechinger, and G. Hug, "Flexibility needs in a 100 % renewable German power system with growing shares of decentralised sector coupling technologies", *Working manuscript*,
- [117] T. Brown, D. Schlachtberger, A. Kies, S. Schramm, and M. Greiner, "Synergies of sector coupling and transmission reinforcement in a cost-optimised, highly renewable European energy system", *Energy*, vol. 160, 720, 2018.
- [118] A. Kemmler, A. Wunsch, and H. Burret, "Entwicklung des Bruttostromverbrauchs bis 2030", 2021, 2021. Available: [https://www.prognos.com/sites/default/files/2021-11/20211116\\_Kurzpaper\\_Bruttostromverbrauch2018-2030.pdf](https://www.prognos.com/sites/default/files/2021-11/20211116_Kurzpaper_Bruttostromverbrauch2018-2030.pdf).
- [119] M. Kühnbach, J. Stute, T. Gnann, M. Wietschel, S. Marwitz, and M. Klobasa, "Impact of electric vehicles: Will German households pay less for electricity?", *Energy Strategy Reviews*, vol. 32, 100568, 2020.
- [120] M. Pehnt, H. Helms, U. Lambrecht, D. Dallinger, M. Wietschel, H. Heinrichs, R. Kohrs, J. Link, S. Trommer, T. Pollok, *et al.*, "Elektroautos in einer von erneuerbaren Energien geprägten Energiewirtschaft", *Zeitschrift für Energiewirtschaft*, vol. 35, no. 3, 221, 2011.
- [121] J. Schäuble, T. Kaschub, A. Ensslen, P. Jochem, and W. Fichtner, "Generating electric vehicle load profiles from empirical data of three EV fleets in Southwest Germany", *Journal of Cleaner Production*, vol. 150, 253, 2017.
- [122] A. Thingvad, C. Ziras, and M. Marinelli, "Economic value of electric vehicle reserve provision in the Nordic countries under driving requirements and charger losses", *Journal of Energy Storage*, vol. 21, 826, 2019.
- [123] B. Lebrouhi, Y. Khattari, B. Lamrani, M. Maaroufi, Y. Zeraouli, and T. Kousksou, "Key challenges for a large-scale development of battery electric vehicles: A comprehensive review", *Journal of Energy Storage*, vol. 44, 103273, 2021.

- [124] S. Powell, G. V. Cezar, L. Min, I. M. Azevedo, and R. Rajagopal, "Charging infrastructure access and operation to reduce the grid impacts of deep electric vehicle adoption", *Nature Energy*, vol. 7, no. 10, 932, 2022.
- [125] M. Arnz and A. Krumm, "Sufficiency in passenger transport and its potential for lowering energy demand", *Environmental Research Letters*, vol. 18, no. 9, 094008, 2023.
- [126] M. Arnz, "Avoid, Shift Or Improve Passenger Transport?: Modelling of Sufficiency Scenarios for the Case of Germany", Ph.D. dissertation, Technische Universität Berlin, 2024.
- [127] O. Ruhnau, *When2Heat Heating Profiles*. *Open Power System Data*, 2019. DOI: <https://doi.org/10.25832/when2heat/2019-08-06>.
- [128] O. Ruhnau, L. Hirth, and A. Praktiknjo, "Time series of heat demand and heat pump efficiency for energy system modeling", *Scientific data*, vol. 6, no. 1, 189, 2019.
- [129] Statistisches Bundesamt (Destatis), *Energy consumption of households*, 2023. Available: <https://www.destatis.de/EN/Themes/Society-Environment/Environment/Environmental-Economic-Accounting/private-households/Tables/energy-consumption-households.html>.
- [130] Fachvereinigung Wärmepumpen Schweiz. "Statistik 2021". (2021), Available: <https://www.fws.ch/wp-content/uploads/2022/05/FWS-Statistiken-2021-V2.pdf>.
- [131] Bundesverband Wärmepumpe (BWP) e.V. und BWP Marketing & Service GmbH, *Absatzzahlen für Wärmepumpen in Deutschland 2020*, 2021. Available: <https://www.waermepumpe.de/presse/zahlen-daten/>, (accessed: 23.12.2021).
- [132] Bundesnetzagentur, *Bundesnetzagentur legt Regelungen zur Integration steuerbarer Verbrauchseinrichtungen fest*, 2023. Available: [https://www.bundesnetzagentur.de/SharedDocs/Pressemitteilungen/DE/2023/20231127\\_14a.html](https://www.bundesnetzagentur.de/SharedDocs/Pressemitteilungen/DE/2023/20231127_14a.html).
- [133] M. Schlemminger, T. Ohrdes, E. Schneider, and M. Knoop, "Dataset on electrical single-family house and heat pump load profiles in Germany", *Scientific Data*, vol. 9, no. 1, 56, 2022.

- [134] M. Barton, B. Lukas, and C. Schweigler, "Wärmepumpen für die Energiewende in Bayern – Gebäudewärmebedarf und Anwendungspotenzial im Jahr 2050", *BWK Energie*, 2022. Available: <https://www.ingenieur.de/fachmedien/bwk/energieversorgung/waermepumpen-fuer-die-energiewende-in-bayern/>.
- [135] N. Damianakis, G. R. C. Mouli, P. Bauer, and Y. Yu, "Assessing the grid impact of Electric Vehicles, Heat Pumps & PV generation in Dutch LV distribution grids", *Applied Energy*, vol. 352, 121878, 2023.
- [136] C. Underwood, "14 - Heat pump modelling", in *Advances in Ground-Source Heat Pump Systems*, S. J. Rees, Ed., Woodhead Publishing, 2016, 387.
- [137] D. Fischer, J. Bernhardt, H. Madani, and C. Wittwer, "Comparison of control approaches for variable speed air source heat pumps considering time variable electricity prices and PV", *Applied Energy*, vol. 204, 93, 2017.
- [138] E. Thrampoulidis, "Transforming the built environment: Leveraging large-scale retrofit and building-level demand flexibility", Ph.D. dissertation, ETH Zurich, 2023.
- [139] M. Puiggròs Vilalta, "Flexibility potential of residential buildings for distribution grid services", M.S. thesis, Universitat Politècnica de Catalunya, 2022.
- [140] N. Orth, J. Weniger, L. Meissner, I. Lawaczek, and V. Quaschnig, "Stromspeicher Inspektion 2022", Hochschule für Technik und Wirtschaft Berlin, 2022. Available: <https://solar.htw-berlin.de/studien/speicher-inspektion-2022/>.
- [141] Agora Energiewende und Forschungsstelle für Energiewirtschaft e. V., "Haushaltsnahe Flexibilitäten nutzen. Wie Elektrofahrzeuge, Wärmepumpen und Co. die Stromkosten für alle senken können.", 2023. Available: [https://www.agora-energiewende.de/fileadmin/Projekte/2023/2023-14\\_DE\\_Flex\\_heben/A-EW\\_315\\_Flex\\_heben\\_WEB.pdf](https://www.agora-energiewende.de/fileadmin/Projekte/2023/2023-14_DE_Flex_heben/A-EW_315_Flex_heben_WEB.pdf).
- [142] J. Figgner, P. Stenzel, K.-P. Kairies, J. Linßen, D. Haberschusz, O. Wessels, G. Angenendt, M. Robinius, D. Stolten, and D. U. Sauer, "The development of stationary battery storage systems in Germany – A market review", *Journal of Energy Storage*, vol. 29, 101153, 2020. DOI: <https://doi.org/10.1016/j.est.2019.101153>. Available: <https://www.sciencedirect.com/science/article/pii/S2352152X19309442>.

- [143] D. Fischer, T. Wolf, J. Wapler, R. Hollinger, and H. Madani, "Model-based flexibility assessment of a residential heat pump pool", *Energy*, vol. 118, 853, 2017.
- [144] M. S. Kany, B. V. Mathiesen, I. R. Skov, A. D. Korberg, J. Z. Thelufsen, H. Lund, P. Sorknæs, and M. Chang, "Energy efficient decarbonisation strategy for the Danish transport sector by 2045", *Smart Energy*, vol. 5, 100063, 2022.
- [145] Statistisches Bundesamt (Destatis), *Bautätigkeit und Wohnungen - Bestand an Wohnungen*, [https://www.destatis.de/DE/Themen/Gesellschaft-Umwelt/Wohnen/Publikationen/Downloads-Wohnen/bestand-wohnungen-2050300217004.pdf?\\_\\_blob=publicationFile](https://www.destatis.de/DE/Themen/Gesellschaft-Umwelt/Wohnen/Publikationen/Downloads-Wohnen/bestand-wohnungen-2050300217004.pdf?__blob=publicationFile), 2022.
- [146] J. Gasser, H. Cai, S. Karagiannopoulos, P. Heer, and G. Hug, "Predictive energy management of residential buildings while self-reporting flexibility envelope", *Applied Energy*, vol. 288, 116653, 2021.
- [147] A. Eicke, L. Hirth, and M. Jonathan, "Mehrwert dezentraler Flexibilität - Oder: Was kostet die verschleppte Flexibilisierung von Wärmepumpen, Elektroautos und Heimspeichern?", 2024. Available: <https://neon.energy/Neon-Mehrwert-Flex.pdf>.
- [148] J. Villar, R. Bessa, and M. Matos, "Flexibility products and markets: Literature review", *Electric Power Systems Research*, vol. 154, 329, 2018. DOI: <https://doi.org/10.1016/j.epsr.2017.09.005>.
- [149] Bundesnetzagentur, *Bericht zum Zustand und Ausbau der Verteilernetze 2021*, 2022.
- [150] McKinsey and Company, *The Impact of Electromobility on the German Electric Grid*, <https://www.mckinsey.com/industries/electric-power-and-natural-gas/our-insights/the-impact-of-electromobility-on-the-german-electric-grid>.
- [151] L. Strobel, J. Schlund, and M. Pruckner, "Joint analysis of regional and national power system impacts of electric vehicles - A case study for Germany on the county level in 2030", *Applied Energy*, vol. 315, 2022. DOI: 10.1016/j.apenergy.2022.118945.
- [152] R. Mehta, D. Srinivasan, A. M. Khambadkone, J. Yang, and A. Trivedi, "Smart Charging Strategies for Optimal Integration of Plug-In Electric Vehicles Within Existing Distribution System Infrastructure", *IEEE Transactions on Smart Grid*, vol. 9, no. 1, 299, 2018.

- [153] S. Deb, A. K. Goswami, P. Harsh, J. P. Sahoo, R. L. Chetri, R. Roy, and A. S. Shekhawat, "Charging Coordination of Plug-In Electric Vehicle for Congestion Management in Distribution System Integrated With Renewable Energy Sources", *IEEE Transactions on Industry Applications*, vol. 56, no. 5, 5452, 2020.
- [154] R. Hemmati and H. Mehrjerdi, "Investment deferral by optimal utilizing vehicle to grid in solar powered active distribution networks", *Journal of Energy Storage*, vol. 30, 101512, 2020.
- [155] N. Brinkel, W. Schram, T. AlSkaif, I. Lampropoulos, and W. van Sark, "Should we reinforce the grid? Cost and emission optimization of electric vehicle charging under different transformer limits", *Applied Energy*, vol. 276, 115285, 2020.
- [156] R. Reibsch, P. Blechinger, and J. Kowal, "The importance of battery storage systems in reducing grid issues in sector-coupled and renewable low-voltage grids", *Journal of Energy Storage*, vol. 72, 108726, 2023.
- [157] J. K. Szinai, C. J. Sheppard, N. Abhyankar, and A. R. Gopal, "Reduced grid operating costs and renewable energy curtailment with electric vehicle charge management", *Energy Policy*, vol. 136, 111051, 2020. DOI: <https://doi.org/10.1016/j.enpol.2019.111051>.
- [158] E. Veldman and R. A. Verzijlbergh, "Distribution Grid Impacts of Smart Electric Vehicle Charging From Different Perspectives", *IEEE Transactions on Smart Grid*, vol. 6, no. 1, 333, 2015.
- [159] D. Pudjianto, P. Djapic, M. Aunedi, C. K. Gan, G. Strbac, S. Huang, and D. Infield, "Smart control for minimizing distribution network reinforcement cost due to electrification", *Energy Policy*, vol. 52, 76, 2013.
- [160] T. Navidi, A. El Gamal, and R. Rajagopal, "Coordinating distributed energy resources for reliability can significantly reduce future distribution grid upgrades and peak load", *Joule*, vol. 7, no. 8, 1769, 2023.
- [161] E. Veldman, M. Gibescu, H. (Slootweg, and W. L. Kling, "Scenario-based modelling of future residential electricity demands and assessing their impact on distribution grids", *Energy Policy*, vol. 56, 233, 2013. DOI: <https://doi.org/10.1016/j.enpol.2012.12.078>.

- [162] M. Baran and F. Wu, "Network reconfiguration in distribution systems for loss reduction and load balancing", *IEEE Transactions on Power Delivery*, vol. 4, no. 2, 1401, 1989. DOI: 10.1109/61.25627.
- [163] A. Heider, F. Moors, and G. Hug, "The Influence of Smart Charging and V2G on the Flexibility Potential and Grid Expansion Needs of German Distribution Grids", in *2023 International Conference on Smart Energy Systems and Technologies (SEST)*, 2023, 1.
- [164] Bundesministerium für Umwelt, Naturschutz und nukleare Sicherheit (BMU). "Klimaschutzprogramm 2030 der Bundesregierung zur Umsetzung des Klimaschutzplans 2050". (2019).
- [165] F. Tuchnitz, N. Ebell, J. Schlund, and M. Pruckner, "Development and evaluation of a smart charging strategy for an electric vehicle fleet based on reinforcement learning", *Applied Energy*, vol. 285, 116382, 2021.
- [166] R. Fachrizal, M. Shepero, D. van der Meer, J. Munkhammar, and J. Widén, "Smart charging of electric vehicles considering photovoltaic power production and electricity consumption: A review", *eTransportation*, vol. 4, 100056, 2020.
- [167] M. Brenna, F. Foadelli, D. Zaninelli, G. Graditi, and M. Di Somma, "Chapter 10 - The integration of electric vehicles in smart distribution grids with other distributed resources", in *Distributed Energy Resources in Local Integrated Energy Systems*, G. Graditi and M. Di Somma, Eds., Elsevier, 2021, 315.
- [168] Agora Verkehrswende, Agora Energiewende, and Regulatory Assistance Project (RAP). "Verteilnetzausbau für die Energiewende, Elektromobilität im Fokus". (2019).
- [169] Reiner Lemoine Institute gGmbH, *SimBEV - Simulation of Battery Electric Vehicles*, <https://simbev.readthedocs.io/en/latest/>.
- [170] Python Software Foundation, *tracemalloc*, <https://docs.python.org/3/library/tracemalloc.html>.
- [171] Python Software Foundation, *time*, <https://docs.python.org/3/library/time.html>.
- [172] Gurobi Optimization, LLC, *Gurobi Optimizer version 10.0.1 build v10.0.1rc0 (win64)*, <https://www.gurobi.com/downloads/gurobi-optimizer-readme-v10-0-1/>, 2023.

- [173] M. L. Bynum, G. A. Hackebeil, W. E. Hart, C. D. Laird, B. L. Nicholson, J. D. Sirola, J.-P. Watson, D. L. Woodruff, *et al.*, *Pyomo Optimization Modeling in Python*. Springer Optimization and Its Applications, 2021, vol. 67.
- [174] M. Held, “Netzdienlich optimaler Einsatz von Flexibilitäten in radialen Verteilnetzen basierend auf einem AC-Lastflussmodell”, *Master Thesis, Technische Universität Berlin*, 2023. Available: [https://reiner-lemoine-institut.de/wp-content/uploads/2023/11/2023\\_MA\\_Maike\\_Held\\_Netzdienlich\\_optimaler\\_Einsatz\\_von\\_Flexibilitaeten.pdf](https://reiner-lemoine-institut.de/wp-content/uploads/2023/11/2023_MA_Maike_Held_Netzdienlich_optimaler_Einsatz_von_Flexibilitaeten.pdf).
- [175] A. Heider, L. Kundert, B. Schachler, and G. Hug, “Grid Reinforcement Costs with Increasing Penetrations of Distributed Energy Resources”, in *2023 IEEE Belgrade PowerTech, IEEE*, 2023, 01.
- [176] E. Taibi, C. Fernández del Valle, and M. Howells, “Strategies for solar and wind integration by leveraging flexibility from electric vehicles: The Barbados case study”, *Energy*, vol. 164, 65, 2018.
- [177] M. Gödde, E. Szczechowicz, T. Helmschrott, C. Matrose, and A. Schnettler, “Approach and main results of the G4V project analyzing the impact of a mass introduction of electric vehicles on electricity networks in Europe”, in *2012 IEEE Transportation Electrification Conference and Expo (ITEC)*, 2012, 1. DOI: 10.1109/ITEC.2012.6243434.
- [178] Bundesministerium für Wirtschaft und Klimaschutz (BMWK), *Erneuerbare-Energien-Gesetz vom 21. Juli 2014 (BGBl. I S. 1066), das zuletzt durch Artikel 4 des Gesetzes vom 3. Juli 2023 (BGBl. 2023 I Nr. 176) geändert worden ist*, 2023. Available: [https://www.gesetze-im-internet.de/eeg\\_2014/BJNR106610014.html](https://www.gesetze-im-internet.de/eeg_2014/BJNR106610014.html).
- [179] G. Reynders, R. Amaral Lopes, A. Marszal-Pomianowska, D. Aelenei, J. Martins, and D. Saelens, “Energy flexible buildings: An evaluation of definitions and quantification methodologies applied to thermal storage”, *Energy and Buildings*, vol. 166, 372, 2018.
- [180] T. Nuytten, B. Claessens, K. Paredis, J. Van Bael, and D. Six, “Flexibility of a combined heat and power system with thermal energy storage for district heating”, *Applied Energy*, vol. 104, 583, 2013.
- [181] G. Reynders, J. Diriken, and D. Saelens, “Generic characterization method for energy flexibility: Applied to structural thermal storage in residential buildings”, *Applied Energy*, vol. 198, 192, 2017.

- [182] D. Kleinhans, *Towards a systematic characterization of the potential of demand side management*, 2014. DOI: 10.48550/ARXIV.1401.4121.
- [183] W. Heitkoetter, B. U. Schyska, D. Schmidt, W. Medjroubi, T. Vogt, and C. Agert, "Assessment of the regionalised demand response potential in Germany using an open source tool and dataset", *Advances in Applied Energy*, vol. 1, 100001, 2021.
- [184] L. Göransson, J. Goop, T. Unger, M. Odenberger, and F. Johnsson, "Linkages between demand-side management and congestion in the European electricity transmission system", *Energy*, vol. 69, 860, 2014.
- [185] A. Zerrahn and W.-P. Schill, "On the representation of demand-side management in power system models", *Energy*, vol. 84, 840, 2015.
- [186] A. G. Tveten, T. F. Bolkesjø, and I. Ilieva, "Increased demand-side flexibility: market effects and impacts on variable renewable energy integration", *International Journal of Sustainable Energy Planning and Management*, Vol 11 (2016), 2016. DOI: 10.5278/IJSEPM.2016.11.4.
- [187] D. Heide, L. von Bremen, M. Greiner, C. Hoffmann, M. Speckmann, and S. Bofinger, "Seasonal optimal mix of wind and solar power in a future, highly renewable Europe", *Renewable Energy*, vol. 35, no. 11, 2483, 2010.
- [188] D. Heide, M. Greiner, L. Von Bremen, and C. Hoffmann, "Reduced storage and balancing needs in a fully renewable European power system with excess wind and solar power generation", *Renewable Energy*, vol. 36, no. 9, 2515, 2011.
- [189] R. Nayak-Luke, R. Bañares-Alcántara, and S. Collier, "Quantifying network flexibility requirements in terms of energy storage", *Renewable Energy*, vol. 167, 869, 2021.
- [190] D. Suna, G. Totschnig, F. Schöniger, G. Resch, J. Spreitzhofer, and T. Esterl, "Assessment of flexibility needs and options for a 100% renewable electricity system by 2030 in Austria", *Smart Energy*, vol. 6, 100077, 2022.
- [191] F. Cebulla, J. Haas, J. Eichman, W. Nowak, and P. Mancarella, "How much electrical energy storage do we need? A synthesis for the U.S., Europe, and Germany", *Journal of Cleaner Production*, vol. 181, 449, 2018.
- [192] Bundesnetzagentur, *Growth in renewable energy in 2023*, 2024. Available: [https://www.bundesnetzagentur.de/SharedDocs/Pressemitteilungen/EN/2024/20240105\\_EEGZubau.html](https://www.bundesnetzagentur.de/SharedDocs/Pressemitteilungen/EN/2024/20240105_EEGZubau.html).

- [193] S. Pfenninger and I. Staffell, "Long-term patterns of European PV output using 30 years of validated hourly reanalysis and satellite data", *Energy*, vol. 114, 1251, 2016.
- [194] I. Staffell and S. Pfenninger, "Using bias-corrected reanalysis to simulate current and future wind power output", *Energy*, vol. 114, 1224, 2016.
- [195] O. Ruhnau, L. Hirth, and A. Praktiknjo, "Heating with wind: Economics of heat pumps and variable renewables", *Energy Economics*, vol. 92, 104967, 2020.
- [196] O. Ruhnau and S. Qvist, "Storage requirements in a 100% renewable electricity system: Extreme events and inter-annual variability", *Environmental Research Letters*, vol. 17, no. 4, 044018, 2022.
- [197] G. Kobiela, S. Samadi, J. Kurwan, A. Tönjes, M. Fishedick, T. Koska, S. Lechtenböhmer, S. März, and D. Schüwer, "CO<sub>2</sub>-neutral bis 2035: Eckpunkte eines deutschen Beitrags zur Einhaltung der 1,5-°C-Grenze; Diskussionsbeitrag für Fridays for Future Deutschland", 2020.
- [198] Y. Wen, Z. Hu, S. You, and X. Duan, "Aggregate Feasible Region of DERs: Exact Formulation and Approximate Models", *IEEE Transactions on Smart Grid*, vol. 13, no. 6, 4405, 2022.
- [199] A. Stawska, N. Romero, M. de Weerd, and R. Verzijlbergh, "Demand response: For congestion management or for grid balancing?", *Energy Policy*, vol. 148, 111920, 2021. DOI: <https://doi.org/10.1016/j.enpol.2020.111920>.
- [200] I. Abdelmottaleb, T. Gómez, J. P. Chaves Ávila, and J. Reneses, "Designing efficient distribution network charges in the context of active customers", *Applied Energy*, vol. 210, 815, 2018.
- [201] I. Abdelmottaleb, T. Gómez, and J. Reneses, "Evaluation Methodology for Tariff Design under Escalating Penetrations of Distributed Energy Resources", *Energies*, vol. 10, 1, 2017.
- [202] R. J. Hennig, D. Ribò-Pérez, L. J. de Vries, and S. H. Tindemans, "What is a good distribution network tariff? - Developing indicators for performance assessment", *Applied Energy*, vol. 318, 119186, 2022.

- [203] J. D. Jenkins and I. J. Pérez-Arriaga, "Improved Regulatory Approaches for the Remuneration of Electricity Distribution Utilities with High Penetrations of Distributed Energy Resources", *The Energy Journal*, vol. 38, no. 3, 63, 2017. Available: <http://www.jstor.org/stable/44203643>.
- [204] Q. Hoarau and Y. Perez, "Network tariff design with prosumers and electromobility: Who wins, who loses?", *Energy Economics*, vol. 83, 26, 2019.
- [205] O. Okur, N. Voulis, P. Heijnen, and P. Lukszo, "Aggregator-mediated demand response: Minimizing imbalances caused by uncertainty of solar generation", *Applied Energy*, vol. 247, 426, 2019.
- [206] Bundesamt für Energie (BFE), *Weiterentwicklung in der Tarifierung von Netz und Energie*, <https://pubdb.bfe.admin.ch/de/publication/download/10513>, 2021.
- [207] F. Li, D. Tolley, N. P. Padhy, and J. Wang, "Framework for Assessing the Economic Efficiencies of Long-Run Network Pricing Models", *IEEE Transactions on Power Systems*, vol. 24, no. 4, 1641, 2009. DOI: 10.1109/TPWRS.2009.2030283.
- [208] T. Schittekatte, I. Momber, and L. Meeus, "Future-proof tariff design: Recovering sunk grid costs in a world where consumers are pushing back", *Energy Economics*, vol. 70, 484, 2018.
- [209] I. Savelli, A. De Paola, and F. Li, "Ex-ante dynamic network tariffs for transmission cost recovery", *Applied Energy*, vol. 258, 113979, 2020.
- [210] S. Young, A. Bruce, and I. MacGill, "Potential impacts of residential pv and battery storage on australia's electricity networks under different tariffs", *Energy Policy*, vol. 128, 616, 2019.
- [211] S. Neuteleers, M. Mulder, and F. Hindriks, "Assessing fairness of dynamic grid tariffs", *Energy Policy*, vol. 108, 111, 2017.
- [212] M. Ansarin, Y. Ghiassi-Farrokhfal, W. Ketter, and J. Collins, "The economic consequences of electricity tariff design in a renewable energy era", *Applied Energy*, vol. 275, 115317, 2020.
- [213] M. D. Trong and Y. Yang, "An investigation on fairness perception for grid tariff models: Evidence from Denmark", *The Electricity Journal*, vol. 36, no. 1, 107240, 2023.

- [214] P. P. Singh, F. Wen, and I. Palu, "Dynamic Network Tariff in Practices: Key Issues and Challenges", in *2021 IEEE 4th International Conference on Computing, Power and Communication Technologies (GUCON)*, IEEE, 2021, 1.
- [215] R. de Sá Ferreira, L. A. Barroso, P. R. Lino, M. M. Carvalho, and P. Valenzuela, "Time-of-Use Tariff Design Under Uncertainty in Price-Elasticities of Electricity Demand: A Stochastic Optimization Approach", *IEEE Transactions on Smart Grid*, vol. 4, no. 4, 2285, 2013.
- [216] F. El Gohary, B. Stikvoort, and C. Bartusch, "Evaluating demand charges as instruments for managing peak-demand", *Renewable and Sustainable Energy Reviews*, vol. 188, 113876, 2023.
- [217] J. Vaughan, S. C. Doumen, and K. Kok, "Empowering tomorrow, controlling today: A multi-criteria assessment of distribution grid tariff designs", *Applied Energy*, vol. 341, 121053, 2023.
- [218] V. Nair and U. Nair, "Selection of electricity tariff designs for distribution networks using analytic network process", *International Journal of the Analytic Hierarchy Process*, vol. 15, no. 2, 2023.
- [219] J.-J. Wang, Y.-Y. Jing, C.-F. Zhang, and J.-H. Zhao, "Review on multi-criteria decision analysis aid in sustainable energy decision-making", *Renewable and Sustainable Energy Reviews*, vol. 13, no. 9, 2263, 2009.
- [220] C. Büttner, J. Amme, J. Endres, A. Malla, B. Schachler, and I. Cußmann, "Open modeling of electricity and heat demand curves for all residential buildings in Germany", *Energy Informatics*, vol. 5, no. 21, 2022.
- [221] D. Kucevic, B. Tepe, S. Englberger, A. Parlikar, M. Mühlbauer, O. Bohlen, A. Jossen, and H. Hesse, "Standard battery energy storage system profiles: Analysis of various applications for stationary energy storage systems using a holistic simulation framework", *Journal of Energy Storage*, vol. 28, 101077, 2020.
- [222] B. Wehrmann, *What German households pay for power*, 2021. Available: <https://www.cleanenergywire.org/factsheets/what-german-households-pay-electricity>, (accessed: 12.07.2022).
- [223] T. Frahm, *Einspeisevergütung für Photovoltaik 2022*, 2022. Available: <https://www.solaranlagen-portal.com/photovoltaik/wirtschaftlichkeit/einspeiseverguetung>, (accessed: 12.07.2022).

- [224] M. Nijhuis, M. Gibescu, and J. Cobben, "Analysis of reflectivity & predictability of electricity network tariff structures for household consumers", *Energy Policy*, vol. 109, 631, 2017.
- [225] R. A. Verzijlbergh, L. J. De Vries, and Z. Lukszo, "Renewable Energy Sources and Responsive Demand. Do We Need Congestion Management in the Distribution Grid?", *IEEE Transactions on Power Systems*, vol. 29, no. 5, 2119, 2014. DOI: 10.1109/TPWRS.2014.2300941.
- [226] International Renewable Energy Agency, Abu Dhabi, *Innovation landscape brief: Time-of-use tariffs*, (accessed: 26.07.2022).
- [227] D. Dallinger and M. Wietschel, "Grid integration of intermittent renewable energy sources using price-responsive plug-in electric vehicles", *Renewable and Sustainable Energy Reviews*, vol. 16, no. 5, 3370, 2012.
- [228] M. Kühnbach, J. Stute, and A.-L. Klingler, "Impacts of avalanche effects of price-optimized electric vehicle charging-Does demand response make it worse?", *Energy Strategy Reviews*, vol. 34, 100608, 2021.
- [229] D. Patteeuw, G. P. Henze, and L. Helsen, "Comparison of load shifting incentives for low-energy buildings with heat pumps to attain grid flexibility benefits", *Applied energy*, vol. 167, 80, 2016.
- [230] J. Stute and M. Kühnbach, "Dynamic pricing and the flexible consumer – Investigating grid and financial implications: A case study for Germany", *Energy Strategy Reviews*, vol. 45, 100987, 2023.
- [231] S. Bjarghov and M. Hofmann, "Grid Tariffs for Peak Demand Reduction: Is there a Price Signal Conflict with Electricity Spot Prices?", in *2022 18th International Conference on the European Energy Market (EEM)*, IEEE, 2022, 1.
- [232] J. Stute and M. Klobasa, "How do dynamic electricity tariffs and different grid charge designs interact? - Implications for residential consumers and grid reinforcement requirements", *Energy Policy*, vol. 189, 114062, 2024.
- [233] A. Heider, J. Huber, Y. Farhat, Y. Hertig, and G. Hug, "How to choose a suitable network tariff? - Evaluating network tariffs under increasing integration of distributed energy resources", *Energy Policy*, vol. 188, 114050, 2024.

- [234] J. Huber, "Evaluation Framework for Network Tariff Structures under Increased Integration of Distributed Energy Resources", *Master Thesis, Power Systems Laboratory, ETH Zurich*, 2022.
- [235] A. Byman, *Social Research Methods. 4th Edition*. Oxford University Press, 2012.
- [236] T. Dresing and T. Pehl, *Praxisbuch Interview, Transkription & Analyse. Anleitungen und Regelsysteme für qualitativ Forschende*. Dr. Dresing und Pehl GmbH, Marburg, 2015.
- [237] S. Kvale and S. Brinkmann, *InterViews: Learning the Craft of Qualitative Research Interviewing*. SAGE Publications, 2009.
- [238] Verband Schweizerischer Elektrizitätsunternehmen (VSE), *Netznutzungsmodell für das Schweizerische Verteilnetz - Grundlagen zur Netznutzung und Netznutzungsentschädigung in den Verteilnetzen der Schweiz*, <https://www.strom.ch/de/media/13220/download>, 2021.
- [239] Stromversorgungsgesetz (StromVG), <https://www.fedlex.admin.ch/eli/cc/2007/418/de>, 2017.
- [240] European Union (EU), *Regulation (EU) 2019/943 of the European Parliament and of the Council of 5 June 2019 on the internal market for electricity*, <https://eur-lex.europa.eu/legal-content/EN/TXT/?uri=CELEX%3A02019R0943-20220623>, 2019.
- [241] T. Schittekatte, "Distribution Network Tariff Design and Active Consumers: A Regulatory Impact Analysis", Ph.D. dissertation, Université Paris Saclay (COMUE), 2019.
- [242] Council of European Energy Regulators (CEER), *CEER Paper on Electricity Distribution Tariffs Supporting the Energy Transition*, 2020. Available: <https://www.ceer.eu/documents/104400/-/-/fd5890e1-894e-0a7a-21d9-fa22b6ec9da0>.
- [243] P. Chanel and J. Limoges, *Overview of Electricity Distribution in Europe - Summary from Capgemini's 2008 European benchmarking survey*, 2008. Available: [https://www.capgemini.com/wp-content/uploads/2017/07/tl\\_Overview\\_of\\_Electricity\\_Distribution\\_in\\_Europe.pdf](https://www.capgemini.com/wp-content/uploads/2017/07/tl_Overview_of_Electricity_Distribution_in_Europe.pdf).
- [244] L. Steg and C. Vlek, "Encouraging pro-environmental behaviour: An integrative review and research agenda", *Journal of Environmental Psychology*, vol. 29, no. 3, 309, 2009.

- [245] J. C. Besley, "Public Engagement and the Impact of Fairness Perceptions on Decision Favorability and Acceptance", *Science Communication*, vol. 32, no. 2, 256, 2010.
- [246] Bundesamt für Energie (BFE), *Energiestrategie 2050*, <https://www.bfe.admin.ch/bfe/de/home/politik/energiestrategie-2050.html/>, 2018.
- [247] Stromversorgungsverordnung (StromVV), <https://www.fedlex.admin.ch/eli/cc/2008/226/de>, 2008.
- [248] T. L. Saaty, *The Analytical Hierarchy Process*, McGraw-Hill, New York, 1980.
- [249] W. C. Wedley, "Combining Qualitative and Quantitative Factors - An Analytic Hierarchy Approach", *Socio-Economic Planning Sciences*, vol. 24, no. 1, 57, 1990.
- [250] T. L. Saaty, "Fundamentals of the Analytic Hierarchy Process", in *The Analytic Hierarchy Process in Natural Resource and Environmental Decision Making*, D. L. Schmoldt, J. Kangas, G. A. Mendoza, and M. Pesonen, Eds. Dordrecht: Springer Netherlands, 2001, 15.
- [251] R. W. Saaty, "The analytic hierarchy process - what it is and how it is used", *Mathematical Modelling*, vol. 9, no. 3, 161, 1987. DOI: [https://doi.org/10.1016/0270-0255\(87\)90473-8](https://doi.org/10.1016/0270-0255(87)90473-8). Available: <https://www.sciencedirect.com/science/article/pii/0270025587904738>.
- [252] Y. Farhat, G. M. Lipsa, and T. Braun, "Evaluate the impact of network tariffs on the Swiss energy transition. A fair cost distribution or a driver to reduce expensive network upgrades?", in *2022 IEEE PES Innovative Smart Grid Technologies Conference Europe (ISGT-Europe)*, 2022, 1. DOI: 10.1109/ISGT-Europe54678.2022.9960540.
- [253] Bundesamt für Energie (BFE), *Bundesgesetz für eine sichere Stromversorgung mit erneuerbaren Energien - Revision Energiegesetz und Stromversorgungsgesetz*, <https://www.news.admin.ch/news/message/attachments/63715.pdf>, 2020.
- [254] M. Kendzioriski, L. Göke, C. von Hirschhausen, C. Kemfert, and E. Zozmann, "Centralized and decentral approaches to succeed the 100% energiewende in Germany in the European context – A model-based analysis of generation, network, and storage investments", *Energy Policy*, vol. 167, 113039, 2022.

- [255] N. Helistö, J. Kiviluoma, J. Ikäheimo, T. Rasku, E. Rinne, C. O'Dwyer, R. Li, and D. Flynn, "Backbone—An Adaptable Energy Systems Modelling Framework", *Energies*, vol. 12, no. 17, 2019.
- [256] F. Wiese, R. Bramstoft, H. Koduvere, A. Pizarro Alonso, O. Balyk, J. G. Kirkerud, Å. G. Tveten, T. F. Bolkesjø, M. Münster, and H. Ravn, "Balmorel open source energy system model", *Energy Strategy Reviews*, vol. 20, 26, 2018.
- [257] S. Pfenninger and B. Pickering, "Calliope: a multi-scale energy systems modelling framework", *Journal of Open Source Software*, vol. 3, 825, 2018. DOI: 10.21105/joss.00825.
- [258] A. Zerrahn and W.-P. Schill, "Long-run power storage requirements for high shares of renewables: Review and a new model", *Renewable and Sustainable Energy Reviews*, 2017. DOI: 10.1016/j.rser.2016.11.098.
- [259] S. Quoilin, I. Hidalgo, and A. Zucker, *Modelling Future EU Power Systems Under High Shares of Renewables: The Dispa-SET 2.1 open-source model*, 2017. DOI: 10.2760/25400.
- [260] *The European Electricity Market Model EMMA Model documentation*, <https://neon.energy/emma-documentation.pdf>.
- [261] *EnergyPlan webpage*, <https://www.energyplan.eu/>.
- [262] G. Limpens, S. Moret, H. Jeanmart, and F. Maréchal, "EnergyScope TD: A novel open-source model for regional energy systems", *Applied Energy*, vol. 255, 113729, 2019.
- [263] A. Alhamwi, W. Medjroubi, T. Vogt, and C. Agert, "GIS-based urban energy systems models and tools: Introducing a model for the optimisation of flexibilisation technologies in urban areas", *Applied Energy*, vol. 191, 1, 2017.
- [264] D. F. Dominković, R. G. Junker, K. B. Lindberg, and H. Madsen, "Implementing flexibility into energy planning models: Soft-linking of a high-level energy planning model and a short-term operational model", *Applied Energy*, vol. 260, 114292, 2020.
- [265] *GridCal documentation*, <https://gridcal.readthedocs.io/en/latest/>.
- [266] E. Taibi, T. Nikolakakis, L. Gutierrez, C. Fernandez del Valle, J. Kiviluoma, T. Lindroos, and S. Rissanen, *POWER SYSTEM FLEXIBILITY FOR THE ENERGY TRANSITION IRENA FLEXTOL METHODOLOGY*, 2018. DOI: 10.13140/RG.2.2.11715.86566.

- [267] S. Hilpert, C. Kaldemeyer, U. Krien, S. Günther, C. Wingenbach, and G. Plessmann, "The Open Energy Modelling Framework (oemof) - A new approach to facilitate open science in energy system modelling", *Energy Strategy Reviews*, vol. 22, 16, 2018.
- [268] *OMEGALpes documentation*, <https://omegalpes.readthedocs.io/en/latest/index.html>.
- [269] M. Howells, H. Rogner, N. Strachan, C. Heaps, H. Huntington, S. Kypreos, A. Hughes, S. Silveira, J. DeCarolis, M. Bazillian, and A. Roehrl, "OSeMOSYS: The Open Source Energy Modeling System: An introduction to its ethos, structure and development", *Energy Policy*, vol. 39, no. 10, 5850, 2011.
- [270] L. Thurner, A. Scheidler, F. Schäfer, J. Menke, J. Dollichon, F. Meier, S. Meinecke, and M. Braun, "Pandapower—An Open-Source Python Tool for Convenient Modeling, Analysis, and Optimization of Electric Power Systems", *IEEE Transactions on Power Systems*, vol. 33, no. 6, 6510, 2018. DOI: 10.1109/TPWRS.2018.2829021.
- [271] T. Brown, J. Hörsch, and D. Schlachtberger, "PyPSA: Python for Power System Analysis", *Journal of Open Research Software*, vol. 6, 2018. DOI: 10.5334/jors.188.
- [272] W. Heitkoetter, W. Medjroubi, T. Vogt, and C. Agert, "Regionalised heat demand and power-to-heat capacities in Germany – An open dataset for assessing renewable energy integration", *Applied Energy*, vol. 259, 114161, 2020.
- [273] A. P. Hilbers, D. J. Brayshaw, and A. Gandy, "Efficient quantification of the impact of demand and weather uncertainty in power system models", *IEEE Transactions on Power Systems*, vol. 36, no. 3, 1771, 2021. DOI: 10.1109/TPWRS.2020.3031187.
- [274] R. Loulou, U. Remme, A. Kanudia, A. Lehtilä, and G. Goldstein, "Documentation for the TIMES model", *Energy Technology Systems Analysis Programme (ETSAP)*, 2005.
- [275] L. Andresen, P. Dubucq, R. Peniche Garcia, G. Ackermann, A. Kather, and G. Schmitz, "Status of the TransiEnt Library: Transient Simulation of Coupled Energy Networks with High Share of Renewable Energy", 2015. DOI: 10.3384/ecp15118695.
- [276] *Urbs documentation*, <https://urbs.readthedocs.io/en/latest/index.html>.

- [277] R. Morrison, T. Wittmann, J. Heise, and T. Bruckner, "POLICY-ORIENTED ENERGY SYSTEM MODELING WITH XEONA", 2020.
- [278] T. Bründlinger, J. E. König, O. Frank, D. Gründig, C. Jugel, P. Kraft, O. Krieger, S. Mischinger, P. Prein, H. Seidl, *et al.*, "dena-Leitstudie Integrierte Energiewende: Impulse für die Gestaltung des Energiesystems bis 2050", *Deutsche Energie-Agentur GmbH (dena), ewi Energy Research & Scenarios gGmbH: Berlin/Köln, Germany, 2018.*